Characterization of the nuclear envelope mechano-transduction in Arabidopsis : from supracellular stress to chromatin remodeling

Rituparna Goswami

Université de Strasbourg

UNIVERSITÉ DE STRASBOURG

École Doctorale des Sciences de la Vie et de la Santé STRASBOURG

ÉCOLE DOCTORALE _414

Institut de Biologie Moléculaire des Plantes, Strasbourg

THÈSE présentée par : **Rituparna GOSWAMI**

soutenue le : **25 septembre 2020**

pour obtenir le grade de : **Docteur de l'université de Strasbourg**

Discipline/ Spécialité : Sciences du vivant- Aspect Moléculaire et cellulaire de la biologie

Characterization of the nuclear envelope mechano-transduction in *Arabidopsis*: from supracellular stress to chromatin remodeling

Membres du Jury

Rapporteur	:	Pr. Ueli GROSSNICKLAUS, UZH, Zurich
Rapporteur	:	Dr. Valérie GAUDIN, DR2, IJPB, Versailles
Examinateur	:	Dr. Cristel CARLES, MC, LFCV, UGA, Grenoble
Examinateur	:	Dr. JM DAVIERE, MC, IBMP, Strasbourg
Directeur de Thèse	:	Dr. ME CHABOUTE, DR2 CNRS , IBMP, Strasbourg
Co-Directeur de Thèse	:	Dr. Olivier HAMANT, DR1 INRA, RDP, ENS, Lyon

Acknowledgement

I would first like to express my gratitude to Pr. Ueli Grossnicklaus, Dr. Valérie Gaudin, Dr. Cristel Carles, Dr. Jean Michel Daviere for their kind acceptance to review my PhD thesis.

I am thankful to my supervisors Dr. Marie Edith Chabouté and Dr. Olivier Hamant for giving me this opportunity to work in this fascinating project. Your constant guidance, support, trust and encouragement have been enlightening to be. You both have been amazing mentors to me, helping me to focus towards the endless possibilities of science and research. Marie, it has been a treat to know you and to work alongside you. Olivier, you are not only exceptional scientist but exceptional human being as well. I hope I will be keep receiving these valuable insights for science and life itself from you.

Institut de biologie moléculaire des plantes (IBMP) and Université de Strasbourg has given me an amazing platform helping me to understand and realise my scientific curiosity. I am thankful to French government and IDEX fellowship for enabling me to pursue research in this vibrant environment. I am grateful to all the team members for their help and care. I will always cherish our elaborate discussions on science but more importantly the non-scientific one. All my friends here and back home, thank you for being there. I want to thank all the teachers and mentors without them I would have been lost.

I want to especially mention my best friend and my husband Dr. Abhijit Sau. You are not only an extremely talented researcher but also an extraordinary person. Your constant kindness, love and care has made this journey of PhD more enjoyable. Your scientific knowledge, objectivity and love of research has been my personal motivation. My little brother, thank you for the bond we share where I can rely anytime, you are my constant cheerer. Last and hugely important acknowledgement goes towards by parents. You are rare blend of intellect, compassion, tolerance, honesty, with a disconnect from materialistic desires who showed me the glory of pursuit of knowledge and enabled me with aids to boldly follow that path. I am humbled for the path you showed, as that led me to understand my own limitless ignorance and to see the world with empathy and compassion. The best teaching of my father I take as mantra of my life is “your behaviour exhibits your education not your marks in tests; if your education doesn’t humble you then it’s irrelevant”. As parents your unconditional love has been a compass in this life and thousands of miles away, I have never felt separated from you for a moment. You are everything and more one could ever hope and ask for.

Nomenclature and list of the abbreviations:

Abbreviations:

Name of the gene and associated function		
Protein	**Full name**	**Function**
AtMEKK1	MITOGEN-ACTIVATED PROTEIN KINASE KINASE KINASE 1	extracellular signal-related kinase
AtMPK3	ARABIDOPSIS MITOGEN-ACTIVATED PROTEIN KINASE 3	extracellular signal-related kinase
AtMPK4	ARABIDOPSIS MITOGEN-ACTIVATED PROTEIN KINASE 4	extracellular signal-related kinase
AtMPK6	ARABIDOPSIS MITOGEN-ACTIVATED PROTEIN KINASE 6	extracellular signal-related kinase
CA	CALCIUM-BINDING EF-HAND FAMILY PROTEIN	Response to karrikin
CESA	CELLULOSE SYNTHASE	Family involved in cellulose deposition
CML	CALMODULINE LIKE PROTEIN	Involved in Ca^{2+} signalling
CPK28	CALCIUM-DEPENDENT PROTEIN KINASE 28	Abscisic acid-activated signalling pathway
CPK32	CALCIUM-DEPENDENT PROTEIN KINASE 32	Abscisic acid-activated signalling pathway
Cre1	CYTOKININ RESPONSE 1	Plant histidine kinase
CRWN1	CROWDED NUCLEI 1	Plant lamin like protein,
CRWN4	CROWDED NUCLEI 4	Plant lamin like protein
CSC	CELLULOSE SYNTHASE COMPLEXES	Cellulose deposition complex in plasma membrane
CSI1	CELLULOSE SYNTHASE INTERACTING PROTEIN 1	Links Microtubule and CSC physically
CSL	CELLULOSE SYNTHASE-LIKE	Glucosyl transferase involved in hemicellulose modification
CYP81D8	CYTOCHROME P450, FAMILY 81, SUBFAMILY D, POLYPEPTIDE 8	response to karrikin
DEK 1	DEFECTIVE KERNEL 1	Membrane protein involved in Ca^{2+} signalling
DREB26	DEHYDRATION RESPONSIVE ELEMENT BINDING 26	Transcription factor
FER	FERONIA	RLK protein involved in cell wall integrity
GCP3	GAMMA-TUBULIN COMPLEX PROTEIN 3	Microtubule Nucleation complex protein
GIP1/GIP2	GCP3 INTERACTING PROTEIN 1/2	Proper microtubule nucleation and CENH3 loading
HOG	HIGH OSMOLARITY GLYCEROL RESPONSE	
KASH	KLARSICHT, ANC-1, AND SYNE HOMOLOGY 1	Outer Nuclear envelope protein interacting with cytoskeleton
MLK1	MUT9 LIKE KINASES 1	Involved in osmosensing pathway

MLK2	MUT9 LIKE KINASES 2	Involved in osmosensing pathway
MSL	MscS-LIKE	Mechanosensitive ion channel
Myb44	MYELOBLASTOMA TRANSCRIPTION FACTOR	Transcription factor involved in abiotic stress response
MZT1	MITOTIC-SPINDLE ORGANIZING PROTEIN 1	Directing γ-tubulin complexes to microtubule organizing centers
NHL3	NDR1/HIN1-LIKE 3	Disease resistance
NMCP	NUCLEAR MATRIX CONSTITUENT PROTEINS	nuclear lamin like protein
PHS1	PROPYZAMIDEHYPERSENSITIVE 1	Involved in salt stress talerance
PIN	PIN-FORMED	Family of Auxin efflux carrier involved in cell polarity
PME	PECTIN METHYLESTERASES	Family of proteins involved in pectin demethylesterification
PtaZFT	Pta ZINC FINGER PROTEIN 2	Transcription factor in Poplar
PRC2	POLYCOMB REPRESSIVE COMPLEXES 2	chromatin-mediated gene repression
PWO1	PROLINE-TRYPTOPHANE-TRYPTOPHANE- PROLINE (PWWP) INTERACTOR OF POLYCOMBS1	chromatin-mediated gene repression
SLN1	SYNTHETIC LETHAL OF N-END RULE 1	Histidine kinase act as osmosensor
SUN1	SAD1P AND UNC-84 PROTEIN 1	Inner Nuclear envelope protein interacting with Nucleoskeleton
SZF1	SALT ZINC FINGER	Transcription facto
TCH2	TOUCH2	Putative role in Calcium signalling
TCH3	TOUCH3	Putative role in Calcium signalling
TCH4	TOUCH4	Cell wall modifying enzyme
THE	THESEUS1	RLK protein involved in cell wall integrity maintenance
TSA1	TONSOKU (TSK)-ASSOCIATING PROTEIN	Protein involved in genomic maintenance
WAK	WALL-ASSOCIATED KINASES	RLK protein involved in cell wall integrity maintenance
XTH	XYLOGLUCAN ENDOTRANS GLUCOSYLASE/ HYDROLASE	Proteins involved in hemicellulose modifications
YAP/TAZ	YES-ASSOCIATED PROTEIN/TRANSCRIPTIONAL CO-ACTIVATOR WITH PDZ-BINDING MOTIF	Transcriptional coactivators downstream of the Hippo signalling pathway

Wild Type and mutant lines		
Abbreviation	**Corresponding gene**	**Reference**
CoL0	Wild Type, ecotype COLUMBIA	×
eli1.1	*Ectopic lignin 1-1*	(Caño-Delgado *et al.*, 2003)
gip1gip2	*GCP3 INTERACTING PROTEIN 1/2*	(Janski *et al.*, 2012)
qua1	*QUASIMODO1*	(Verger *et al.*2018)
WS	Wild Type, ecotype Wassilewskija	×
WS*Col0	Wild Type, ecotype COLUMBIA * Wassilewskija	https://www-arabidopsis-org.insb.bib.cnrs.fr/servlets/TairObject?id=90&type=species_variant https://www.arabidopsis.org/servlets/TairObject?id=392&type=species_variant

Marker lines		
Abbreviation	**Description**	**Reference**
Arabidopsis crwn1 PSUN1::SUN:GFP	Crossing of *crwn1* and WT PSUN1::SUN:GFP	×
Arabidopsis crwn4 PSUN1::SUN:GFP	Crossing of *crwn4* and WT PSUN1::SUN:GFP	×
Arabidopsis eli1-1 PSUN1::SUN:GFP	Crossing of *eli1-1* and WT PSUN1::SUN:GFP	×
Arabidopsis gip1gip2 p35S::SUN1-YFP	Transformation of *gip1gip2* via floral dipping with *p35S::AtSUN1-YFP*	(Batzenschlager *et al.*, 2013)
Arabidopsis WT PSUN1::SUNGFP	×	(Graumann *et al.,* 2010)

Other abbreviations	
ABA	Abscisic Acid
AFM	Atomic Force Microscopy
ATP	Adenosine Tri Phosphate
Ca^{2+}	Calcium Ion
CFM	Cellular Force Microscopy
CMR	Cell Monolayer Rheology
CMT	Cortical Microtubule
DMSO	Dimethyl Sulfoxide
ECM	Extra Cellular Matrix
FA	Focal Adhesion
FESEM	Field-Emission Scanning Electron Microscopy
GFP	Green Fluorescent Protein
INM	Inner Nuclear Membrane
LINC	Linker Of Nucleoskeleton And Cytoskeleton
MAMP	Microbial-Associated Molecular Pattern-Triggered Immunity
MCA	Mid1-Complementing Activity
MCF7	Michigan Cancer Foundation-7
MPa	Megapascal
MSCs	Mesenchymal Stem Cells
MTC	Magnetic Twisting Cytometry
NaCl	Sodium Chloride
NADP	Nicotinamide Adenine Dinucleotide Phosphate
ONM	Outer Nuclear Membrane
OS	Optical Stretching
OSCA1	Reduced Hyper Osmolarity-Induced $[Ca^{2+}]_I$ Increase 1
OT	Optical Tweezer
PI	Propidium Iodide
PTM	Particle-Tracking Micro Rheology
RALF	Rapid Alkalinisation Factor
RLK	Receptor Like Kinase
ROS	Reactive Oxygen Species
SAM	Shoot Apical Meristem
SEM	Scanning Electron Microscopy
SF	Stress Fibers
SPM	Spinning Plate Microscopy

Table of contents

Introduction- 15-104

Introduction

Preface-

The biochemical and molecular characterisation of biological processes has been a major focus of study in biology in the second half of the twentieth century. Scientist have identified and characterized countless molecular players and strong hypotheses regarding the associated mechanisms have been put forward. Yet, biological organisms are also physical objects. Thus, the identified pathways must be integrated in a more physical framework too, and at all scales. Indeed, mechanical properties of living material may contribute to a global control of these molecular pathways and help us to understand how these pathways coordinate to generate physiological responses from cell division to differentiation during development. Although physical explanation of biological systems was already vibrant in the 19th century (see e.g. Sachs, Hofmeister, D'Arcy Thompson), the field gained momentum in last decades with the technological improvements in live imaging, micromechanics and computational modelling allowing the study of the physical properties of biological systems.

Last few decades have seen enormous rise in biomechanics and mechanotransduction studies. Mechanical properties of biological material have been measured at different scales. Several mechanosensor elements have been identified and their role in force transduction, characterized. Mechanical signalling is particularly hard to study because forces are in essence invisible and because the transduction of mechanical signals is coupled with that of biochemical signals. In fact, mechanical signals impact on biological processes both through biophysical and biochemical modulations of cellular mechanosensors. An even more difficult question to address is how mechanical signals reach the nucleus.

During my PhD research work I have focused to understand the nuclear mechanics and its role in mechanotransduction. I have chosen the dividing region of root tip of the plant *Arabidopsis thaliana*, as a model system. This system is suitable for live imaging of nuclei and can be easily perturbed by osmotic stress. To introduce the context and relevance of my work, I will first present the mechanics of living systems at different scales with an emphasis on plants. Next, I will detail the range of tools that made these studies possible, notably by adapting existing methods to the constraints of plant systems. Then I will describe the known mechanotransduction pathways. In this section I will dissect the animal mechanotransduction pathways and then switch to putative mechanisms in plants with a more detailed analysis of key candidates. In the last part, I will focus on the nucleus to introduce my work. I will present

the morpho-mechanical properties of the nucleus and how manipulation of these properties serves as readouts of cellular and multicellular processes *via* signalling pathways leading to modified gene expression.

.

1. The structural elements of living organisms

In this first part, I will describe the general role of mechanics behind the processes of life, focusing on the mechanical features of multicellular organisms, at different scales, and how they contribute to biological processes.

1.1. Mechanics Basics (definitions)

Mechanics is the branch of science dealing with characteristics of material under the influence of forces. The architecture of any object is largely determined by its mechanics. This paradigm extends to living organisms as well. In words of the Professor Thomas D'Arcy Wentworth Thompson written in his seminal book On Growth and Form '*to see how . . . the form of living things . . . can be explained by physical considerations, and to realise that in general no organic forms exist save such as are in conformity with ordinary physical laws'* (Thompson, 1917). He describes the shape as '*diagram of forces*' in which the external and internal forces forms a balance to maintain the form. The shape change is manifested by the forces it endures.

To measure stress (often noted sigma), one needs to normalize force by the geometry of the material. Stress is defined as a force per unit area and it is measured in Pascal or Newton per square meter. Although stress could be of various types, the most studied types of stress could be normal (either tensile or compressive) or shear stresses. When the force acts perpendicular to the cross-section of the object, it is defined as normal stress while the shear stress works parallel to the cross-section.

Force makes relative change (deformation) in the dimension of the object. When normalized by the initial geometry, it is measured as strain (often noted epsilon). Like normal and shear stresses, there are normal and shear strains. Usually, when stress increases, strain increases too. The slope between stress and strain corresponds to Young's Modulus (often noted E) and reflect the elastic mechanical properties of the material. Depending on the strain from the mechanical stress exerted on a material, materials could be elastic, viscous, plastic, visco-plastic, visco-elastic, elasto-viscous properties (Figure 1). When the material is deformed following Hooke's law, the strain becomes proportional to the stress and when the stress is withdrawn it goes back to its absolute original form it is called elastic. When the material does not go back to an original form it is called plastic. Viscous material can resist the deformation but when they deform permanently only after a threshold stress it shows a plastic component

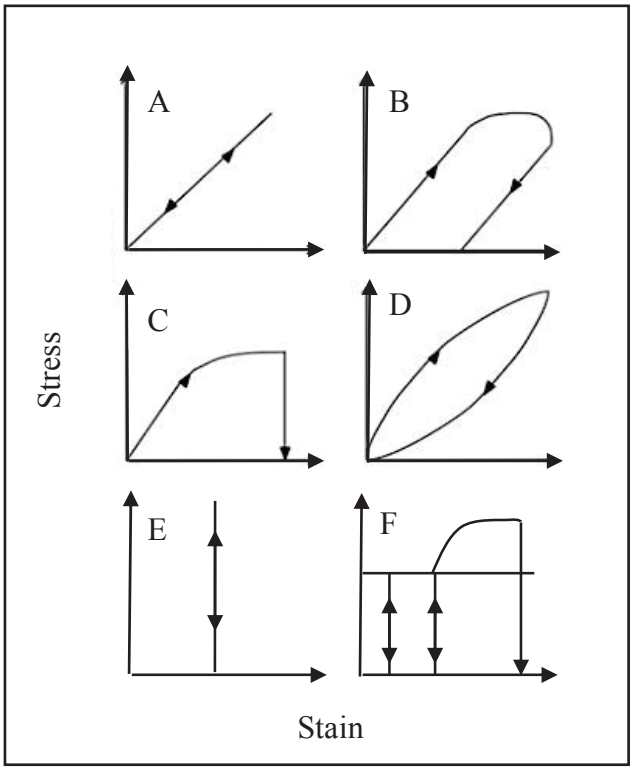

Figure 1. Graphical representation of mechanical properties of material

(A) Elastic: Material is deformed via application of stress and goes back to original when the stress is withdrawn
(B) Elasto-plastic : Partial recovery of original shape
(C) Plastic : material deforms permanently in response to stress
(D) Visco-elastic : Original form is recovered with a delay in time
(E) Viscous : Material capable of resisting deformation.
(F) Visco-plastic : Material resist deformation up to a threshold but permanent deformation occurs after that.

and the material is called visco-plastic. For some material the shape of the material could go back to the original but with a time delay showing both viscous and elastic properties.

The hold of mechanics on the behaviour of a living thing could be studied in different dimensions, starting from organism to tissue to cell and to molecular levels (Figure 2).

1.2. Living organisms as multiscale mechanical objects

1.2.1. Organism scale

The study of the mechanical properties of living systems and associated biological processes gained momentum in last few decades (Ingber, 2008).

If we compare organisms with an inflated balloon, where the thin wall of the balloon exerts compressive force on the inside air; in turn the balloon wall remains under tension with the force exerted on it with the air inside. The tension and compression force balance each other on the balloon wall. When we try to increase the volume of the balloon with more air, the walls get thinner reaching to a new equilibrium of tension-compression balance. When a structure carry pre-existing tensile stress before an external load is applied, the initial state of the structure is called 'prestressed'.

Drawing a circle on the side of an object allows to quantify the deformation. For instance, when an object is extended vertically, the circles become ellipses with a major axis in the vertical orientation (Figure 3). This however may be more complex depending on whether the material properties are inhomogeneous, or if the deformation follows a more complex spatio-temporal pattern. Needless to say, living organisms rather belong to the latter category. Despite such simplifications, the use of mechanical models is of great help to understand the bases of growth and deformation in developing organisms

While studying the mechanical properties of organism, a presence of prestressed condition is observed such as in arteries (Fung & Liu, 1989), human brain (Budday *et al.*, 2014), blood vessels (Fung, 1991), developing embryo (Beloussov & Grabovsky, 2006). This stressed mechanics contributes to the shape and mechanical properties of the organism.

Adapted from Hamant, 2013

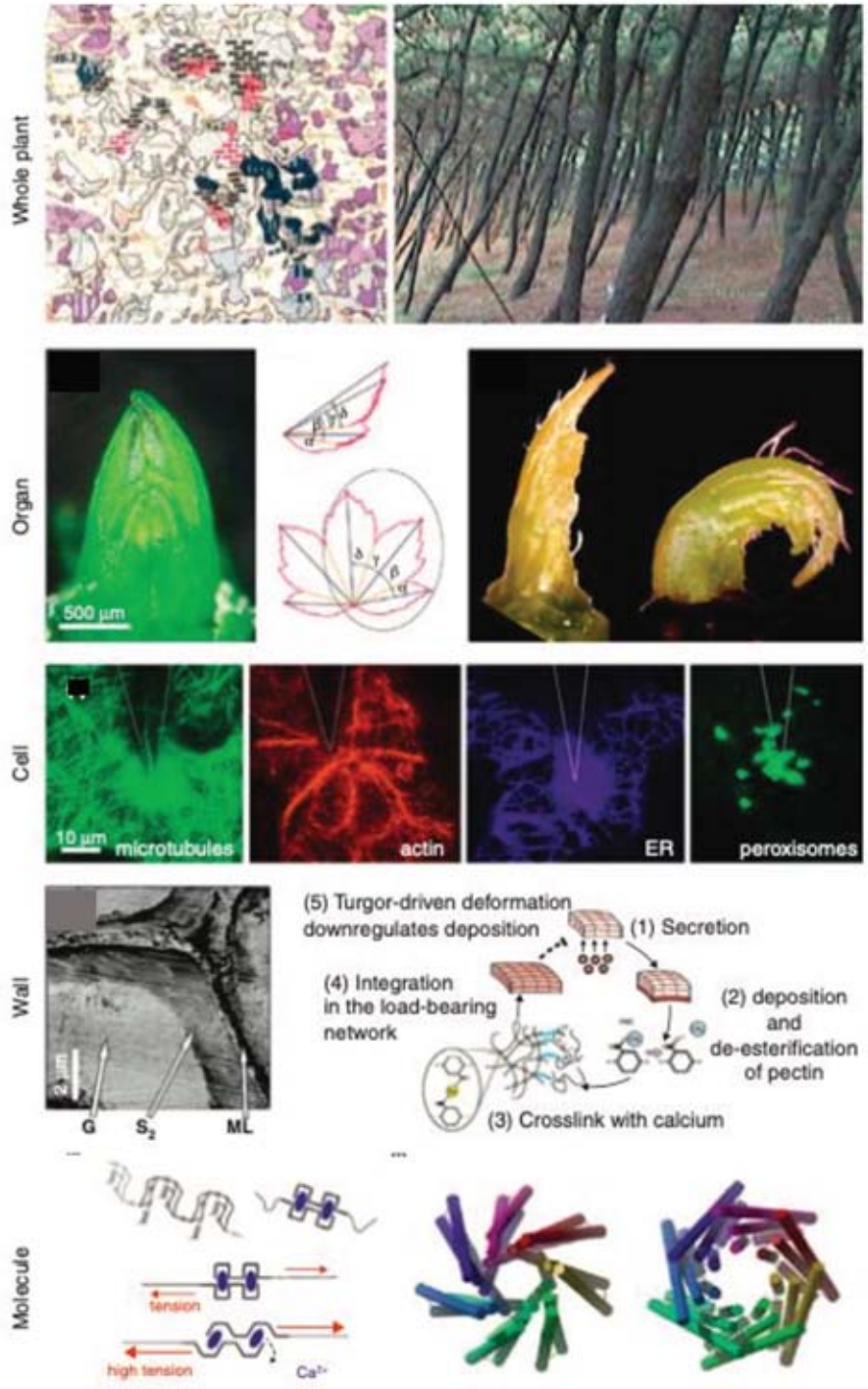

Figure 2. Mechanical stress impact plant at different scales

Physical stress contributes to the posture and shape at organism level. Plant population map shows the summit of the isolated Mount Mezenc (center) in central France is characterized by the presence of *Juniperus nana* (pink), a dwarf plant adapted to high winds. At organ level leaf development could be controlled by the presence of other leaf feedbacking on the shape of the 1st one. External force is able to perturb cellular organisation by interacting with cytoskeleton and subcellular organelle. Cell wall stiffness is a major mechanical readout of the cell. At a molecular level cell wall pectin and mechanosensing ion channels are able to change under direct stretching via pressure. Adapted from Hamant, (2013).

A very early experiment in 1980s showed that the arteries remains in a perpetual stressed condition. If we think the artery as a three-layered cylinder, the outer layer is in tensile whereas the inner layer in under compressive stress. By a simple experiment of cutting an artery in particular angle a quantification of the stress can be done with the parameters of the angle of the cut and the furthest point on the disk (Fung, 1991). The convolved shape of the mammalian gut brings another interesting example of organ development led by mechanical force: mechanical forces are instrumental to explain such three-dimensional tissue folding. Savin *et al.,* indeed showed that if the mesentery is separated from the gut tube via physical of chemical means the loops of the intestine uncoils to a straight tube and the mesentery contracts. Such elastic behaviours show that the mesentery tissue was under tension, while the gut tube was under compression; the resulting balance leads to folding and looping of the gut (Savin *et al.*, 2011).

Organs are formed by complex organisation of tissue. The mechanical properties of these next level organisation contribute to the form and function of the organism.

1.2.2. Tissue as a mechanical object

Tissues have a wide range of elastic properties with brain as an example of soft tissue with a Young's modulus of less than 1 kPa (Georges *et al.*, 2006) while bones being the stiffest in vertebrates with a stiffness in the GPa range (Keller *et al.*, 1990).

In a seminal article Engler *et al.*, showed that depending on the stiffness of the matrix (the medium where the cells grow), Mesenchymal Stem Cells could become neurogenic, myogenic or osteogenic (Figure 4) (Engler *et al.,* 2006). This gives us the idea about the importance of tissue mechanics in the context of differentiation and development as tissue is the *in-situ* matrix for cells in a living organism.

Note that the measured stiffness of the tissue is not the sum of individual elements, but instead, it highly depends on the structure and topology of the tissue. For instance, collagen is present

Adapted from Beloussov and Grabovsky - 2006

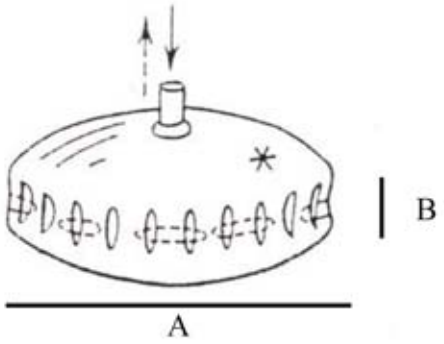

Figure 3. Inflation (solid arrow) of a flattened balloon generates on its surface a series of vertical folds, while its deflation (dotted arrow) produces a series of horizontal folds

If we assume the diameter of the balloon is A and height B, here the A>B. Folds are the structures created along of the height of the balloon when the above-threshold inflation or deflation force works on the balloon. In each case, the number of folds is quite precise and depends upon the balloon's geometry. This shows how a regular complicated pattern can be created by applying no more than one volume changing force.

Adapted from Beloussov and Grabovsky (2006).

in all tissues, but these tissues exhibit different stiffnesses. Collagen is a stiff acellular component present in all kind of tissues including skin, bones, tendon, teeth, cartilage, cornea. Individual collagen fibrils (type I from rat tail) shows elastic modulus ranging from 3.75 GPa to 11.5 GPa when measured by AFM in air and at room temperature (Wenger *et al.*, 2007). Whereas the tissues collagen is associated with could be very stiff like bone with elastic modulus of 12.1 (± 4.14) GPa (Keller *et al.*, 1990), with a low stiffness like cornea with elastic modulus of 0.2 -1 MPa (Orssengo, 1999) or with intermediate stiffness in skin (elastic modulus of 0-50 MPa) (Yang *et al.*, 2015) depending on the specialized hierarchical organization of collagen fibrils (Sherman *et al.*, 2015). This depicts a scenario where the physical characteristics of the individual collagen does not portray the actual characteristic of the tissue.

In addition, the physico-chemical properties of molecular elements, and their combination, geometry, e.g. through tissue topology, affects the structural features of the tissue. In turn, this may also affect cell properties. It has been shown computationally that the hexagonal packing of cells in the epithelial (animal) / epidermal (plant), affects the cell shape when the shape is function of mechanical property of the cell (balance between internal pressure and shape derived tension). Also, in the same study the cell division plane was affected by the tissue packing in a way the orientation of the plane was shown to be biased by the position of the long axis of the neighbouring cell and as a result again affects the cell shape and mechanics (Gibson *et al.*, 2011). In plants, tissue topology was recently shown to prescribe heterogeneous turgor pressure in tissues (Long *et al.*, 2020).

1.2.3. Cell as a mechanical object

In any tissue, the functional unit is the cell. This entails a local and global coordination. In the end, the mechanics of cells become an important piece of the puzzle to understand the mechanics behind an organism.

As in tissues, a range of Young's modulus have been measured in different types of cells: 1.7 ± 2.2 kPa for 3T3 fibroblasts (Mahaffy *et al.*, 2004), 1–2 kPa for osteoblasts (Takai *et al.*, 2005), 1.8 ± 0.3 kPa for fibroblasts (Ricci *et al.*, 1997), 1.5–5.5 kPa for endothelial cells (Costa *et al.*, 2006), and 0.3–30 kPa for bone marrow stromal cells (Simon *et al.*, 2003).

Adapted from Engler *et al.*, 2006

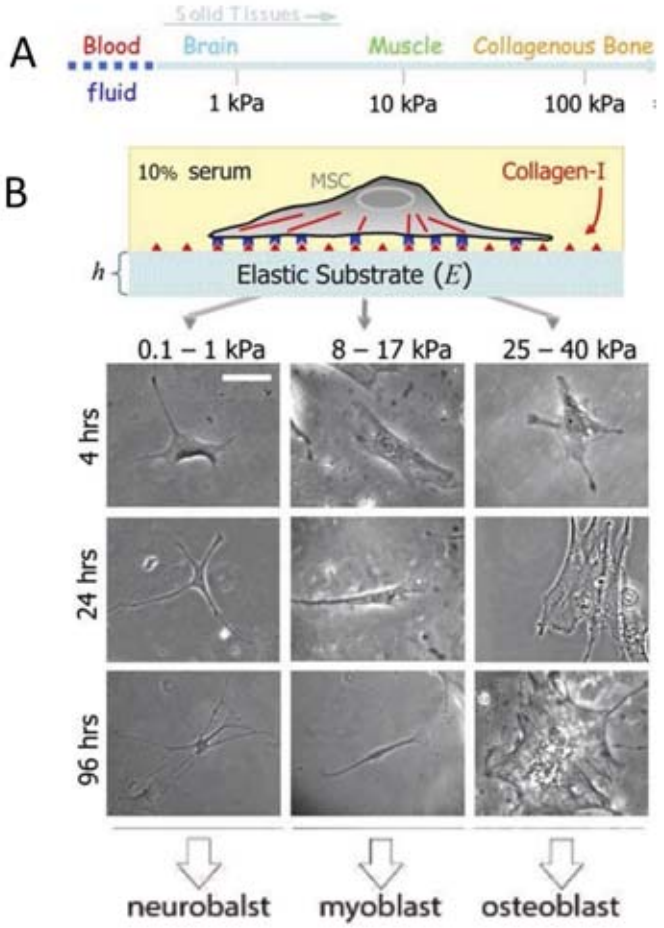

Figure 4. Impact of tissue elasticity on the fate of mesenchymal stem cell

(A) Solid tissues exhibit a range of stiffness, as measured by the elasticmodulus, *E*.

(B) Mesenchymal stem cells differentiate in neuroblast or myoblast or osteoblast depending on the different elasticity of the substrate it is growing (the substrate elasticity is determined depending on the tissue elasticity of the different types of cells).

Adapted from Engler *et al.*, (2006).

Stem cells are the building block of living material with the properties of both self-renewal and diversification meaning it can generate similar cells as parent cell and cells with differential abilities (Lanza & Atala, 2014). Numeral studies have been conducted to decipher the molecular players behind stem cell-ness and differentiation (Martí *et al.*, 2013). Geometrical and mechanical cues are increasingly integrated in the corresponding regulatory network (Higuchi *et al.*, 2013). AFM measurement have been done to quantitatively study the mechanical parameters. Studies have shown that the stiffness of stem cells increased when stem cells loose their stemness abilities, which could be seen as a loss of malleability. AFM measurement of elastic modulus via a spherical 5- μm-diameter glass bead of pluripotent, multipotent and unipotent stem cells shows a decreasing stiffness with pluripotent being the softest and the unipotent being the stiffest (Hammerick *et al.*, 2011). Hammerick *et al.*, compared the elastic properties of fibroblasts (E = 3.5 kPa), fibroblast- induced pluripotent stem cells (E = 1.3 kPa), human Adipose derived Stem Cells (E = 5.2 kPa), human Adipose derived Stem Cells – induced pluripotent stem cells (E = 0.9 kPa) and human Embryonic Stem cell (E = 1.2 kPa). It appears again that pluripotency correlates with softer cells.

But in a completely opposite trend, Titushkin & Cho, observed during the process of osteogenesis in human Mesenchymal Stem Cells, Young's modulus decreases from 3.2 ± 1.4 kPa in medium compared to 1.7 ± 1.0 kPa after differentiation (Titushkin & Cho, 2007). This was later confirmed by a study in human amniotic fluid-derived stem cells where Young's modulus of undifferentiated cells was 3.97 ± 0.53 kPa significantly higher than that of fully differentiated osteoblasts 1.52 ± 0.63 kPa. This loss in stiffness also have been observed during adipogenesis where adipocytes (0.9 ± 0.8 kPa) becomes softer than Human adipose-derived adult stem (2.6±1.6 kPa)(Darling *et al.*, 2008).

This difference in stiffness is shown to be originated from cytoskeletal differences. Hammerick *et al.*, showed higher accumulation of cytoskeletal proteins in differentiated cells when compared with the induced pluripotent cell. In hMSC cells, the main structural contributor is the actin cytoskeleton which is present as thick bundles correlating with the mechanical stability these stem cells need, during their adjustment to a plethora of environmental cues, including mechanical cues. On the other hand, the osteoblasts need to be more elastic and compliant to withstand the mechanical stress which correlates with a thin dense mesh like arrangement of the actin cytoskeleton giving rise to an overall lower stiffness for these differentiated cells (Titushkin & Cho, 2007). As a note of caution, it should be mentioned that

Adapted from Mao and Baum - 2015

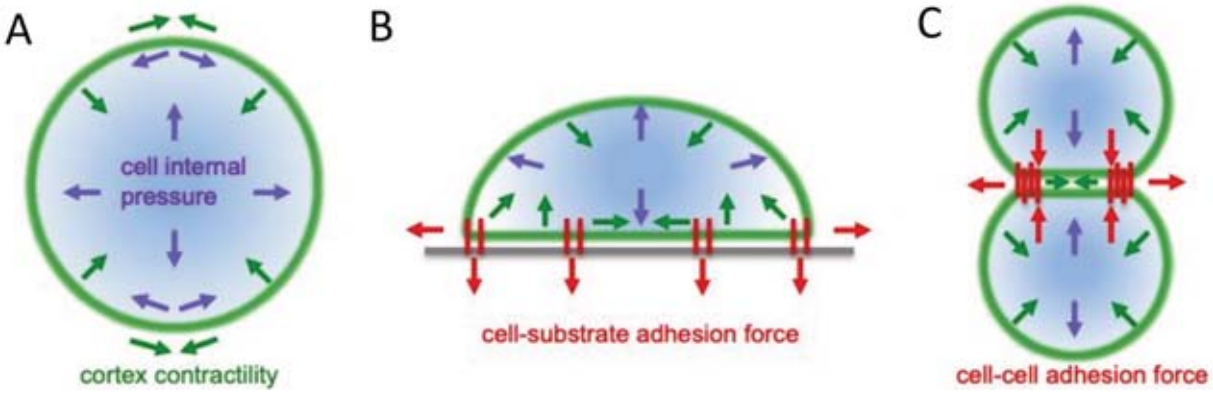

Figure 5. Influence of mechanics on cell shape

(A) For single animal cells cell shape is a balance of the outward expansion forces from the internal cell pressure (blue arrows) and the inward contractile forces generated by the actomyosin cortex (green arrows). This isotropic balance of forces generates a spherical cell.
(B) When a cell adheres to a substrate, adhesion generates additional forces which act on the cell to lower the effective surface tension acting along the cell–substrate interface (red arrows). As a result the cell–substrate contact area increases, causing the cell to spread on the substrate.
(C) Cell–cell adhesion forces create a similar effect, lowering inter-cellular tension, and increasing the cell–cell contact area.

Adapted from Mao and Baum (2015).

this apparent Young's modulus comes with a simple quasi-elastic approximation but the biological materials have viscous component which needs to be taken into account more often.

In addition to direct measurements, the mechanical properties of the cell can be inferred indirectly through morphometry (Paluch & Heisenberg, 2009). In case of animals, the shape of the cells is decided by internal forces *via* cytoskeletal and external forces from environment (Mao & Baum, 2015). In a tissue context, cells are subjected to matrix and other cells and the interaction of a particular cell with them is regulated by mechanics (Figure 5). Thus, mechanics regulates the cellular function such as division, polarisation, movement or differentiation (discussed in depth in later paragraphs) in animal cells. In plants, due to their sessile nature, intriguing mechanical aspects will control their developmental in response to environmental cues.

1.3. The unique aspects of plant mechanics

1.3.1. Plants are pre-stressed structures

The pre-stressed state is shared across all kingdoms. Typically, all walled organisms build an internal pressure, with a balance between tension in the envelope and a compressed content. Plants are walled organisms, and what may be unique about their mechanics is the high stiffness of their walls, which allow them to build up high turgor pressure too, in the MPa range (Figure 6). Because all cells are glued to one another, what is true at the scale of individual cells, may be true also at the organ scale. In other words, plants exhibit self-similarity, at least to some extent.

A prestressed structure acquires a stable state when tension and compression is balanced (Wang *et al.*, 2002). This can be found in individual cells, where a spherical shape would prescribe isotropic tensile stress in the wall, whereas an elongated cell would experience anisotropic tensile stress in its wall. This is also true at the tissue scale. For example, in Shoot Apical Meristem (SAM) (the tissue of origin for the areal organs) the central zone exhibits a spherical shape where tensile stresses are predicted to be isotropic, whereas, in the organ-meristem boundary region, highly anisotropic stresses are associated with the saddles shape geometry(Hamant *et al.*, 2008).

A simple yet classic experiment with a dandelion stem can reveal the internal stress pattern in growing plants. If you cut lengthwise the bottom of the dandelion stem curls upwards as a

Adapted from Brulé *et al.,* 2016

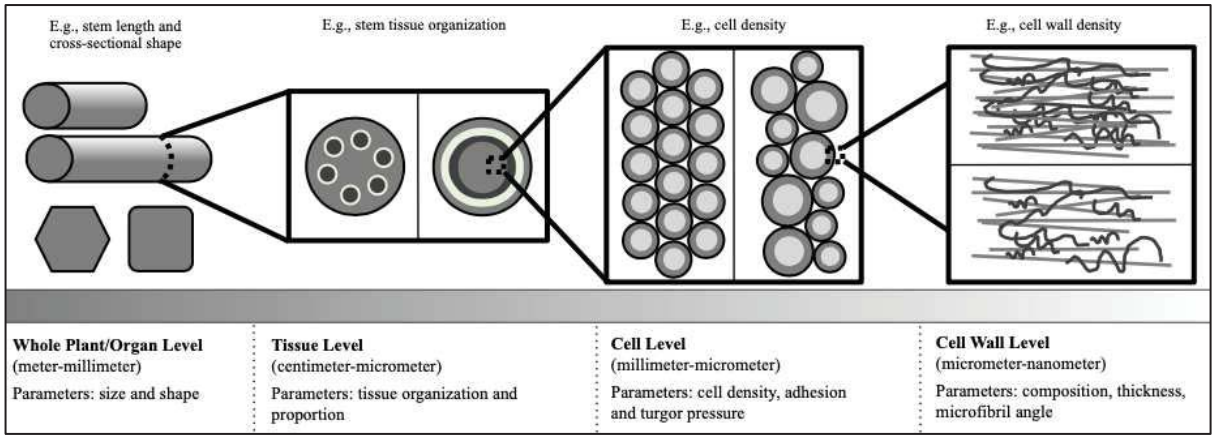

Figure 6. Plant architecture influences the mechanics at different scale of organisation

Adapted from Brulé *et al.,* (2016).

result of the release of longitudinal tension between the inner and outer tissues. This reveals the existence of a balance of forces inside the plant before the perturbation (Hamant & Traas, 2010). Similarly, after peeling, the sunflower hypocotyl epidermis contracts, meaning that it was under tension before (Kutschera & Niklas, 2007). This leads us to a pressure vessel analogy of plant tissue where a compressed mass is covered by a tensed layer (Figure 7). Decades of research suggest that the plant epidermis is under tension to balance the inner turgor pressure from the plant cells. This gives the idea to view whole plant as a big cell comparing the epidermis with cell wall (Kutschera & Niklas, 2007).

Apart from internal stress, plants are regularly subjected to external mechanical stress notably gravity and wind. This may be one of the evolutive advantage of prestressed structures: they are robust to environmental fluctuations. To compare with a pre-stressed inanimate object, suspension bridge withstands high winds because of their pre-stressed design. In a similar fashion the prestressed mechanics of plant stems would help them withstand huge force of wind.

The unit of plant architecture is the rigid plant cell encaged in a cell wall which is comparable with extracellular matrix dictating the adhesion and interaction of cells with other cells as well as with biotic/abiotic factors. Plant cells balance the exerted external forces and the generated internal forces to maintain a stable architecture. This cellular mechanics is the key to understand the modulation of cell size and shape, cell wall production, cell-cell interaction to provide mechanical support to a stable architecture and promote growth. Although single cells are not very common in plants, root hairs and pollen tubes serve as very common models to study the single cell mechanics in plants. Micro indentation technics have revealed that in pollen tubes the growing apical region has lower stiffness than the distal region (Geitmann & Ortega, 2009). Thus, the key players of mechanics in plant at the cellar level are turgor pressure and the rigid cell wall.

1.3.2. Turgor pressure

Turgor pressure is a hydrostatic force imposed by the cytoplasm to the cell wall in walled cells like plant, fungus or bacteria. Walls are typically 0.1 to 1μM thick in growing cells. This cell wall and the plasma membrane parts the outer and inner compartments with different solute concentrations thus creating a hydrostatic pressure (the wall pushing on the cell content) of osmotic origin, which in the end put the wall under tension (Cosgrove, 1993; Schopfer, 2006)

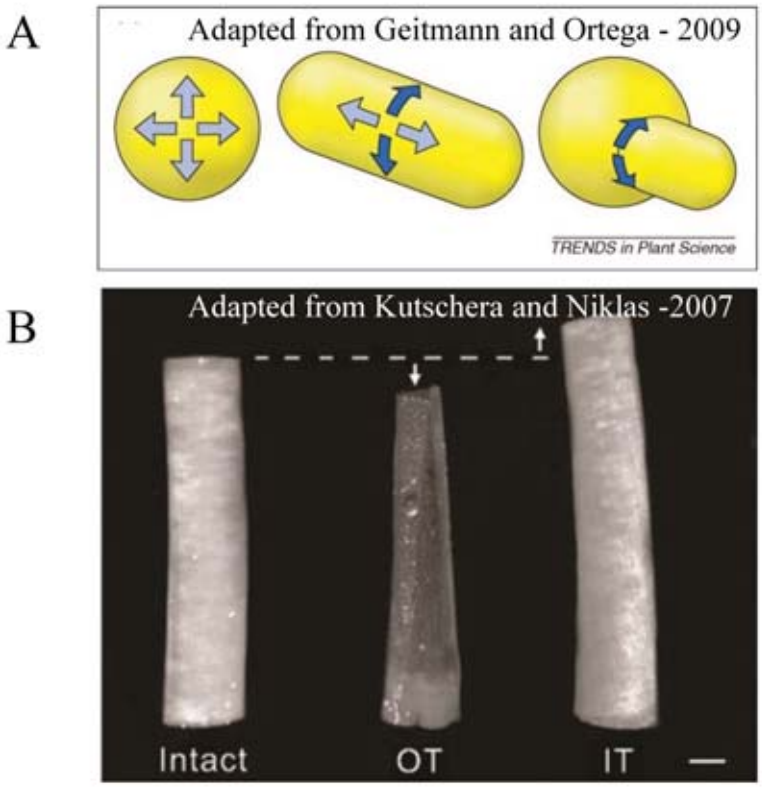

Figure 7. Pressure vessel analogy of tissue mechanics

(A) Surface stress patterns of a thin-shelled pressure vessels. Depending on the geometry of the vessel stress could be isotropic (spherical) or anisotropic (cylindrical). When a outgrowth occurs in an isotropic environment the local stress ins highest at the boundary. Adapted from Geitmann and Ortega (2009).

(B) Biological tissue which has a similar mechanic as thin walled pressure vessel. For example ,when the outer teguments (OTs) from etiolated sunflower hypocotyls are under tension whereas the inner teguments (Its) are under compression (scale bar: 1 mm) Adapted from Kutschera and Niklas (2007).

(Figure 8). In essence, turgor pressure is non-directional. However, turgor pressure can vary in intensity. When turgor pressure is high, plant maintains a state of turgidity where the hydrostatic pressure has valued many times higher than atmospheric pressure, getting as high as 3- 20 bar (0.3 MPa to 2 MPa) (Beauzamy *et al.*, 2015a,b). Turgor pressure decreases in condition of drought (which includes freezing conditions) or in presence of salts in the environment. This property is also apparent in certain developmental stages. Typically, when seeds maturate, they accumulate many osmolytes and progressively enter in life slowed. Interstingly, the same osmolytes (e.g. trehalose, proline) are present in response to drought, freezing or life slowed (Xiong *et al.*, 2002; Pareek *et al.*, 2017; Sharma *et al.*, 2019) .

By definition, turgor pressure depends on wall properties. When the wall becomes softer, water enters, the volume of the cell increases, and turgor pressure increases. The cell usually responds by mechanically reinforcing its cell wall, and turgor goes back to normal. Experimentally, it is really challenging to decouple the mechanics of turgor pressure and cell wall composition. In particular, the tensile stress would only depend on the cell wall thickness if the wall were mechanically uniform. However, the cell wall is a chemically and mechanically composite entity, and a complex active material.

1.3.3. Cell wall

The presence of walls in plant tissues named the “cell”, by analogy with the walled cells of monasteries (Hooke *et al.*, 1665). Plant cells are the mechanical unit of plant and smallest entities that build an internal hydrostatic pressure to resist osmotic pressure. The rigid cell wall confers the ability to withstand such extreme forces. Most biological processes including growth, differentiation, nutrition, immunity… depends on the cell wall.

After cell division, when the two daughter nuclei are reforming, a gel like phragmoplast is formed and serve as a scaffold for the cell plate assembly with subsequent cell wall formation separating the two daughter cells. This phragmoplast is mainly formed with pectin polymers and other components are accumulating(Cosgrove, 2005). Primary cell walls are composed of cellulose fibers embedded in matrix formed by other polysaccharides (pectin, hemicellulose) and structural proteins (Figure 9). The wall is formed in a way that it is able to stretch during growth, yet possesses an extreme tensile strength (Wolf *et al.*, 2012). Upon differentiation, secondary cell wall can form, and are characterised by higher cellulose content with long microfibrils and increased crystallinity (discussed later). At that stage, cells cannot grow

Adapted from Landrein and Hamant - 2013

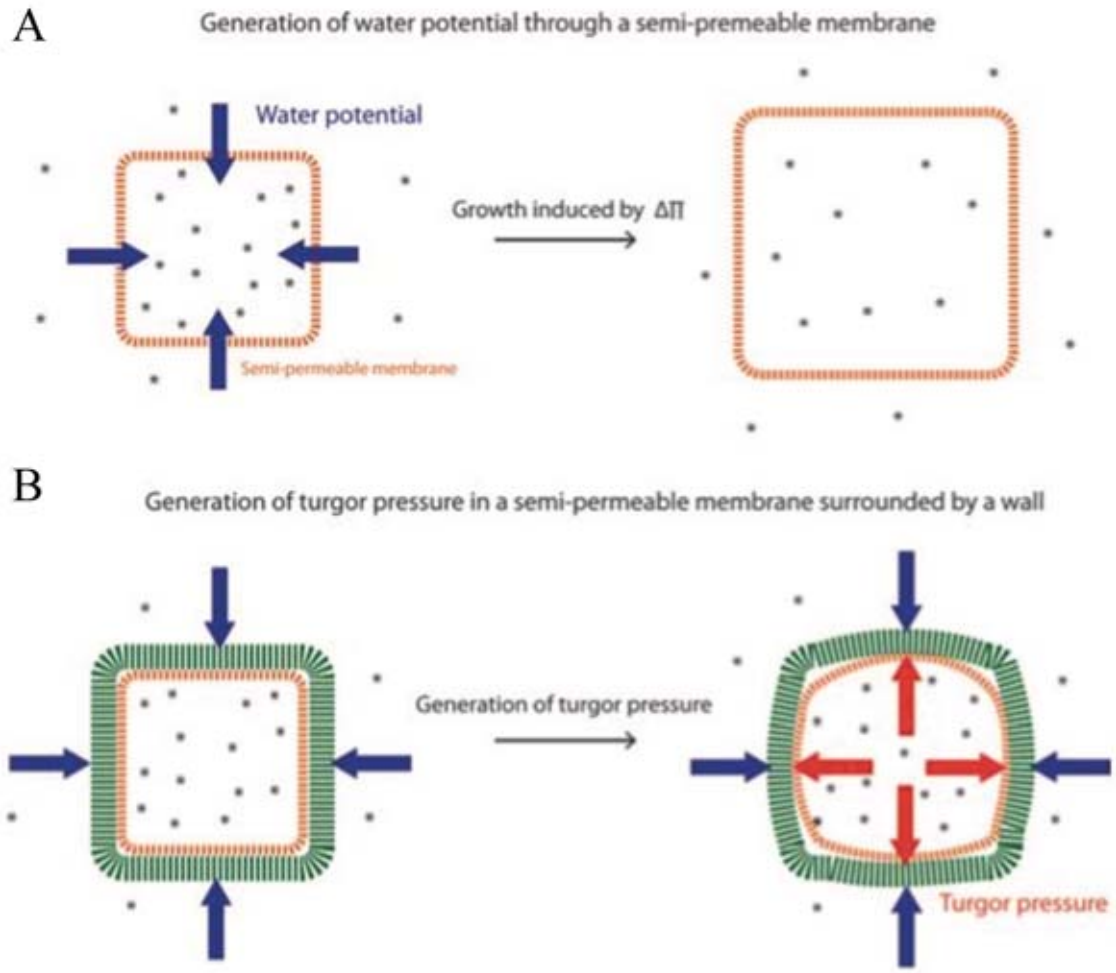

Figure 8. Turgor pressure generation in plants

(A) Higher solute concentration in one of two compartments separated by just a semipermeable membrane leads to water uptake by the compartment with higher solute concentration. Water uptake increases the volume until osmotic balance is reached.

(B) Plant cell membrane water uptake is restricted by a rigid cell wall. The difference in osmotic composition creates a constant hydrostatic pressure which corresponds to turgor pressure.

Adapted from Landrein and Hamant (2013).

anymore. Lignification is a characteristic phenomenon for the final formation of secondary cell wall. It also helps water proofing, notably in xylem vessels (Roppolo & Geldner, 2012). As the cellulose stands as the main load-bearing component of the cell wall mechanics I will discuss its features in more details.

Cellulose synthase and cellulose deposition

Cellulose forms hierarchal organisation strata contributing to the mechanical identity of the cell wall (Figure 10). Cellulose is a fibrous polymer chain of D- Glucose units linked by β-1,4-glycosidic bonds (Figure 11A). This is the most abundant biopolymer on Earth, as it constitutes the larger portion of primary and secondary cell wall. Parallel chains of 500 to 14 000 β-1,4-glucose linked by hydrogen bonds and van der Waals forces and by xyloglucans chains forms microfibrils (Figure 10). This microfibrils are 3-5 nm wide and could reach many micrometres in length. When forming bundles, they appear as a straight line in high resolution imaging (FESEM and AFM) of cell wall (Cosgrove, 2005).

Another parameter contributing towards the structural properties of cellulose is crystallite shape and size and crystallinity. Any solid matter that crystallises has their units organised in a periodic manner. In case of cellulose, depth analysis revealed two crystalline structures (called allomorphs of each other) (Figure 10): in case of plant the dominant one is Iβ with monoclinic unit cell during crystallisation, while Iα with triclinic unit cell is more abundant in primitive organisms. But cellulose microfibrils could also be present in cell wall in a non-crystallisable form, called the amorphous organisation (Rongpipi *et al.*, 2019). In higher plants the inner layer of cell wall is rich in amorphous cellulose microfibrils (Harris *et al.*, 2012). The degree of order in this organisation is referred to crystallinity which is the ratio of crystalline to crystalline plus amorphous portion of volume of cell wall. Crystallinity is an important determinant of the physical properties of the wall, such as stiffness and strength. When the crystallinity increases, it results into increased Young's modulus, tensile strength, density, and hardness (Lionetto *et al.*, 2012). Many micromechanical models of wood strength take into account this crystallinity of cellulose as well (Rongpipi *et al.*, 2019).

As the turgor pressure is isotropic, the mechanical anisotropy of the wall translates the pressure into a directional cue. This mainly depends on cellulose microfibrils orientation, and thus on their initial deposition in the cell wall. Cellulose is deposited in the cell wall by a membrane-bound protein called CELLULASE SYNTHASE (CESA). The family of genes expressing

Adapted from Cosgrove 2005

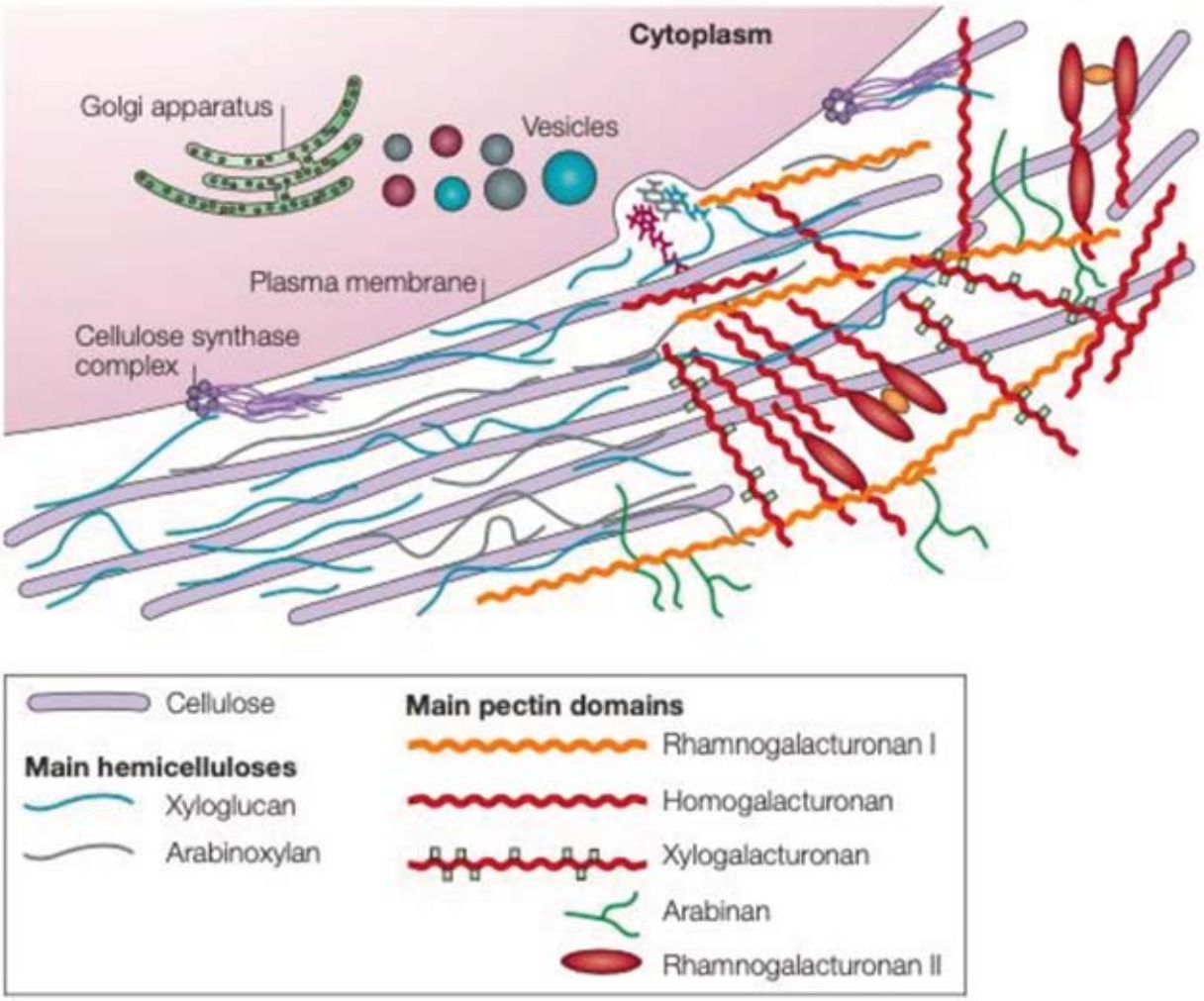

Figure 9. Components of primary cell wall in plants

Primary cell wall in plants is composed of cellulose microfibrils crosslinked with hemicellulose and embedded in a matrix made of hemicellulose and pectins. Cellulose microfibrils are synthesised by large hexameric complexes in the plasma membrane, while the hemicellulose and pectins are deposited in the cell wall after being synthesised in Golgi apparatus. Adapted from Cosgrove, (2005).

CESA was found in 1990s (Pear *et al.*, 1996) by molecular and genetic studies. In case of *Arabidopsis Thaliana* 10 CESA genes (12 for maize, 9 for rice, 8 for barley, 7 for aspen..) are found and they are differentially expressed in various tissues and cell types (Somerville, 2006; Taylor, 2008) but belongs to a big family of proteins called CELLULOSE SYNTHASE-LIKE (CSL) proteins. CESA proteins have a glycosyl transferase domain and can form dimers by two adjacent zinc fingers in the N-terminal region (Cosgrove, 2005). In case of angiosperms CESA is organised in a rosette called CELLULOSE SYNTHASE COMPLEXES (CSC) (Figure 9) made of six rosette subunits formed by six CESA subunits encoded by three different CESA genes. Different CESA subunits are put together to form the cellulose microfibrils in different types of cell wall, for example CESA1, CESA3 and CESA6 mainly contribute to primary cell wall formation whereas CSCs formed with CESA4, CESA7 and CESA8 dominate in secondary cell wall deposition (Cosgrove, 2005). The cellulose synthases proteins possess a constant rotary as well as bidirectional linear movement in the plasma membrane (Paredez, 2006). This trajectory of CSCs correlates with the cortical microtubule (CMT) but a linear movement could still occur even in the absence of that guidance though at a slower rate and for shorter distance (Chan and Coen 2020). Indeed, the microfibril arrays have a similar orientation as the CMTs but they do not immediately loose their directionality in absence of CMTs. This suggests a self-organising feature of cellulose by the forces created by polymerization and crystallization of the cellulose microfibrils where microtubules act as a scaffold provider (Emons *et al.*, 2007). It thus seems that CMTs are rather catalysing rapid changes in cellulose microfibrils orientation.

Other proteins like KORRIGAN, COBRA, KOBITO interacts with CSC and thus indirectly contribute to the physical properties of cellulose microfibrils. For example, mutation in KORRIGAN, a membrane-bound endoglucanase, results into reduced cellulose crystallinity (Nicol *et al.*, 1998). Microtubules and CSCs are connected physically via CELLULOSE SYNTHASE INTERACTING PROTEIN 1 (CS1). As microtubules contribute hugely to the mechanical stability of the plant cell this physical link is a highly intriguing point to study in the context of mechanics. In addition to cellulose microfibrils, other wall components contribute to its mechanics.

Matrix and matrix deposition

Cell wall has a composite configuration where structure, physico-chemical properties are the determinant of its mechanics (Chebli & Geitmann, 2017). Although cellulose is the primary

Adapted from Rongpipi *et al.*, 2019

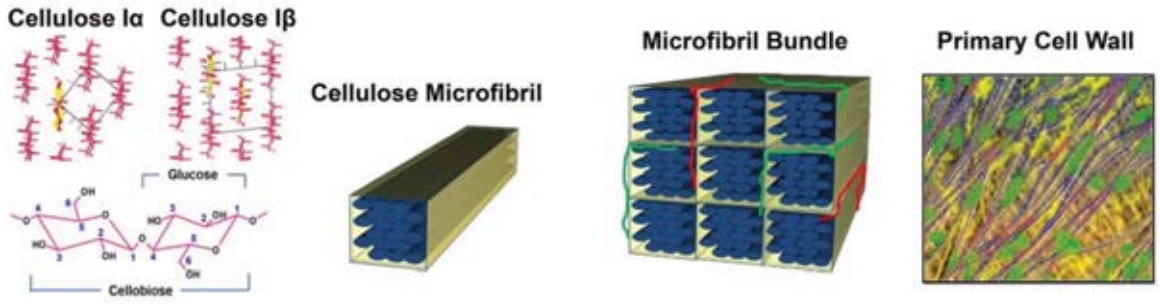

Figure 10. Hierarchies of primary cell wall formation by cellulose microfibrils

Cellulose is polymer β 1-4 D glucose. Cellulose could form two crystalline structure called cellulose Iα and Iβ . Parallel chains of cellulose forms a cellulose microfibril which forms bundles with help of matric components. Microfibrils are the lower order structure of the primary cell wall organisation and it is the main load bearing component as well. Adapted from Rongpipi *et al.*, (2019).

load bearing component in the cell wall present in both primary and secondary cell wall, cellulose is embedded in a matrix made of other polysaccharides and structural proteins. Cellulose-cellulose and cellulose-matrix interactions controls the strength and malleability of cell wall contributing to the wall mechanics (Cosgrove & Jarvis, 2012).

The current model suggests cellulose interacts with hemicellulose and they are embedded in hemicellulose-pectin matrix. The hemicellulose has similar backbone as cellulose but due to their branching and modifications they cannot form the fibrous structure like cellulose microfibrils (Figure 9). The main hemicelluloses are xyloglucan, arabinoxylan and (gluco)mannans (Figure 11B). They form crosslinks between cellulose fibres forming a network and also can sometimes act as a matrix filling substrate. The type and abundance of hemicellulose is important contributor in the mechanics of cell wall as well as their crosslinking ability with the cellulose microfibrils (Scheller & Ulvskov, 2010). Note that it has been shown that xyloglucans interact with only a small portion of the cellulose surface despite their high affinity towards cellulose (Wang *et al.*, 2012). *CELLULOSE SYNTHASE-LIKE (CSL*) proteins are responsible of the synthesis of the β-D-GLYCAN backbone of hemicelluloses. Hemicelluloses are also modified by XYLOGLUCAN ENDOTRANS GLUCOSYLASE/ HYDROLASE (XTH) family of proteins. These proteins cut and ligate glycans helping in the formation of the hemicellulose and their integration on preformed matrix. Importantly, these proteins have recently been shown to form hybrid structures between cellulose and hemicellulose. This in turn form mechanical hotspots in the walls, which are likely to be instrumental in the wall mechanics (Cosgrove, 2014).

Another important primary cell wall component is a complex and heterogenous polysaccharide called pectin (Figure 9). Quantitatively, pectin is usually the most abundant component in primary walls. For instance, in dicotyledonous plants around 35% of the cell wall dry weight is made of pectin. The major pectin elements are rhamnogalacturonan I, rhamnogalacturonan II, homogalacturonan, xylogalacturonan, apiogalacturonan, arabinan, and arabinogalactan (Figure 11C). Alternating residues of galacturonic acid and rhamnose with side branches of pectin domains forms rhamnogalacturonan I. Galacturonic acid can form linear chain homogalacturonan, whereas xylose branching occurs in xylogalacturonan. Their ability to form gel like network is reduced by blocking the carboxyl group via methyl esterification. Pectin can change their mechanical properties and in turn that of the cell wall by forming networks with variable stiffness depending on the degree of methyl-esterification. Indeed, upon

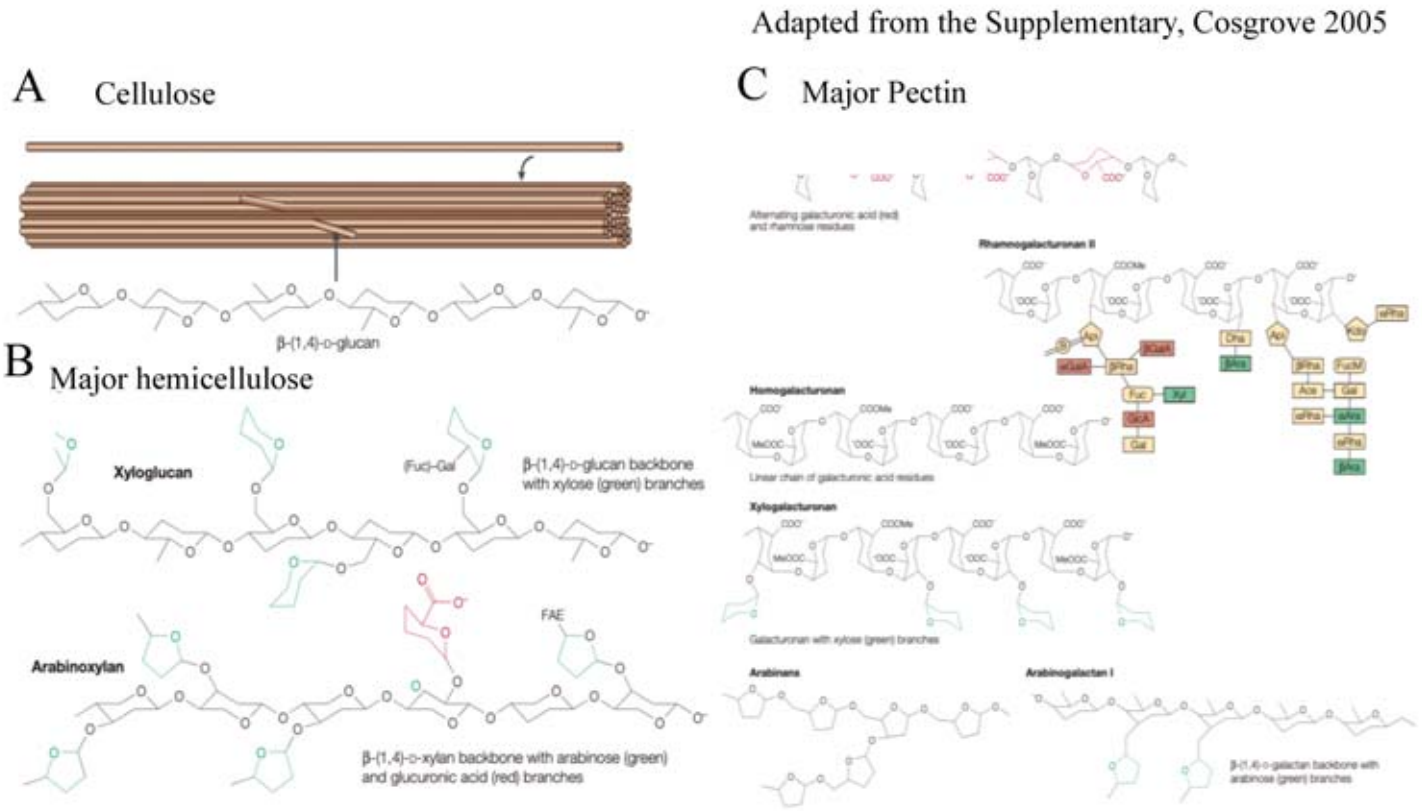

Figure 11. Different polysaccharides present in primary cell wall formation

(A) Cellulose is a β-1,4-glucose chain.
(B) Major hemicellulose component of a primary cell wall is xyloglucan and arabinoxylan polysaccharides with a backbone of β-1,4 D xylose chain.
(C) Structures of main polysaccharidic components of pectin.

Adapted from Cosgrove (2005), supplementary information.

demethylesterification, acidic pectin are either the target of pectate lyases which degrade pectin and would rather soften the cell wall. Alternatively, such acidic pectin can instantly become stiffer when chelated by calcium ions (Wolf *et al.*, 2009). Demethylesterification is mediated by Pectin Methylesterases (PME) which are tightly regulated and belong to large gene families. For example, 66 PMEs (and 64 Pectin Methylesterase inhibitor) are present in the Arabidopsis genome (Pelloux *et al.*, 2007). This allows pectin to contribute to the mechanical properties of the cell wall growing cells depending on the plant species, developmental status, type of cell with the help of varying degrees of pectin methyl esterification (Palin & Geitmann, 2012).

Although the 90% of the cell wall dry weight is made of polysaccharides, a few other proteins also contributes to the properties of the cell wall. These additional proteins help in remodelling of the cell wall, such as extensin which interacts with pectin (Lamport *et al.*, 2011; Borassi *et al.*, 2016).

As inferred above with the case of PMEs, the cell wall is also a compartment that hosts wall regulators. Beyond wall modifying enzymes, the pH-dependent expansin is one of the best studied protein in plant biology, and it would induce cell wall loosening by removing Hydrogen-bounds between cellulose and hemicellulose (Cosgrove, 2005).

1.4. Conclusion

Here I have discussed the mechanical properties of biological material. Animals and plants share similarity in the basic way of their mechanics work, yet there are huge differences in the level of magnitude of physical properties as well as proteins involved in mechanical properties. In case of plants, the high hydrostatic pressure and stiff cell wall is a major determinant of their mechanics. Thus, it becomes important to be able to measure the mechanical properties of plant cells and tissues in a robust way. In the next segment I will discuss the techniques used to measure such properties.

2. Measuring the mechanical properties of living systems

When a material encounters mechanical force, mechanical properties of the material like the stiffness and the geometry relates to the amount of force needed to produce certain deformation. To analyse the mechanical properties, stress and strain need to be considered.

2.1. Mathematical formalization: the case of elastic properties

Because forces are invisible, they can only be deduced from deformation. Conversely, to measure force, deformation or mechanical properties, one only needs to have a quantification for two of these variables. In an elastic material, if stress is imposed and strain is measured, one can deduce the slope which represents the stiffness (Young's modulus).

To articulate more mathematically, tensile or compressive stress (σ) produced by a given force (F) normal to a material of surface area (A) is

$$\sigma = F/A$$

In a particular example where a mechanically homogenous material under tensile force, and a particular dimension (length) increases from L_0 to L. This deformation is measured by the normal strain (ε) which is defined as

$$\varepsilon = (L - L_0)/L_0$$

Hooke's (observed by Robert Hooke) law for a 1D spring with a spring constant k the force (F) is measured as

$$F = - k (L- L_0)$$

Hooke's law for 3D materials for the stress (σ) to strain (ε) and Young's modulus (E) is

$$\sigma = E\varepsilon$$

By solving these equations and measuring the measurable quantities under a known force (F) in an experimental set up (which are Stress (σ) to strain (ε)) we can deduce the Young's modulus (Hamant & Traas, 2010). In next part I will discuss about the tools used to experimentally measure these quantities as minutely and as robustly as possible.

2.2. A critical view on rheometric techniques

Mechanical properties are measured by exerting stress and quantifying strain or vice versa. Depending on the samples and the resolution of the measurement needed, the suitable method is chosen. Biological materials are heterogenous, complex anisotropic samples. An extra layer of difficulty is imported with the presence of the time-dependent viscous element to the properties of the material (Parre & Geitmann, 2005; Balland *et al.*, 2005). In the last decades several technological advances have helped to get better tools to measure the mechanical properties more and more accurately.

Yet, challenges still remain in this area in the context of consistency in the results or crossing the specificity barrier (being able to apply same techniques to multiple scales). There are differences sometimes when measurement from several techniques of the same material is done. Wu *et al.,* observed in 2018 that mechanical measurement of the MCF-7 human breast cancer cells (cultured in same environmental condition) from seven different technologies are different even by two orders of magnitude (Wu *et al.*, 2018). Though the underlying principle was same, different technologies, including atomic force microscopy (AFM), magnetic twisting cytometry (MTC), particle-tracking microrheology (PTM), parallel-plate rheometry, cell monolayer rheology (CMR), and optical stretching (OS) were used. These methods differed in level of mechanical stress and speed of deformation faced by the cells, the geometry of the mechanical probe, the probe–subject contact area, the probed location on cell, and environmental factor.

It is clear that depending on the magnitude of the force and the geometry of the probe we can measure the properties of material at a global or local scale as well as various magnitude (from tissue to cell to actin fibres (Wu *et al.*, 2018).

2.3. Large scale measurements

The stiffness of a material (elasticity of elastic modulus) is quantified in a number of ways including bending, tension, compression, vibration, and acoustic excitation test. Classical tests at low spatial resolution have been used to measure the mechanical properties of organs for a long time. One of the much-studied tissue in animal is bone tissue, notably to measure its bending stiffness. Such tests are used for plant organs, and in particular in the case of branches

Adapted from Sharir *et al.,* 2008

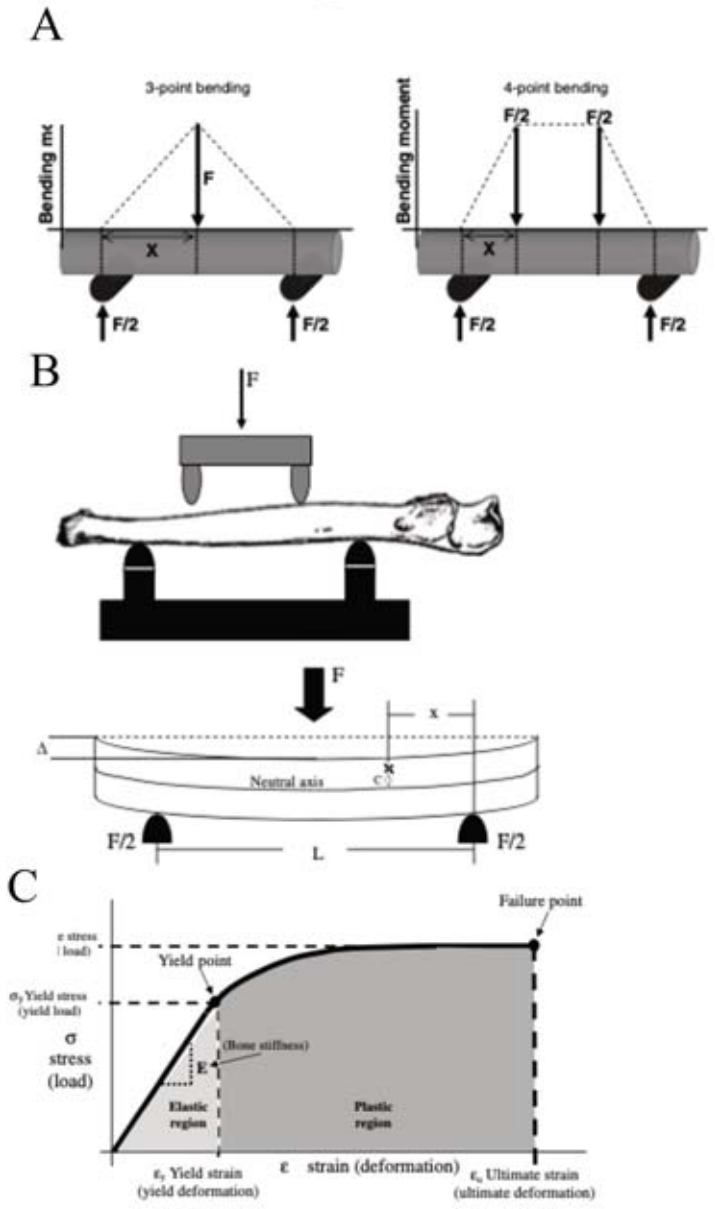

Figure 12. Bending experiment to measure mechanical properties

(A) A simple illustration of force exertion in two different types of bending experiments called 3-point bending and 4-point bending.
(B) experimental setup of the 2 different bending experiment
(C) The stress–strain curve obtained by loading a sample of compact bone in tension. E is the stiffness of the material (Young's modulus for isotropic materials).

Adapted from Sharir *et al.,* (2008).

and trees producing woods (Lindström *et al.*, 2002), stalks of sunflower or corn (İnce *et al.*, 2005; Robertson *et al.*, 2014, 2015), wheat stems (Esehaghbeygi *et al.*, 2009).

Bending tests are mostly three- or four-point tests (Figure 12A). In a classical 3-point bending test the material is positioned between two supports and the force is exerted precisely in the middle of the support via mechanical loading (Figure 12B). In the 4-point bending method the force is exerted at the 2-equidistance point from the support (Sharir *et al.*, 2008) (Figure 12B). By measuring the deflection of the material at the point of maximal force and load we can calculate the stiffness of the material via a force-deflection graph where stress and strain plotted against each other (Figure 12C). The bending test is frequently used for its simple sample preparation, low loads and readily measurable deformation (Lopez *et al.*, 2014; Robertson *et al.*, 2014) . But the drawbacks include poor spatial resolution and inaccurate Young's modulus assumption.

Another family of tests are tensile tests (Figure 13). They have been used in wood (Kretschmann, 2008) or in stems of corn (Zhang *et al.*, 2016), rice or *Arabidopsis* (Varanasi *et al.*, 2012). Most of the cases whole tissue and organs are used (McQueen-Mason *et al.*, 1992; Park & Cosgrove, 2012; Miedes *et al.*, 2013; Kim *et al.*, 2015; Saxe *et al.*, 2016). Tensile testing could be uniaxial (where the stretching is done from one side) or biaxial (Stretched on both sides). The force required for the stretching is measured and the elastic modulus is calculated. The force is applied in several ways but the most common are single application loading increasing towards rupturing of the sample or cyclic application where a smaller quantity of force is given and withdrawn repeatedly. The stress-strain curve consists of an elastic and a plastic region, where the slope of the elastic region is used to determine the elastic modulus (Figure 13A) (Young's modulus for a homogenous linear elastic material). The difficulties associated with this technique are the need to accurately position the sample according to the axis of force application, to grip the tissue to avoid slippage or damage (Figure 13B), to avoid any damage at the sample ends before and during the installation (Robinson & Kuhlemeier, 2018).

Elastic modulus could be measured by compressive force application (Figure 14). Compression testing is done in maize stalks (Al-Zube *et al.*, 2017) or in woods (Kretschmann, 2008) as well. A compressive load is applied at a particular rate to the sample and strain (deflection) is measured. The compressive elastic modulus is the slope of the linear portion for the stress-strain curve which gives the measurements for the stiffness under compressive stress.

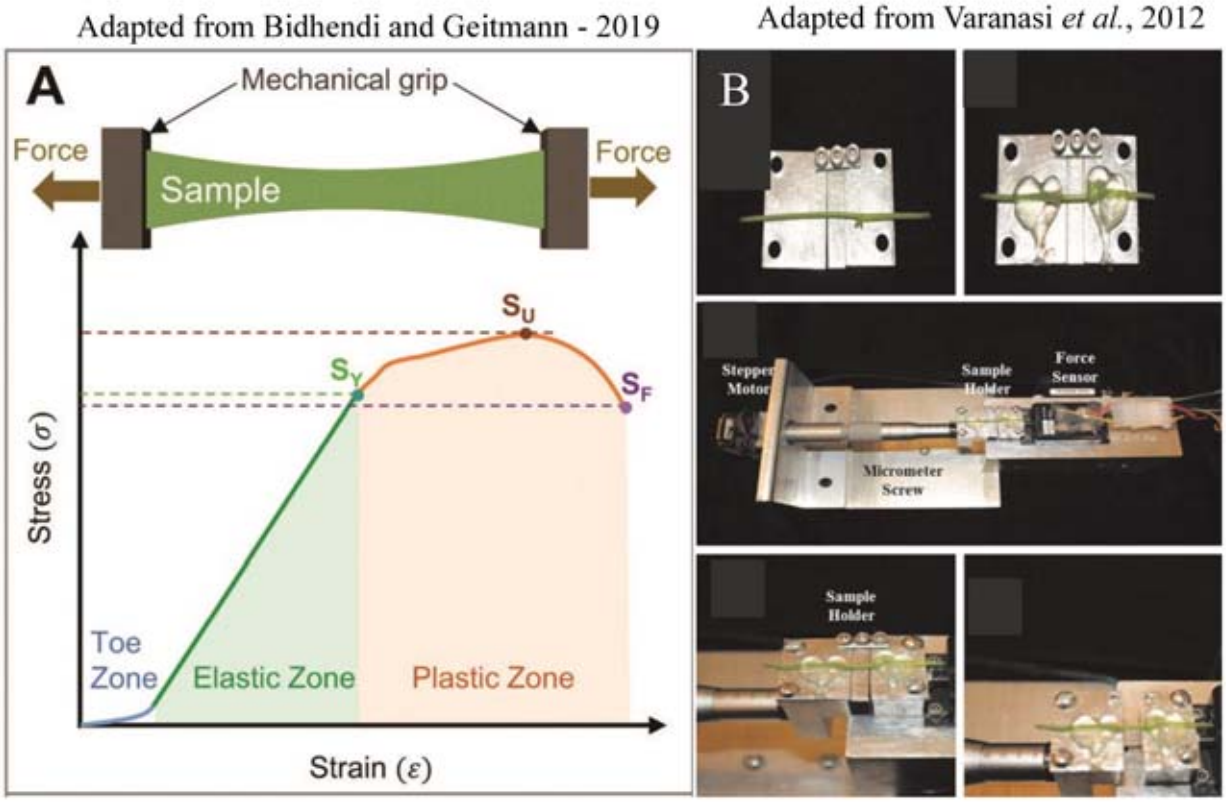

Figure 13. Experimental designing of tensing testing

(A) Illustration of a sample in a tensile testing experiment where the force could be exerted in both way and sample needs to be firmly gripped to the apparatus. The stress-strain curve to calculate the elastic modulus of a deforming sample. Adapted from Bidhendi and Geitmann (2019).

(B) Image of an actual apparatus there force is exerted by stretching in a single direction where the other end of the sample attached to the apparatus remains still. Use of glue is done to secure the attachment of the plant tissue as strongly as possible. Adapted from Varanasi *et al.,* (2012).

When the sample size reduces it becomes more challenging to use these classical measurement techniques. Fine tuning of this techniques and using other vibration of acoustic techniques are done.

2.4. Microscale measurements

At the cellular or subcellular levels, measuring mechanical property demands an ability to exert force and measure deformation at a microscopic amplitude which makes the job very challenging. Several micromanipulation techniques have been adapted to overcome such challenges. Generally the rheological behaviour (a passive mechanical measurement) is studied by micropipette aspiration (Hochmuth, 2000), magnetic twisting cytometry (Fabry *et al.*, 2001), and optical stretchers (Guck *et al.*, 2005) but the active mechanical behaviour could be studied by measuring the deformation of a compliant gel generated by traction forces of a cell (Munevar *et al.*, 2001). Whereas both the active and passive mechanical properties are studied mainly by indentation techniques as Atomic force microscopy (AFM) (Alcaraz *et al.*, 2003; Webster *et al.*, 2011) , Cellular Force microscopy (CFM) (Routier-Kierzkowska *et al.*, 2012; Felekis *et al.*, 2015) the parallel plates technique (Desprat *et al.*, 2005; Mitrossilis *et al.*, 2009) Optical tweezers (OT) (Balland *et al.*, 2005; Nussenzveig, 2018).

Micropipette aspiration is a widely used technique in the field of micromechanical manipulation. A pressure drop is generally applied via a micropipette and the edges are observed via microscopy (Figure 15A). This technique was readily used in case of single cell rheometry (Hochmuth, 2000) but then extended to the nucleus as well (Guilak *et al.*, 2000).

Another local micromechanical technique is magnetic twisting cytometry (Figure 15D). Ferrimagnetic beads coated with Arg-Gly-Asp containing peptide and bonded with integrins of a cell/nuclear surface were magnetised horizontally. Then they are twisted vertically by an external homogeneous magnetic field. This gives information about the response to the direct mechanical manipulation of cellular and subcellular components(Fabry *et al.*, 2001). Cells have been studied with the help of this techniques reveals a cytoskeletal continuum to the nucleus leading to a change in the nuclear shape via cyclic magnetic forces (Hu *et al.*, 2005).

Adapted from Al-Zube *et al.*, 2017

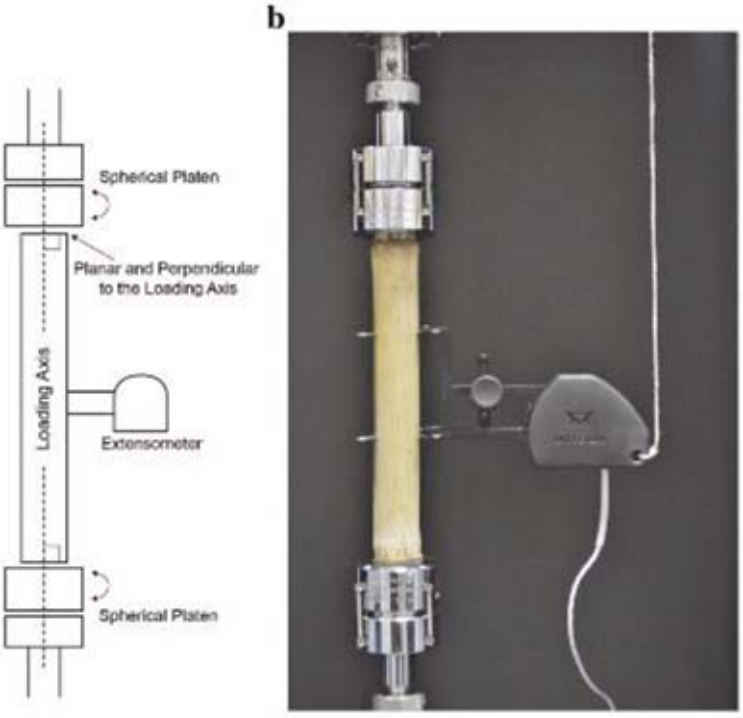

Figure 14. Compressing testing apparatus

A schematic diagram depicting geometric features of an ideal compression test and a image of a actual compressor. Adapted from Al-Zube *et al.*,(2017).

Atomic force microscopy (AFM) is an indentation technique (Figure 15C) using the principles of the scanning probe microscopy (SPM), to measure mechanical properties of a wide range of material depending on the morpho-mechanical properties of the probe and the indentation parameters. The surface of the sample is scanned by a tip jointed to the cantilever (the probe) with a radius of usually a few nanometres and detection is done via probe-sample interaction forces to generate a 3D map (Figure 16B) with a resolution of few nanometres (Bovio *et al.*, 2019). This tip can be used to apply precise force which results in a local deformation called indentation and helps to determine mechanical properties such as elastic modulus or viscoelastic properties (Figure 16A). Many other indentation techniques are presently used in varying conditions of sophistication, resolution, application able to measure forces in the range of picoNewtons and spatial resolution ranging in Ångströms. In AFM the position of a flexible cantilever attached to a rigid tip is monitored by a reflecting laser and the position change of laser in the photodiode gives the information of position change in the cantilever. Now with a cantilever of known spring constant (Figure 16B) helps to determine the force generated by the deflexion of the cantilever by the sample. Spring constant is a critical information during indentation which is calibrated by thermal tuning (Lévy & Maaloum, 2002) and by deflecting it on an infinitely stiff material. This constant needs to be carefully assessed depending on the material properties to measure: the cantilever needs to be flexible enough to deflect yet rigid enough to deform. The tip geometry (Figure 16C) directly determines the probe-sample contact surface (Figure 16D) which is an important parameter for the computational models that are used to deduce the Young's modulus. For these reasons choosing the appropriate probe with appropriate cantilever spring constant and tip geometry is hugely significant while measuring the mechanical properties of a sample. Though most indentation techniques are limited to outer layer of the material, AFM studies have been extended to inner layer as well. AFM has been used to measure cell mechanics properties of cells in culture, that are normally inside tissues. For example, when Li *et al.,* showed that cancerous MCF7 cells have lower Young's moduli compared to benign MCF-10A cells (Li *et al.*, 2008). AFM can also be used on fixed tissue section (with the drawback that only relative properties can be deduced, absolute values being highly dependent on fixation). AFM is also adapted to study the mechanics of isolated nuclei (Dahl *et al.,* 2005) but also nuclei inside cells, in animals only (Liu *et al.*, 2014; Moeendarbary & Harris, 2014).

Adapted from Fal *et al*., 2017

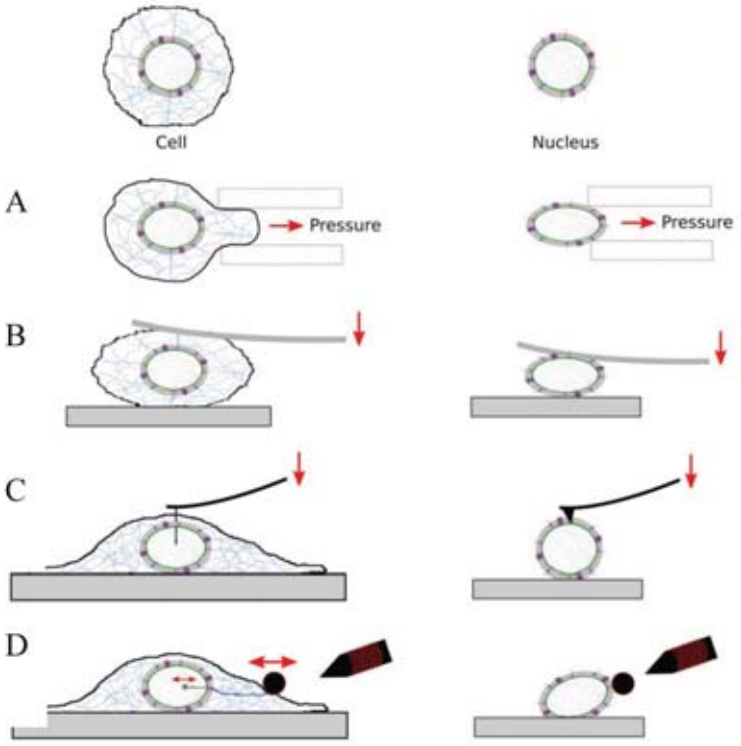

Figure 15. Different micromanipulation techniques to estimate the mechanical property at a microscopic level Cell (left) and Nucleus (right)

(A) Micropipette aspiration to measure and observe deformation at cell/nuclear level.
(B) Compression between microplates.
(C) Indentation techniques like CFM, AFM.
(D) Magnetic bead based rheometry.

Adapted from Fal et *al.,* (2017).

An alternative to AFM to obtain the global properties of the cell or the nucleus is the parallel plate techniques (Figure 15B). The basic principal of this technique is to capture the object between two parallel microplates (where one plate is flexible with a calibrated stiffness and the other plate is more than 100 times stiffer and nonflexible compared to the former) and then to apply a force to measure the deformation (Bufi *et al.*, 2015). An inverted microscope is coupled with the plates in a way that they capture the side view of the object trapped in between. This device is used to calculate Young's modulus of a biological object like cell or nucleus by calculating the change in shape with the analysis of the images recorded (Mitrossilis *et al.*, 2009).

For smaller force values, optical tweezers (OT) are vastly used as single molecular and cellular studies. Optical tweezers (Zhang & Liu, 2008) use a highly focused laser beam to trap a neutral particle and exert a precisely controlled force to manipulate the trapped particle and carry mechanical measurement in the pN range (Figure 17A). When the object is deflected from its equilibrium trapping position (the displacement of the object via the light is measured by a detector), a force is exerted to restore the position, this follows the Hooks law allowing us to measure the elastic modulus (Figure 17B). This technique is not only used to characterise the cell membrane (Nussenzveig, 2018) but also have been used for studying the mechanics of DNA even the mechanics of entire Chromosome of *Escherichia Coli* (Heller *et al.*, 2014). Magnetic tweezers can develop larger forces, and have been used to deform cells, even in the context of a living embryo (Desprat *et al.*, 2008).

2.5. Advantages and Difficulties in Plants

The interdisciplinary study of physics and botany dates back to Aristotle. The founding fathers of modern plant biomechanics are found in the 19th century, starting with Wilhem Hofmeister (Hofmeister, 1863) and several other scientists like Sachs, Kraus, Errera, Schwendener, Berthold, Thompson.

Plant biomechanics has importance not just only for crop sciences, forestry or ecological reasons but from a fundamental scientific understanding of living systems. Mechanics of trees with woody and non-woody was studied with the help of applied mechanical engineering and compared with hydrostatic living tissues. The mechanistic view of plants resisting breakage, of being penetrated by pathogens, and herbivory can be studied under the light of already

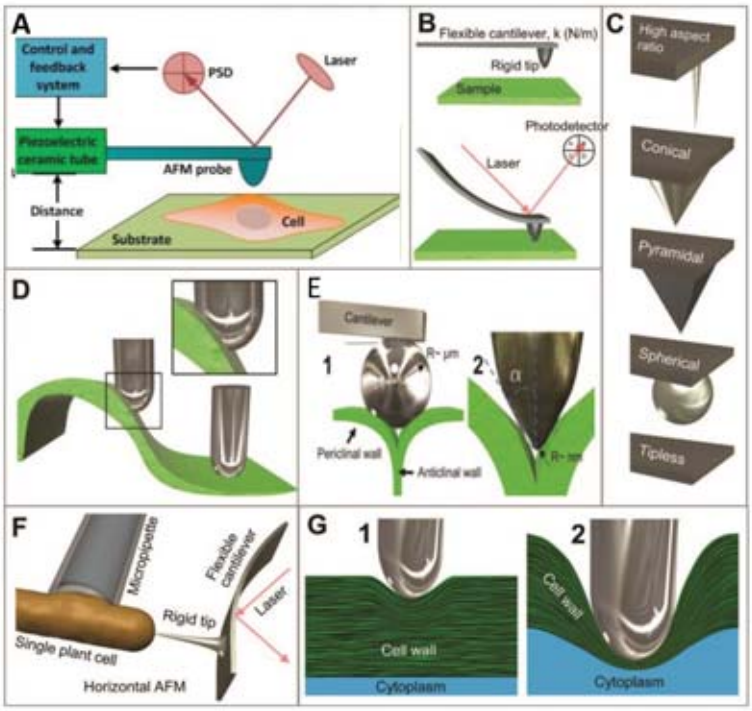

Figure 16. Representation of AFM set up and principle of measurement

(A) Principle of AFM. The piezoelectric ceramic tube drives the AFM probe move vertically to maintain a constant interaction force between sample surface and AFM tip. The interaction force is detected by a laser reflected off the backside of the cantilever. Adapted from Li *et al,.* (2017).

(B) Force measurement and topographical imaging in a typical cantilever-based indentation system as in common AFMs. Forces arising due to proximity of or contact between the rigid tip and the sample result in the bending of the flexible cantilever. Changes in direction of the laser beam reflected off the surface of the cantilever allow measurement of forces, based on the bending of the cantilever of a known spring constant (k). Adapted from Bidhendi and Geitmann (2019).

(C) Great variability exists between indenter tip geometries, sizes, and aspect ratios. Size and geometry of tips affect the force measurement and topographical imaging artefacts. Adapted from Bidhendi and Geitmann (2019).

(D) Tip geometry and curvature of the specimen influence the contact quality and therefore the measured forces. Adapted from Bidhendi and Geitmann (2019).

(E) Effect of fine topographical features of the cell such as cell borders. With a (1) large probe, the probing tip of the indenter may not come into contact with the cell border, and access deep trenches. Further, the deformation may not be limited only to the target structure being investigated. (2) A sharper probe tip enables studying the finer cellular features. In either case, the tip of the probe may or may not reach the deep valleys between the cells. Reinforcement by vertical anticlinal walls may contribute to the 'sensed' stiffness. Adapted from Bidhendi and Geitmann (2019).

(F) Horizontal AFM set-up to probe perpendicularly to the highly curved regions of a single plant cell. The cell may be immobilized by exertion of a negative pressure via a micropipette.

(G) The depth of the indentation determines to what extent the inner layers of a single wall and the turgor pressure contribute to the measured forces. Adapted from Bidhendi and Geitmann (2019).

established physical concepts of fracture mechanics and the concept of toughness whereas fluid mechanics helped to model the water flow by non-living xylem tissue (Moulia, 2013).

Although concepts were already studied in the 19th century (see e.g. Errera, 1886 and the comparison between plant cells and soap bubbles), the experimental study of plant biomechanics at the cellular and subcellular scale is more recent. The micromanipulation techniques widely used in animal cell including micropipette aspiration or magnetic twisting are not used to study the cellular mechanics of plants. This is a result of the presence of a non-deformable wall as well as the fact that a huge amount of force would be needed to manipulate plant cells due to their high wall stiffness and turgor pressure. Paul Green has been a pioneer in the experimental investigation of plant cells from the 1960s onwards, notably developing the pressure probe (Green, 1968). Cell wall anisotropy leading to a heterogenous mechanics is an important part of plant developmental mechanism and on the other hand it is another barrier on the way of success of rheometric techniques. Plant protoplasts are spheroid structures devoid of cell walls could be used as a system for studying single cell mechanics. Several studies have taken advantage of this system, for instance to analyse the impact of centrifugal forces on the plant cytoskeleton (Wymer *et al.*, 1996). The protoplast system has also been studied with the parallel plate technique to measure mechanical properties: Durand-Smet *et al.,* showed that the plant protoplasts have surprisingly similar behaviour as the animal cells where as they are three order of magnitude (1000 times) softer than that of walled plant cells (Milani *et al.*, 2011). These leads to the conclusion that plant cells needs a tailored approach in the context of mechanical studies.

2.6. Advancement in plants

Plant tissue and cells have different mechanics but they are clearly mechano-reactives. There are several developments towards using micromechanical techniques suited for the needs to study plant biomechanics.

Indentation based techniques are widely used in plant tissue and cell wall. Milani *et al.,* showed with the help of AFM and combining fluorescence microscopy that the shoot apical meristem tip has stiff cell wall compared to flanking regions (Milani *et al.*, 2011). The role of cell wall modifying enzymes (expansin) to modify cell wall mechanics via changing the crosslinking polymer has been studied by combining AFM and field-emission scanning electron microscopy (FESEM) (Marga *et al.*, 2005). Pollen tube is a highly investigated system using indentation to

Adapted from Nussenzveig - 2018

A

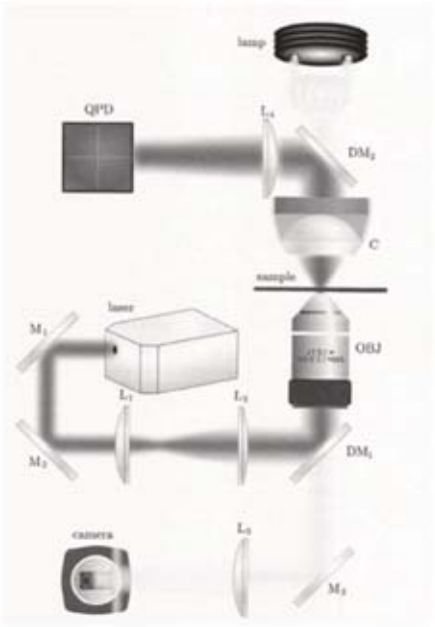

B

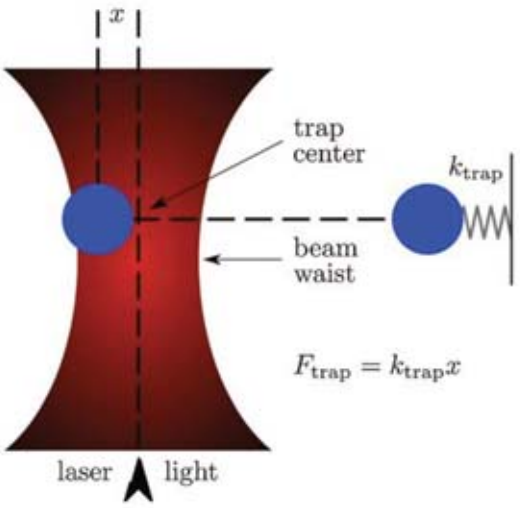

Figure 17. Generic optical tweezers instrument set up and principal mechanism

(A) A highly focused leaser beam is focused on a sample after passing through a upright microscope objective to trap a particle in the sample holder. An independent visible light beam from another light source make the visualisation at real time possible.

(B) Trap restoring force F_{trap} for small object displacements x is measured to determine the mechanical properties of the sample.

Adapted from Nussenzveig (2018).

understand the mechanics leading to its interesting growth phenotype and the role of cell wall mechanics behind it (Parre & Geitmann, 2005). Peaucelle *et al.,* used AFM indentation to show the role of pectin dimethyl transferase regulating cell wall mechanics and growth (Peaucelle *et al.*, 2015). Despite these studies a robust protocol applicable to cells from varying location delivering reproducible and absolute values remains challenging.

One of the biggest issues in measuring the mechanics of plant cells *in situ* is the topography of the sample (Figure 16E). This curvature of the tissue may lead to errors. Measurements are thus usually taken in the flattest portions of the tissue and cells (Peaucelle *et al.*, 2015). Tip growing cells possess a huge curvature making it difficult to study by conventional AFM setup. A 90° rotation of a conventional AFM makes the cantilever perpendicular to the region of interest (Figure 16F). These kinds of set up have been described (Ounkomol *et al.*, 2009) where the plant cells need to be hold perpendicularly for example by microfluidic system (Nezhad *et al.*, 2013) or by using micropipette.

Interestingly, depending on the indentation depth AFM includes information about only the outer cell wall (shallow indentation), turgor pressure (deeper indentation) or even deeper tissue properties (AFM tomography) (Figure 16G). Bovio *et al.,* showed that by appropriate analysis of single indentation curves, the measurement for cell wall elasticity and turgor pressure could be done (Bovio *et al.*, 2019).

Although the inherent cell wall anisotropy is neglected and an average of elastic modulus is calculated by indentation techniques, there is often underestimation of Young's modulus when compared to tensile testing (Bidhendi & Geitmann, 2019). Tensile testing at cellular level has been used to measure the mechanics of a whole cell. Several sample handling problems and the discrepancy between the stress pattern generated and the *in vivo* ones, result into scarce use of this test to determine mechanical property at cellular level.

2.7. Conclusion

Different tools used to study the mechanical properties of material have been adapted to the study of plant mechanics as well. Classical tests have been able to study the properties of plant material at a macroscopic level. At a microscopic level with the help of microscopy several micromanipulation techniques have been developed, adjusted and successfully used according to characteristics of the plant cells. Studying these properties in different growth conditions

help to investigate the changes in these properties, and is the first step to understand and quantify the origin of mechanical stress in tissues. Changes in mechanics generates mechanical signal and also simultaneously mechanical forces brings changes in mechanics. This means that cells are active systems. How they perceive and transduce such mechanical signals is the focus of the next section.

3. Forces as instructive cues: mechanotransduction

The relationship between mechanical force and biological processes is both universal and ubiquitous. Physical forces shape the form and function of living organism either by exogenous forces from the environment or the endogenous forces. Organisms have developed elaborate mechanism not only to passively respond to such forces, but also to use them as instructive signals. In animals, mechanical forces are implicated in most biological processes, such as posture control, bone or muscle formation, or stem cell differentiation.

Plants are also able to sense mechanical forces. For example, in *Arabidopsis* plants, if they are touched and brushed regularly (10 passes per day) they become shorter, in a process called thigmomorphogenesis (Jensen *et al.*, 2017) (Figure 18). Basically, plant cells translate an elastic deformation (either through touch or wind) into a plastic response (stiffer walls, and reduced growth;(Braam, 2004).

Like animals, plants also respond to the forces associated with their own shape and growth: deformation, stretching and/or compression during plant development will generate mechanical stress, and the perception of such cues can impact morphogenesis in a feedback loop. The Shoot Apical Meristem has become a model system to study the link between growth and mechanical cues. The central zone of the SAM has an isotropic elastic (or visco elastic) strain pattern related to its dome shape. In contrast, tissue invagination and differential growth at the organ-meristem boundary region prescribes anisotropic stresses (Robinson *et al.*, 2013). Several molecular targets (microtubules, PIN1 auxin efflux carriers, phospholipids, gene expression) have been shown to respond to such cues, in turn contributing to SAM function and shape.

Internal forces can also take part in shaping the trees and regulating their functions. Thus, plants maintain their upright position by sensing their own body mass. Vertical stress produced by the weight of an upright stem will stimulate cambial activity to balance radial growth. For example, in a recent study by Alonso-Serra et al., showed that radial growth is controlled by mechanical stimulus generated by change in vertical loading (Alonso-Serra *et al.*, 2020).

These external or internal stimuli need to reach tissue and cellular level to be able to activate the responses.

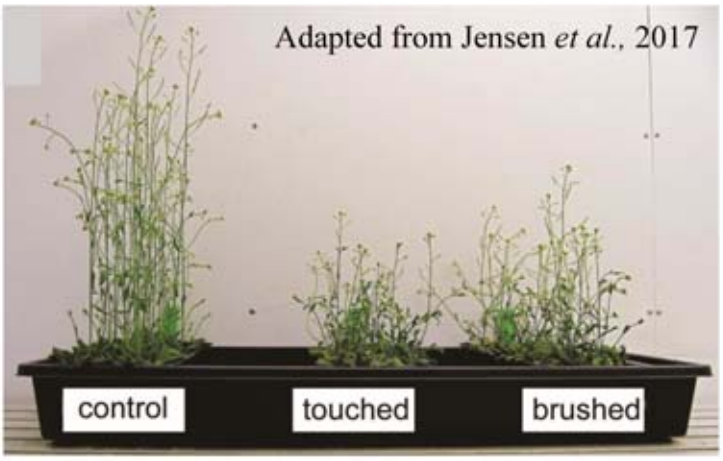

Figure 18. Response of plants to mechanical stimuli

Arabidopsis seedings become shorter after 10 days of hand touching or touching with paintbrush (10 times per day) and they retain this morphological change induced by touch signalling until senescence (Plastic). Adapted from Jensen *et al.,* (2017).

3.1. Propagation of forces across the tissue

Because plant cells are glued to each other, forces can propagate across several cell files. In particular, there is increasing evidence that the epidermis is under tension in plant aerial tissues (Figure 19A). Hofmeister showed in a very early work in this field that the epidermis of the growing plant tissue is under tension due to the elongation of the inner layers which was later supported with direct measurement of the tensile forces on the epidermal peel (Hofmeister, 1863) and later described as Kutschera's "epidermal-growth-control hypothesis". In other words, inner tissues of the stem would be the motor of growth, while the epidermis would resist and limit it (Kutschera & Niklas, 2007).

More recently, a genetic approach was used to reveal this tension and deduce the associated patterns in tissues. Plant cells are connected via the middle lamella, a pectin rich structure maintaining the plant cells together. Defects in pectin synthesis result in cell-cell adhesion defects as observed in *quasimodo1 (qua1)* plants. *QUA1* encodes a glycosyltransferase that is required for pectin synthesis and cell adhesion (Mouille *et al.*, 2007). Verger *et al*., used the gaping pattern in *qua1* aerial organs to deduce the tensile stress pattern in these tissues, while also showing that epidermal continuity is required for the supracellular cytoskeletal response to stress (Figure 19B) (Verger *et al.,* 2018).

Interestingly, many epithelia are also under tension in animal systems, and cell-cell adhesion has been shown to be promoted by such forces, while allowing their propagation across the tissue (Galletti *et al.*, 2016).

Cells are the units of multicellular organisms. To understand how the mechanical forces are sensed and used at organ and tissue level we need to understand the mechanical force propagation inside the cells.

3.2. Mechanotransduction at the cell cortex

Mechanical signals have many instructive roles in cellular processes. Each cell is able to sense their physical environment and respond accordingly. Mechanical forces propagate inside the cell, either directly through the mechanical deformation of structural elements of the cells, and/or indirectly through a relay via biochemical cascades. Both relate to mechanotransduction. Here I will discuss some the key players enabling mechanotransduction.

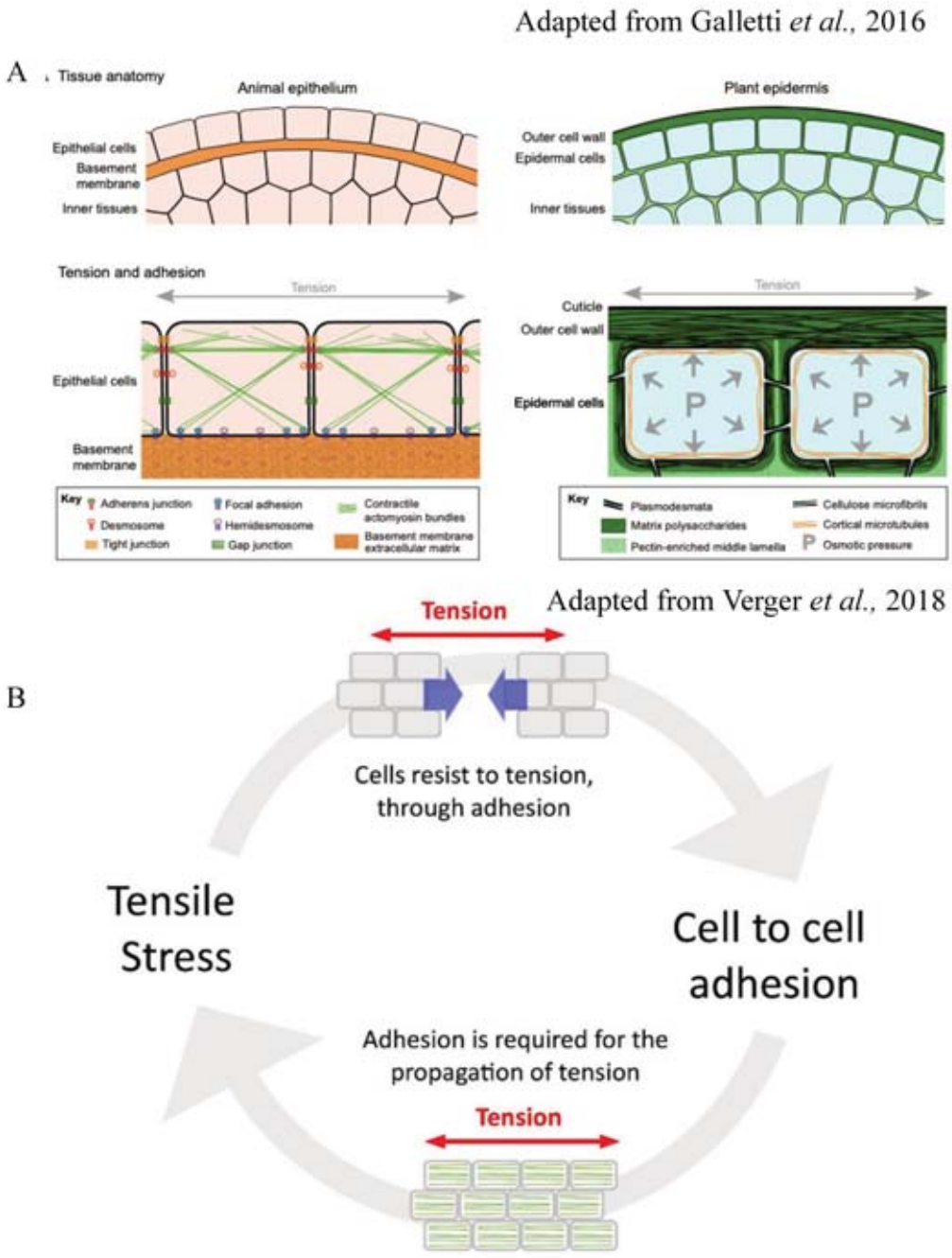

Figure 19. Tissue under tension

(A) Demonstration of the stress in tissue by taking epidermal tissue as example. In both cases epidermis in under tension generated by internal structures. Epidermal cells are tightly regulated via cell architecture and cell-cell adhesion. Adapted from Galletti *et al.,* (2016).

(B) Schematic representation of the relationship between tensile stress and cell to cell adhesion in the epidermis. Tensile stress pulls the cells apart while cell to cell adhesion is required to allow the normal propagation of tensile stress in the epidermis. Adapted from Verger *et al.,* (2018).

3.2.1. Wall mechanosensing

Cell wall being the outermost component of a cell, takes part in the molecular process of mechanotransduction in plants. Cell wall itself can act as a mechanosensor and triggers downstream signalling. For example, calcium-dependent changes in cell wall pectate chemistry are sensitive to the tension present in the cell wall (isolated from *Chara corallina*). Ladder like antiparallel chains of homogalacturonan (poly-α-(1–4)-D-galacturonate) creates an "eggbox" like structure sustaining Ca^{2+} via coordination bond. Upon a threshold of stretch (e.g. by extending the wall), these chains are distorted and break the structure holding this Ca^{2+} leading to cell wall loosening (Figure 2 - molecule). This newly generated Ca^{2+} only be chelated by newly supplied pectate in turn causing the change in mechanical property of the wall (Proseus & Boyer, 2007). Recently Haas *et al.,* showed that homogalacturonan nanofilaments can expand independent of turgor pressure upon demethylation in the anticlinal walls of pavement cells. The change between the quaternary formation of methylated homogalacturonan (three screw symmetry helical chains arranged on a hexagonal lattice) to demethylated homogalacturonan (rectangular lattic) promotes radial swelling and axial contraction in these cells helping in maturation of the shape (Haas *et al.*, 2020).

Cell wall can also sequester signalling molecules (beyond calcium) which can directly interact with plasma membrane or soluble molecules could be released upon mechanical stress. Plasma membrane harbours receptors for signalling peptides like Rapid Alkalinisation Factor (RALF) peptides that are trapped in cell wall by non-covalent bond (Mecchia *et al.*, 2017). Mechanical signalling induces stress or strain of the wall may able to release these peptides and transduce the signal forward (Ackermann & Stanislas, 2020).

The cell wall is physically attached to the plasma membrane. Even during plasmolysis, the plant cell wall is firmly attached to the plasma membrane via 'Hechtian Strands' – a structure visualised almost 100 years back which may act as a hub for cell wall integrity sensing(Yoneda *et al.*, 2020).

Interestingly, in animal cells, discrete multiprotein complexes form in the area where the plasma membrane is in contact with the stiff surface namely the Focal Adhesion (FA) sites serving as a nexus for the cell-ECM force transmission (Figure 20). FA is the active mediator of mechanical cues from extracellular milieu to the intracellular cytoskeleton. For that, it builds a complex multicomponent structure with a transmembrane and intracellular part

Adapted from Martino *et al.*, 2018

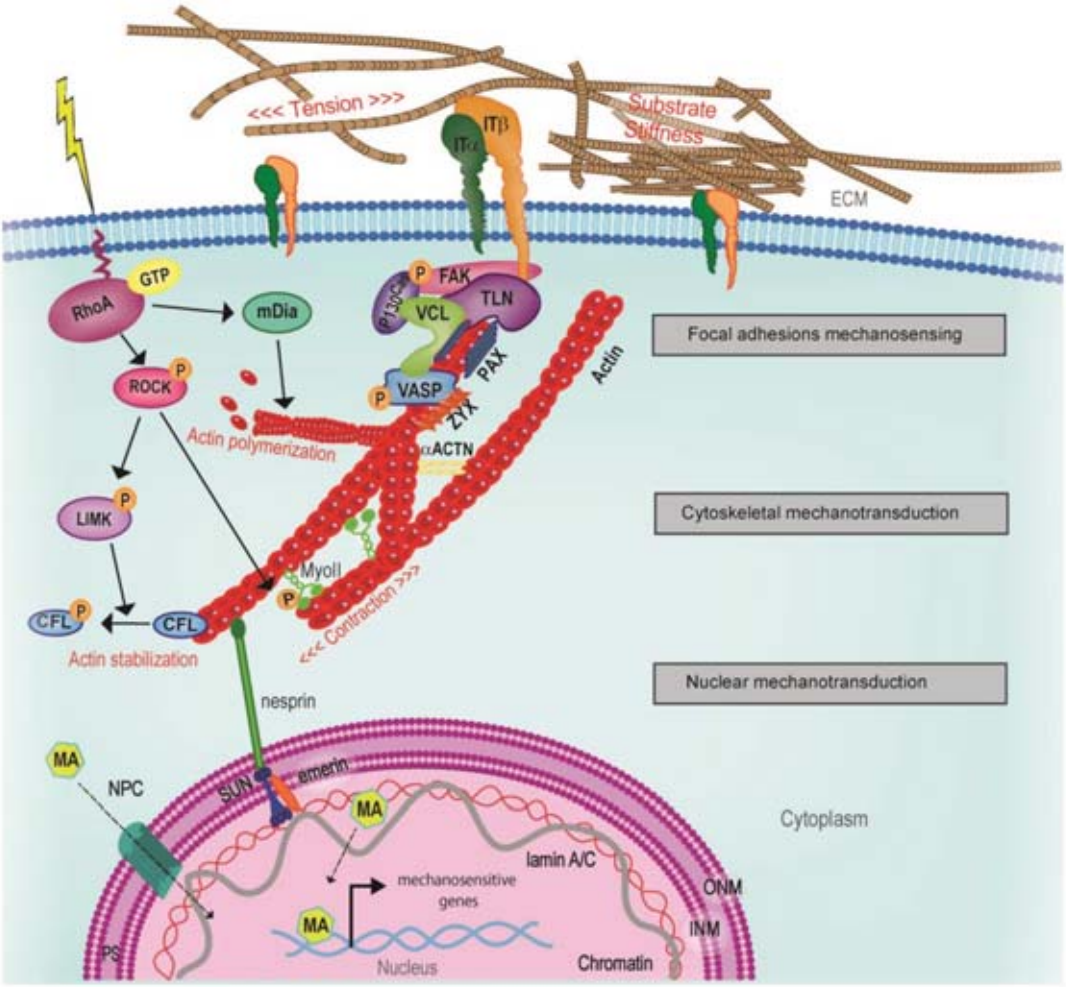

Figure 20. Animal cell mechanotransduction pathway

Schematic illustration of the cellular mechanoresponsive elements and there interactions have been done in a single animal cell.

(ACTN, actinin; CFL, cofilin; FAK, focal adhesion kinase; INM, inner nuclear membrane; IT, integrin; LIMK, LIM kinase; mDia, Diaphanous-related formin-1; MyoII, myosin II; NPC, nuclear pore complex; ONM, outer nuclear membrane; PAX, paxillin; PS, perinuclear space; ROCK, Rho-associated protein kinase; TLN, talin; VASP, vasodilator-stimulated phosphoprotein; ZYX, zyxin.)

Adapted from Martino *et al.*, (2018).

where some of the components are mechanosensitive but others play role in the signal transduction. The composition of the FA depends on the tissue and cellular context, dictated by the ECM composition and mechanics. A size proportionate tension generation by FA was proved to be directly correlated with the amount of cytoskeletal and signalling proteins recruited at these multiprotein complexes (Goffin *et al.*, 2006). Whether plant cells have an homolog of such sites, beyond Hechatian's strands, remains to be investigated.

3.2.2. Mechanosensing at the plasma membrane

The plasma membrane contributes to mechanosensing through its composition and physical properties and through the factors it hosts, such as mechanosensitive channels, transporters and receptors (Figure 21).

Direct sensing of force should be mediated by conformational changes of components in cell wall and being sensed by the downstream receptor proteins. As the appropriate structural integrity of the cell is linked to maintaining cell plasticity, plant cell has developped elaborate mechanisms to sense any damage and neutralise it. This is called cell wall integrity maintenance signalling (Bacete & Hamann, 2020). In the model plant *Arabidopsis*, several receptor-like kinases (RLK) are involved in such process which generally consists of an extracellular domain to sense the cell wall stress, central transmembrane domain, and an intracellular kinase domain for downstream signalling (Ackermann & Stanislas, 2020). They form the biggest gene family in *Arabidopsis* (600 genes) with notable roles of wall-associated kinases (WAKS) and the *Catharanthus roseus* RLK family (crRLKs). WAKS are able to interact with pectin in a Ca^{2+}-dependent way (Decreux & Messiaen, 2005). Recent studies have revealed detailed involvement of two of the seventeen crRLKs namely THESEUS1 (THE1) and FERONIA (FER) in this pathway. Shih *et al.,* showed the role of FER in [Ca^{2+}] signalling during mechanical strain on plant and how *Arabidopsis fer* mutants become impaired in mechanical aspects of growth (Shih *et al.*, 2014). FER could have important role in sensing cell wall composition as the extracellular domain of FER binds with the dimethyl-esterified homogalacturonan, a major structural domain of pectin *in vitro*. Indeed, in absence of FER cells loses the shape and integrity in Arabidopsis root. FER helps in mechanical balancing of the cell wall integrity after salt stress (Feng *et al.*, 2018).

Adapted from Ackermann and Stanislas , 2020

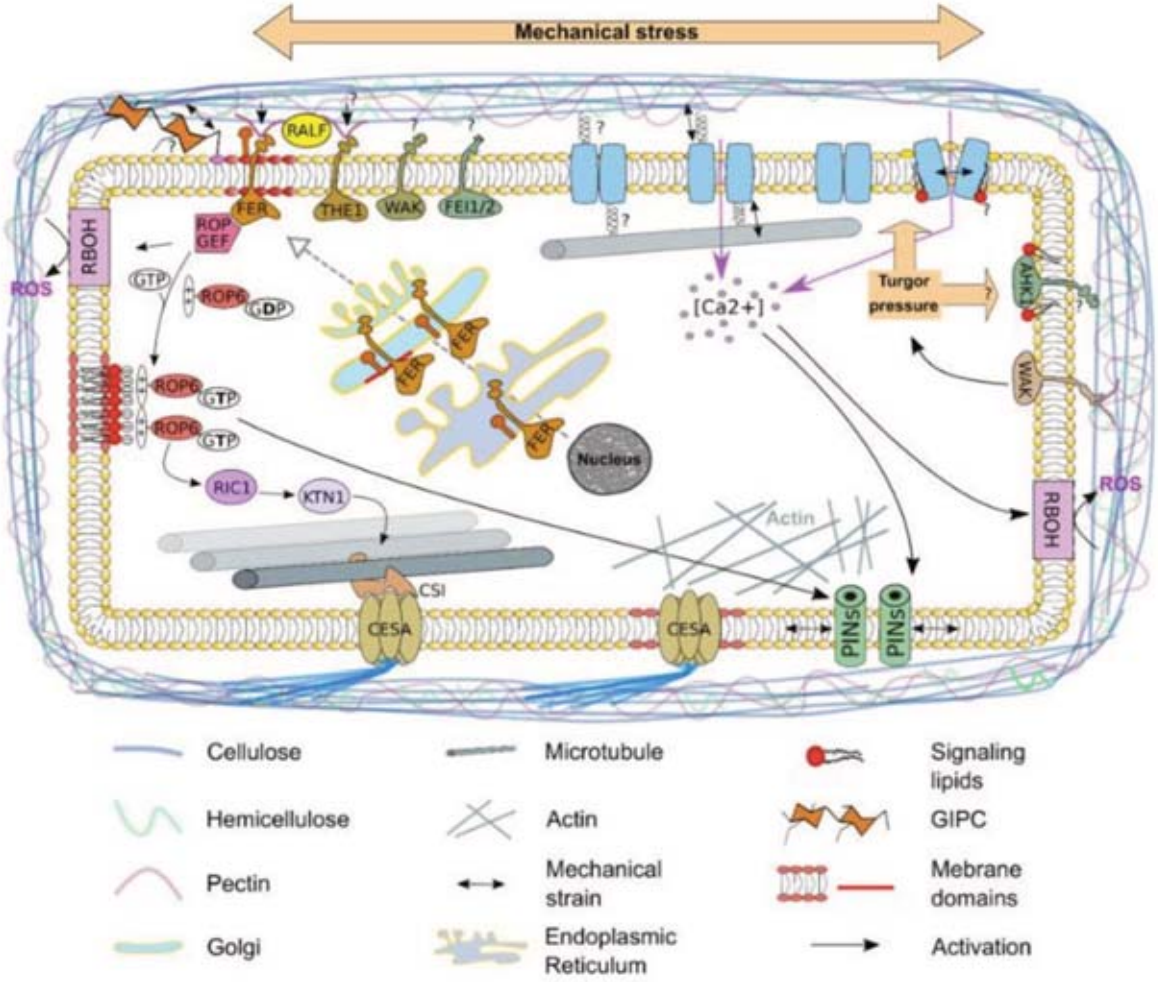

Figure 21. Role of the plasma membrane in mechano-sensing

Mechanical stress can modify the composition and/or organization of the cell wall. This may be perceived by transmembrane receptor kinases such as FERONIA (FER), THESEUS1 (THE1), WALL-ASSOCIATED KINASE (WAK) and FEI1 - FEI2 receptor-like kinases. Selective opening of stretch- activated channels can open when a mechanical tension is pulling them or by a modification of the membrane tension, that may be regulated by the membrane curvature and a specific lipid composition of the plasma membrane. Adapted from Ackermann and Stanislas, (2020).

Analogs of such mechanosensors exist in animal cells too, providing point of comparison with plant mechnosensing. In particular, the extra cellular domains of integrins directly contact the ECM (RGD motifs in fibronectins, that are unmasked after stretching the ECM) and the intracellular domain interacts with the cytoskeleton via the core of FA. The core of FA is formed by a number of docking proteins. The affinity of integrins towards the ECM can be manipulated by mechanical stimuli (Chen *et al.*, 2012) leading to the formation of the FA (Oria *et al.*, 2017; Strohmeyer *et al.*, 2017). Integrins also play important role in forming the balance between cell own mechanical state and the mechanical force coming from exterior which is highly dependent on equilibrium of β3 and β1 integrins (Milloud *et al.*, 2017). The diversity in the structure and composition of integrins make them as the basement for cellular mechanosensing. FA core as well contributes in the process of mechanosensing by changing composition. For example, in presence of force a FA core molecule Talin interacts with its partner protein Vinculin more readily helps to propagate the deformation to the actin cytoskeleton.

Another way of mechanical signals to act on a cell is via the mechanosensitive ion channels (Figure 22). When the lipid bilayer is challenged by large anisotropic force it changes the conformation of these channels where the mechanical force is a direct gating stimulus, allowing ions to pass depending on the present ion gradient. Within a few milliseconds the mechanical stimuli changes into electrochemical signal. MS channels show huge diversity depending on the organisms.

Mechanosensitive ion channels take part in a range of physiological phenomenon in plants like the hyper-osmotic and hypo-osmotic stress, gravity perception, vibration, touch pollen tube growth etc (Peyronnet *et al.*, 2014). 5 types of MS channels have been identified in the context of mechano signalling (Hamant & Haswell, 2017) namely MscS-like (MSL), Mid1-Complementing Activity (MCA), Reduced Hyperosmolality Induced Ca^{2+} Increase (OSCA), two-pore potassium (TPKand Piezo ion channels (Figure 23). Among the 10 MSL ion channels localised at the plasma membrane, MSL9 and MSL 10 has been shown to genetically regulate mechanosensitive ion channel activity (Haswell *et al.*, 2008; Maksaev & Haswell, 2012). Ca^{2+} signalling is interlinked with mechanical signalling. Absence of MCA1 and MCA2 (stretch activated Ca^{2+} channels) leads to *Arabidopsis* roots impaired in touch signalling (Nakagawa *et al.*, 2007).

Adapted from Monshausen and Haswell - 2013

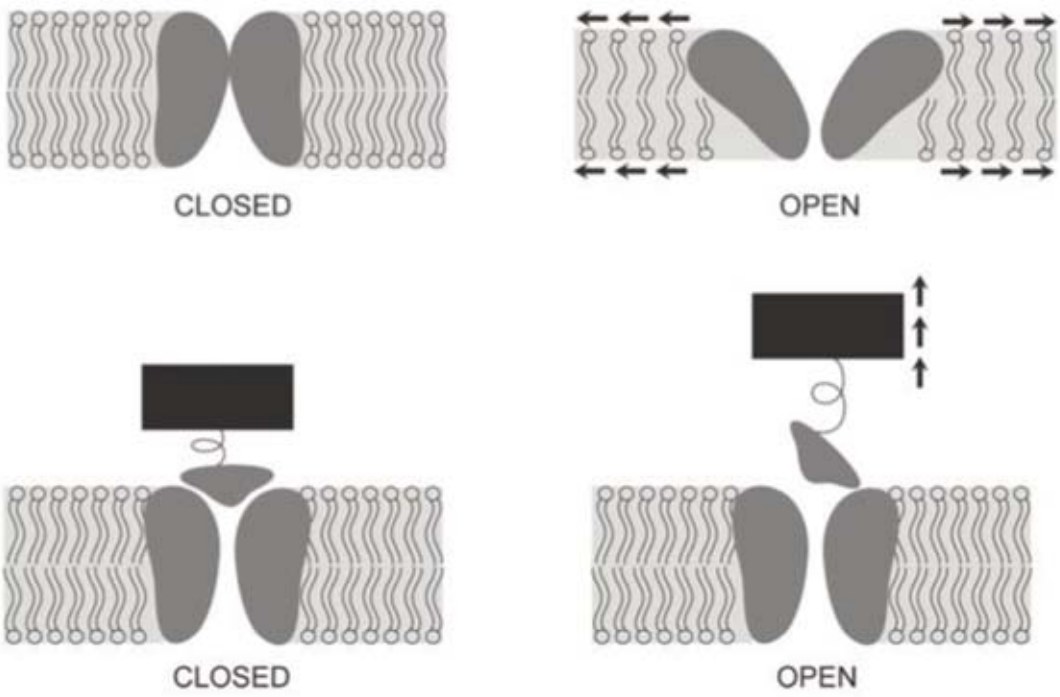

Figure 22. Simplified illustration of mechanosensitive ion channels

Mechano sensitive ion channels could directly open in response to the physical stress on plasma membrane leading to membrane tension or membrane thinning. Opening of ion channels could also be achieved by opening of a 'trapdoor' domain which is in turn bound with other mechanoresponsive element inside the cell (like cytoskeleton). Adapted from Monshausen and Haswell, (2013).

In contrast to RLKs, MS channels are more conserved across kingdoms. For instance, MscL (MS channel Large conductance) and MscS (Small conductance) are found in bacteria. Similarly, Piezo channels are found in all Eukaryotes, and have a key role in animal development. The role of Piezo in plants remains to be investigated, although downstream factors, such as calpain, have been involved in mechanosensing in both kingdoms (Tran *et al.*, 2017).

These mechanosensing factors are also integrated: RLKs and MS channels can work in synergy. For instance, the sensitivity of Piezo could be increased 10 fold by adding the ECM molecules like collagen, whereas actin cross-linker filamin A is able to decrease the sensitivity. This postulates a scenario where the ECM, ion channels, cytoskeleton act together during mechanotransduction (Cox *et al.*, 2019).

3.2.3. Cortical cytoskeleton

Upon wall digestion, the rheology of the protoplast depends on the balance between osmotic pressure and the cortical microtubules. Indeed, upon wall digestion and microtubule digestion, the protoplast inflates (Durand-Smet *et al.*, 2014). Beyond this direct structural role, cortical microtubules in plant cells mainly control the mechanical properties of the wall through cellulose deposition.

Microtubule are the primary cytoskeletal protein in plants. It is organised in B type hollow cylinder (approximately 24 nm in diameter) of 13 protofilaments, where each filament is made of longitudinal heterodimers of α- and β-tubulin monomers interacting with other α- and β monomers respectively (Hashimoto, 2015). In interphase, the microtubule arrays are organised beneath the plasma membrane as Cortical microtubule (CMT) array anchored to the membrane (mechanism not yet fully understood) with occasional cross-bridging (Barton *et al.*, 2008). The Cellulose Synthase Complex A (CESA) located in plasma membrane is guided by CMTs and attached CMTs via Cellulose Synthase Interacting 1 (CSI1) protein (Paredez, 2006) (Figure 24 A-B). In this way CMTs influence the deposition of Cellulose microfibrils which in turn controls the directionality under tensile stress and determining the cell shape. CMT dynamics and orientation depends on the stress pattern: CMTs usually align with the direction of maximal tensile stress, either in intact tissues or after mechanical perturbations. This response involves self-organization processes. In particular, the severing of microtubule promotes such self-organization, and catalyse the CMT alignement with stress (Uyttewaal *et al.*, 2012). MT

Adapted from Hamant and Haswell - 2017

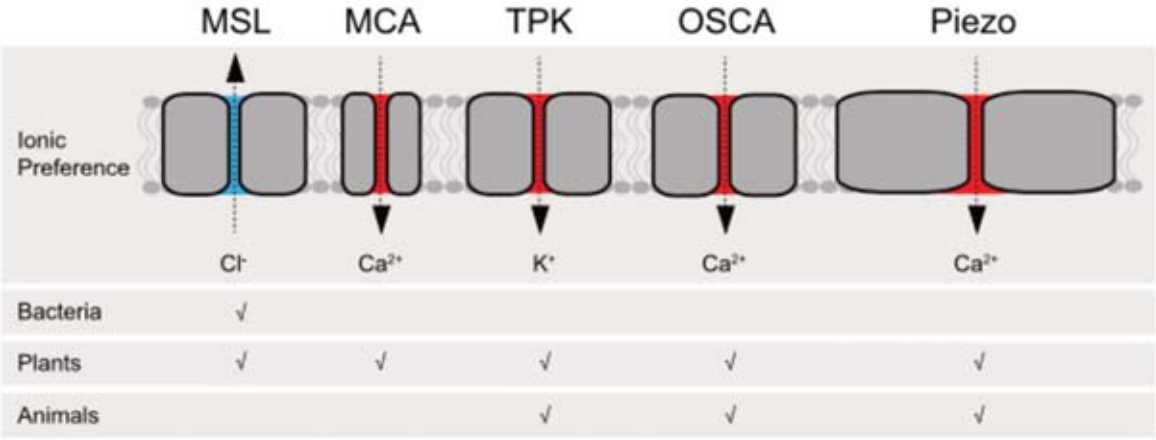

Figure 23. Mechanosensing by ion channels in plasma membrane

Families of likely plant mechanosensitive ion channels. From left to right: MscS-like (MSL), Mid1-Complementing Activity (MCA), Two Pore Potassium (TPK), Reduced hyperosmolality-induced [Ca2+] increase (OSCA), and Piezo channel families, with their proposed primary ion permeability. The presence of homologs in bacterial, plant, and/or animal genomes is indicated with a checkmark. The predominant ion flux is shown for each channel, but for simplicity no directionality nor specificity is shown .

Adapted from Adapted from Hamant and Haswell (2017).

nucleation occurs at the cortex but MT initiation from the nuclear surface may also control CMT organization in *A. thaliana,* showing connection between nucleus and cortex (Ambrose & Wasteneys, 2014).

In animals, the cell cortex is richer in actin filaments. Interestingly, actin filaments have also been shown to align with maximal tension. F-actin bundles and myosin II crosslinked (with the help of actinin, filamin etc) to form the stress fibers (SF). Actin contractibility via motor protein myosin II ensures the cellular contractibility. Stress fibers transmit the mechanical force from ECM via FAs to the inside of the cell but also in the vice versa in case of "inside-out signalling" (Cramer *et al.*, 1997; Pellegrin & Mellor, 2007; Naumanen *et al.*, 2008). A unique structure made of actomyosin is surrounding the nucleus called perinuclear cap which directly connects the nuclear membrane with FA in animals (Kim *et al.*, 2012; Shiu *et al.*, 2018). FA can reinforce SF stabilisation, for example zyxilin determines the SF stabilisation during mechanical loading. On the other hand, SF also modulate FA composition for example vinculin loading under force. Actin severing protein cofilin is another major mechanosensing molecule, in an activated dephosphorylated form, it cuts the F-actin chain making them vulnerable to depolymerisation. But mechanical stimulation promotes phosphorylation of cofilin leading to stabilisation of the cytoskeleton (Martino *et al.*, 2018).

Stress fiber is directly link with microtubules – the stiffest cytoskeletal component. Microtubule mediates biological processes such as intracellular trafficking, mitotic spindle formation, cell polarity. In response to mechanical force in dividing cells mitotic spindle have been shown to be aligned parallelly to the force (Martino *et al.*, 2018).

Depending on the nucleation and depolymerisation of actin and MT networks with the help of crosslinker proteins cell can generate force and create mechanical identity of the cell which can be transferred to outside of the cell via FA complex.

Plants has substantially different mechanical property compared to animal contributed by the fact that osmotic pressure in animal cells is in the kPa range while turgor pressure in the MPa range in case of plants. Several molecular players have been identified in plants and mechanical force has been shown to regulate processes at subcellular level. But it is still a matter of great uncertainty that how these highly pressurised cells relay the information of the force from out the cell to nucleus via the cytoplasm.

Adapted from Landrein and Hamant, 2013

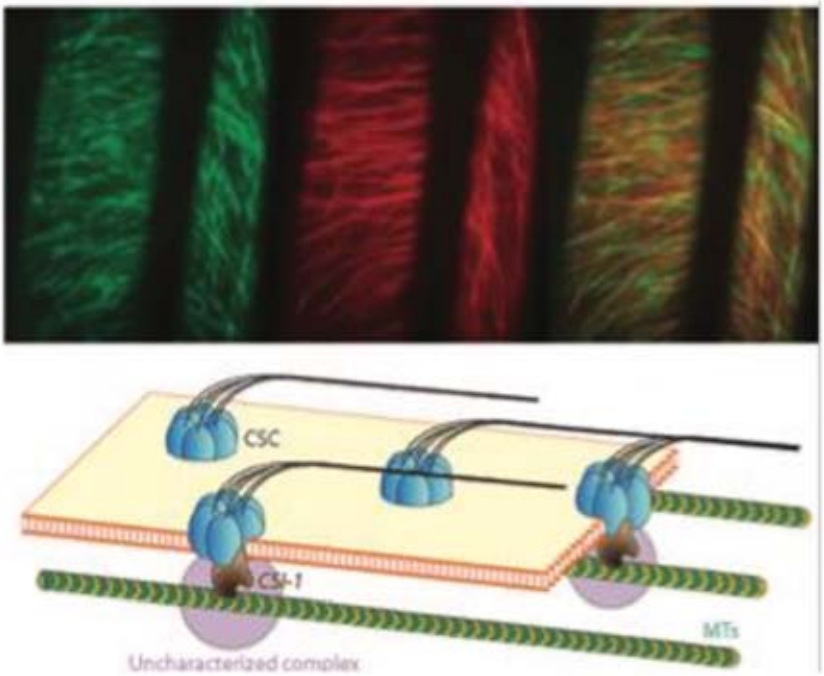

Figure 24. Cellulose deposition is corelated with cortical microtubules

(A) Cortical microtubules colocalises with the cellulose synthesis trajectory. Cellulose synthase complex is illuminated with YFP-CESA6 (green) and the microtubule is tagged with CFP-TUA1 (red).
(B) Simple illustration of how cellulose microfibrils deposition by cellulose synthase complex (CSC) is guided by cortical microtubule where the cellulose synthase interacting protein 1 (CSI 1).

Adapted from Landrein and Hamant (2013).

3.3. The cell response to osmotic stress as a form of mechanotransduction

3.3.1. Definition: Osmotic stress

When two compartments are separated by semipermeable membrane, water diffuses to the compartment with higher solute concentration until the two compartment reaches same solute concentration, and the phenomenon is called osmosis. In presence of hypertonic solution (hyper-osmotic stress) outside the cell, water is lost from inside the cell causing plasmolysis (in animals cell shrivel, in plants plasma membrane are detached from the cell wall), whereas hypo-osmotic stress leads to water intake and cell swelling (in animals and in plants (Figure 25). There are two main ways to manage osmotic stresses: osmoregulation (either through osmolyte management or through compartmentalization (e.g. the animal body is most often a close to iso-osmotic environment) and resistance (e.g. in walled organisms, like bacteria, fungi and plants (Hyskova & Ryslava, 2018) (Figure 8). All living organisms use both strategies to manage osmotic stresses.

Plants cells are able to actively regulate the osmotic pressure by synthesising osmolytes or they are passively regulated by changes in extracellular solute concentration. This passive strategy is in the core of the key response when they are exposed to salt, drought, freezing or heat stress (Conde *et al.*, 2011). Although precise interactions of cellular mechanics, turgor pressure and osmosis are not well elucidated yet, increasing or decreasing the solute concentration on either side of the plant cell, or vacuole (major accumulator of water in plant cells), water uptake and cell wall elasticity will directly affect turgor pressure.

This change in pressure creates a force on the membrane and is called osmotic stress which has a mechanical component. Changes in cell wall property upon osmotic stress may be indirect e.g. through the activation of H^+-ATPases which generate higher pH in the extracellular compartment leading to wall loosening and Ca^{2+} intake. This consequently activates reactive oxygen species (ROS) production in the apoplast such as H_2O_2, which will activate peroxidases inducing cell wall stiffening. In anyway, these changes will collide with the cell mechanics by manipulating main contributors of cell mechanics – cell wall and the turgor pressure (Ackermann & Stanislas, 2020). The ion channels facilitating such solute exchanges are modified by the mechanical stress generated by a physiological mechanical force -the osmotic stress.

Adapted from Campbell and Reece - 2008

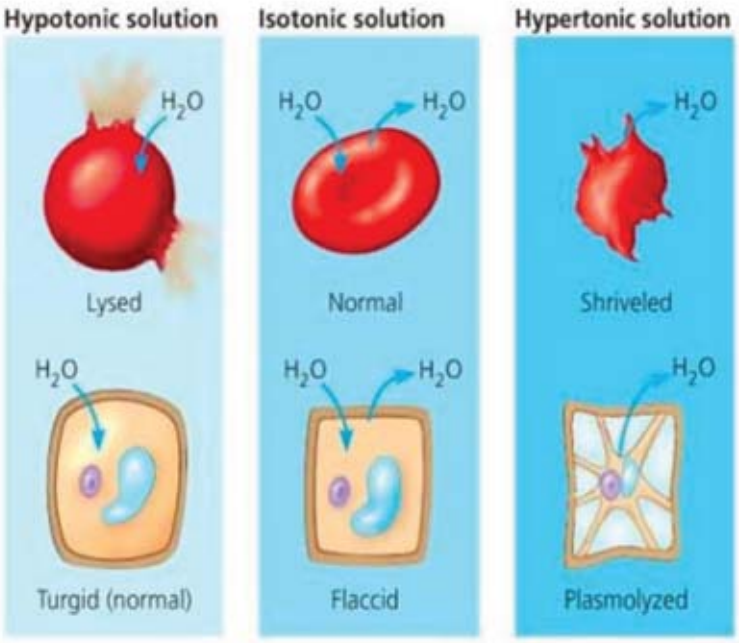

Figure 25. Osmotic stress in single cell

Living cells responses to different osmotic stress. An animal cell is highly sensitive towards osmotic changes where as a plant cell encased by wall has complex response to osmotic imbalance. Hyper osmotic tress leads to shrinkage of cell. Hypoosmotic stress in animal leads to the lysis of cell where as plant cell has cell wall to protect them from such lysis leading to build up of huge hydrostatic pressure.

Adapted from Campbell and Reece, (2008).

3.3.2. Osmosensing and signalling pathway

In yeast, two main osmosensors are histidine kinase SLN1(Synthetic Lethal of n-end rule 1) and SHO1, which signal the HOG (high osmolarity glycerol response) MAPK pathway. Due to their sessile life, plants have evolved osmo-sensory pathways (Figure 26), since plants need constant presence of water for their biological processes from organism to cellular levels (ie , maintenance of turgor). In plants, osmotic stress may be sensed in part by transmembrane protein kinases and by stretch-activated channels. Indeed SLN1 homolog ATHK1 can act as stress sensor and transduces the signal to downstream MAPK pathway (Wohlbach *et al.*, 2008) but it seems not proven as a key osmosensor (Kumar *et al.*, 2013). Others putative osmosensors in plant are, the histidine kinase cytokinin response 1 (Cre1) which is regulated in a similar way as SLN1 by turgor pressure (Reiser *et al.*, 2003) and the mechanosensitive ion channel, like reduced hyper osmolarity-induced $[Ca^{2+}]_i$ increase (OSCA 1)- which is activated by hyperosmolarity (Yuan *et al.*, 2014). Membrane tension and mechanosensitive ion channel activation (tension in membrane never have been correlated with channel closure) link osmotic and mechano-signalling. Finally, the receptor like kinases act as osmosensing in plants via sensing the cell wall modifications (Haswell & Verslues, 2015). After osmosensing, plants transfer the signal and respond by producing protective proteins or stress regulating gene expression. Many of these pathways are regulated by Abscisic Acid (ABA) (Verslues & Juenger, 2011; Christmann *et al.*, 2013). Downstream osmotic sensing, MAPK signalling pathway is activated, through protein phosphorylation and protein/protein interaction. In *Arabidopsis*, AtMEKK1, AtMPK3, AtMPK4 and AtMPK6 are activated (Conde *et al.*, 2011).

3.3.3. Hyperosmotic stress

Hyperosmotic stress is a common phenomenon encountered by plants when water availability in the plant environment is less (drought stress) and leads to higher solute concentration. It induces ABA-related stress response, with the production of protective proteins like dehydrins or accumulation of compatible solutes like proline. Hyperosmotic stress may also be induced by higher solute concentration outside cell leading to plasmolysis of the cell for example, when treating plants with low molecular weight solutes like mannitol, NaCl. These solutes can enter cell wall and induce detachment of plasma membrane from cell wall. However, when cells are treated with long polymer like polyethylene glycol or when the soil dries both the cell wall and the plasma membrane shrinks together leading to cytorrhysis. These two mechanisms show

Adapted from Haswell and Verslues - 2015

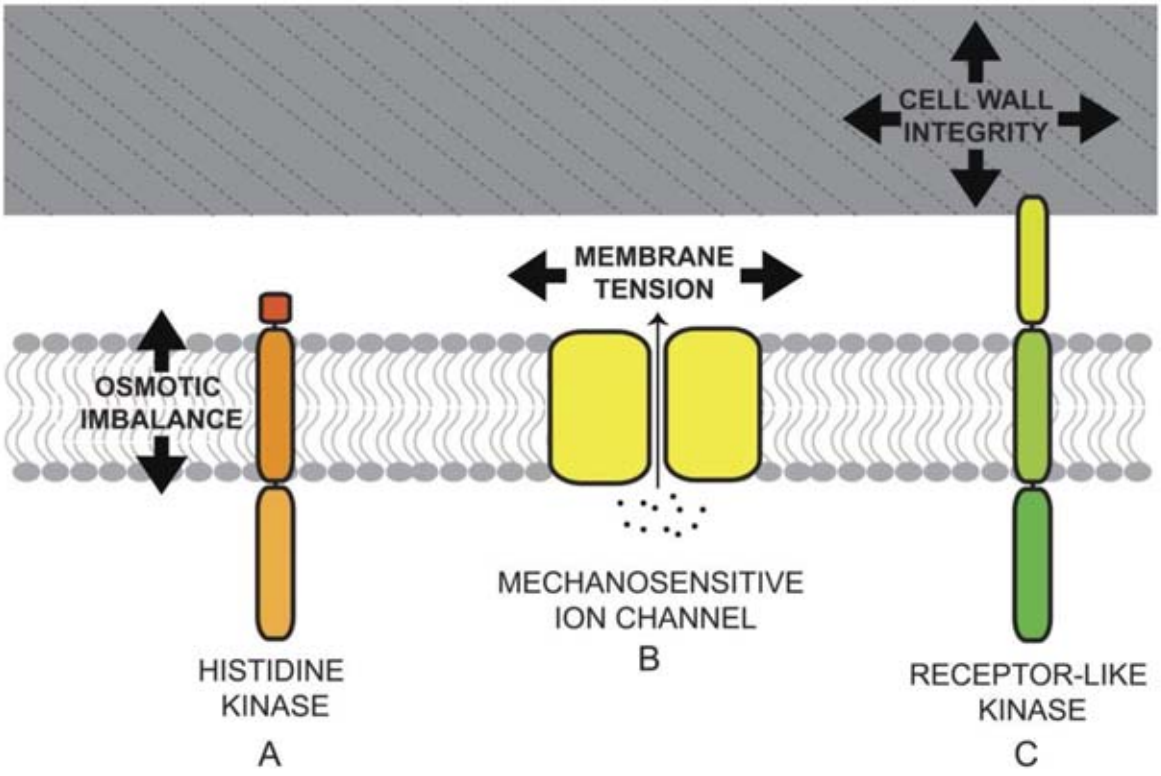

Figure 26. Potential osmosensing mechanisms in plant cells

(A) Histidine kinases could be activated by osmotic imbalance across the plasma membrane, initiating a signal transduction pathway similar to the high osmolarity glycerol response 1 pathway in *Saccharomyces cerevisiae*.

(B) Ion channels that are opened in response to planar membrane tension or membrane bending could respond to both protoplast swelling or shrinking. The release of ions in response to hypoosmotic swelling would be similar to the MscS/MscL "osmotic release valve" paradigm in *Escherichia coli*. In addition, the entry of Ca2+ through an opened MS ion channel could have downstream signaling properties.

(C) Cell wall integrity-monitoring mechanisms could involve receptor-like kinases with extracellular domains capable of sensing the movement or disruption of cell wall components. The cell wall is presented as a gray box. The plasma membrane is represented as a bilayer of gray lipid molecules.

Adapted from Haswell and Verslues , (2015).

different downstream effects and may be sensed by different modules (Haswell & Verslues, 2015).

Hyperosmotic stress creates a pressure and induces other signalling molecules which could affect the intracellular organelles and molecules. One highly studied organelle is nucleus which has the chromatin inside. In plants hyper osmotic stress have been linked with chromatin modification. Wang et al., showed that hyper osmotic stress induces global Phosphorylation of Histone H3 at Threonine 3 in *Arabidopsis*. This response depends on an osmosensing pathway using MUT9 Like kinases (MLK 1 and MLK 2) (Wang *et al.*, 2015).

3.3.4. Hypoosmotic stress

Hypo osmotic stress occurs in physiological conditions where the outside environment has less solute than inside leading to water intake to the cell. This condition is mimicked with a presence of excess water in the surroundings of a cell and organism. Cell swelling is a common outcome, whereas in case of plant it is a normal state where the plant cell wall faces extreme pressure and pushes onto the cell wall making the cells turgid.

But physiological conditions with prolonged hypoosmotic stress exist too. Hypoosmotic stress is generated where the plants stuck in an environment with higher water volume than normal such as during flood or in case of tropical rain forest plants (Teo *et al.*, 2009). In some cases, rapid rewetting of dry soil also leads to hypoosmotic stress to plants. In case of isolated cells equilibrated with a medium with salt or sugar, treatment with distilled water will reproduce the effects of hypoosmotic stress but in plants it is limited by the mechanics of cell wall (Haswell & Verslues, 2015).

Plant water system highly depends on the vacuole. It has been shown that the vacuole is under hypoosmotic stress during normal growth condition in *Arabidopsis*. The dynamic response of hypo-osmotically stressed vacuole needs mechanosensitive ion channels MSL2 and MSL3. Hypo osmotic stress also induces ROS generation mediated by NADPH-oxidases which depends on calcium signalling. Water homeostasis after such stress is ensured by the activation of metabolic and gene expression reprogramming via MAPK pathway (Cazalé *et al.*, 1999). A mechanosensitive channel MSL 8 has been demonstrated essential in case of hypoosmotic shock in pollen during rehydration (Hamilton *et al.*, 2015).

Water ensures not only the mechanics of plant system it is the main medium to transduce nutrients, signals and hormones across plant tissue but even presence of excess water can cause nutrient deprivation in plants.

3.3.5. Conclusion on the nexus between osmotic stress and mechanical stress

Here I have discussed how osmotic stress and mechanical stress are intertwingled in the cell and the underlying molecular pathways. In response to hyperosmotic stress the mechanoresponsive elements of the cells are hugely affected. As I have discussed the role several mechanosensitive channels and receptors play important role in this context. It is still unclear how plant actually sense the osmotic signal outside the cell and transfer it inside. But the responses have been widely studied in case of hyper osmotic stress. Mounting evidence suggests that microtubule is an important downstream target for osmotic stress. Decades earlier, microtubules in *Zea mays* root cells have been shown to reorient from transverse to oblique/longitudinal (to the root axis) under ionic osmotic (KCl) stress (Blancaflor & Hasenstein, 1995). Several microtubule associated proteins plays important role in salt stress tolerance such as PROPYZAMIDEHYPERSENSITIVE 1 (PHS1) (Fujita *et al.*, 2013) or AtKATANIN1 (Yang *et al.*, 2019). More generally, the highly dynamic characteristics of cortical microtubule i.e. rapid polymerisation and depolymerisation capacity is important for plants to withstand salt stress (Shoji *et al.*, 2006; Wang *et al.*, 2007). As microtubule is one of the key factor of the mechanical identify of cell, these changes in microtubules also changes the mechanical status of the cell and leading to interconnected signalling system and response of osmotic and mechanical stresses.

As hypo osmotic stress is considered as a physiological condition in case of plants it has not gained so much attention from the plant scientists. In addition, osmotic sensing is used by plant during desiccation of seeds or pollen and again rehydrating them.

4. Plant cell responses to mechanical signals

Wide range of cellular activities are responsive to mechanical cues and influence cell morphology, cell motility or durotaxis, cellular growth, polarity, cell division and differentiation, or cell fate decision.

4.1. Cell growth

Mechanical stress drives the rate and direction of cell expansion in plants. During cell differentiation, plant cells grow 10-1000 folds but could reach to 300000-fold during xylem vessel maturation. In plant cells the expansive growth depends on the mechanics of cell wall and the changes occurred through biomechanical responses to tensile stresses created by the turgor pressure (Figure 27). Cell deform both reversibly and irreversibly (Figure 27C). Reversible cell expansion is observed during elastic cell deformation via turgor pressure. One classic example is the opening of stomata by elastic deformation of the guard cells. An intake of K_+ ions decreases the osmotic potential leading to a hypoosmotic stress and increased turgor pressure in the guard cells and opening of the stomata (Humble & Raschke, 1971). Irreversible cell growth is associated with plastic deformation of the cell wall under turgor pressure directly by the stress relaxation by cell wall modification (Cosgrove, 1986) (Figure 27B). The cell wall mechanics (e.g. cell wall extensibility - φ) is modified to make the cell wall softer, then the turgor pressure (without actually changing) becomes higher than the pressure needed for plastic deformation (yielding pressure Y) of a cell. Growth continues until the new wall material thickens the cell enough to be balanced with the difference of osmotic potential (Δπ) again (Boyer *et al.*, 1985). A conceptual formalization of the underlying biophysics of cell growth (increase cell volume V over time, dV/dt) via water intake and cell wall loosening comes from Lockhart equation:

$$\frac{dV}{Vdt} = \frac{\varphi L}{\varphi + L}(\Delta\pi - Y)$$

Here L is water conductance coefficient. This equation relate osmotic pressure and the mechanical properties of the cell, and channels the rate of cell growth. The mechanosensors and wall integrity sensors mentioned above are likely involved in setting or sensing the Y threshold, at least indirectly.

Adapted from Cosgrove, 2016

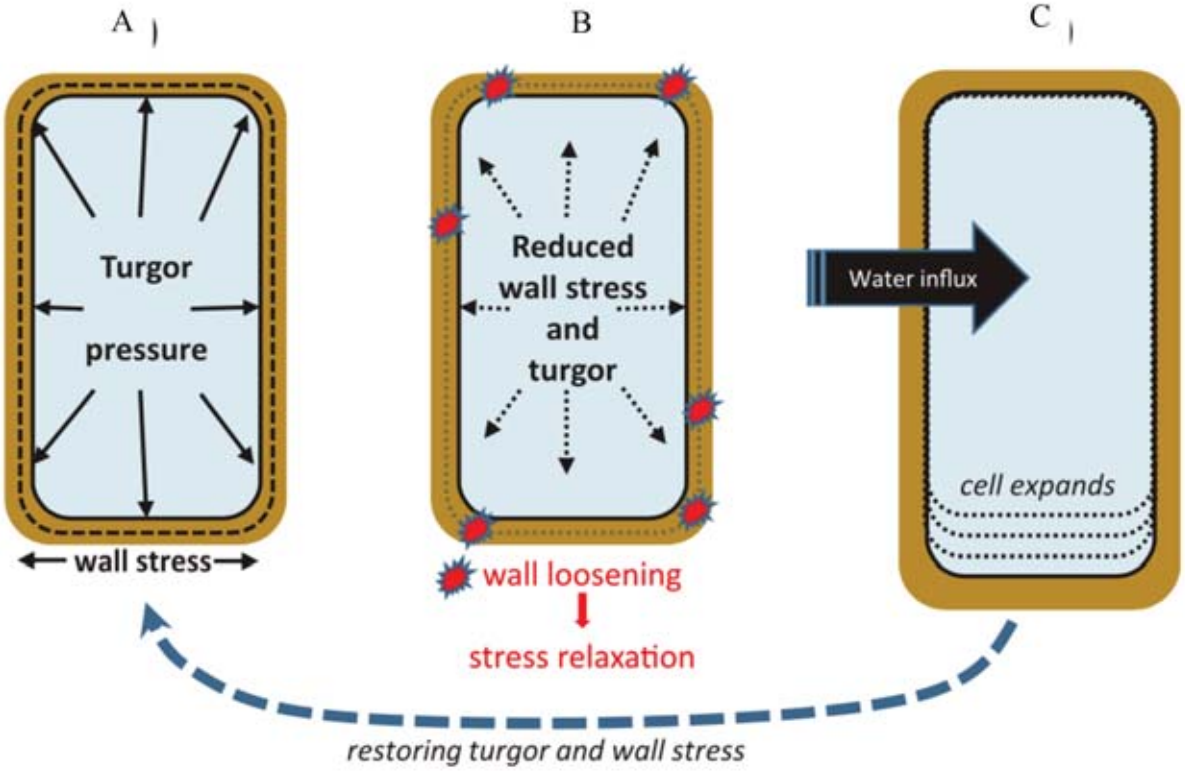

Figure 27. Biophysics of plant cell growth

(A) Nongrowing turgid cell with a hydrostatic turgor pressure balanced at the cell wall.
(B) While growing the cell wall loosens and the turgor pressure relaxes.
(C) In an elastic scenario water enters the cell and restores the turgor pressure but in a plastic scenario when the pressure exceeds the yielding pressure irreversible growth of cell take place.

Adapted from Cosgrove, (2016).

The directionality of during the growth comes from the anisotropic structures of the cell like cellulose microfibrils or the microtubule networks as discussed earlier. Briefly, the alignment of CMTs would ensure the directional expansion of cells. In turn, elongated plant cells may prescribe tensile stress patterns that reinforce such CMT alignment, in a positive feedback loop. More complex plant cell shapes can also be maintained by such feedback loop. In particular, this has been shown for jigsaw puzzle pavement cells (Sampathkumar *et al.*, 2014).

4.2. Cell division

Building on the effects of mechanical forces on cell growth, it also affects other determinants of morphogenesis, cell division. By orienting the division plane, plant cells modify their shape and the topology of the tissue. Previously it has been shown cell division plane of symmetric division follows one of the shortest division paths, as in soap bubbles (Errera, 1886; Besson & Dumais, 2011). This probabilistic division plane rule follows a molecular mechanism where geometry derived cues are processed and cytoskeletal microtubule help in integrating the information (Besson & Dumais, 2011). Such geometrical cues may be in part translated into mechanical cues. As mentioned above, an elongated cell may have higher transverse tensile stresses. Several studies have established the role of tensile stress in manipulating the cell division plane orientation (Lintilhac & Vesecky, 1984; Louveaux *et al.*, 2016). In particular, when the tissue experiences highly anisotropic supracellular tensile stresses, as in the boundary region of Shoot Apical Meristem, cells divide along such tensile stresses, independent of cell geometry (Figure 28). Single cell ablation in a tissue region of isotropic stress distribution like the center of the Shoot Apical meristem was done. The resulting change in the cell division plane orientation followed the maximal tension (Louveaux *et al.*, 2016). This rule is likely shared across kingdoms: in human cells (HeLa) the role of external force in cell division has been directly demonstrated by uni-axial stretching of the cells around ~25%. Reorientation of mitotic spindle and the division plane was observed following the external stress (Fink *et al.*, 2011).

4.1 Cell polarity

Cell polarity is a crucial process for symmetry breaking, through the asymmetric distribution of molecules like proteins and lipids biochemically and biomechanically. Plant cells can be polar in single cells like pollen tube growth or root hair development, and in tissues. In particular, the polarity of the auxin efflux carrier PIN-FORMED1 (PIN1) plays an essential

Adapted from Louveaux *et al.,* 2016

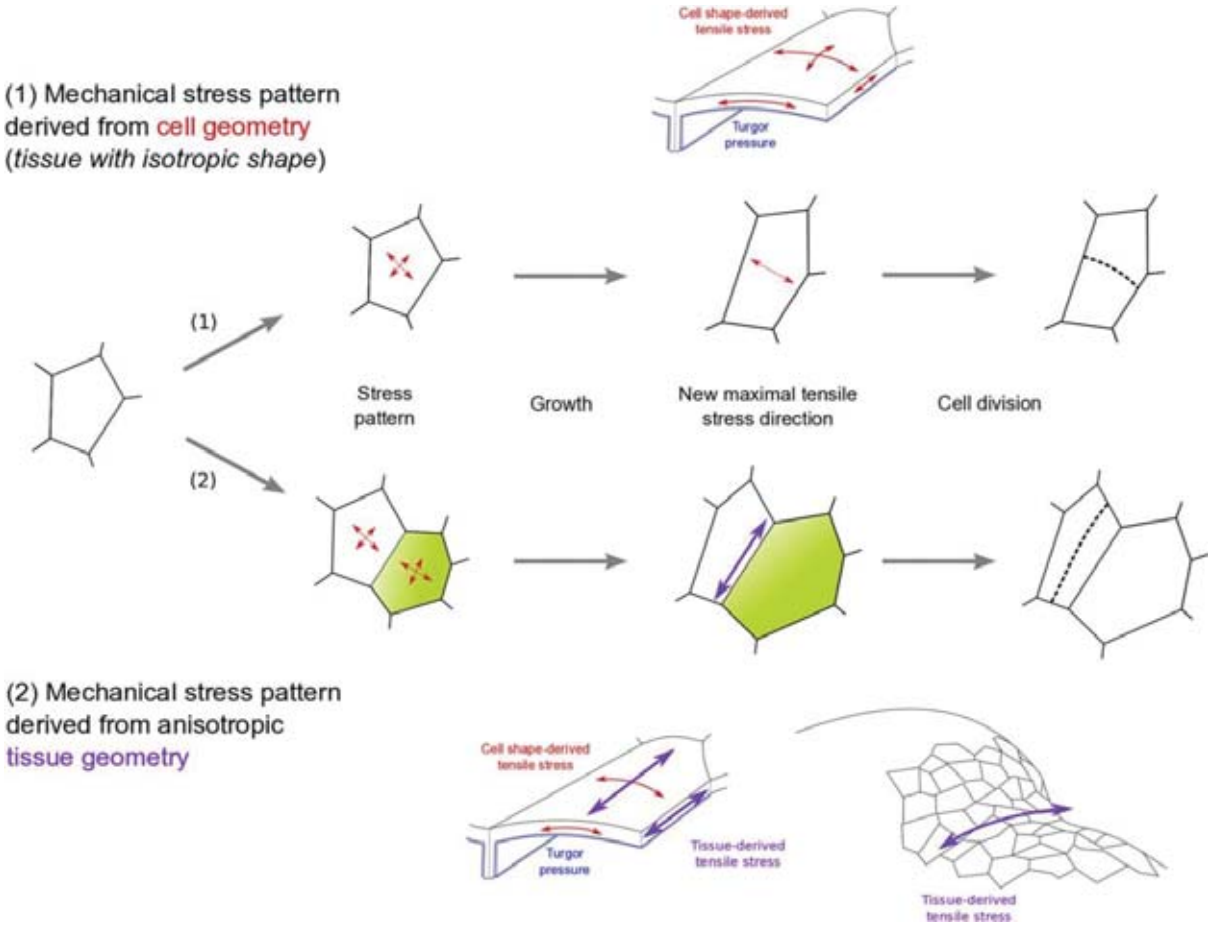

Figure 28. Mechanical stress regulated division rule determines the cell division plane

Plant cells follow Besson Dumais rule of cell division when the cell shape is spherical and the stress can only be derived from cell geometry. Cells follow one of the shortest pathway. But when the cell shape is anisotropic as well as its under anisotropic growth induced stress the cell division plane orients according to maximal tensile stress which followed mechanical cell division rule. Adapted from Louveaux *et al.,* (2016).

role if defining auxin maxima and patterning organogenesis in plants (Wisniewska, 2006). When CMTs reorient according to changes in maximal tensile stress directions (Hamant *et al.*, 2008), their orientation also correlates with PIN polarity (Heisler *et al.*, 2010). Nakayama *et al.,* showed that growth induced mechanical strain could increase PIN1 (plasma membrane under highest tensile stress shows increased PIN1 accumulation) mediated-auxin accumulation in tomato shoot apical meristem (Nakayama *et al.*, 2012). Several external mechanical stresses like osmotic treatments (hyper and hypoosmotic mannitol stress), external force applications (by pushing with a glass rod), membrane modulations (chemical interaction with plasma membrane using DMSO and ethanol) directly modulated the PIN1 localisation (hypoosmotic stress or glass rod pushing increased tension and PIN1 density, whereas hyperosmotic stress or DMSO decreased membrane tension and PIN1 density) and in turn contribute to the auxin-mediated cell polarity correlating with the degree of mechanical stress (Nakayama *et al.*, 2012). Altogether this suggests that mechanical stress contributes to PIN1 polarity (Figure 29).

4.3. Cell fate

The role of mechanical stress in determining cell fate is by far the most debated. In animal system single Mesenchymal Stem Cell fate can be modulated by changing stiffness of the extracellular matrix they grow on (Engler *et al.*, 2006). In plants it has been proposed that epidermal cell fate determination could be under mechanical control (Figure 30). Epidermal cells are strongly adhering with each other forming a monolayer between the plant and the outer environment and it is under tension (Galletti *et al.*, 2016). Embryonic protodermal cell fate is determined only once during morphogenesis and then inherited through divisions for the whole life cycle of plant on the surface of tissue and organs. The specification and/or maintenance of epidermal identity in the early embryo, depends upon the gene DEFECTIVE KERNEL 1 (DEK1) which encodes an integral membrane protein with a CALPIN like domain involved in Ca^{2+} signalling. The role of Ca^{2+} as secondary signalling molecule in mechanical signal transduction is well established. DEK has been identified as a mechanosensor in the epidermis by regulating Ca^{2+} activated mechanosensitive ion channel (Tran *et al.*, 2017). This postulates a scenario where the epidermal tension in sensed by the cells via DEK1 which activates Ca^{2+} dependent mechanotransduction pathway leading to epidermal cell fate determination and maintenance (Malivert, 2018).

Adapted from Li *et al.*, 2012

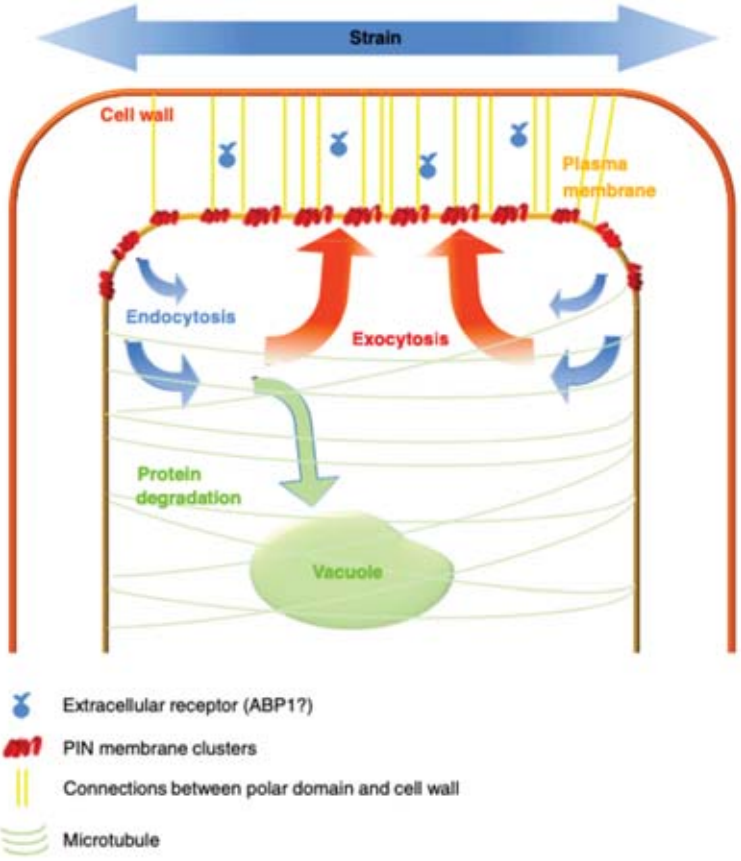

Figure 29. Illustration of mechanical control over cell polarity

Mechanical inputs from cell wall via PIN1 is integrated in the cell and results into changed membrane mechanics loading. Resulting differential distribution of membrane molecules leads to the established of cell polarity. Adapted from Li *et al.*, (2012)

Adapted from Malivert *et al.,* 2018

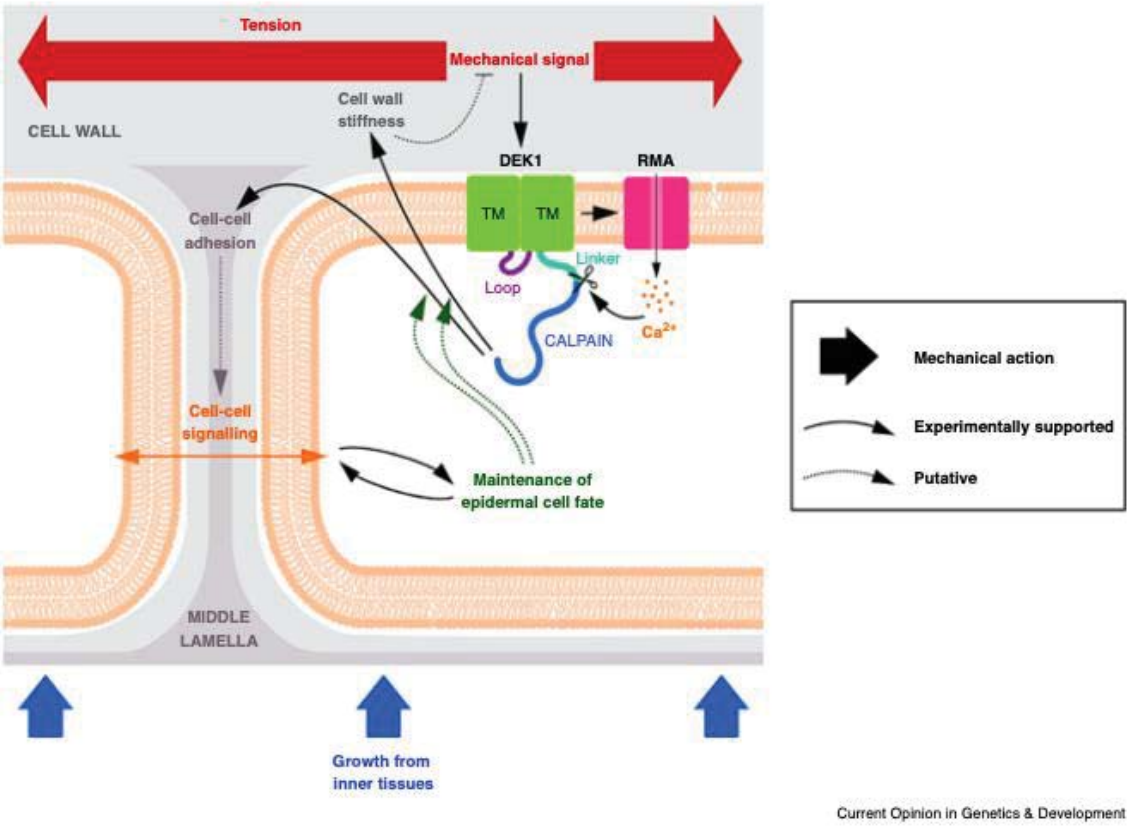

Figure 30. Epidermal cell fate under mechanical control

Epidermal cells layer is a tightly regulated tissue with cell-cell signalling and also under tension from the inner tissue. DEK1 senses the tension the epidermal cells via which activates Ca^{2+} dependent mechanotransduction pathway leading to epidermal cell fate maintenance. Adapted from Malivert *et al.,* (2018).

4.4. Conclusion

Mechanical signals contribute to several biological processes including growth, division, polarity and differentiation. As these signals enters the cell, they need to reach the nucleus to device the responses. In the next part I will discuss the role of nucleus as a mechanical object and how mechanical signals reach and inferred by this organelle.

Ref.: Ms. No. COPLBI-D-19-00047
57: Cell signaling and gene regulation
Current Opinion in Plant Biology

Is the plant nucleus a mechanical rheostat?

Rituparna Goswami[a,b], Atef Asnacios[c], Olivier Hamant[b*] and Marie-Edith Chabouté[a*]

[a] Institut de biologie moléculaire des plantes, CNRS, Université de Strasbourg, 67084 Strasbourg, France

[b] Laboratoire de Reproduction et Développement des Plantes, Université de Lyon, UCB Lyon 1, ENS de Lyon, INRA, CNRS, 69364 Lyon, France

[c] Laboratoire Matières et Systèmes Complexes, Université de Paris, CNRS, Université Paris-Diderot, 75013 Paris, France

*Correspondence: marie-edith.chaboute@ibmp-cnrs.unistra.fr ; olivier.hamant@ens-lyon.fr

Abstract

Beyond its biochemical nature, the nucleus is also a physical object. There is accumulating evidence that its mechanics plays a key role in gene expression, cytoskeleton organization, and more generally in cell and developmental biology. Building on data mainly obtained from the animal literature, we show how nuclear mechanics may orchestrate development and gene expression. In other words, the nucleus may play the additional role of a mechanical rheostat. Although data from plant systems are still scarce, we pinpoint recent advances and highlight some differences with animal systems. Building on this survey, we propose a list of prospects for future research in plant nuclear mechanotransduction and development.

The nucleus as a physical object

Cells are physical objects that react to tension, compression or friction in tissues. Conversely, cells can adapt or resist to such forces by modulating their mechanical properties. This applies to the matrix [1], the cytoskeleton [2], as well as the nucleus [3], with important consequences in gene expression and development [4]. Here we review key features of nuclear mechanics and mechanotransduction, based on data from mammalian and yeast cells.

The nucleus has specific mechanical features. When probed through the diffusion of internalized nanoparticles, the nuclear structure reveals transient ~300 nm sized micro-domains

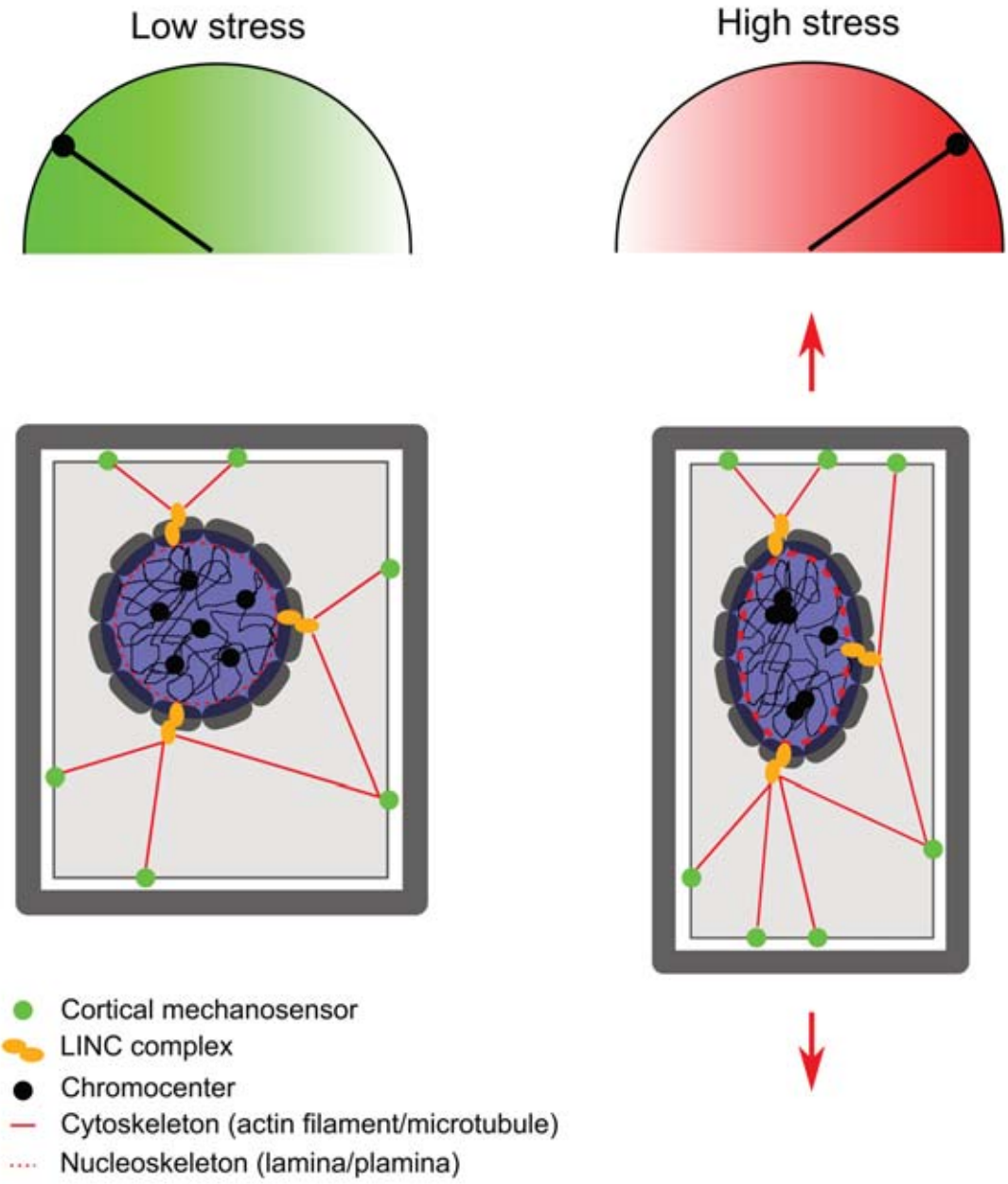

Figure 1. Mechanical force influences cell and nuclear shape
Under high cell stress, the nucleus is more compact with nucleoskeleton enrichment and spatial chromatin reorganization.

with elastic trapping and low elastic moduli (~20 Pa) and viscosities (~50 Pa.s) [5]. When the whole nucleus is deformed under constant loading (creep experiment), it displays a time-scale free weak power law behavior, with a viscoelastic modulus ranging from 1 to 10 kPa, and an exponent α~0.2-0.3 [6]. This corresponds to a mechanical behavior dominated by elasticity, with, at a typical time scale of a second, an apparent elastic modulus of about 5 kPa, and an apparent viscosity of ~300 Pa.s.

Importantly, the nucleus viscoelastic modulus correlates with cell identity. For example, during human stem cell differentiation, nuclei stiffen ~6-fold relative to cell cytoplasm. Consistently, nuclei of primary human fibroblasts are ~2 times stiffer than nuclei from Marrow-derived human stem cells and their stiffness correlates with the level of expression of lamins [7]. However, the nucleus also displays a plastic behavior and strain hardening (stiffening with increased deformation) reminiscent of the non-linear stress-strain relationship of chromatin fibers [6].

Thus, the nucleus may be considered as a complex mechanical rheostat able to respond to environmental mechanical stresses, with elastic, viscous and plastic behaviors that are, at least in part, related to chromatin structure and state. In fact, in contrast to the classical view of nuclear mechanics depending mainly on a stiff nucleoskeleton (lamins) surrounding a softer nucleoplasm (chromatin), recent studies indicate that modifications of histone state are sufficient to dictate nuclear rigidity independently of lamins [8].

The ability of the nucleus to react to forces also entail energy requirements and dissipation. In that sense, and like most biological objects, the nucleus belongs to the family of active materials [9]. The idea that the nucleus may be an active mechanosensitive element has gained more and more momentum in the past decades [10], also building on the characterization of its structural elements and their physical link to the cytoskeleton [11,12]. In sum, there is now ample evidence that the mechanical properties of the main mechanically-relevant elements of the nucleus (nuclear envelope, lamins and chromatin) modulate nuclear mechanosensing, leading to the concept of a nuclear rheostat ([13], Figure 1).

The dynamic mechanical properties of chromatin

Heterochromatin is enriched at the nuclear periphery, which is a rather silent transcriptional environment [14–16], while euchromatin is organized in topologically associated active domains, which define regulatory units inside the chromosome territories. While topologically associated active domains are found in rice and cotton, “boundary-like regions” were mainly found in Arabidopsis allowing separation of transcriptionally active regions from inactive regions [17–19].When the balance shifts towards an increase of the transcriptionally less active, condensed heterochromatin, and decrease of the gene-rich transcriptionally active less condensed euchromatin, nuclei from mammalian cells become stiffer [8,20,21]. In plants, only one study was performed in differentiated tissues using mutants showing decondensed heterochromatin (*ddm1*, *atxr5atxr6*) and no obvious nuclear deformation was observed (nuclear sphericity and volumes). However, the analyses were conducted on fixed nuclei that can modify mechanical properties of the nucleus [22]. The nucleus also follows a power-law rheology when subjected to osmosis regulation [6]: isolated nuclei from epidermal cells increase their volume up to 200% and dilute the DNA content, whereas the nucleus becomes wrinkled, due to chromatin condensation, in high salt concentrations.

The dynamic mechanical properties of lamins

The lamina is a stiff nucleoskeleton meshwork including lamins A/C and B. While lamin A/C and B interact with heterochromatin at the nuclear periphery [23], only lamin A/C interacts with euchromatin via lamin-associated polypeptide 2α allowing a more direct regulation of gene expression [24]. Because lamin A interacts with chromatin, they can regulate nuclear viscosity, whereas lamin B rather modulate nuclear elasticity [25,26]. Interestingly using super-resolution microscopy, lamin B1 forms an outer concentric ring, in a curvature-dependent localization to restrain outward protrusions of the stiff lamin A/C network facing the chromatin [25]. Such organization may help to explain the differential mechanical properties of lamins [25,26]. Lamin A was shown to scale with tissue stiffness: both transcription and protein levels are increasing during differentiation in human cells [25] whereas lamins unfolding, through their phosphorylation, was induced by cells growing on soft matrix [28].

In plants, while NE architecture is mainly conserved [29], no true lamin exists. Yet specific

functional homologs are present [30]. This includes the CRWN/NMPC coiled-coil domain proteins found initially in carrot as NMPC [31] and further identified in Arabidopsis as CRWN1-4 [32,33]. Using FRET experiments, CRWN1 was shown to interact with the nucleoplasm N-terminus domain of SUN1 [34]. Other proteins were shown to interact physically with SUN1 using yeast two hybrid, such as the plant specific lamin-like KAKU4 [35] or the chromatin associated protein PWO1 [34]. In Arabidopsis while CRWN1 and KAKU4 may maintain nuclear morphology through their interaction with the NE, they can deform the NE independently [35]. Interestingly, genetic interactions between single and double mutants, reveal that *PWO1* and *CRWN1* control nuclear size and shape in the same genetic pathway [36]. However the scaling of nuclear deformation with mechanical stress response has not yet been investigated in plants.

The nuclear envelope as a mechanical integrator

The NE has its own mechanical properties, the elasticity, viscosity and plasticity of the NE is supported and modulated by several key proteins [37]. It consists of two lipid bilayer membranes, namely outer (ONM) and inner (INM) nuclear membranes, which are separated by a ∼35–50 nm perinuclear space. These membranes fuse together at the sites of Nuclear Pore Complex (NPC) giving rise to an ultra-donut topology [38]. The geometric gap between the nuclear membranes is mostly maintained via the SUN1 and SUN2 proteins [39]. SUN1 and SUN2 proteins are located at the INM and interact, via their C-terminus SUN domain (Sad1/UNC-84 homology domain), with the KASH (Klarsicht/ANC-1/SYNE homology) domain of KASH family proteins located at the ONM. These SUN-KASH complexes, also known as LINC complexes (LInker of Nucleoskeleton and Cytoskeleton) are found across all eukaryotes [39–43]. In the case of vertebrates, SUN1 is also connected to lamins A/C [44].

In a cellular context, the dynamics of actomyosin and microtubules can generate compressive and pulling stresses on the nucleus [45]. The NE plays a key intermediary role. For instance, disrupting the perinuclear actin cap through actin depolymerization leads to an increase of nuclear volume in mouse fibroblasts [46]. Similarly, untethering chromatin from the inner nuclear membrane induces nuclear deformation and reduces nuclear rigidity in *S. pombe* [47]. In plants, the presence of a large vacuole may further constrain the nucleus in a thin cytoplasmic compartment. Consistently, actin depolymerization in leaf epidermal cells does not change the

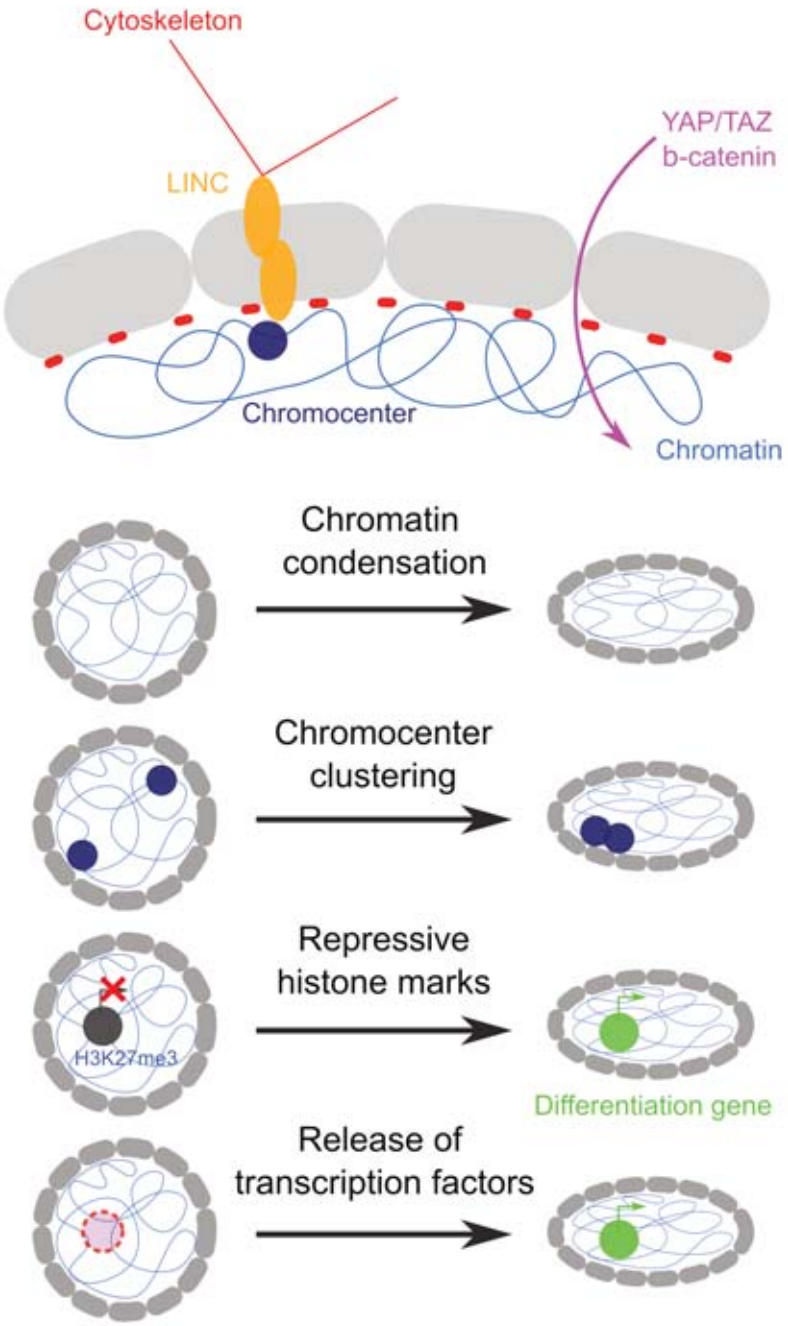

Figure 2. Chromatin is under the regulation of mechanical stress

Changes of nuclear architecture under mechanical stress lead to chromatin condensation, clustering of chromocenters, repressive histone mark modifications inducing altered accessibility for the transcription of differentiated gene, and release of transcription factors from the nuclear periphery.

elongated shape of the nuclei [48]. Yet, LINC complexes are associated to actin via Myosin XI-i in plant cells [49] and impaired LINC functions prevent nuclear elongation in differentiated tissues [50,51]. Therefore, plant nucleus shape also depends on NE factors and the cytoskeleton.

The mechanical regulation of gene expression through the nucleus properties

Because the cytoskeleton and NE components are relatively stiff, cortical mechanical cues can change nucleus shape rapidly, leading to subsequent chromatin changes (Figure 2). For instance, the perinuclear actin cap can induce nuclear deformation mediated by LINC complexes and lamins A/C in 30 seconds [11,52,53]. Disrupting LINC complexes through SUN1 perturbation in fibroblasts cells leads to different transcriptional responses on soft versus stiff substrates [4]. Unfolding of lamins through their dephosphorylation affect gene expression within 10 minutes [28]. Last, destabilization of lamins under stress will induced global chromatin reorganization, release of sequestrated transcription factors as well as modifications in setting repressive histone marks H3K27me3 mediated by the polycomb complex PRC2 [54] (Figure 2).

In parallel to the propagation of stress through the internal structural elements of the cell, cortical cues may indirectly reach the nucleus through protein translocation to the nucleus. In particular, the well-known Hippo pathway-YAP/TAZ involves the traffic of the transcriptional activator ß-catenin from the cytoplasm to the nucleoplasm through the NPC [55]. Note that because NPCs are directly connected to nucleoskeleton, chromatin, and LINC complexes [56], the passive nuclear entry of the co-transcriptional factor YAP also depends on the physical deformation of the nucleus [57].

Chromatin is actually a site where mechanical and biochemical cues largely overlap [7,8,21,47]. In response to mechanical stress, changes in gene transcription may be modified either by changes of gene position inside the nucleus or by changes of the chromatin state itself. For instance, direct stretching of chromatin through mechanical forces (using RGD-coated magnetic beads) can induce expression of a GFP-tagged gene in hamster cellular line, and this involves actin and LINC complexes. This is triggered through a change in the spatial chromatin organization, i.e. a change in the location of the transgene [12]. Upon cell mechanical constraint, actomyosin induces the nuclear translocation of HDAC3 leading to decreased level

of histone acetylation (permissive mark for gene expression) in mouse embryo fibroblast cells leading to a geometry-dependent transcriptional response. Such response is reversible [58,59]. On the contrary, inhibition of actin leads to the recruitment of the histone methyltransferase G9a to the NE and thus increases the level of repressive marks H3K9me2/3 in T-lymphocyte cells [60]. Interestingly, using an active 3D chemo-mechanical model, also integrating cell geometric constraints, one can predict nuclear mechanics and architecture patterns [61].

Functional implications of nuclear shaping in development

During development, tissue change their shape or mechanical status, and the resulting mechanical conflicts can transduce mechanical cues to cells and, arguably, nuclei. Although most of the knowledge on nuclear mechanics and mechanotransduction has been generated from studies in single cells in culture, this should also apply to cells in a tissue context. This starts to be addressed [62].

For instance, during epidermal morphogenesis in humans, actin-driven force decreased the level of the lamin-binding protein emerin at the INM inducing a loss of anchoring of heterochromatin at the NE and changes in transcriptional programs mediated by the polycomb PRC2, with important consequences for cell identity [63]. Furthermore, impaired NE functions, notably lamins A, lead to a wide range of diseases called laminopathies, such as muscular dystrophies and progeria [64]. Thus, nuclear mechanics shows functional regulation or correlation through a range of physical and pathological condition.

Plant tissues are usually much stiffer than animal ones, because plant cells are highly pressurized with a turgor pressure in the MPa range, and surrounded by a stiff cell wall. Yet, plant cells are still experiencing mechanical conflicts, the pattern of which is determined by tissue shape and growth. Cortical microtubule arrays play a major role in guiding cellulose synthase complex (CSC) to regulate the cell wall and its physical properties. Cortical microtubules align with the direction of maximal tensile stress in the cell wall, thereby reinforcing the cell wall to resist tensile stress [65]. γ tubulins are present at the NE, where they nucleate cytoplasmic microtubules, together with MZT1-homolog GIP proteins [66]. Interestingly, γ tubulins are also found at the INM in a complex with SUN1 and GIPs which

form a complex with the centromeric chromatin via CENH3 [67,68]. Therefore, the GIP-γ tubulin hub might have a specific role in nuclear mechanotransduction in plants.

Impaired GIP activity lead to irregular shape and lobulated nuclei in both meristems and differentiated root tissues [69] as well as severe developmental defects in development, with the presence of callus on differentiated tissues [66]. Such effects are not shared with other NE proteins. In particular, most of the nuclear envelope proteins characterized in LINC complexes identified so far regulate nuclear shape, yet, they do not necessarily induce major developmental defects when impaired [50,51]. This may in part be due to genetic redundancy. For instance, single *crwn* mutants have no growth defects, *crwn1crwn2* as well as *crwn1crwn2crwn4* showed increasing severity in their development, like stunted plants [33]. When compared to wild type, these mutants exhibit smaller and denser nuclei with fewer, more aggregated, chromocenters. Interestingly, only CRWN1 and CRWN4 allow tethering of heterochromatin at the nuclear periphery [68]. CRWN1 interacts with PWO1, and both control nuclear size [36]. PWO1 physically interacts with the polycomb complex PRC2 mediating H3K27me3 repressive marks [71]. Whereas mechanical regulation of nuclear architecture was linked to cell fate decisions in mammals, this remains to be explored in plants [72,73].

Perspectives for plant science: the role of the nucleus in multi-stress responses

In contrast to animals, plants exhibit a plastic postembryonic development that largely depends on environmental cues. In line with the established role of nuclear mechanics in animal development, plant development also relies on nuclear mechanotransduction. Yet the exact role of nuclear shape, mechanics and structural elements in signaling and development remains to be investigated. Conducting this research in plants will not only unravel conserved and divergent mechanisms in a walled context, it will also help to understand how the nucleus integrates cues from the environment.

In a recent study in Arabidopsis, we show the importance of nuclear mechanics in roots exposed to osmotic stresses. Throughout mechanical assessment of nucleus stiffness by atomic force microscopy and microrheometry, we revealed that hyperosmotic stress leads to nucleus shrinking, stiffening and chromatin remodeling. We also observed a strong induction of touch-response genes. Importantly, these responses were reversible upon return to iso-osmotic

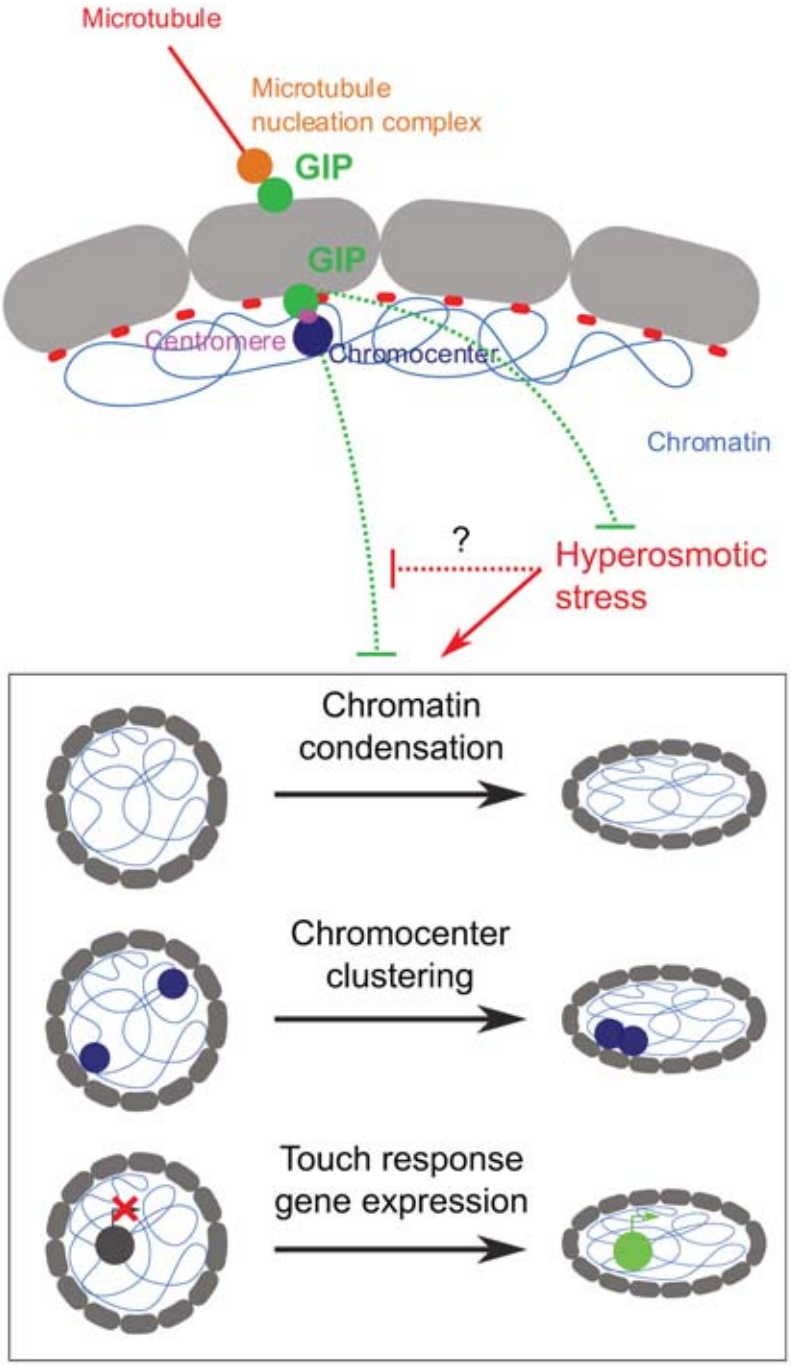

Figure 3. Nuclear mechanical response in plants under hyperosmotic stress
Upon hyperosmotic stress, the nucleus is more compact with clustered chromocenters and induction of touch-response gene expression. The nuclear envelope proteins GIPs may act as negative regulators of this response.

conditions. We propose that chromatin behaves like a mechanosensitive gel in response to osmotic stresses (Figure 3) [74].

Interestingly, the *gip1gip2* mutant nuclei mimicked a hyper-osmotic phenotype, with reduced nucleus volume and sphericity. We also find that touch-response genes are constitutively induced in the mutant. This further suggests that not only NE envelope proteins play an important role in growth-derived mechanical cues, but they may also be involved in the plant response to its mechanical environmental environment. Consistently, we also found that *gip1gip2* plants are more resistant to harsh osmotic conditions. This suggests that the absence of GIP may actually prime the plant to hyperosmotic conditions (Figure 3).

Based on these recent results, and building on the comparative analysis of nucleus mechanics and mechanotransduction in animals, we thus propose that the nucleus also acts as a mechanical rheostat in plants. Why would plants be competitive model systems to address this question? Plant cells do not move. Thus the relation between tissue stress and nucleus phenotype is more direct and readily amenable to be investigated in plants. Furthermore, the analysis of multi-stress responses is also facilitated in plants due to their plastic development and sessile nature, meaning that eco-devo study of nuclear mechanotransduction can be envisioned in plants. Altogether, this introduces nuclear mechanotrasnduction as a new field of research in the plant community, with implications going far beyond a comparison with animal nuclei.

REFERENCES AND RECOMMENDED READING

Papers of particular interest, published within the period of review, have been highlighted as:

*of special interest

Bi et al., 2017 Genome Res.: Using the nucleoporin NUP136/NUP1 fused to GFP in RE-ChIP experiments in different Arabidopsis tissues, the authors show that 10 to 20% of chromosome regions are anchored at the nuclear periphery and are enriched in TE and H3K27me3-marked genes.

Nmezi et al., 2019 PNAS: Using high resolution microscopy STORM, the authors show that Lamin B1 forms an outer concentring ring adjacent to the INM, the localization of which is

strain-dependent. Lamins B stabilize nuclear shape and prevents protusions from the underlying Lamins A/C network.

Chumova et al., 2019 Cells: In Arabidopsis, the γ tubulin initially associated with the microtubule nucleation complexes at the ONM, are found to co-localize with SUN at the INM. They are also present in complexes associated with GIP, suggesting new roles of these proteins at the NE.

Szabo et al., 2019 Sci Adv.: In this article, the authors perform an interkingdom comparison of nuclear architecture through the analysis of topologically associating domains.

Damodaran et al., 2018, Mol Biol Cell: The authors show the importance of fibroblast geometry in changing the chromatin condensation state and the transcriptional response to compressive forces.

Shivashankar, 2019, Curr. Opin. Cell Biol.: In this review, the author discusses the contribution of mechanical cues in changing nuclear architecture and cell fate transitions in mammals.

Miroshnikova et al., 2019, Curr. Opin Gen. Dev: The authors present the latest advances linking mechanics and epigenetic gene regulation during differentiation.

** of outstanding interest

Stephens et al., 2018 Mol Biol. Cell: The authors show that modifications of histone state are sufficient to dictate nuclear rigidity independently of lamin perturbation. For instance, chromatin decompaction via increased acetylation is sufficient to decrease nuclear stiffness without perturbing lamins.

Mikulski et al., 2019 Plant Cell: The authors show that PWO1, which interacts with the polycomb complex PRC2, also interact physically with lamin-like CRWN1. This reveals mechanisms for repressing chromatin at the nuclear periphery in plants.

Hu et al., 2019 Genome biol.: The authors show that lamin-like CRWN1 is needed to anchor

repressed chromatin domains to the nuclear periphery in Arabidopsis. CRWN1 has a direct interaction with repressive heterochromatin regions, highlighting chromatin interaction with the plamina in Arabidopsis.

Alisafaei et al., 2019, Proc Natl Acad Sci U S A.: The authors develop a 3D chemo-mechanical model considering the reciprocity in dynamics between extracellular matrix, cytoskeleton and nucleus using micropatterning experiments.

Goswami et al., 2020 Current Biol. : In this paper, the authors propose that plant nuclei may act as a mechanical rheostat in response to osmotic stress with concomitant changes in nuclear rigidity, shape and mRNA levels of touch-response gene. The absence of GIP/MZT1 may prime the plant to respond to hyperosmotic conditions.

ACKNOWLEDGMENTS

The authors were supported by the Centre National de la Recherche Scientifique (CNRS, defi Mecanobio, NEstress 2016-2018), by Fondation Schlumberger pour l'Education et la Recherche (FSER 2016-2018), by the European Research Council Grants ERC-2013-CoG-615739 "MechanoDevo", by the IdEX international PhD program (unista, Strasbourg) and by HFSP Grant 2018, RGP, 009. This study was partially supported by the labex «Who AM I ?», labex ANR-11-LABX- 0071 and the Université de Paris, Idex ANR-18-IDEX-0001 funded by the French Government through its «investments for the future» program. We apologize to our colleagues whose work we were not able to discuss because of space constraints.

References

1. Engler AJ, Sen S, Sweeney HL, Discher DE: **Matrix elasticity directs stem cell lineage specification**. *Cell* 2006, **126**:677–689.
2. Durand-Smet P, Chastrette N, Guiroy A, Richert A, Berne-Dedieu A, Szecsi J, Boudaoud A, Frachisse JM, Bendahmane M, Hamant O, et al.: **A comparative mechanical analysis of plant and animal cells reveals convergence across kingdoms**. *Biophys J*

2014, **107**:2237–2244.

3. Lovett DB, Shekhar N, Nickerson JA, Roux KJ, Lele TP: **Modulation of Nuclear Shape by Substrate Rigidity**. *Cell Mol Bioeng* 2013, **6**:230–238.
4. Alam SG, Zhang Q, Prasad N, Li Y, Chamala S, Kuchibhotla R, Kc B, Aggarwal V, Shrestha S, Jones AL, et al.: **The mammalian LINC complex regulates genome transcriptional responses to substrate rigidity**. *Sci Rep* 2016, **6**:38063.
5. Tseng Y, Lee JSH, Kole TP, Jiang I, Wirtz D: **Micro-organization and visco-elasticity of the interphase nucleus revealed by particle nanotracking**. *J Cell Sci* 2004, **15**:2159–2167.
6. Dahl KN, Engler AJ, Pajerowski JD, Discher DE: **Power-law rheology of isolated nuclei with deformation mapping of nuclear substructures**. *Biophys J* 2005, **89**:2855–2864.
7. Pajerowski JD, Dahl KN, Zhong FL, Sammak PJ, Discher DE: **Physical plasticity of the nucleus in stem cell differentiation**. *Proc Natl Acad Sci U S A* 2007, **104**:15619–15624.
8. Stephens AD, Liu PZ, Banigan EJ, Almassalha LM, Backman V, Adam SA, Goldman RD, Marko JF: **Chromatin histone modifications and rigidity affect nuclear morphology independent of lamins**. *Mol Biol Cell* 2018, **29**:220-233.
9. Fletcher DA, Geissler PL: **Active Biological Materials**. *Annu Rev Phys Chem* 2009, **60**::469-486.
10. Wang N, Tytell JD, Ingber DE: **Mechanotransduction at a distance: mechanically coupling the extracellular matrix with the nucleus**. *Nat Rev Mol Cell Biol* 2009, **10**:75–82.
11. Poh YC, Shevtsov SP, Chowdhury F, Wu DC, Na S, Dundr M, Wang N: **Dynamic force-induced direct dissociation of protein complexes in a nuclear body in living cells**. *Nat Commun* 2012, **3**:866.
12. Tajik A, Zhang Y, Wei F, Sun J, Jia Q, Zhou W, Singh R, Khanna N, Belmont AS, Wang N: **Transcription upregulation via force-induced direct stretching of chromatin**. *Nat Mater* 2016, **15**:1287–1296.
13. Thorpe SD, Lee DA: **Dynamic regulation of nuclear architecture and mechanics—a rheostatic role for the nucleus in tailoring cellular mechanosensitivity**. *Nucleus* 2017, **8**:287–300.
14. Fransz P, De Jong JH, Lysak M, Castiglione MR, Schubert I: **Interphase chromosomes**

in Arabidopsis are organized as well defined chromocenters from which euchromatin loops emanate. *Proc Natl Acad Sci U S A* 2002, **99**:14584–14589.

15. Bi X, Cheng YJ, Hu B, Ma X, Wu R, Wang JW, Liu C: **Nonrandom domain organization of the Arabidopsis genome at the nuclear periphery**. *Genome Res* 2017, **27**:1162–1173.
16. Fransz P, de Jong H: **From nucleosome to chromosome: a dynamic organization of genetic information**. *Plant J* 2011, **66**:4–17.
17. Liu C, Cheng YJ, Wang JW, Weigel D: **Prominent topologically associated domains differentiate global chromatin packing in rice from Arabidopsis**. *Nat Plants* 2017, **3**:742-748.
18. Wang C, Liu C, Roqueiro D, Grimm D, Schwab R, Becker C, Lanz C, Weigel D: **Genome-wide analysis of local chromatin packing in Arabidopsis thaliana**. *Genome Res* 2015, **25**:246–256.
19. Szabo Q, Bantignies F, Cavalli G: **Principles of genome folding into topologically associating domains**. *Sci Adv* 2019, **5(4):eaaw1**:1–12.
20. Furusawa T, Rochman M, Taher L, Dimitriadis EK, Nagashima K, Anderson S, Bustin M: **Chromatin decompaction by the nucleosomal binding protein HMGN5 impairs nuclear sturdiness**. *Nat Commun* 2015, **6**, **6138.**
21. Stephens AD, Banigan EJ, Adam SA, Goldman RD, Marko JF: **Chromatin and lamin A determine two different mechanical response regimes of the cell nucleus**. *Mol Biol Cell* 2017, **28**:1984–1996.
22. Poulet A, Duc C, Voisin M, Desset S, Tutois S, Vanrobays E, Benoit M, Evans DE, Probst A V, Tatout C: **The LINC complex contributes to heterochromatin organisation and transcriptional gene silencing in plants**. *J Cell Sci* 2017, **130**:590–601.
23. Gruenbaum Y, Foisner R: **Lamins: Nuclear Intermediate Filament Proteins with Fundamental Functions in Nuclear Mechanics and Genome Regulation**. *Annu Rev Biochem* 2015, **84**:131–164.
24. Gesson K, Rescheneder P, Skoruppa MP, Von Haeseler A, Dechat T, Foisner R: **A-type Lamins bind both hetero- and euchromatin, the latter being regulated by lamina-associated polypeptide 2 alpha**. *Genome Res* 2016, **26**:462–473.
25. Swift J, Ivanovska IL, Buxboim A, Harada T, Dingal PC, Pinter J, Pajerowski JD, Spinler KR, Shin JW, Tewari M, et al.: **Nuclear lamin-A scales with tissue stiffness and**

enhances matrix-directed differentiation. *Science (80-)* 2013, **341**:1240104.

26. Swift J, Discher DE: **The nuclear lamina is mechano-responsive to ECM elasticity in mature tissue**. *J Cell Sci* 2014, **127**:3005–3015.
27. Nmezi B, Xu J, Fu R, Armiger TJ, Rodriguez-Bey G, Powell JS, Ma H, Sullivan M, Tu Y, Chen NY, et al.: **Concentric organization of A- and B-type lamins predicts their distinct roles in the spatial organization and stability of the nuclear lamina**. *Proc Natl Acad Sci U S A* 2019, **116**:4307–4315.
28. Buxboim A, Swift J, Irianto J, Spinler KR, Dingal PC, Athirasala A, Kao YR, Cho S, Harada T, Shin JW, et al.: **Matrix elasticity regulates lamin-A,C phosphorylation and turnover with feedback to actomyosin**. *Curr Biol* 2014, **24**:1909–1917.
29. Fal K, Asnacios A, Chabouté M-E, Hamant O, Chaboute ME, Hamant O: **Nuclear envelope: a new frontier in plant mechanosensing?** *Biophys Rev* 2017, **9**:389–403.
30. Ciska M, Moreno Diaz de la Espina S: **The intriguing plant nuclear lamina**. *Front Plant Sci* 2014, **5**:166.
31. Masuda K, Xu ZJ, Takahashi S, Ito A, Ono M, Nomura K, Inoue M: **Peripheral framework of carrot cell nucleus contains a novel protein predicted to exhibit a long alpha-helical domain**. *Exp Cell Res* 1997, **232**:173–181.
32. Dittmer TA, Stacey NJ, Sugimoto-Shirasu K, Richards EJ: **LITTLE NUCLEI Genes Affecting Nuclear Morphology in Arabidopsis thaliana**. *Plant Cell* 2007, **19**:2793–2803.
33. Wang H, Dittmer TA, Richards EJ: **Arabidopsis CROWDED NUCLEI (CRWN) proteins are required for nuclear size control and heterochromatin organization**. *BMC Plant Biol* 2013, **13**:200.
34. Graumann K: **Evidence for LINC1-SUN associations at the plant nuclear periphery**. *PLoS One* 2014, **9**:e93406.
35. Goto C, Tamura K, Fukao Y, Shimada T, Hara-Nishimura I: **The Novel Nuclear Envelope Protein KAKU4 Modulates Nuclear Morphology in Arabidopsis**. *Plant Cell* 2014, **26**:2143–2155.
36. Mikulski P, Hohenstatt ML, Farrona S, Smaczniak C, Stahl Y, Kalyanikrishna, Kaufmann K, Angenent G, Schubert D: **The chromatin-associated protein pwo1 interacts with plant nuclear lamin-like components to regulate nuclear size**. *Plant Cell* 2019, **31**:1141–1154.
37. Rowat AC, Foster LJ, Nielsen MM, Weiss M, Ipsen JH: **Characterization of the elastic**

properties of the nuclear envelope. *J R Soc Interface* 2005, **2**:63–69.

38. Torbati M, Lele TP, Agrawal A: **Ultradonut topology of the nuclear envelope**. *Proc Natl Acad Sci* 2016, **113**:11094–11099.
39. Crisp M, Liu Q, Roux K, Rattner JB, Shanahan C, Burke B, Stahl PD, Hodzic D: **Coupling of the nucleus and cytoplasm: role of the LINC complex**. *J Cell Biol* 2006, **172**:41–53.
40. Graumann K, Runions J, Evans DE: **Characterization of SUN-domain proteins at the higher plant nuclear envelope**. *Plant J* 2010, **61**:134–144.
41. Zhou X, Graumann K, Evans DE, Meier I: **Novel plant SUN-KASH bridges are involved in RanGAP anchoring and nuclear shape determination**. *J Cell Biol* 2012, **196**:203–211.
42. Zhou X, Graumann K, Wirthmueller L, Jones JDG, Meier I: **Identification of unique SUN-interacting nuclear envelope proteins with diverse functions in plants**. *J Cell Biol* 2014, **205**:677–692.
43. Murphy SP, Simmons CR, Bass HW: **Structure and expression of the maize (Zea mays L.) SUN-domain protein gene family: evidence for the existence of two divergent classes of SUN proteins in plants**. *BMC Plant Biol* 2010, **10**:269.
44. Haque F, Lloyd DJ, Smallwood DT, Dent CL, Shanahan CM, Fry AM, Trembath RC, Shackleton S: **SUN1 interacts with nuclear lamin A and cytoplasmic nesprins to provide a physical connection between the nuclear lamina and the cytoskeleton**. *Mol Cell Biol* 2006, **26**:3738–3751.
45. Gundersen GG, Worman HJ: **Nuclear positioning**. *Cell* 2013, **152**:1376–1389.
46. Kim DH, Li B, Si F, Phillip JM, Wirtz D, Sun SX: **Volume regulation and shape bifurcation in the cell nucleus**. *J Cell Sci* 2015, **129**:457.
47. Schreiner SM, Koo PK, Zhao Y, Mochrie SGJ, King MC: **The tethering of chromatin to the nuclear envelope supports nuclear mechanics**. *Nat Commun* 2015, **6**:7159.
48. Sakamoto Y, Takagi S: **LITTLE NUCLEI 1 and 4 regulate nuclear morphology in Arabidopsis thaliana**. *Plant Cell Physiol* 2013, **54**:622–633.
49. Tamura K, Iwabuchi K, Fukao Y, Kondo M, Okamoto K, Ueda H, Nishimura M, Hara-Nishimura I: **Myosin XI-i links the nuclear membrane to the cytoskeleton to control nuclear movement and shape in Arabidopsis**. *Curr Biol* 2013, **23**:1776–1781.
50. Tamura K, Goto C, Hara-Nishimura I: **Recent advances in understanding plant nuclear envelope proteins involved in nuclear morphology**. *J Exp Bot* 2015, **66**:1641–

1647.

51. Meier I, Richards EJ, Evans DE: **Cell Biology of the Plant Nucleus. TL - 68**. *Annu Rev Plant Biol* 2017, **68 VN-r**:139–172.
52. Chambliss AB, Khatau SB, Erdenberger N, Robinson KD, Hodzic D, Longmore GD, Wirtz D, Robinson DK, Hodzic D, Longmore GD, et al.: **The LINC-anchored actin cap connects the extracellular milieu to the nucleus for ultrafast mechanotransduction**. *Sci Rep* 2013, **3**:1087.
53. Lombardi ML, Jaalouk DE, Shanahan CM, Burke B, Roux KJ, Lammerding J: **The interaction between nesprins and sun proteins at the nuclear envelope is critical for force transmission between the nucleus and cytoskeleton**. *J Biol Chem* 2011, **286**:26743–26753.
54. Osmanagic-Myers S, Foisner R: **The structural and gene expression hypotheses in laminopathic diseases - Not so different after all**. *Mol Biol Cell* 2019, **30**:1786–1790.
55. Dupont S, Morsut L, Aragona M, Enzo E, Giulitti S, Cordenonsi M, Zanconato F, Le Digabel J, Forcato M, Bicciato S, et al.: **Role of YAP/TAZ in mechanotransduction**. *Nature* 2011, **474**:179–183.
56. Jahed Z, Soheilypour M, Peyro M, Mofrad MR: **The LINC and NPC relationship - it's complicated! TL - 129**. *J Cell Sci* 2016, **129 VN-**:3219–3229.
57. Elosegui-Artola A, Andreu I, Beedle AEM, Lezamiz A, Uroz M, Kosmalska AJ, Oria R, Kechagia JZ, Rico-Lastres P, Le Roux AL, et al.: **Force Triggers YAP Nuclear Entry by Regulating Transport across Nuclear Pores**. *Cell* 2017, **171**:1397-1410 e14.
58. Jain N, Iyer K V, Kumar A, Shivashankar G V: **Cell geometric constraints induce modular gene-expression patterns via redistribution of HDAC3 regulated by actomyosin contractility**. *Proc Natl Acad Sci U S A* 2013, **110**:11349–11354.
59. Damodaran K, Venkatachalapathy S, Alisafaei F, Radhakrishnan A V., Jokhun DS, Shenoy VB, Shivashankar G V.: **Compressive force induces reversible chromatin condensation and cell geometry–dependent transcriptional response**. *Mol Biol Cell* 2018, **29**:3039–3051.
60. Zhang X, Cook PC, Zindy E, Williams CJ, Jowitt TA, Streuli CH, MacDonald AS, Redondo-Muñoz J: **Integrin α4β1 controls G9a activity that regulates epigenetic changes and nuclear properties required for lymphocyte migration**. *Nucleic Acids Res* 2015, **44**:3031–3044.
61. Alisafaei F, Jokhun DS, Shivashankar G V, Shenoy VB: **Regulation of nuclear**

architecture, mechanics, and nucleocytoplasmic shuttling of epigenetic factors by cell geometric constraints. *Proc Natl Acad Sci U S A* 2019, **16**:13200–13209.

62. Fernandez-Sanchez M-E, Brunet T, Röper J-C, Farge E: **Mechanotransduction's Impact on Animal Development, Evolution, and Tumorigenesis**. *Annu Rev Cell Dev Biol* 2015, **31**:373–397.
63. Le HQ, Ghatak S, Yeung C-YCY, Tellkamp F, Günschmann C, Dieterich C, Yeroslaviz A, Habermann B, Pombo A, Niessen CM, et al.: **Mechanical regulation of transcription controls Polycomb-mediated gene silencing during lineage commitment**. *Nat Cell Biol* 2016, **18**:864–875.
64. Horn HF, Brownstein Z, Lenz DR, Shivatzki S, Dror AA, Dagan-Rosenfeld O, Friedman LM, Roux KJ, Kozlov S, Jeang K-T, et al.: **The LINC complex is essential for hearing**. *J Clin Invest* 2013, **123**:740–750.
65. Hamant O, Heisler MG, Jonsson H, Krupinski P, Uyttewaal M, Bokov P, Corson F, Sahlin P, Boudaoud A, Meyerowitz EM, et al.: **Developmental patterning by mechanical signals in Arabidopsis**. *Science (80-)* 2008, **322**:1650–1655.
66. Janski N, Masoud K, Batzenschlager M, Herzog E, Evrard JL, Houlne G, Bourge M, Chaboute ME, Schmit AC: **The GCP3-interacting proteins GIP1 and GIP2 are required for gamma-tubulin complex protein localization, spindle integrity, and chromosomal stability**. *Plant Cell* 2012, **24**:1171–1187.
67. Batzenschlager M, Lermontova I, Schubert V, Fuchs J, Berr A, Koini MA, Houlne G, Herzog E, Rutten T, Alioua A, et al.: **Arabidopsis MZT1 homologs GIP1 and GIP2 are essential for centromere architecture**. *Proc Natl Acad Sci U S A* 2015, **112**:8656–8660.
68. Chumová J, Kourová H, Trögelová L, Halada P, Binarová P: **Microtubular and Nuclear Functions of γ-Tubulin: Are They LINCed?** *Cells* 2019, **8**:259.
69. Batzenschlager M, Masoud K, Janski N, Houlne G, Herzog E, Evrard JL, Baumberger N, Erhardt M, Nomine Y, Kieffer B, et al.: **The GIP gamma-tubulin complex-associated proteins are involved in nuclear architecture in Arabidopsis thaliana**. *Front Plant Sci* 2013, **4**:480.
70. Hu B, Wang N, Bi X, Karaaslan ES, Weber AL, Zhu W, Berendzen KW, Liu C: **Plant lamin-like proteins mediate chromatin tethering at the nuclear periphery**. *Genome Biol* 2019, **20**:1–18.
71. Hohenstatt ML, Mikulski P, Komarynets O, Klose C, Kycia I, Jeltsch A, Farrona S,

Schubert D: **PWWP-DOMAIN INTERACTOR OF POLYCOMBS1 interacts with polycomb-group proteins and histones and regulates arabidopsis flowering and development**. *Plant Cell* 2018, **30**:117-133.

72. Shivashankar G V: **Mechanical regulation of genome architecture and cell-fate decisions**. *Curr Opin Cell Biol* 2019, **56**:115–121.
73. Miroshnikova YA, Cohen I, Ezhkova E, Wickström SA: **Epigenetic gene regulation, chromatin structure, and force-induced chromatin remodelling in epidermal development and homeostasis**. *Curr Opin Genet Dev* 2019, **55**:46–51.
74. Goswami R, Asnacios A, Milani P, Graindorge S, Houlné G, Mutterer J, Hamant O, Chabouté M-E: **Mechanical Shielding in Plant Nuclei**. *Curr Biol* 2020, in press.

Figure legends

Figure 1: Changes of cell and nuclear shapes under mechanical stress.
Under high cell stress, the nucleus is more compact with nucleoskeleton enrichment and spatial chromatin reorganization

Figure 2: The features of chromatin under mechanical stress
Changes of nuclear architecture under mechanical stress lead to chromatin condensation, clustering of chromocenters, repressive histone mark modifications inducing altered accessibility for the transcription of differentiated gene, and release of transcription factors from the nuclear periphery

Figure 3: Nuclear mechanical response in plants under hyperosmotic stress
Upon hyperosmotic stress, the nucleus is more compact with clustered chromocenters and induction of touch-response gene expression. The nuclear envelope proteins GIPs may act as negative regulators of this response.

Objective of the thesis

Mechanical signaling has been increasingly integrated into biological processes during the last few decades. For instance, the physical properties of cell is modulated via the stiffness of the matrix (Engler *et al.*, 2006b), of the cytoskeleton (Durand-Smet *et al.*, 2014b), and this can span to the nucleus (LOVETT *et al.*, 2013) resulting in changes in gene expression (Alam *et al.*, 2016b). Although most of the focus has been on cortical mechanosensing (i.e. matrix, plasma membrane and cytoskeleton), the idea that nucleus may be an active mechanosensitive element has gained momentum during the past few years (Wang *et al.*, 2009b): How does mechanical forces affect nuclear morphology and mechanics? How is this signal selectively transmitted to the nucleus? Is the nuclear envelope only a platform and gate between two cellular compartments, or has it an active mechanical role? Does mechanical stress directly affect chromatin organization and gene expression – globally or specifically?

The goal of my thesis is to decipher the role of nuclear envelope in nuclear mechanotransduction taking *Arabidopsi*s root meristem as a model system. Using hyperosmotic stress as an experimental physiological mechanical stress, I study the impact of osmolarity on nucleus shape and stiffness, linking it with chromatin remodeling and gene expression. Then I investigate the roles of actors at the nuclear envelope which regulate nuclear shape, focusing on GIP proteins. These regulatory proteins are found in both nuclear and cytosolic compartments close to the nuclear envelope, in connection with centromeric heterochromatin and microtubules, respectively (Janski *et al.*, 2012; Batzenschlager *et al.*, 2013, 2015), making them ideal transduction candidates between the cytosol and the nucleus. Then, due to the involvement of CRWN1 and CRWN4 in maintaining chromatin organization at the nuclear periphery (Wang *et al.*, 2013; Hu *et al.*, 2019), I compare the potential contribution of the nucleoskeleton elements in the hyperosmotic stress response in meristematic cells to that of GIP. Finally, by observing the effect of the cell wall property on nuclear phenotype, I study the effect of *in situ* changes in mechanical properties of the cell cortex on nucleus features, with or without hyperosmotic stress. Altogether, the goal of this PhD is to provide the first bases of the nuclear mechanotransduction in Arabidopsis.

Chapter I

Morphomechanics of nuclei:

linking subcellular form and function in *Arabidopsis*

Preface-

The function of the nucleus is not limited to transcription, DNA replication and repair; the nucleus is also physical object which contributes to mechanosensing and mechanotrasnduction. As discussed in the introduction, mechanical signals can reach the nuclear envelope to modify genome architecture and to induce responsive genes. Nuclear size, shape and mechanics can vary inter and intra cellularly depending on form and function of the cell. But typically, nucleus is the largest (with a diameter of ~5 to 20 μm) and the stiffest organelle inside a cell(Dahl *et al.*, 2008). Being such a structural element inside the cell, it is thus not surprising to find interplays between the mechanical properties of the nucleus and its functions.

The nuclear envelope is a barrier at the nucleo-cytpoplasmic interface of a eukaryotic cell. It also has its own mechanical properties, notably thanks to its nucleoskeleton at the nucleus cortex and thanks to chromatin inside the nucleus. In this first chapter, I studied the changes of nuclear shape and mechanics under hyper and hypoosmotic stress, while also linking these parameters to gene expression levels.

Hyper osmotic stress, such as salt or mannitol stresses, are known to induce array of stress responsive genes (Seki *et al.*, 2002; Sewelam *et al.*, 2014; Ghorbani *et al.*, 2019)in abscisic acid dependent and independent pathway ensuring stress tolerance and response (Yamaguchi-Shinozaki & Shinozaki, 2006). For instance, *Arabidopsis* microarray gene expression data by meta-analysis approach shows a set of 4540 up-regulated Differential Expressed Genes (DEGs) in the leaf tissue among which 1643 (36%) and 2897 (64%) of them were up-regulated in response to drought and salt stress, respectively. While, 6906 DEGs were upregulated in root tissue (1.5- fold higher than leaves) among which 3150 (46%) and 3756 (54%) were in response to drought and salt stress, respectively (Ghorbani *et al.*, 2019). In each tissue major transcription factors families were induced by these osmotic stresses and belong to AP2/ERF, MYB and NAC as well as bZIP, HSF, C2H2 and WRKY transcription factor families (Ghorbani *et al.*, 2019). In an earlier study, the dehydration response after 24h has been shown to upregulate genes which are important in the mechanical stress response after (105 out of 421 dehydration induced genes overlapped with touch induced genes) including 33 xyloglucan endotransglucosylase/hydrolase (XTH), 10 calmodulin-like (CML) protein genes(Urano *et al.*, 2016). This suggests a strong coupling between osmotic and mechanical stress, and a role of the nucleus, through transcription, in this process.

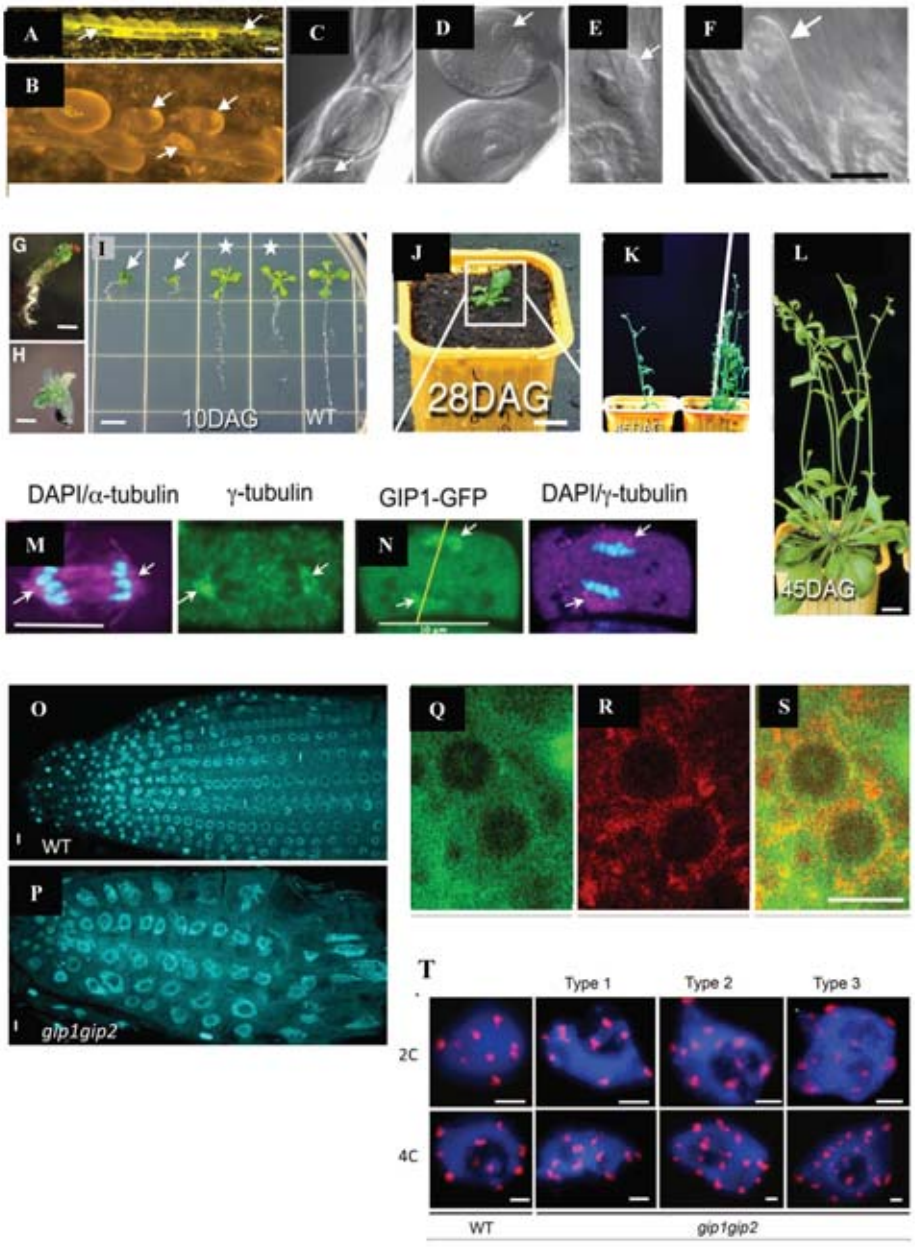

Figure 1. Defective developmental stages of *gip1gip2* and colocalization of GIP with gamma tubulin/ Microtubule cytoskeleton and ER components

(A-L) Absence of GIPS in *gip1gip2* knockdown mutant generates phenotypic change at the organism level. Adapted from Janski *et al.,* (2012).

(M-N) GIP1-GFP colocalises with gamma tubulin (N) which colocalises with alpha tubulin (magenta) (M). Gamma tubulin (M) and GIP1 (N) are green. Chromatin is stained with DAPI (Cyan). Adapted from Janski *et al.,* (2012).

(O-P) Nuclear shape and root meristem organisation are disturbed in *gip1gip2* double mutant. Adapted from Batzenschlager *et al.,* (2013).

(Q-S) Colocalization (S) of AtGIP1-GFP (green) (Q) and the ER AtTSA1 (red) (R) proteins observed at the nuclear envelope. Adapted from Batzenschlager *et al.,* (2013).

(T) Defective centromeric cohesion is observed in *gip1gip2*. Centromeric signals are labelled by the 180 pb centromeric repeats (FISH probe) and chromatin is DAPI stained (Blue). Adapted from Batzenschlager *et al.,* (2015).

At the chromosomal level hyperosmotic stress is able to act and change chromatin structure. For example, when protoplasts isolated from root-tip cells of *Triticum turgidum* are subjected to a short term (30 mins) but high osmotic stress of 1M mannitol, chromatin coalescence occurs and chromosomes also form a clustered mass which is separated from the nuclear envelope in interphase cells (Komis *et al.*, 2002). Later Wang et al., showed in Arabidopsis plants subjected to PEG that the relative heterochromatic fraction is increasing due to the clustering of chromocenters upon hyperosmotic stress in root meristematic cells (Wang *et al.*, 2015). Because nuclear mechanics also depend on chromatin status, this suggests that osmotic stress may change the mechanical properties of the nucleus.

Next, I focus on analysis the nuclear response and physiological correlation in *gip1gip2* plants under hyperosmotic stress where the small regulatory GIP (GCP (gamma tubulin complex protein) 3 interaction Protein) proteins are knocked-down. There are two GIP proteins present in *Arabidospis*, GIP1 has 71 amino acids with a molecular weight of 7.8 kDa and GIP2 is 7.4 kDa having 67 amino acids. At the structural level three alpha helixes are present in each protein (Batzenschlager *et al.*, 2013). Homologues of GIP are found is several organisms including *S. pombe* and mammals but not in *S. cerevisiae,* and GIPs show wide conservation from fungi to humans. In plants, a GIP gene duplication was observed and might be linked to the conquest of terrestrial habitats. These proteins are very conserved among plant species, where AtGIP1 may shares sequence identity varying from 41 to 78%.

GIPs are found associated with the MT nucleation complexes (Janski *et al.*, 2012), as shown for the human GIP homologue MOZART1, and are crucial for proper formation of mitotic spindle as for GIPs (Hutchins *et al.*, 2010; Janski *et al.*, 2012). In eukaryotes, these GIP homologues are found important in regards with MT nucleation and MT organisation arrays (Lin *et al.*, 2016; Huang *et al.*, 2020).

Knockdown *gip1gip2* plants show pleiotropic phenotypes in development, notably a reduced growth at the root and shoot levels and plants were sterile (Janski *et al.*, 2012) (Figures 1A - 1L). The root meristem organization is impaired and the cellular level the morphology is disturbed with often large irregular and bulging shape (Janski *et al.*, 2012). The double mutant exhibits higher ploidy level with the presence of aneuploidy too (Batzenschlager *et al.*, 2015) and as a consequence considerably enlarged nucleus in all the plant tissue irrespective of differentiated or undifferentiated (Figures 1O - 1P). Morphology of the nucleus is disturbed as well with a lobulated wavy nuclear phenotype (Janski *et al.*, 2012). NPC density and shape are

altered in *gip1gip2*, as well as an irregular distribution of the inner nuclear membrane marker AtSUN1(Batzenschlager *et al.*, 2013) indicating highly disorganized nuclear envelope. GIP proteins have unique dual localization in *Arabidopsis* at the centromere and microtubule nucleation sites (Janski *et al.*, 2012; Batzenschlager *et al.*, 2015). Notably they are found located at the nuclear envelope in interphase cells. GIPs form a protein complex with the variant histone CENH3 – a marker of the centromere in cycling cells, and are important for ensuring proper recruitment of CENH3 at the centromere. In the mutant *gip1gip2*, the centromeric cohesion is also impaired (Batzenschlager *et al.*, 2015) (Figure 1T). GIPs also interact with TSA1, described as TONSOKU (TSK)-associating protein where TSK/MGO3/BRU1 is described as a nuclear factor involved in DNA damage responses and epigenetic gene regulation (Takeda *et al.*, 2004) (Figures 1Q - 1S). TSA1 is found associated at the nuclear envelope and with endoplasmic reticulum (Batzenschlager *et al.*, 2013).

Changed nuclear morphology of *gip1gip2* is associated with reduced levels of GIP1 and GIP2 in both compartments of the cell – nucleus and cytoplasm. GIP are dynamic molecules at the nuclear envelope (Batzenschlager *et al.*, 2013) with regulatory roles at the nucleocytoplastic interface in plant cells, by helping the microtubule nucleation recruitment at the outer nuclear membrane (Figures 1M -1N) and centromere regulation close to the chromocenters at the inner nuclear membrane. Because of its key role in cytoskeleton and chromatin organization GIPs may have important functions in nuclear mechanics and possibly nuclear mechanotransduction.

In this chapter we show that the nuclear stiffness correlates with hyper and hypo - osmotic stresses leading to differential expression of mechanically induced genes. We also show that *gip1gip2* mimics the hyperosmotic stress response, with stiff nuclei and enhanced expression of mechanosensitive genes. This chapter includes an article that was recently published in Current Biology (Goswami *et al.*, 2020), and an additional discussion about the regulation of mechanically induced genes.

Article

Current Biology

Mechanical Shielding in Plant Nuclei

Graphical Abstract

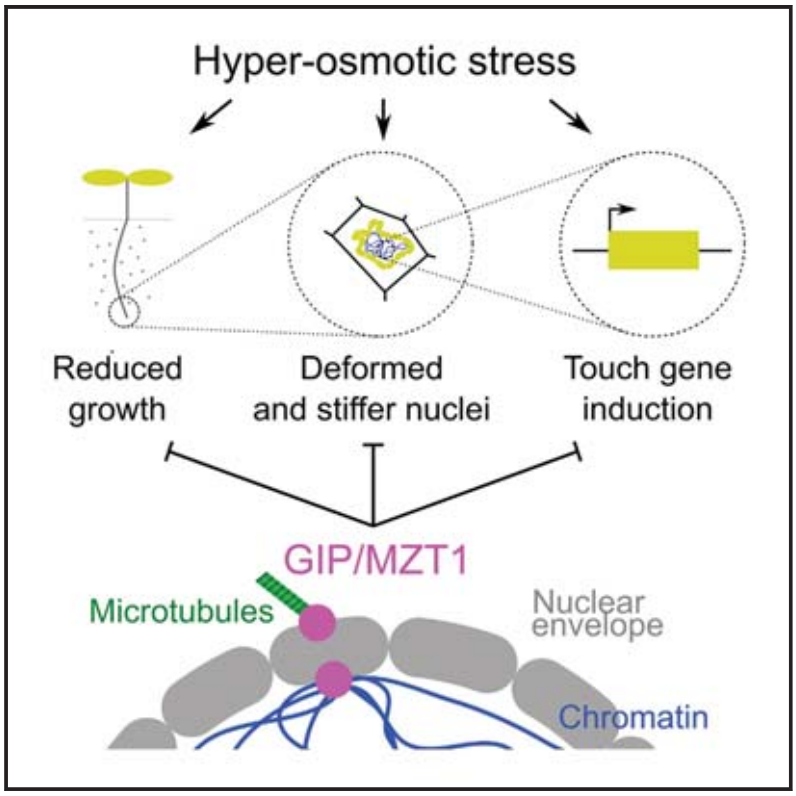

Authors

Rituparna Goswami, Atef Asnacios, Pascale Milani, ..., Jérôme Mutterer, Olivier Hamant, Marie-Edith Chabouté

Correspondence

olivier.hamant@ens-lyon.fr (O.H.), marie-edith.chaboute@ibmp-cnrs.unistra.fr (M.-E.C.)

In Brief

Goswami et al. unravel the nuclear response to hyperosmotic stress in plants. Nuclear shrinking and stiffening correlate with high expression levels of touch response genes. The functional analysis of the GIP/MZT1 proteins reveals a role of nuclear envelope factors in this response and may help us to better understand how plants resist drought.

Highlights

- Hyperosmotic stress reversibly leads to stiffer and smaller nuclei in *Arabidopsis*
- Hyperosmotic stress reversibly induces the expression of touch response genes
- The nucleus response to hyperosmotic stress is phenocopied in the *gip1gip2* mutant
- The *gip1gip2* mutant exhibits enhanced resistance to hyperosmotic stress

Goswami et al., 2020, Current Biology *30*, 1–13
June 8, 2020
https://doi.org/10.1016/j.cub.2020.03.059

CellPress

Please cite this article in press as: Goswami et al., Mechanical Shielding in Plant Nuclei, Current Biology (2020), https://doi.org/10.1016/j.cub.2020.03.059

Current Biology
Article

Mechanical Shielding in Plant Nuclei

Rituparna Goswami,[1,2] Atef Asnacios,[3] Pascale Milani,[4] Stéfanie Graindorge,[1] Guy Houlné,[1] Jérôme Mutterer,[1] Olivier Hamant,[2,*] and Marie-Edith Chabouté[1,5,*]
[1]Institut de Biologie Moléculaire des Plantes, CNRS, Université de Strasbourg, Strasbourg 67084, France
[2]Laboratoire de Reproduction et Développement des Plantes, Université de Lyon, UCB Lyon 1, ENS de Lyon, INRAE, CNRS, Lyon 69364, France
[3]Laboratoire Matière et Systèmes Complexes, Université de Paris, CNRS, Université Paris-Diderot, Paris 75013, France
[4]BioMéca, ENS de Lyon, Lyon 69364, France
[5]Lead Contact
*Correspondence: olivier.hamant@ens-lyon.fr (O.H.), marie-edith.chaboute@ibmp-cnrs.unistra.fr (M.-E.C.)
https://doi.org/10.1016/j.cub.2020.03.059

SUMMARY

In animal single cells in culture, nuclear geometry and stiffness can be affected by mechanical cues, with important consequences for chromatin status and gene expression. This calls for additional investigation into the corresponding physiological relevance in a multicellular context and in different mechanical environments. Using the *Arabidopsis* root as a model system, and combining morphometry and micro-rheometry, we found that hyperosmotic stress decreases nuclear circularity and size and increases nuclear stiffness in meristematic cells. These changes were accompanied by enhanced expression of touch response genes. The nuclear response to hyperosmotic stress was rescued upon return to iso-osmotic conditions and could even lead to opposite trends upon hypo-osmotic stress. Interestingly, nuclei in a mutant impaired in the functions of the gamma-tubulin complex protein 3 (GCP3) interacting protein (GIP)/MZT1 proteins at the nuclear envelope were almost insensitive to such osmotic changes. The *gip1gip2* mutant exhibited constitutive hyperosmotic stress response with stiffer and deformed nuclei, as well as touch response gene induction. The mutant was also resistant to lethal hyperosmotic conditions. Altogether, we unravel a stereotypical geometric, mechanical, and genetic nuclear response to hyperosmotic stress in plants. Our data also suggest that chromatin acts as a gel that stiffens in hyperosmotic conditions and that the nuclear-envelope-associated protein GIPs act as negative regulators of this response.

INTRODUCTION

All living organisms are able to sense and respond to mechanical forces during their development [1]. Typically, in animal cells, mechanical stress affects the cytoskeleton at the cell cortex [2]. Mechanical stress also has intracellular effects on nuclear shape and stiffness [3, 4], and this may ultimately impact 3D chromatin organization and gene expression [5–8]. This either implies propagation of mechanical signals through the nucleus via biochemical cascades, or more directly through the linker of nucleoskeleton and cytoskeleton (LINC) complexes at the nuclear envelope [9–11]. Thus, the stress born by the cytoskeleton can be transmitted to the nucleoskeleton, composed of lamins, and to chromatin [12–14]. Changes in tension levels at the nuclear envelope can also impact the entry of transcription factors [15]. Yet the interplay between nuclear shape and stiffness, and its contribution to nuclear function, are still not fully understood in animals [16–18] and are completely unknown in plants.

Mechanical stress can be induced by changing osmotic conditions, through modification of the internal hydrostatic pressure that affects the cell cortex [19]. Thus, the role of membrane tension in cell polarity can be revealed by modifying the osmolarity of the medium in which single cells in culture are kept [20]. Hyperosmotic stress was also shown to shrink the nucleus through an uneven distribution of macromolecules between cytoplasm and nucleoplasm [21] and to affect gene expression by modifying chromatin compaction [3]. Under natural conditions, high salinity and drought are the most frequent causes of osmotic stress in plants [22]. Osmotic stress leads to changes in chromatin remodeling and gene expression to protect the cell [23–25].

As in animals, gene expression in plants is in part under mechanical control. For instance, the expression of 2.5% of the genome is significantly affected by a gentle touch in *Arabidopsis* [26, 27]. Furthermore, the expression of the transcription factor *PtaZFP2* linearly correlates with stem bending in poplar [28], and the expression level of the homeodomain master regulator SHOOT MERISTEMLESS scales to tissue folding and can be induced by mechanical perturbation during organogenesis at the shoot apical meristem [29]. Yet whether osmotic conditions affect nuclear mechanics and shape and whether gene expression relates to such modifications is unknown.

Variation in nuclear shape is observed in mutants impaired in LINC components or in plant-specific proteins found at the nuclear envelope. Among them are the plant lamin-like proteins (KAKU4, NEAP, and CRWN1–4) [30–33], as well as the human MZT1 homologs, gamma-tubulin complex protein 3 (GCP3) interacting proteins (GIPs) 1 and 2 [34]. GIP1 and GIP2 are associated with the microtubule nucleation complexes via the GCP3 [35, 36]. They are also found to be associated with centromeric

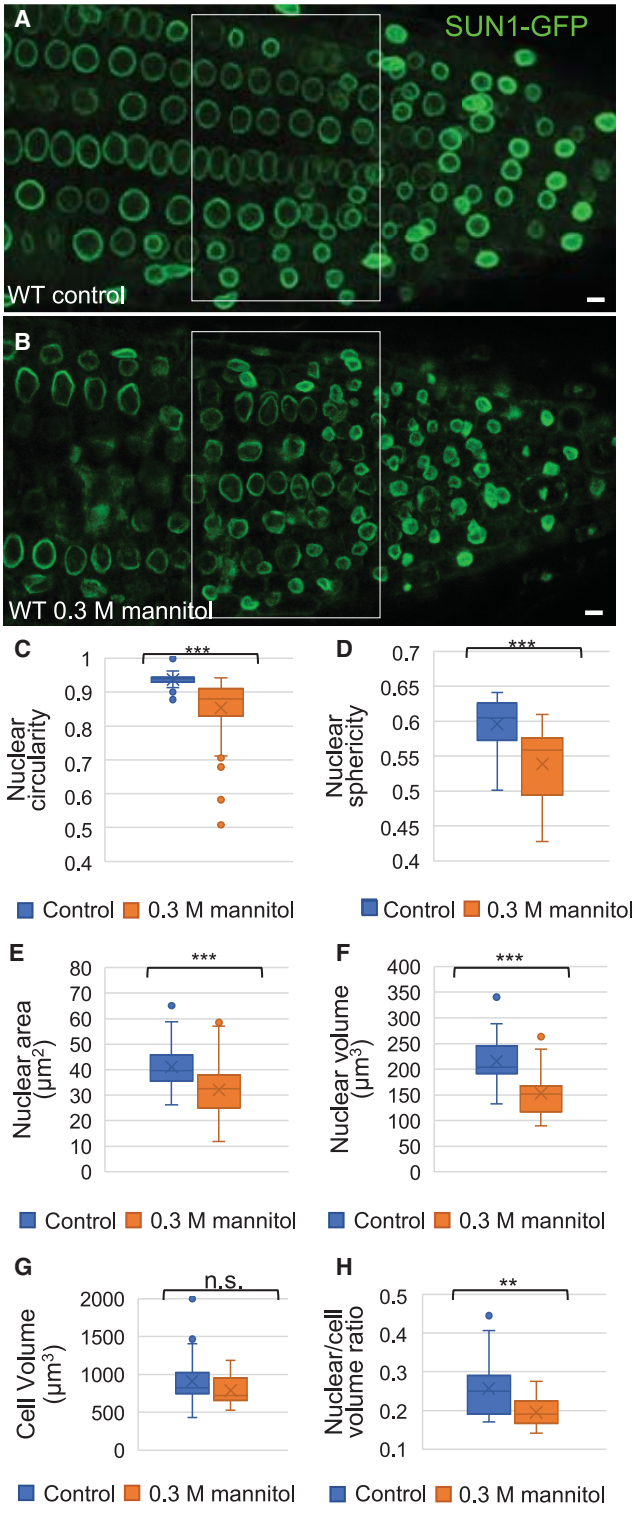

Figure 1. Nuclear Shape Is Altered in the Presence of Hyperosmotic Stress in WT *Arabidopsis* Root Tips

(A and B) Confocal analysis of nuclear shape in root tips of 9-day-old seedlings expressing SUN1-GFP in absence (A) or presence (B) of a 16-h-long treatment with 0.3 M mannitol (Z max, optical sections of 0.7 μm). Representative images are presented. Scale bars, 5 μm.

(C–F) Quantification of various nuclear parameters in 2D and 3D dimensions. Measurements were performed in the region delineated by the white frame in (A) and (B). In 2D, nuclear circularity (C) and nuclear area (E) were evaluated on control (n = 99) and treated (n = 98) plants. The p values after Student's t test are 3.23e−16 and 2.12e−11, indicating significant differences between the data; ***p < 0.001. In 3D, nuclear sphericity (D) and volume (F) were evaluated on control and treated plants (n = 20). The p values after Student's t test are 0.0006 and 0.00012, respectively, indicating significant differences between the data; ***p < 0.001.

(G and H) Differential effects of osmotic stress on cell and nuclear volumes. Cell volume (G) and nuclear/cell volume ratio (H) were also evaluated on the same samples used for 3D measurements. The p values after Student's t test are 0.193 and 0.0001, indicating non-significant differences in changes in cell volume between control and treated samples but a significant change in nuclear/cell volume (***p < 0.001) related to main change of nuclear volume in response to hyperosmotic stress.

See also Figure S1.

chromatin [34, 37] (see Figure 2A). Here, we explore the relation between nuclear stiffness and morphology in the multicellular context of the *Arabidopsis* root tip. Combining hyperosmotic stress, *gip1gip2* mutations, nuclear shape, and micro-rheometric measurements, as well as RNA sequencing (RNA-seq) analysis, we show that nuclear stiffness and touch gene expression scale with the osmotic environment of the cell. In addition, we show that plants defective in GIP proteins exhibit this response constitutively, correlating with an increased ability of the plant to resist hyperosmotic stress.

RESULTS

Hyperosmotic Stress Decreases Nuclear Circularity and Size in Root Tip Cells

Building on results obtained in animal cells where osmotic stress affects nuclear shape [21], we tested the nuclear response to hyperosmotic stress in *Arabidopsis* root tips. Nine-day-old *Arabidopsis* seedlings expressing the nuclear envelope SUN1-GFP marker [38] were exposed to 0.3 M mannitol for 16 h (Figure 1). Nuclear shape was analyzed by confocal microscopy, focusing on the central part of the root meristem and the external layers of the root (epidermis and cortex; see white frames in Figures 1A and 1B).

Whereas most nuclei displayed round shapes in untreated seedlings, the treated nuclei exhibited irregular shapes and reduced size (Figures 1A and 1B). Nuclear circularity was equal to 0.936 ± 0.001 in control seedlings (n = 99) and 0.854 ± 0.008 in treated seedlings (n = 98), which is significantly different from the control (p = 3.23e−16; Figure 1C). Nuclear area reached 75% of its initial area, from 41.1 ± 0.8 μm^2 in untreated seedlings to 32.1 ± 1.0 μm^2 in treaded seedlings (p = 1.63e−11; Figure 1E). Similar findings were observed when considering the 3D nature of the nuclei (see Method Details): nuclear sphericity decreased from 0.59 ± 0.01 in control plants (n = 20) to 0.53 ± 0.01 in treated plants (n = 20; p = 0.0006; Figure 1D) and, upon hyper-osmotic stress, nuclear volume reached 71% of its initial volume (n = 20; p = 0.0001; Figure 1F). As the trends in 2D and 3D are comparable, and because 3D measurements are more difficult to extract in our confocal microscopy setup, we mainly focused our analysis on 2D measurements in the following experiments.

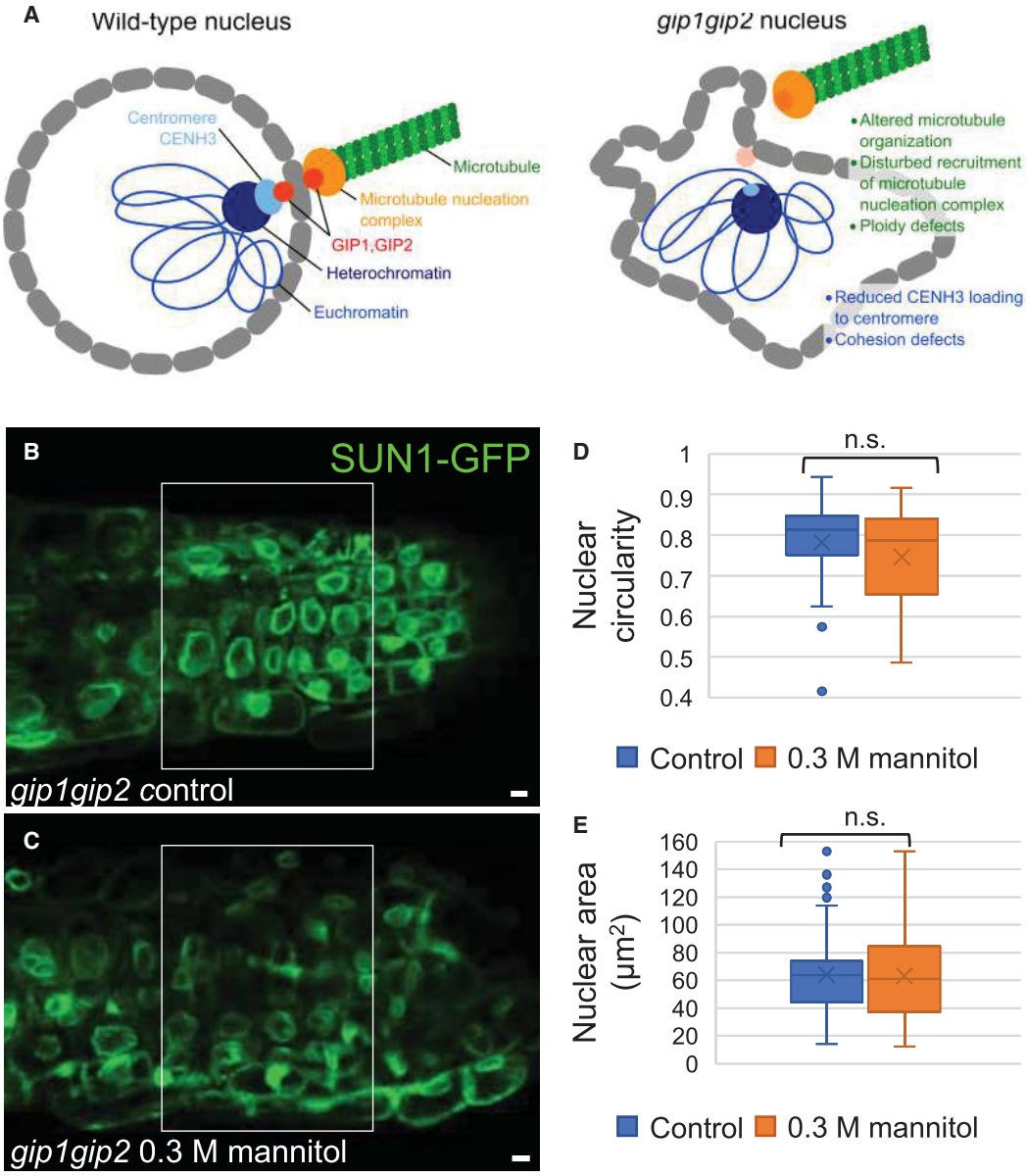

Figure 2. Nuclear Shape Defects Are Stable in the *gip1gip2 Arabidopsis* Root Tip upon Hyperosmotic Stress

(A) Graphical representation (not to scale) of the localization of GIP protein in normal WT conditions and *gip1gip2* knocked down phenotype at the sub-cellular level.

(B and C) Confocal analysis of nuclear shape in root tips (Z max, optical sections of 0.7 μm) in 9-day-old *gip1gip2* seedlings expressing SUN1-GFP in absence (B; n = 74) or presence (C; n = 45) of a 16-h-long treatment with 0.3 M mannitol. Scale bars, 5 μm.

(D and E) Quantification of nuclear parameters, circularity (D) and nucleus area (E), was evaluated on control and treated plants. The p values after Student's t test are 0.11 and 0.87, respectively, indicating no significant differences between the data (n.s.). Measurements were performed in the region delineated by the white frame in (B) and (C).

See also Figure S2.

Interestingly, under lower osmotic stress conditions, i.e., 0.15 M mannitol, no nuclear deformation could be detected in root meristems, indicating the presence of a threshold in the response ($n_{control} = 54$; $n_{treated} = 68$; $p = 0.16$ and 0.17 for nuclear circularity and area, respectively; Figures S1A–S1D). To confirm that the response is not mannitol specific, we also tested another osmolyte. A 0.15 M NaCl treatment, similar in osmolarity to 0.3 M mannitol, induced a decrease in nuclear circularity and area comparable to that observed with 0.3 M mannitol (circularity of 0.84 ± 0.01 and area of 32.0 ± 1.8 μm^2 after treatment; $n_{control} = 91$; $n_{treated} = 51$; $p = 1.98e{-}8$ and 0.0043, respectively; Figures S1E–S1H).

In order to see whether changes in nuclear geometry could reflect changes in cell shape [39], we analyzed cytoplasmic

detachment from the cell wall in our root meristem under hyperosmotic stress (0.3 M mannitol). This effect was mild, and the overall cell shape was not modified (Figures S1I–S1K; see white arrows in Figures S1J and S1K). As the impact on the nucleus is in contrast severe, the nucleocytoplasmic volume ratio decreased significantly from 0.25 ± 0.01 to 0.19 ± 0.01 (n = 20; p = 0.0022), although the cell volume remained unchanged (p = 0.19; Figures 1G and 1H). Altogether, this demonstrates that hyperosmotic shock in root meristems decreases nuclear circularity and area without significantly changing cell volume.

Nuclear Shape Defects in *gip1gip2* Mimic Hyperosmotic Stress

The *gip1gip2* knocked down mutant is impaired in the recruitment of microtubule nucleation complexes and centromeric chromatin architecture, leading to ploidy defects [36, 37] (Figure 2A). The mutant also exhibits severe developmental defects. Root growth is altered and is variable from mild to strong phenotype (Figure S2A). As previously shown, root meristem nuclei from *gip1gip2* SUN1-GFP seedlings exhibit shape defects [34] (Figure 2B) that resemble that of wild-type (WT) nuclei under hyperosmotic stress (Figure 1B). To go beyond this qualitative comparison, we characterized the nuclear shape of the mutant. Nuclear circularity in *gip1gip2* was equal to 0.78 ± 0.01 (n = 74; Figure 2D), which was significantly lower than the untreated WT (0.936 ± 0.001; n = 99; p = 2.19e−26; see Figure 1C). However, nuclear area was increased in *gip1gip2* and reached 63.8 ± 3.5 μm^2 on average (n = 74; Figure 2E) to compare to 41.1 ± 0.8 μm^2 in untreated WT (n = 99; p = 9.79e−12; see Figure 1D). Increased average nuclear area may relate to increased ploidy levels in the mutant [36, 37]. In order to compare nuclear area between WT and mutant independently of ploidy, we analyzed 2C flow-sorted root nuclei. The 2C WT and 2C *gip1gip2* nuclei exhibited an area of 31.1 ± 2.1 μm^2 and 21.4 ± 1.8 μm^2, respectively. Thus, 2C *gip1gip2* nuclei exhibit significantly smaller nuclei when compared with 2C WT nuclei ($n\ 2C_{WT}$ = 18 and $n\ 2C_{gip1gip2}$ = 19; p = 0.0014; Figure S2F). This demonstrates that *gip1gip2* has more compact nuclei than the WT nuclei. This confirms that *gip1gip2* nuclei fully mimic WT nuclei under hyperosmotic stress, at least from a geometric standpoint.

Next, we investigated whether hyperosmotic stress could aggravate the *gip1gip2* phenotype. To do so, we treated *gip1-gip2* seedlings with 0.3 M mannitol, as shown above for the WT. In such conditions, no more deformation was observed in *gip1gip2* nuclei (Figures 2B and 2C): nuclear circularity (0.74 ± 0.02; n = 45) and nuclear area (62.8 ± 5.5 μm^2; n = 45) were not significantly different from the untreated *gip1gip2* control (0.78 ± 0.01 and 63.8 ± 3.5 μm^2, respectively; n = 74; p = 0.118 and 0.875, respectively; Figures 2D and 2E). Note that we reached the same conclusions when analyzing *gip1gip2* seedlings with milder phenotypes (Figures S2B–S2E). Altogether, these results suggest that *gip1gip2* may constitutively activate a hyperosmotic-like response.

gip1gip2 Mutants Resist High Hyperosmotic Stress

If the *gip1gip2* mutant nuclei already exhibit a hyperosmotic-like response, this may also prime the plant to resist to hyperosmotic conditions. In order to test that hypothesis, we analyzed the mutant phenotype upon 0.4 M and 0.6 M mannitol treatment. In these severe hyperosmotic conditions, widespread cell death occurred in WT root meristems (Figures 3A and 3B). In contrast, most of the *gip1gip2* root tip cells from seedlings, exhibiting a mild phenotype, survived the treatment (Figures 3A and 3B).

In the surviving WT cells, nuclei were strongly deformed upon treatment with 0.4 and 0.6 M mannitol, when compared with iso-osmotic control, showing nuclear circularity of 0.81 ± 0.01 and 0.84 ± 0.01, respectively, compared with 0.85 ± 0.01 in control, and nuclear area of 31.9 ± 1.4 and 28.6 ± 1.1 μm^2, respectively, compared with 43.7 ± 1.7 in control ($n_{control}$ = 38; $n_{0.4\ M}$ = 39; $n_{0.6\ M}$ = 41; p values for control versus 0.4 M and control versus 0.6 M are 2.903e−9 and 1.51e−6 and 1.60e−10 and 3.58e−10 for nuclear circularity and area, respectively; Figures 3C and 3D). Furthermore, when compared with 0.3 M mannitol (nuclear circularity = 0.85 ± 0.01 and nuclear area = 32.1 ± 1.0 μm^2) (Figures 1C and 1E), nuclear circularity was even more reduced at 0.4 M mannitol (p = 0.038), and the nuclear area was lower at 0.6 M mannitol (p = 0.019). No significant differences were observed between 0.4 M and 0.6 M mannitol (p = 0.094 and 0.075, respectively, for nuclear circularity and area; Figures 3C and 3D). This indicates a threshold in the response to hyperosmotic stress for the WT. In contrast, the *gip1gip2* nuclear shapes remained unchanged in these harsher osmotic conditions ($n_{control}$ = 58; $n_{0.4\ M}$ = 22; $n_{0.6\ M}$ = 43; p values, control versus 0.4 M and control versus 0.6 M, are 0.33 and 0.61 and 0.99 and 0.53 for nuclear circularity and area, respectively; Figures 3E and 3F). This suggests that a maximum of nuclei deformation exists in the WT and that *gip1gip2* already reaches it in control conditions.

To test how the *gip1gip2* mutant root grows in such harsh osmotic conditions, we analyzed the impact of such conditions on root length in the WT and mutant. Nine-day-old seedlings were grown in normal conditions and then transferred on 0.4 M and 0.6 M mannitol for 2 days. In the WT, final root length was decreased by a factor 5 after transfer to 0.4 M (n = 13; p = 3.8e−7) and by a factor 18 after transfer to 0.6 M mannitol (n = 12; p = 3.54e−5; Figure 3G). Although we also saw an impact on root length in *gip1gip2*, this was much milder: final *gip1gip2* root length was decreased by a factor 2 after transfer to 0.4 M (n = 10; p = 0.0029) and by a factor 4.4 after transfer to 0.6 M mannitol (n = 13; p = 1.74e−6; Figures 3G and S3A). Note that the *gip1gip2* mutant also seemed to resist to such harsh conditions even in the long term: after 15 days in harsh osmotic conditions, the *gip1gip2* exhibited reduced leaf senescence when compared with the WT (n = 14; Figures 3H and 3I).

Next, we measured root growth for 5 days in our standard hyperosmotic conditions (0.3 M mannitol) using WT as well as mild and severe *gip1gip2* mutants. As expected, in these conditions, root growth was dramatically reduced in the WT (Figure 3J; $n_{control}$ = 6; $n_{treated}$ = 7; $p < 0.01$). In contrast, compared with the untreated control, root growth was only slightly affected in the mild *gip1gip2* mutants ($n_{control}$ = 7; $n_{treated}$ = 6; $0.05 < p < 0.01$; Figures 3I and S3B) and unchanged in the severe *gip1gip2* mutants ($n_{control}$ = 6; $n_{treated}$ = 7; $p > 0.05$; Figures 3J and S3B).

Altogether, we identify three nuclear responses to hyperosmotic stress in the WT: up to 0.15 M mannitol, nuclear shape is

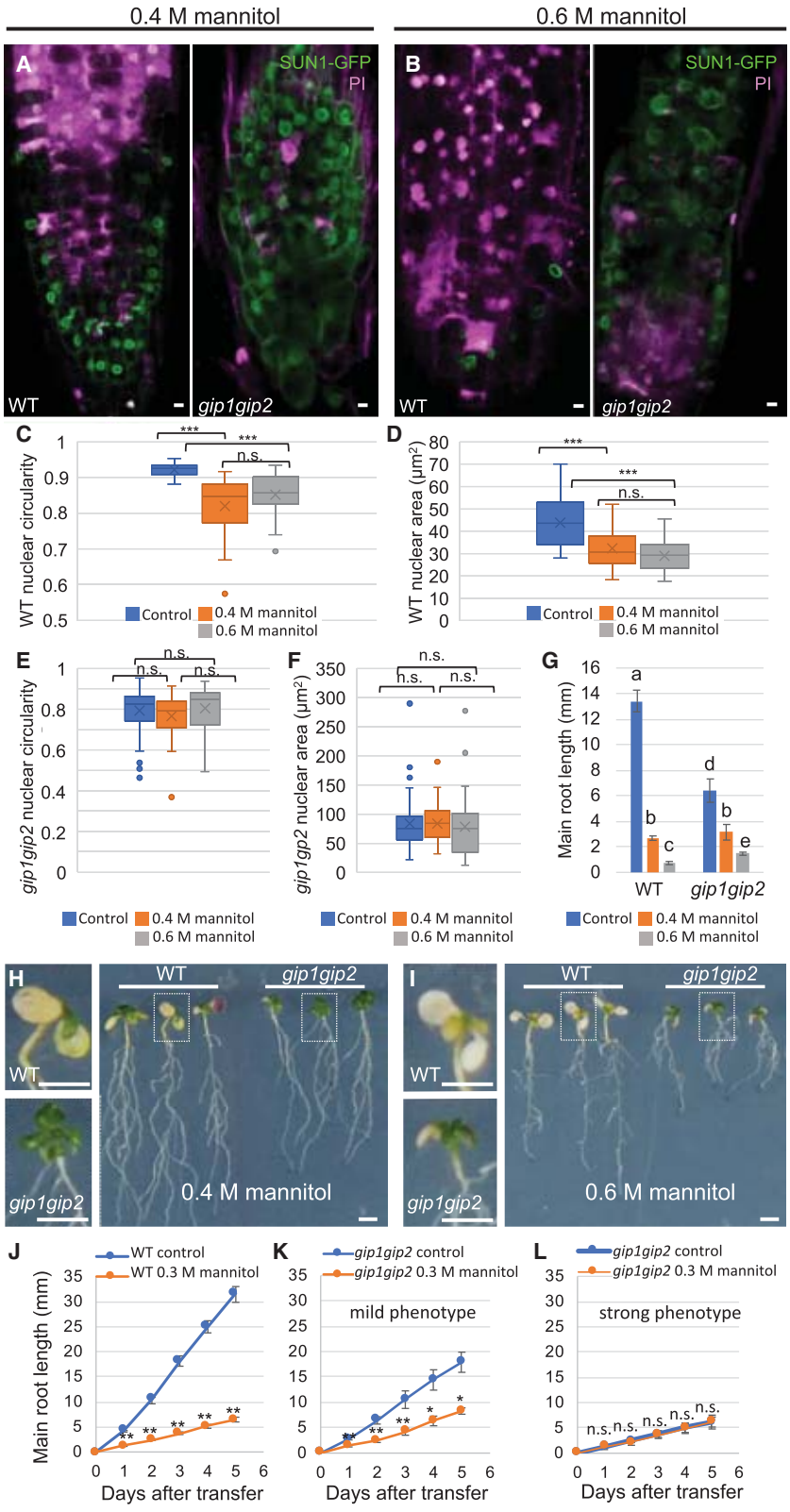

Figure 3. Resistance of *gip1gip2* Root Tip Cells to Severe Hyperosmotic Conditions

(A and B) Confocal analysis of root meristems of 9-day-old seedlings expressing SUN1-GFP in presence of 0.4 M (A) and 0.6 M (B) mannitol stress (16 h treatment) in WT (n = 8 and n = 5, respectively) and mild *gip1gip2* (n = 10). Dead cells were revealed with propidium iodide staining (magenta). Scale bars, 5 µm.

(C and D) Quantification of nuclear parameters, the circularity (C) and the area (D) of the nuclei, was evaluated in WT in both mannitol treatments compared with control ($n_{control}$ = 38, $n_{0.4\ M}$ = 39, and $n_{0.6\ M}$ = 41). Between control/0.4 M and control/0.6 M, p values (Student's t test) are 2.903e−9 and 1.515e−6 and 1.604e−10 and 3.581e−10, respectively, for each parameter, indicating a significant change between control and severe hyperosmotic conditions (***p < 0.001). No significant change (n.s.) was observed between nuclear parameters at 0.4 M and 0.6 M mannitol with p values of 0.094 and 0.075 for nuclear circularity area, respectively.

(E and F) Quantification of nuclear circularity (E) and area (F) of the nuclei in mild *gip1gip2* in both mannitol treatments compared with control ($n_{control}$ = 57; $n_{0.4\ M}$ = 22; $n_{0.6\ M}$ = 43). Using Student's t test, no significant changes (n.s.) were observed between control/0.4 M or control/0.6 M with p values of 0.329 and 0.614 and 0.989 and 0.534 for nuclear circularity and area, respectively, or between 0.4 M and 0.6 M conditions with p values of 0.195 and 0.617, respectively.

(G–I) Mild *gip1gip2* phenotype compared with WT using 9-day-old seedlings transferred for 2 days on 0.4 M and 0.6 M mannitol as well as on control media. (G) Main root growth was evaluated through the measurement of root length on growth control conditions (n_{WT} = 12; $n_{gip1gip2}$ = 10), 0.4 M mannitol (n_{WT} = 13; $n_{gip1gip2}$ = 10), and 0.6 M mannitol (n_{WT} = 12; $n_{gip1gip2}$ = 13). Using Mann Whitney test, different letters above the error bars indicate significant differences at p < 0.01. Three individual experiments were repeated. (H and I) Leaf senescence phenotype in WT and *gip1gip2* seedlings maintained on 0.4 M (H) and 0.6 M mannitol (I) for 15 days. Representative images are presented; on each figure, the left panel presents magnification of WT and *gip1gip2* leaf rosettes, respectively. Scale bars, 0.2 cm.

(J–L) Mild (K) and strong (L) *gip1gip2* phenotypes compared with WT (J) using 9 day-old seedlings transferred to 0.3 M mannitol for 5 days. Every day, main root length was measured on control media: WT (n = 6), mild *gip1gip2* (n = 7), and strong *gip1gip2* (n = 6) and on 0.3 M mannitol: WT (n = 7), mild *gip1gip2* (n = 6), and strong *gip1gip2* (n = 7). Using Mann Whitney test, differences between control and treated samples were evaluated for each time point, for WT (**p < 0.01), mild (*p > 0.05; **p < 0.01), and strong *gip1gip2* phenotypes (p > 0.05, n.s.). See also Figure S3.

stable; at 0.3 M mannitol, nuclei shrink and become more circumvoluted; and above 0.3 M mannitol, nuclei are even more deformed and cells die, consistent with growth defects under such harsh hyperosmotic conditions. Because the *gip1gip2* mutant nuclei are already more compact than the WT, this may also prime the mutant to resist hyperosmotic stress.

Nuclear Deformation upon Hyperosmotic Stress or with Defective GIPs Correlates with Nuclear Stiffening

In theory, wavy nuclear envelope could result from cytoplasmic forces acting on a soft nucleus (in which case the cytoskeleton would shape the nucleus upon hyperosmotic stress) or from nuclear factors shaping and stiffening the nucleus (in which case, the nucleoskeleton and/or chromatin would shape the nucleus upon hyperosmotic stress). To discriminate between these two scenarios, we isolated nuclei from root meristems and checked their shape. Although extracted nuclei appeared smaller than nuclei in tissues, shape defects were still maintained in WT extracted nuclei upon mannitol treatment ($n_{control\ WT} = 33$; $n_{treated\ WT} = 57$; $p = 2.7\ e{-9}$ and 0.0079 for nuclear circularity and area, respectively; Figures S4A, S4B, S4E, and S4F). No significant difference in area or circularity was observed in extracted *gip1gip2* nuclei after mannitol treatment ($n_{control\ gip1gip2} = 34$; $n_{treated\ gip1gip2} = 53$; $p = 0.94$ and 0.083 for nuclear circularity and area, respectively; Figures S4C, S4D, S4G, and S4H). This suggests that the impact of hyperosmotic stress on nuclear shape mainly depends on the nucleus itself.

This prompted us to test the intrinsic physical properties of the nucleus. To do so, we measured the stiffness of isolated nuclei from untreated and treated WT root tips. First, we adapted a micro-rheometry approach, initially developed to measure whole-cell stiffness [40, 41]: the nucleus is compressed between two microplates, one flexible and the other one more rigid; the stiffness of the sample is deduced from the deflection of the flexible microplate, the stiffness of which is calibrated (Figures 4A–4C; see Method Details). Root meristematic nuclei were isolated from 9-day-old untreated or treated seedlings using a fluorescence-activated cell sorting (FACS)-based protocol and they were then resuspended in Murashige and Skoog (MS) medium with or without mannitol (as in whole plant treatments; see Method Details). Note that nuclear envelope integrity was confirmed by the presence of SUN1-GFP and microtubules (Figures S4I and S4J). WT nuclei, that were resuspended in control medium, exhibited an elastic modulus of 0.39 ± 0.07 kPa (n = 17; Figure 4D; Video S1). In contrast, WT nuclei, that were resuspended in hyperosmotic conditions, were about 10 times stiffer (4.15 ± 1.78 kPa; n = 11; p = 0.0029; Figure 4D; Video S2). This shows that reduced nuclear circularity and area upon hyperosmotic stress correlates with increased nuclear stiffness. If true, this should apply to *gip1gip2* nuclei too. Consistently, we found that *gip1gip2* mutant nuclei were also stiffer than WT nuclei (2.88 ± 1.38 kPa; n = 17; p = 0.0001; Figure 4D) and with a stiffness value comparable to that of mannitol-treated WT nuclei (p = 0.643; Figure 4D). Therefore, it seems that not only *gip1gip2* mutants mimic the effect of hyperosmotic stress observed on WT nuclear shape, but they also mimic its impact on nuclear stiffness.

To validate these results *in planta*, we used atomic force microscopy (AFM). A sharp tip is attached on a flexible cantilever, which stiffness is calibrated. The deformation of the cantilever as it contacts the sample is monitored via a laser beam reflecting from the top surface of the cantilever into a photodetector. This provides force-displacement curves from which the mechanical properties of the sample can be derived (Figures 4E, S4L, and S4M). Nuclei from WT and *gip1gip2* root meristems from 9-day-old seedlings were analyzed after *in situ* cell wall digestion and meristem squashing (Figures 4F and 4H). The cantilever was applied on the nuclei *in planta* on poly-L-lysine-coated Petri dishes (Figures 4F and 4H). After acquiring matrix forces curves (Figures 4G and 4H, inset, and S4L and S4M), topography and rigidity maps were obtained using the PeakForce QNM (quantitative nanomechanical mapping) mode (Figures 4G and 4I). Note that we found no significant difference in the elastic modulus of the WT nuclei by AFM, whether nuclei were isolated with FACS buffer or measured on squashed root tips (Figure S4K), thus validating our comparative approach. Although absolute values were higher than in micro-rheometry, our AFM measurements confirmed the trend: nuclei from untreated WT root tips exhibited an elastic modulus of 37.4 ± 3.6 kPa (n = 13), whereas *gip1gip2* mutant nuclei were much stiffer, at 89.0 ± 8.3 kPa (Figure 4J; n = 14; p = 0.0018). Thus, *gip1gip2* nuclei are significantly stiffer than those of the WT, whether nuclear stiffness is measured by micro-rheometry or AFM.

Altogether, we show that hyperosmotic stress leads to increased nuclear stiffness, which correlates with decreased nucleus size and area. This trend is mimicked in *gip1gip2* mutants. Because nuclear shape and stiffness can affect gene expression, we next checked whether hyperosmotic stress and *gip1-gip2* mutation also have consistent effects on the transcriptome.

Hyperosmotic Stress and *gip1gip2* Mutation Induce Overlapping Transcriptional Stress Responses

First, we analyzed gene expression in *gip1gip2* mutants using total RNA sequencing and qRT-PCR. We used *gip1gip2* mutant populations from 9-day-old seedlings, with either mild or strong phenotypes (Figure S2A). Using a next-generation sequencing (NGS) approach (Illumina), we analyzed 125-bp reads. Principal-component analysis (PCA) revealed three different groups matching plant phenotypes (DESeq2 package). This approach generated a list of the shared most upregulated genes in mild and severe *gip1gip2*, when compared with WT (Figure S5A). A list of differentially expressed genes was then selected with *Z* score calculations using Benjamini-Hochberg corrections of 0.05 for false discovery rate (FDR). The *gip1gip2* mutant displayed major deviations from the WT in stress response genes, as annotated through their Gene Ontology (Table S1). In particular, the *gip1gip2* transcriptome shared 57% of the transcripts identified in the transcriptome of touched plants [26], with a statistical significance of the overlap (representation factor R = 7.8 with a probability $p < 4.661e{-231}$ using hypergeometric test; Figure 5A).

Conversely, a significant overlap with the transcriptome of *gip1gip2* was obtained when considering WT seedlings treated with high concentration of mannitol (21.4% of overlapping transcripts) or high concentration of sodium chloride (28.6% of overlapping transcripts; Figures S5B and S5C; R = 3.9 and 2.9, respectively, and an exact hypergeometric probability $p < 2.904e{-118}$) [42].

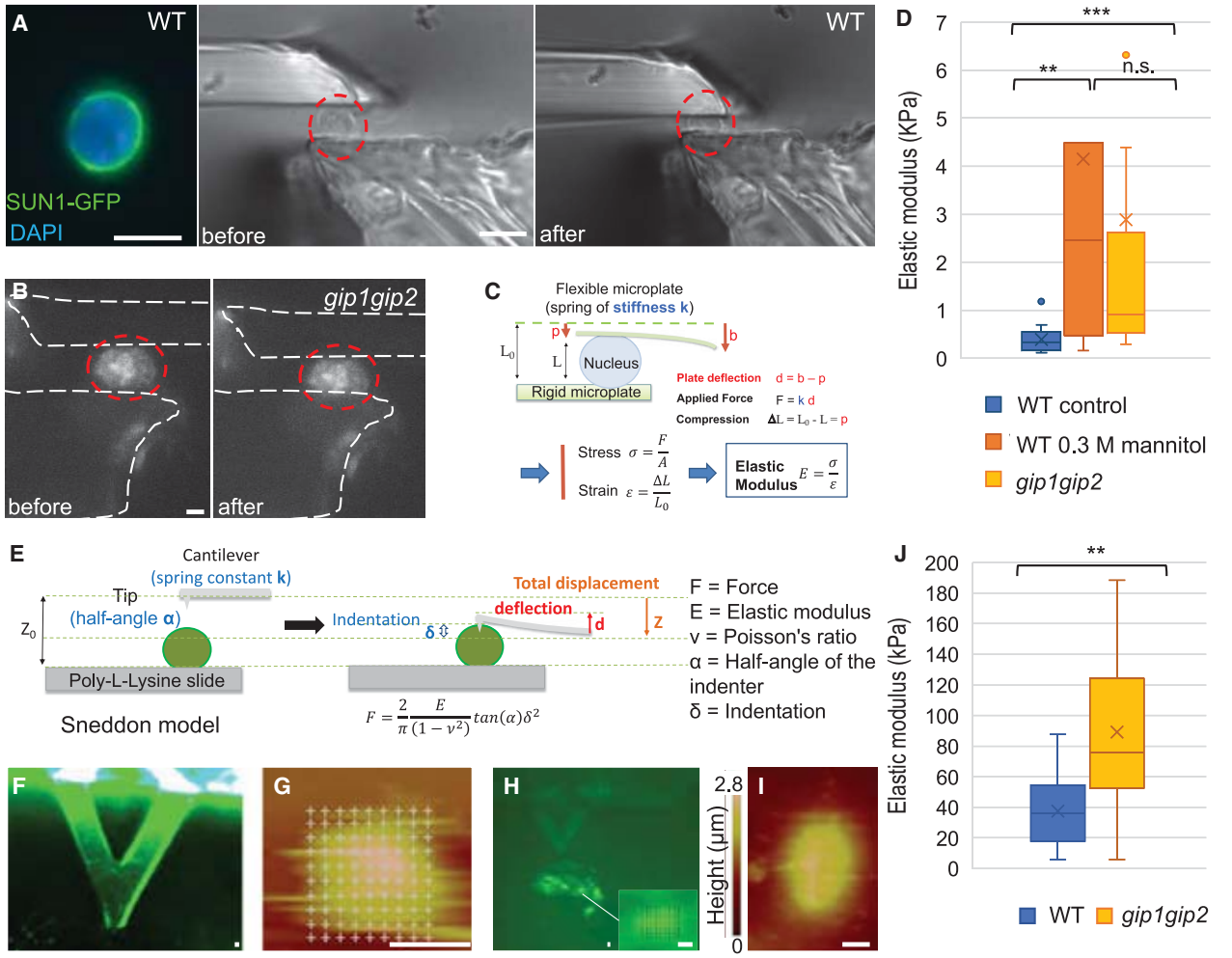

Figure 4. Hyperosmotic Stress and *gip1gip2* Mutations Stiffen the Nuclei

(A–D) Micro-rheometry on isolated nuclei. (A) Left, fluorescence imaging of an isolated WT SUN1-GFP nucleus (green) stained with DAPI (blue). Middle and right, bright field imaging of an isolated nucleus (see dashed red circle) trapped between two microplates, one rigid (bottom) and the other flexible (top) with calibrated stiffness. The nucleus is compressed under an uniaxial fore. Imaging of the nucleus before (middle) and after (right) compression allows one to visualize nuclear deformation. Compared with that of a *gip1gip2* nucleus (B), deformation is high, reflecting the low stiffness of the WT nuclei. (B) Fluorescence imaging of a *gip1gip2* SUN1-GFP nucleus trapped (left) and compressed (right) in the micro-rheometer: almost no deformation occurred, reflecting its high stiffness. Scale bar, 5 μm. (C) Principle of the micro-rheometry to measure nuclear stiffness. The force applied to the nucleus is F = kd, where d is the deflection of the flexible microplate of spring constant k. The elastic modulus was obtained by dividing the force F by the apparent contact area and relative nuclear shortening between the plates, i.e., nuclear strain. (D) Comparison between the elastic moduli (kPa) of *gip1gip2* (n = 17) and WT SUN1-GFP nuclei treated (n = 11) or not (n = 17) with 0.3 M mannitol is shown; p values from Mann-Whitney tests are WT/WT treated: 0.0029 (significant $p < 0.01$); WT/*gip1gip2*: 0.000107 (significant $p < 0.001$); and WT treated/*gip1gip2*: 0.643 (n.s.).

(E–J) AFM analysis of nuclei from root meristems. (E) Principle of the AFM to measure nuclear stiffness. (F–H) The AFM tip was positioned on a nucleus (GFP signal) isolated from root squashing after cell wall digestion of WT (F) and *gip1gip2* (H), and the acquisition of a matrix of force curves (100 curves) was acquired for WT (G) and *gip1gip2* nuclei (H, right inset). (G–I) Topography was obtained in WT (G) and mutant (I) with the PeakForce QNM (quantitative nanomechanical mapping). Scale bars, 5 μm. (J) Comparison of the elastic moduli between WT (n = 14 nuclei in 3 independent roots) and *gip1gip2* nuclei in control conditions (n = 13 nuclei in 3 independent roots); p values from Mann-Whitney test are 0.00288 (significant $p < 0.01$).

See also Figure S4 and Videos S1 and S2.

Among the most upregulated touch response genes (76 genes), 60 were also upregulated in *gip1gip2*. To check whether this response is specific to GIP, we analyzed the expression of these genes in the transcriptomic data of another nuclear envelope mutant, *cpr5*. This nucleoporin mutant exhibits major defects in nuclear shape and plant development [43]. Yet, although 23.6% of the transcriptome of *cpr5* overlapped with that of *gip1gip2* (Figure S5D; R = 3.2 with $p < 9.70e{-}57$, using hypergeometric test), only 7 genes were found to overlap with the most upregulated touch response genes. This suggests that the GIP-dependent nuclear deformation and gene expression profile exhibit some degree of specificity, with a more prominent link to mechanical stress.

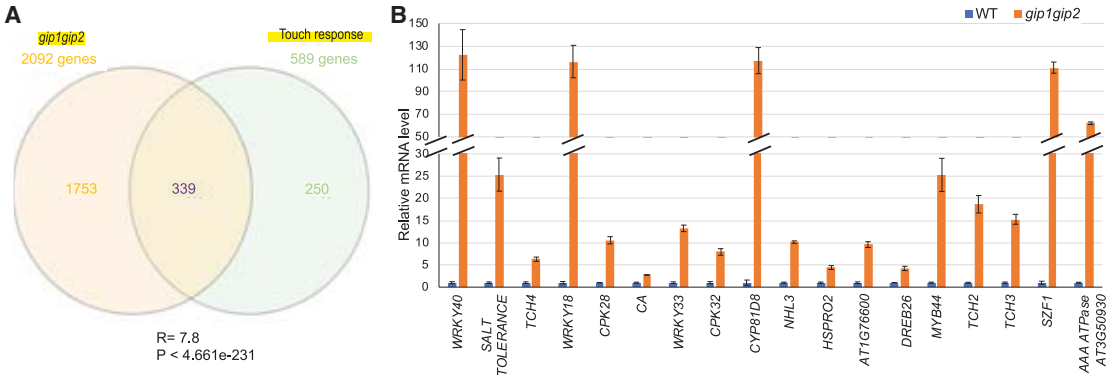

Figure 5. Transcriptomic Analysis of *gip1gip2* Compared with WT

(A) Venn diagram shows the overlap between upregulated genes in *gip1gip2* and the touch response in WT [26]. R factor and p value are indicated using the hypergeometric test.

(B) Relative transcript levels of 18 touch-induced genes (Figure S5E) in *gip1gip2* compared with WT. qRT-PCR was performed on RNA isolated from 9-day-old seedlings using specific primers, with 3 technical replicates and 3 biological replicates. SDs are indicated.

See also Figure S5 and Tables S1 and S2.

Then, we focused our analysis on a subset of 18 touch response genes, based on their established induction in response to mechanical perturbations [26, 44], such as the *TOUCH* gene family (Figure S5E). First, we validated the expression of the selected 18 genes using qRT-PCR (Figure 5B). qRT-PCR was performed on 9-day-old *gip1gip2* and WT seedlings using specific primers for the 18 selected genes (Table S2). As expected, we found significantly increased transcript levels in *gip1gip2* for these 18 genes. The induction was also stronger in the severe *gip1gip2* mutant than in the mild one (Figure S5E). More specifically, mechanosensitive genes, such as *TCH2*, *TCH3*, *TCH4*, *WRKY33*, *WRKY40*, *CPK28*, *CPK32*, *calcium-binding EF-hand gene*, *AT1G76600*, *DREB26*, *NHL3*, and *HSPRO2*, displayed 3- to 16-fold higher transcript levels in *gip1gip2*, when compared with WT (Figure 5B). The transcript levels of genes encoding the salt tolerance zinc fingers, the transcription factors WRKY18, WRKY40, Myb44, and SZF1, as well as the cytochrome CYP81D8 and the AAA-type ATPase family member were even more increased, from 20- up to 120-fold in *gip1gip2* compared to WT (Figure 5B). Interestingly, none of these 18 genes were found upregulated in *cpr5* (Figure S5E, 18 genes with TAIR_ID database).

To check whether similar transcript level changes were observed upon hyperosmotic stress, we performed similar analyses on the 0.3 M mannitol-treated seedlings compared with control plants. Under hyperosmotic stress, 9-day-old seedlings exhibited a response comparable to that of *gip1gip2*, albeit to a lower extent with mRNA levels changing from 2.4- to 53-fold (Figure 6A). Note that similar results were also obtained when analyzing the mRNA levels in roots only, allowing us to formally correlate nuclear deformation and transcriptional response under hyperosmotic stress in root meristematic nuclei (Figure S6A).

As we observed that 0.15 M mannitol is not sufficient to induce a detectable change in nuclear shape, we also analyzed gene expression in these milder conditions. As expected, under such low stress conditions (0.15 M mannitol), no significant induction could be observed for the selected genes (i.e., below a 2-fold induction; Figure S6D). This further correlates changes in nuclear shape with gene expression, including the threshold in the cellular response to hyperosmotic stress.

Last, we found that most of the mechanosensitive genes were induced in the *gip1gip2* mutant upon a 0.3 M mannitol treatment, albeit to a lesser extent when compared with WT, upto 4.3-fold change in mRNA level (Figure S6C), consistent with the observation that *gip1gip2* already exhibits a close to maximal nuclear shape deformation before mannitol treatment.

Transcriptional Nuclear Responses to Hyperosmotic Stress Are Reversible

If the impact of hyperosmotic stress on transcriptome is associated with nuclear mechanics, it should be reversible. To test this hypothesis, we exposed 9-day-old seedlings to hyperosmotic stress for 16 h and then transferred them back to normal medium for 7 h. As a control, 9-day-old seedlings were exposed to normal medium for 16 h and then transferred to fresh normal medium for an additional 7 h. We then analyzed the expression of the 18 selected genes listed above using RNA extracted from whole seedlings. Upon recovery, none of genes exhibited a significant induction (i.e., below a 2-fold change induction), when compared with the untreated control (Figure 6B). Similar results were observed when using RNA extracted from roots (Figure S6B). The reversibility in expression is consistent with the idea that the induction of these genes relates to hyperosmotic stress. In order to correlate changes of gene expression upon recovery to changes in nuclear morphology, we also analyzed nuclear shape upon release of hyperosmotic stress. After a 0.3 M mannitol treatment, root meristematic nuclei exhibited a deformed shape as previously shown, when compared with non-treated plants (Figures 7A and 7B). Although nuclear shape remained unchanged after the additional 7 h in the control medium (Figure 7C), the deformed nuclei observed in treated plants retrieved their original shape upon their transfer to control medium for 7 h (Figure 7D). No statistical differences in nuclear circularity and area could be detected between treated and

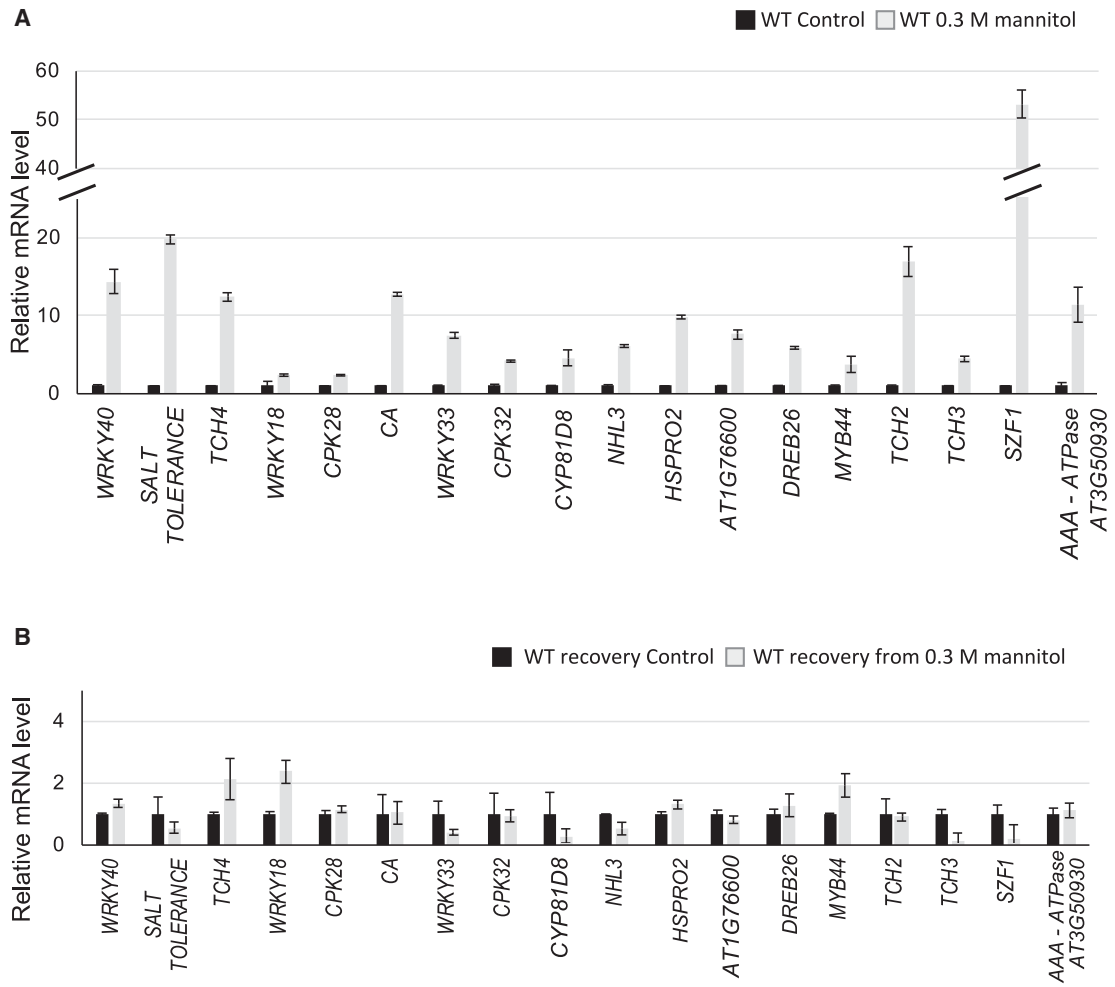

Figure 6. Relative mRNA Level in Response to Hyperosmotic Stress

Analysis of the relative mRNA levels of selected touch-induced genes in 9-day-old seedlings in presence of 0.3 M mannitol during 16 h (A) and after 7 h of recovery (B) on normal growth medium compared with control (no treatment). qRT-PCR was performed using RNA extracted from 9-day-old seedlings and specific primers, with 3 technical replicates and 3 biological replicates. SDs are indicated. See also Figure S6 and Table S2.

untreated plants upon recovery ($n_{control}$ = 70; $n_{treated}$ = 61; p = 0.74 and 0.56, respectively; Figures 7E and 7F).

Nuclear Stiffening upon Hyperosmotic Stress Is Reversible

To link these changes to mechanical properties of the nucleus, we performed measurements of nuclear stiffness on WT nuclei after mannitol treatment and upon recovery. Using both micro-rheometry and AFM, we found that mannitol-treated nuclei indeed become softer when the osmolarity of the medium is decreased. In the end, mannitol-treated-then-rescued nuclei exhibited an apparent elastic modulus that was comparable to that of the untreated iso-osmotic control (in AFM, p values control versus recovery = 0.46; in micro-rheometry, p values control versus recovery = 0.778; Figures 7G and 7H).

Interestingly, DAPI staining of the nuclei under micro-rheometry measurements revealed changes in the organization of the bright DAPI-stained chromocenters associated with pericentromeric heterochromatin located at the nuclear periphery [45]. Although in control and recovery nuclei (Figures S7A and S7D), the chromocenters were scattered as bright DAPI signals at the nuclear periphery, they appeared more clustered in the mannitol-treated nuclei (Figure S7C). Conversely, when we treated the seedlings with hypo-osmotic stress (16 h water incubation), the chromocenters were more diffuse in isolated nuclei while the size of the nuclei was increasing ($n_{control}$ = 45; $n_{treated}$ = 32; p = 9.06e−8; Figures S7B and S7H). Such nuclei seemed very soft and fragile. However, we could not quantitatively assess this trend: only very few nuclei could be handled for micro-rheometry measurements (n = 5), providing no statistically significant bias (p = 0.265; Figure 7H). We believe that we could only measure the stiffer nuclei, because the softer ones were probably, in essence, too weak mechanically to be micro-manipulated. Consistent with this hypothesis, the nuclei that we could mechanically test were indeed significantly smaller (mean area 27.6 ± 8 μm^2) than those that we could not handle (n = 8; mean area 63.4 ± 10 μm^2, with a p value of 0.047).

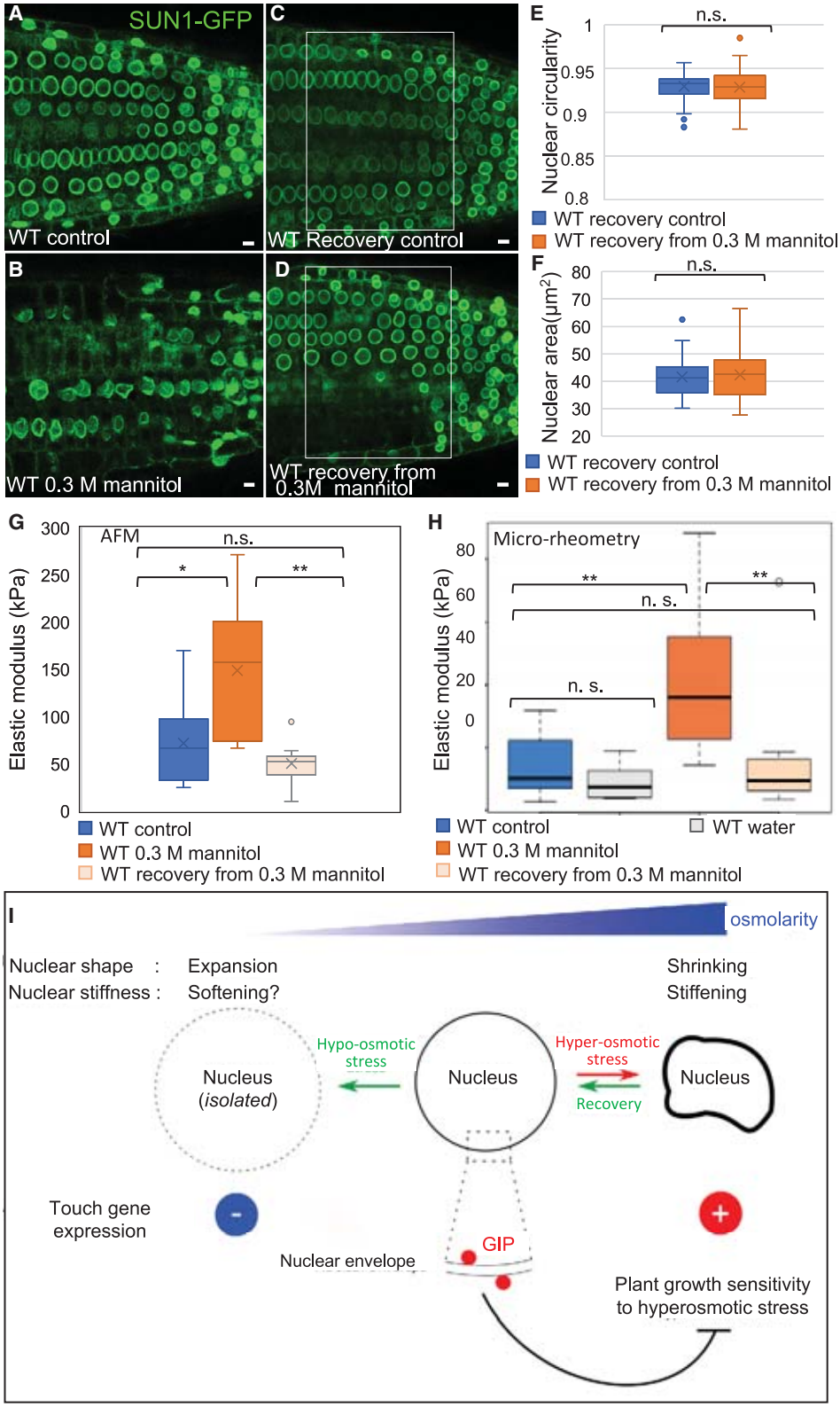

Figure 7. Changes of Nuclear Shape and Elastic Modulus Are Reversible upon Hyperosmotic Stress

(A–D) Representative images of nuclei in root meristems. Nine-day-old WT SUN1-GFP seedlings are presented: control (A) and treated seedlings with 0.3 M mannitol (B) for 16 h; control (C) and mannitol-treated seedlings (D) upon recovery on normal growth medium for 7 h. Scale bars, 5 μm.

(legend continued on next page)

The discrepancy in DAPI staining was also observed at the tissue level when analyzing nuclei in the root tips of WT, mannitol, or water-treated seedlings (Figures S7E–S7G). However, we could not detect a significant increase of the nuclear area in root meristems of seedlings treated with water compared with control plants ($n_{control} = 164$; $n_{treated} = 174$; $p = 0.4$; Figure S7I). In addition, there was no clear changes in circularity ($p = 0.12$; Figure S7J), suggesting that the multicellular environment may prevent such hypo-osmotic environment to exist *in vivo*. Yet, except for *HSPRO2*, in such hypo-osmotic conditions, we could observe a strong decrease in the transcript level of touch-induced genes when compared with WT control, between 1.47- and 333-fold change (Figure S7M). However, the response was very limited in *gip1gip2* with a fold change between 1.14 and 3.84 (Figure S7N), and no further nuclear deformation was observed as well (Figures S7K and S7L).

Altogether, the reversibility of the nucleus response to hyperosmotic stress further supports a scenario in which nuclear shape and stiffness homeostasis is under control, linked to transcriptional program, and for which the GIP proteins play a major, negative, regulatory role. Conversely, the nuclear response to hypo-osmotic stress leads to nuclear expansion on isolated nuclei and negative regulation of the touch gene expression *in planta* (Figure 7I).

DISCUSSION

We show that a reduction of both nuclear area (by 20%) and circularity (by 9%), an increase in nuclear stiffness (by a factor of 3 to 10), as well as a significant induction of touch response genes occur in a narrow window of hyperosmotic conditions (above 0.3 M and below 0.4 M mannitol). Importantly, these responses are reversible when returning to iso-osmotic conditions, suggesting a mechanical response of the nucleus. Mechanistically, this behavior may involve GIP/MZT1 proteins because *gip1gip2* mimic all the observed responses in a constitutive way. Because the *gip1gip2* nuclei are constitutively stiff, we propose that their increased resistance to hyperosmotic stress is in part provided by mechanical shielding through nuclear stiffening (Figure 7I).

Nuclear shape and stiffness may easily be related: nucleoplasm crowding following hyperosmotic stress may reduce nucleus size and increase its internal density and thus its stiffness. Yet the observation that a similar phenotype exists in the *gip1gip2* mutant suggests that this response is not only passive but actively regulated by nuclear envelope components, likely through the global spatial reorganization of chromatin. These data in a tissue context echo the role of nuclear mechanics in single cells in animals. Indeed, the structural elements of the nucleus are essential to drive nuclear shape and transcriptional gene regulation [46]. For instance, nucleus stiffness positively scales with matrix stiffness, and this response involves lamin A and is accompanied by transcriptional changes [47]. Although maintenance of nuclear shape depends in part on the nucleoskeleton and chromatin [18, 48], these components do not have overlapping roles: lamin A would provide a robust enough structure to resist large nuclear deformation, while chromatin would govern nuclear stiffness in smaller deformations [49]. Of note, in line with our results, nuclear deformations in response to hyperosmotic stress were also observed in isolated chondrocytes and were accompanied by chromatin condensation in specific regions within the nucleus [3]. More recently, NaCl-induced hyperosmotic stress was shown to disrupt chromatin organization, with associated transcriptional changes as well [50]. The exact relationship between hyperosmotic stress and gene expression remains to be fully characterized in plants. Our analysis introduces the contribution of nuclear shape, stiffness, and nuclear envelope factors in this network.

This work also raises new questions: how could the nuclear envelope control the nuclear response to osmotic conditions? As nuclear pores are too permissive to allow a pressure build-up inside the nucleus, this may likely involve chromatin itself. This proposition is consistent with the reported impaired centromeric chromatin organization in the *gip1gip2* [37]. Thus, GIP would indirectly control the gel-like properties of chromatin in response to osmotic conditions. Chromatin remodeling can also make nuclei more compact in animal cells [51], and chromatin can become more compact upon hyperosmotic treatment in plants [52]. Therefore, our proposition may also be applicable beyond the plant kingdom. As we also found that a mutant better resists hyperosmotic stress than the WT, our work not only integrates nuclear mechanics in the plant response to drought, it may also open the way for a better understanding of how plants cope with water stress.

STAR★METHODS

Detailed methods are provided in the online version of this paper and include the following:

- KEY RESOURCES TABLE
- LEAD CONTACT AND MATERIALS AVAILABILITY
- EXPERIMENTAL MODEL AND SUBJECT DETAILS
  - Plants

(E and F) Quantification of nuclear parameters, circularity (E) and nuclear area (F), upon recovery on control and treated plants. The p values after Student's t test are 0.73 and 0.56, respectively, indicating no significant changes between untreated and recovering samples (n.s.). Measurements were performed in the region delineated by the white frame in (C) and (D).

(G) Evaluation of elastic moduli using AFM on nuclei from squashed and lysed root meristem of seedlings treated with mannitol (n = 10) and upon recovery (n = 10) from a mannitol treatment compared with control (n = 7). Using Mann Whitney test, p values are 0.027 between control and mannitol (*), 0.0004 between mannitol and recovery (**), and 0.46 (n.s.) between control and recovery.

(H) Evaluation of elastic moduli using micro-rheometry on isolated nuclei from seedlings treated with mannitol (n = 11) and upon recovery (n = 8) compared with control (n = 7) or seedlings treated with water (n = 5) is shown. Using Mann Whitney test, p values are 0.005 between control and mannitol (**), 0.0045 between mannitol and recovery (**), 0.778 (n.s.) between control and recovery, and 0.265 (n.s.) between control and water.

(I) Graphical summary of the changes in nuclear shape and mechanics related to osmotic stress and touch gene expression. Implication of GIPs in plant growth sensitivity to hyperosmotic stress is also shown. See also Figure S7.

SUPPLEMENTAL INFORMATION

Supplemental Information can be found online at https://doi.org/10.1016/j.cub.2020.03.059.

ACKNOWLEDGMENTS

This work was supported by the Centre National de la Recherche Scientifique (CNRS) (defi Mecanobio, NEstress 2016-2018), by Fondation Schlumberger pour l'Education et la Recherche (FSER) (2016-2018), by the European Research Council grants ERC-2013-CoG-615739 "MechanoDevo," by the IdEX international PhD program (unista, Strasbourg), and by HFSP grant 2018, RGP, 009. This study was partially supported by the labex «Who AM I ?», labex ANR-11-LABX- 0071, and the Université de Paris, Idex ANR-18-IDEX-0001 funded by the French Government through its «Investments for the Future» program. We acknowledge discussions with members of the COST Action CA1612 INDEPTH network. We thank J. Fuchs (IPK, Gatersleben) for providing us flow cytometry sorting of nuclei as well as S. Koechler and A. Alioua at IBMP Gene Expression Analysis platform. We are grateful to K. Graumann for providing fluorescent-tagged SUN1 lines, as well as to Elise Hoffmann, L. Barret, and P. Johann to Berens for their technical help. We thank Jean-Pierre Henry for fruitful discussions about nuclear pores and mechanical regulation.

AUTHOR CONTRIBUTIONS

Conceptualization, A.A., M.-E.C., and O.H.; Methodology, A.A., J.M., M.-E.C., O.H., and P.M.; Investigation, A.A., G.H., M.-E.C., P.M., and R.G.; Writing – Original Draft, M.-E.C., O.H., and R.G.; Writing – Review & Editing, A.A., M.-E.C., O.H., P.M., R.G., and S.G.; Funding Acquisition, A.A., M.-E.C., and O.H.; Visualization, A.A., P.M., R.G., and S.G.; Resources, M.-E.C.; Supervision, M.-E.C. and O.H.

DECLARATION OF INTERESTS

The authors declare no competing interests.

Received: July 9, 2019
Revised: February 5, 2020
Accepted: March 23, 2020
Published: April 23, 2020

REFERENCES

1. D'Arcy Thompson, W. (1917). On Growth and Form (Cambridge University).
2. Discher, D.E., Janmey, P., and Wang, Y.L. (2005). Tissue cells feel and respond to the stiffness of their substrate. Science *310*, 1139–1143.
3. Irianto, J., Swift, J., Martins, R.P., McPhail, G.D., Knight, M.M., Discher, D.E., and Lee, D.A. (2013). Osmotic challenge drives rapid and reversible chromatin condensation in chondrocytes. Biophys. J. *104*, 759–769.
4. Lovett, D.B., Shekhar, N., Nickerson, J.A., Roux, K.J., and Lele, T.P. (2013). Modulation of nuclear shape by substrate rigidity. Cell. Mol. Bioeng. *6*, 230–238.
5. Uhler, C., and Shivashankar, G.V. (2017). Regulation of genome organization and gene expression by nuclear mechanotransduction. Nat. Rev. Mol. Cell Biol. *18*, 717–727.
6. Miroshnikova, Y.A., Nava, M.M., and Wickström, S.A. (2017). Emerging roles of mechanical forces in chromatin regulation. J. Cell Sci. *130*, 2243–2250.
7. Cho, S., Irianto, J., and Discher, D.E. (2017). Mechanosensing by the nucleus: from pathways to scaling relationships. J. Cell Biol. *216*, 305–315.
8. Maharana, S., Iyer, K.V., Jain, N., Nagarajan, M., Wang, Y., and Shivashankar, G.V. (2016). Chromosome intermingling-the physical basis of chromosome organization in differentiated cells. Nucleic Acids Res. *44*, 5148–5160.
9. Dupont, S., Morsut, L., Aragona, M., Enzo, E., Giulitti, S., Cordenonsi, M., Zanconato, F., Le Digabel, J., Forcato, M., Bicciato, S., et al. (2011). Role of YAP/TAZ in mechanotransduction. Nature *474*, 179–183.
10. Alam, S.G., Zhang, Q., Prasad, N., Li, Y., Chamala, S., Kuchibhotla, R., Kc, B., Aggarwal, V., Shrestha, S., Jones, A.L., et al. (2016). The mammalian LINC complex regulates genome transcriptional responses to substrate rigidity. Sci. Rep. *6*, 38063.
11. Mammoto, A., Mammoto, T., and Ingber, D.E. (2012). Mechanosensitive mechanisms in transcriptional regulation. J. Cell Sci. *125*, 3061–3073.
12. Poh, Y.C., Shevtsov, S.P., Chowdhury, F., Wu, D.C., Na, S., Dundr, M., and Wang, N. (2012). Dynamic force-induced direct dissociation of protein complexes in a nuclear body in living cells. Nat. Commun. *3*, 866.
13. Tajik, A., Zhang, Y., Wei, F., Sun, J., Jia, Q., Zhou, W., Singh, R., Khanna, N., Belmont, A.S., and Wang, N. (2016). Transcription upregulation via force-induced direct stretching of chromatin. Nat. Mater. *15*, 1287–1296.
14. Hampoelz, B., Azou-Gros, Y., Fabre, R., Markova, O., Puech, P.H., and Lecuit, T. (2011). Microtubule-induced nuclear envelope fluctuations control chromatin dynamics in Drosophila embryos. Development *138*, 3377–3386.
15. Elosegui-Artola, A., Andreu, I., Beedle, A.E.M., Lezamiz, A., Uroz, M., Kosmalska, A.J., Oria, R., Kechagia, J.Z., Rico-Lastres, P., Le Roux, A.L., et al. (2017). Force triggers YAP nuclear entry by regulating transport across nuclear pores. Cell *171*, 1397–1410.e14.
16. Kirby, T.J., and Lammerding, J. (2018). Emerging views of the nucleus as a cellular mechanosensor. Nat. Cell Biol. *20*, 373–381.
17. Stephens, A.D., Liu, P.Z., Kandula, V., Chen, H., Almassalha, L.M., Herman, C., Backman, V., O'Halloran, T., Adam, S.A., Goldman, R.D., et al. (2019). Physicochemical mechanotransduction alters nuclear shape and mechanics via heterochromatin formation. Mol. Biol. Cell *30*, 2320–2330.
18. Alisafaei, F., Jokhun, D.S., Shivashankar, G.V., and Shenoy, V.B. (2019). Regulation of nuclear architecture, mechanics, and nucleocytoplasmic shuttling of epigenetic factors by cell geometric constraints. Proc. Natl. Acad. Sci. USA *116*, 13200–13209.
19. Durand-Smet, P., Gauquelin, E., Chastrette, N., Boudaoud, A., and Asnacios, A. (2017). Estimation of turgor pressure through comparison between single plant cell and pressurized shell mechanics. Phys. Biol. *14*, 055002.
20. Asnacios, A., and Hamant, O. (2012). The mechanics behind cell polarity. Trends Cell Biol. *22*, 584–591.
21. Finan, J.D., and Guilak, F. (2010). The effects of osmotic stress on the structure and function of the cell nucleus. J. Cell. Biochem. *109*, 460–467.
22. Xiong, L., Schumaker, K.S., and Zhu, J.K. (2002). Cell signaling during cold, drought, and salt stress. Plant Cell *14* (*Suppl*), S165–S183.

23. Kim, J.M., Sasaki, T., Ueda, M., Sako, K., and Seki, M. (2015). Chromatin changes in response to drought, salinity, heat, and cold stresses in plants. Front. Plant Sci. *6*, 114.
24. Kreps, J.A., Wu, Y., Chang, H.S., Zhu, T., Wang, X., and Harper, J.F. (2002). Transcriptome changes for Arabidopsis in response to salt, osmotic, and cold stress. Plant Physiol. *130*, 2129–2141.
25. Zeller, G., Henz, S.R., Widmer, C.K., Sachsenberg, T., Rätsch, G., Weigel, D., and Laubinger, S. (2009). Stress-induced changes in the Arabidopsis thaliana transcriptome analyzed using whole-genome tiling arrays. Plant J. *58*, 1068–1082.
26. Lee, D., Polisensky, D.H., and Braam, J. (2005). Genome-wide identification of touch- and darkness-regulated Arabidopsis genes: a focus on calmodulin-like and XTH genes. New Phytol. *165*, 429–444.
27. Braam, J. (2005). In touch: plant responses to mechanical stimuli. New Phytol. *165*, 373–389.
28. Coutand, C., Chevolot, M., Lacointe, A., Rowe, N., and Scotti, I. (2010). Mechanosensing of stem bending and its interspecific variability in five neotropical rainforest species. Ann. Bot. *105*, 341–347.
29. Landrein, B., Kiss, A., Sassi, M., Chauvet, A., Das, P., Cortizo, M., Laufs, P., Takeda, S., Aida, M., Traas, J., et al. (2015). Mechanical stress contributes to the expression of the STM homeobox gene in Arabidopsis shoot meristems. eLife *4*, e07811.
30. Goto, C., Tamura, K., Fukao, Y., Shimada, T., and Hara-Nishimura, I. (2014). The novel nuclear envelope protein KAKU4 modulates nuclear morphology in Arabidopsis. Plant Cell *26*, 2143–2155.
31. Pawar, V., Poulet, A., Détourné, G., Tatout, C., Vanrobays, E., Evans, D.E., and Graumann, K. (2016). A novel family of plant nuclear envelope-associated proteins. J. Exp. Bot. *67*, 5699–5710.
32. Wang, H., Dittmer, T.A., and Richards, E.J. (2013). Arabidopsis CROWDED NUCLEI (CRWN) proteins are required for nuclear size control and heterochromatin organization. BMC Plant Biol. *13*, 200.
33. Dittmer, T.A., Stacey, N.J., Sugimoto-Shirasu, K., and Richards, E.J. (2007). LITTLE NUCLEI genes affecting nuclear morphology in Arabidopsis thaliana. Plant Cell *19*, 2793–2803.
34. Batzenschlager, M., Masoud, K., Janski, N., Houlné, G., Herzog, E., Evrard, J.L., Baumberger, N., Erhardt, M., Nominé, Y., Kieffer, B., et al. (2013). The GIP gamma-tubulin complex-associated proteins are involved in nuclear architecture in Arabidopsis thaliana. Front. Plant Sci. *4*, 480.
35. Janski, N., Herzog, E., and Schmit, A.C. (2008). Identification of a novel small Arabidopsis protein interacting with gamma-tubulin complex protein 3. Cell Biol. Int. *32*, 546–548.
36. Janski, N., Masoud, K., Batzenschlager, M., Herzog, E., Evrard, J.L., Houlné, G., Bourge, M., Chabouté, M.E., and Schmit, A.C. (2012). The GCP3-interacting proteins GIP1 and GIP2 are required for γ-tubulin complex protein localization, spindle integrity, and chromosomal stability. Plant Cell *24*, 1171–1187.
37. Batzenschlager, M., Lermontova, I., Schubert, V., Fuchs, J., Berr, A., Koini, M.A., Houlné, G., Herzog, E., Rutten, T., Alioua, A., et al. (2015). Arabidopsis MZT1 homologs GIP1 and GIP2 are essential for centromere architecture. Proc. Natl. Acad. Sci. USA *112*, 8656–8660.
38. Graumann, K., Runions, J., and Evans, D.E. (2010). Characterization of SUN-domain proteins at the higher plant nuclear envelope. Plant J. *61*, 134–144.
39. Versaevel, M., Grevesse, T., and Gabriele, S. (2012). Spatial coordination between cell and nuclear shape within micropatterned endothelial cells. Nat. Commun. *3*, 671.
40. Desprat, N., Richert, A., Simeon, J., and Asnacios, A. (2005). Creep function of a single living cell. Biophys. J. *88*, 2224–2233.
41. Durand-Smet, P., Chastrette, N., Guiroy, A., Richert, A., Berne-Dedieu, A., Szecsi, J., Boudaoud, A., Frachisse, J.M., Bendahmane, M., Hamant, O., and Asnacios, A. (2014). A comparative mechanical analysis of plant and animal cells reveals convergence across kingdoms. Biophys. J. *107*, 2237–2244.
42. Sewelam, N., Oshima, Y., Mitsuda, N., and Ohme-Takagi, M. (2014). A step towards understanding plant responses to multiple environmental stresses: a genome-wide study. Plant Cell Environ. *37*, 2024–2035.
43. Gu, Y., Zebell, S.G., Liang, Z., Wang, S., Kang, B.-H., and Dong, X. (2016). Nuclear pore permeabilization is a convergent signaling event in effector-triggered immunity. Cell *166*, 1526–1538.e11.
44. Ghosh, R., Mishra, R.C., Choi, B., Kwon, Y.S., Bae, D.W., Park, S.-C.C., Jeong, M.-J.J., and Bae, H. (2016). Exposure to sound vibrations lead to transcriptomic, proteomic and hormonal changes in Arabidopsis. Sci. Rep. *6*, 33370.
45. Fransz, P., De Jong, J.H., Lysak, M., Castiglione, M.R., and Schubert, I. (2002). Interphase chromosomes in Arabidopsis are organized as well defined chromocenters from which euchromatin loops emanate. Proc. Natl. Acad. Sci. USA *99*, 14584–14589.
46. Isermann, P., and Lammerding, J. (2013). Nuclear mechanics and mechanotransduction in health and disease. Curr. Biol. *23*, R1113–R1121.
47. Swift, J., Ivanovska, I.L., Buxboim, A., Harada, T., Dingal, P.C., Pinter, J., Pajerowski, J.D., Spinler, K.R., Shin, J.W., Tewari, M., et al. (2013). Nuclear lamin-A scales with tissue stiffness and enhances matrix-directed differentiation. Science *341*, 1240104.
48. Stephens, A.D., Banigan, E.J., and Marko, J.F. (2019). Chromatin's physical properties shape the nucleus and its functions. Curr. Opin. Cell Biol. *58*, 76–84.
49. Stephens, A.D., Banigan, E.J., Adam, S.A., Goldman, R.D., and Marko, J.F. (2017). Chromatin and lamin A determine two different mechanical response regimes of the cell nucleus. Mol. Biol. Cell *28*, 1984–1996.
50. Amat, R., Böttcher, R., Le Dily, F., Vidal, E., Quilez, J., Cuartero, Y., Beato, M., de Nadal, E., and Posas, F. (2019). Rapid reversible changes in compartments and local chromatin organization revealed by hyperosmotic shock. Genome Res. *29*, 18–28.
51. Heo, S.J., Thorpe, S.D., Driscoll, T.P., Duncan, R.L., Lee, D.A., and Mauck, R.L. (2015). Biophysical regulation of chromatin architecture instills a mechanical memory in mesenchymal stem cells. Sci. Rep. *5*, 16895.
52. Wang, Z., Casas-Mollano, J.A., Xu, J., Riethoven, J.-J.M., Zhang, C., and Cerutti, H. (2015). Osmotic stress induces phosphorylation of histone H3 at threonine 3 in pericentromeric regions of Arabidopsis thaliana. Proc. Natl. Acad. Sci. USA *112*, 8487–8492.
53. Martin, M. (2011). Cutadapt removes adapter sequences from high-throughput sequencing reads. EMBnet.journal *17*, 10–12.
54. Cheng, C.Y., Krishnakumar, V., Chan, A.P., Thibaud-Nissen, F., Schobel, S., and Town, C.D. (2017). Araport11: a complete reannotation of the Arabidopsis thaliana reference genome. Plant J. *89*, 789–804.
55. Huang, W., Sherman, B.T., and Lempicki, R.A. (2009a). Bioinformatics enrichment tools: paths toward the comprehensive functional analysis of large gene lists. Nucleic Acids Res. *37*, 1–13.
56. Huang, W., Sherman, B.T., and Lempicki, R.A. (2009b). Systematic and integrative analysis of large gene lists using DAVID bioinformatics resources. Nat. Protoc. *4*, 44–57.
57. Kim, D., Langmead, B., and Salzberg, S.L. (2015). HISAT: a fast spliced aligner with low memory requirements. Nat. Methods *12*, 357–360.
58. Liao, Y., Smyth, G.K., and Shi, W. (2014). featureCounts: an efficient general purpose program for assigning sequence reads to genomic features. Bioinformatics *30*, 923–930.
59. Love, M.I., Huber, W., and Anders, S. (2014). Moderated estimation of fold change and dispersion for RNA-seq data with DESeq2. Genome Biol. *15*, 550.
60. Livak, K.J., and Schmittgen, T.D. (2001). Analysis of relative gene expression data using real-time quantitative PCR and the 2(-Δ Δ C(T)) method. Methods *25*, 402–408.

STAR★METHODS

KEY RESOURCES TABLE

REAGENT or RESOURCE	SOURCE	IDENTIFIER
Chemicals, Peptides, and Recombinant Proteins		
D-Mannitol	Duchefa	Cat. No. M0803
Pectinase	Sigma	Product No. 17389
Cellulase	Yakult Pharmaceutical Industry	https://www.yakult.co.jp/ypi/en/product/laboratory.html
Pectolyase Y-23	Duchefa	Product No. P8004.0001
PIPES	euromedex	REF 1124
Propidium iodide	SigmaAldrich	Product No.P4170
Cyber green	Roche	Cat. No. REF 04707516001
Critical Commercial Assays		
Nuclei extraction buffer: Cystein UV precise P,	Sysmex, Partec	Ref 05-5002
Nucleospin RNA Plant kit	Macherey-Nagel, Düren	Ref 740949.50
QuBit RNA HS assay kit	Thermo Fisher Scientific, Waltham, USA	Cat. No. Q32855
Bioanalyser 2100	Agilent Technologies, Santa Clara, USA	
Deposited Data		
GEO transcriptomic data	GSE133011	
Experimental Models: Organisms/Strains'		
Arabidopsis gip1gip2	[36]	Cross between *gip1* (GABI_213D01) and *gip2* (FLAG_36406)
Arabidopsis pSUN1::SUN1-GFP	[38]	
Arabidopsis gip1gip2 p35S::SUN1-YFP	[34]	Transformation of *gip1gip2* via floral dipping with *p35S::AtSUN1-YFP*
Arabidopsis: WT Col-0 x Ws	https://www-arabidopsis-org.insb.bib.cnrs.fr/servlets/TairObject?id=90&type=species_variant https://www.arabidopsis.org/servlets/TairObject?id=392&type=species_variant	Cross between WT Columbia-0 (NASC stock number: N1092) and WT Wassilewskija (NASC stock number: N2223)
Oligonucleotides		
Primers for qPCR, see Table S2	This paper	N/A
Software and Algorithms		
ImageJ	https://imagej.net/Welcome	RRID:SCR_003070
Nugsec	https://github.com/mutterer/NucSeg	N/A
Nanoscope Analysis	Bruker	N/A
FastQC (v0.10.1)	N/A	https://www.bioinformatics.babraham.ac.uk/projects/fastqc/
The PeakForce ® QNM	Bruker	N/A
cutadapt (v1.8.1).	[53]	https://cutadapt.readthedocs.io/en/stable/installation.html
Araport11	[54]	https://www.araport.org/
DESeq2 package (v1.22.2).	[55]	https://bioconductor.org/packages/release/bioc/html/DESeq2.html
Hisat2 (v2.1.0)	[56]	https://ccb.jhu.edu/software/hisat2/index.shtml
DAVID	[57, 58]	https://david.ncifcrf.gov/
Zeiss LSM 700 microscope	https://www.zeiss.com/	N/A
FeatureCounts (v1.6.2).	[59]	https://doi.org/10.1093/bioinformatics/btt656

LEAD CONTACT AND MATERIALS AVAILABILITY

All plant lines are available for sharing. Further information for resources and reagents should be forwarded and attended by the Lead Contact, Marie-Edith Chabouté (marie-edith.chaboute@ibmp-cnrs.unistra.fr).

EXPERIMENTAL MODEL AND SUBJECT DETAILS

Plants

Wild-type *pSUN1::SUN1-GFP* and *gip1gip2 SUN1-GFP* lines were described previously [34, 38]. The *gip1gip2* mutant (Col-0 x Ws genetic background) [36] was investigated for transcriptomic analyses, using 2 types of phenotypes i.e., T12 (mild phenotype) and T34 (strong phenotype), as described in Figure S2. WT, i.e., Col-0 x Ws, was used as a control. Seedlings were grown *in vitro* on 1/2 Murashige and Skoog (MS) medium (SERVA Electrophoresis) in presence of 1% sucrose and 1.2% agar at 20°C under long day conditions (16-h light 70 μmol/m2 per second of fluorescent lighting/8-h dark).

METHOD DETAILS

Osmotic stress conditions for nuclear property analyses

For osmotic treatments, sterilized seeds were germinated on ½ MS medium and 9-day-old seedlings were transferred in ½ MS liquid medium containing 0.3 M mannitol for 16h (hyperosmotic stress) or water (hypoosmotic stress). As a control, seedlings were transferred to ½ MS liquid medium.

Plant growth analysis under hyperosmotic stress conditions

Seedlings were grown for 9 days on ½ MS medium and then transferred to medium containing 0.3 M, 0.4 M, or 0.6 M mannitol. Three independent experiments were performed. Pictures of plates were taken before and after treatment either every day after treatment (0.3 M mannitol) or after 2 days of treatment (0.4 and 0.6 M mannitol). Root growth was evaluated using the segmented line measure tool plugin in ImajeJ using a line traced between 2 points.

Propidium iodide and DAPI staining on whole mount roots

Root meristem of 9-day-old seedlings were observed using confocal microscopy. Staining with 2μg/mL propidium iodide (Sigma Aldrich) reveals cell wall in viable cells and the nucleus in dead cells. Chromatin staining was performed on SUN1-GFP seedlings by incubating the roots in FACS buffer containing DAPI (2μg/mL) for 10 min and roots were observed immediately afterward.

Nuclei preparation for micro-rheometry analysis

Nuclei were prepared by chopping root tips from 9-day-old seedlings in a Petri dish with a razor blade in 400 μl of ice-cold commercial nuclei isolation buffer containing DAPI (Cystein UV precise P, Sysmex Partec, Germany) and samples were filtered through a 30 μm mesh filters to remove debris. Nuclei were then concentrated in a pellet after a 5 min centrifugation 3000 rpm at 4°C. Pellet was either resuspended in culture medium with or without mannitol and kept on ice before micro-rheometry measurements.

Micro-rheometry measurement of nuclear stiffness

The experimental chamber was filled with medium containing nuclei. One isolated nucleus was captured between two parallel microplates, one rigid, the other flexible with a calibrated stiffness k. The force applied on the nucleus upon compression was given by F = k d, were d is the flexible plate deflection. Measurements were carried out with flexible plates of spring constants 3.1 mN/m and 12.8 mN/m. The contact areas between the plates and the nucleus were estimated by assuming a circular contact. The apparent contact diameters D_F and D_R (respectively for the flexible and rigid plate) where then measured on bright field images. Then the stress σ applied on the nucleus was defined as F/A, where A is the contact area, with $A = \pi D^2/4$. However, since D_F and D_R had usually different values, leading to two different estimations of the stress value on the flexible and rigid plates, we retained their mean value $\sigma = 8F/\pi\,[D_F^2+D_R^2]$. The uniaxial nucleus strain perpendicular to plates was defined as $\varepsilon = (L\text{-}L_0)/L_0$, where L_0 and L are respectively the nucleus length (distance between the parallel microplates) before and after compression. The nucleus was submitted to increasing compression steps, and the values of ε and σ were reported for each step. Stress-strain data $\sigma(\varepsilon)$ were then fitted by a linear relationship the slope of which was retained as the value of the apparent elastic modulus of the nucleus, $E = \sigma/\varepsilon$.

AFM – material and analyses

Roots from 9-day old seedlings were put on poly L-lysin plates and cell wall was digested in 100 μl of digestion mix (2.5% pectinase, 2.5% cellulase, 2.5 pectolyase in MTBS buffer as previously described [37]. Then root tip was squashed and covered by MTBS buffer to isolate the nuclei (50 mM Pipes, 5 mM EGTA, and 5 mM MgSO4, pH 6.9 in presence of 0.1% Triton X-100). Atomic force microscopy was performed using Bioscope catalyst (Bruker) which was coupled with an optical epifluorescence macroscope (MacroFluo-Leica) equipped with a long distance Mitutoyo 10x air objective lens. The PeakForce ® QNM (Quantitative Nanomechanical Mapping) mode was used for this study. The selected AFM cantilever had a theoretical spring constant of 0.4N/m and the pyramidal tip had a theoretical curvature radius < 40nm. Before each experiment, the defiection sensitivity of the cantilever was calibrated on Sapphire

and its spring constant was also calibrated by thermal tuning. A matrix of force curves was acquired using the following parameters: Images: 100 μm^2, 128px^2, PeakForce setpoint = 1-5nN, Force curves: Ramp size = 2-5 μm, applied force = 8-10nN. The quantifications of the elastic modulus based on raw force curves were achieved with the processing software Nanoscope Analysis (Bruker). Briefly, the quantification of the apparent elastic modulus (Ea) was extracted via the application of a theoretical model (Sneddon) for an indentation I < 100 nm. The measured elastic modulus reflected the stiffness of the nucleus. Each curve was analyzed individually.

RNA extraction and sequencing

Total RNA was extracted from 9-day-old seedlings using the Nucleospin RNA Plant kit (Macherey-Nagel, Düren, Germany) according to manufacturer's instructions. For each preparation around 30 mg of frozen plant material were ground in extraction buffer in a Precelly 24 crusher (Bertin Technologie, Montigny-les-Bretonneux, France) for 2 × 30 s at 3600 rpm in presence of 0.75/1.0 mm glass beads. Purified RNAs were resuspended in 40 μl water. Quantity and quality of the extracted RNAs were determined using QuBit RNA HS assay kit (Thermo Fisher Scientific, Waltham, USA) and a Bioanalyser 2100 (Agilent Technologies, Santa Clara, USA), respectively. RNA Seq was done by Fasteris SA (Plan-les-Ouates, Switzerland) on samples of 2 μg of RNA in 20 μl. The sequencing was performed on Illumina in 125bp on single end mode.

Transcriptomic data analysis

Raw reads were quality checked with FastQC (v0.10.1) and cleaned with cutadapt (v1.8.1). Mapping was performed against the *Arabidopsis thaliana* reference genome (from Araport11) using Hisat2 (v2.1.0) and the read counting was done using FeatureCounts (v1.6.2). Differential expression analysis and corresponding graphs were done using the DESeq2 package (v1.22.2). Finally the GO analysis was done with the latest version of the DAVID online tool.

RNA extraction and Real-Time qRT-PCR

Either whole 9-day-old seedlings or root tips from 9-day-old seedlings were collected and snap-frozen in liquid nitrogen. For each experiment, 3 independent biological replicates were used. Total RNA was extracted following the kit 'NucleoSpin® RNA Plant, Macherey-Nagel' protocol (Macherey-Nagel, Düren, Germany). For qRT-PCR, 2.5 μg of RNA were used to synthesize cDNA using specific primers, random hexamer primers (IDT), and the protocol "SuperScript® IV (SSIV) First-strand and cDNA Synthesis Reaction" (Invitrogen). qRT-PCR was performed on Light Cycler thermocycler 480 II (Roche) using specific primers and SYBR Green Master Mix (Bio-Rad), according to the manufacturer's instructions. All primers used are described in Table S2. The cDNA quantification was made with the ΔΔCt method, which considers the amplification efficiency ([1+E]- ΔΔCt) and was normalized to ACTIN2 [60].

Confocal Microscopy

Confocal images were recorded with a Zeiss LSM 700 microscope equipped with 20 × /0.8 NA lens. The excitation and emission wavelengths for the fluorescent protein GFP are 488 nm and 510 nm, respectively. For propidium iodide observations, the excitation and emission wavelengths were 555 nm and 617 nm, respectively. Images were captured using Z stacks with 0.7 μm Z slice intervals. For DAPI observations, the excitation and emission wavelengths were 405 nm and 500 nm, respectively. Observations were performed in multi-tracking mode using 405-, 488-, or 555-nm laser excitation.

QUANTIFICATION AND STATISTICAL ANALYSIS

Nuclear parameters measurements

The confocal images were analyzed using ImageJ. The nuclear circularity was measured using the NucSeg ImajeJ macro tool developed by J. Mutterer (IBMP). This tool gives a detailed analysis of several nucleus parameters including circularity ($4\pi \times$ area/ $perimeter^2$). A circularity of 1 corresponds to a perfect circle. Nuclear volume and sphericity were evaluated using 3D manager and segmentation editor in Fiji (ImageJ). The volume of the 3D object is evaluated in calibrated unit, *i. e.* the number of voxels multiplied by the calibrated volume of one voxel. Compactness (sphericity) is the normalized ratio between the surface and the volume, it should be close to value 1 for a perfect sphere. Measurements were performed in the epidermal and cortex layers of the root, i.e., the more external cellular layers directly exposed to mannitol.

Statistical tests

The distribution of the data was evaluated using Shapiro-Wilk test to determine if it follows a normal law. Accordingly, we used either two tailed Student-t test or Mann-Whitney test. The Student t test was performed to study the significance of the difference between two populations for nuclear circularity and area data. The variances of the population in all the sets of data were tested using F-test. For low data number, Mann-Whitney test was used. Sample size and statistical tests are indicated in the figure captions.

DATA AND CODE AVAILABILITY

This work does not involve the production of large datasets and uses published plugins or image analysis tools.

Current Biology, Volume *30*

Supplemental Information

Mechanical Shielding in Plant Nuclei

Rituparna Goswami, Atef Asnacios, Pascale Milani, Stéfanie Graindorge, Guy Houlné, Jérôme Mutterer, Olivier Hamant, and Marie-Edith Chabouté

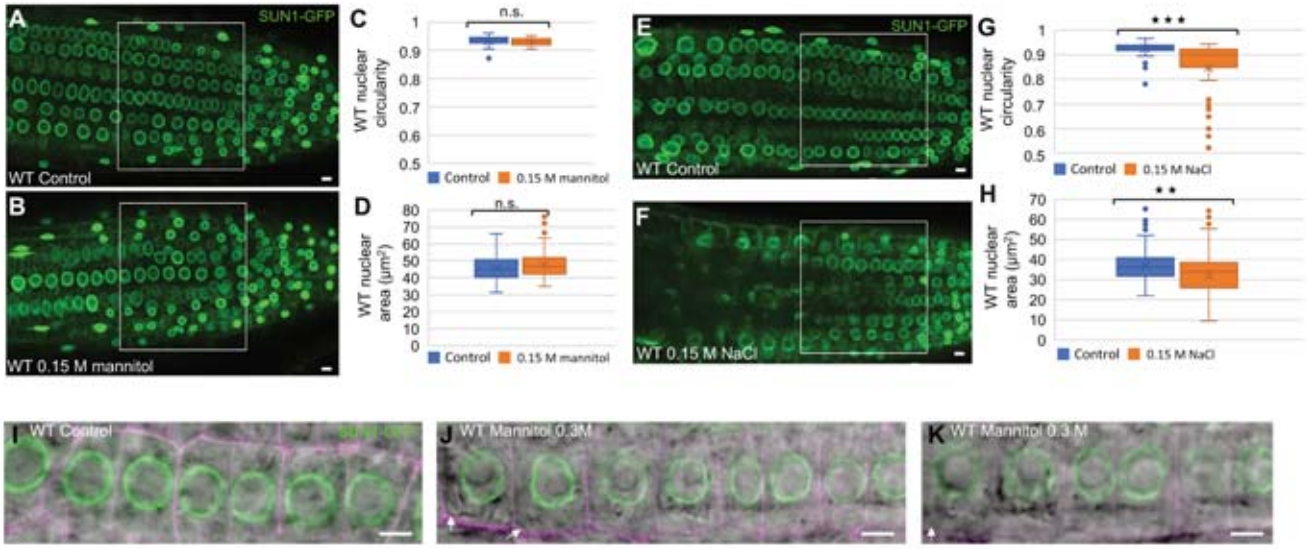

Figure S1. Cell and nuclear shape analysis in root meristems under various osmotic conditions related to Figure 1 : (A-D) in the presence of 0.15 M mannitol (A-B) Representative images of root meristems of 9-day-old seedlings expressing SUN1-GFP in absence (A) or presence (B) of 0.15 M mannitol (16h-treatment). Scale bars are 5 µm. (C-D) Quantification of the nuclear circularity (C) and area (D). The *p*-values after Student's t-test are 0.163 and 0.168, respectively, indicating no significant nuclear changes after 0.15 M mannitol treatment (n.s.). $n_{control} = 54$; $n_{treated} = 57$. (E-H) in the presence of 0.15 M NaCl. (E-F) Representative images of root meristems of 9-day-old seedlings expressing SUN1-GFP in absence (E) or presence (F) of 0.15 M NaCl (16h-treatment). Scale bars are 5 µm. (G-H) Quantification of the nuclear circularity (G) and area (H). Using Student's t –test, the *p*-values are 1.9e-8 and 0.0043, respectively, indicating significant changes (***$p \leq 0.001$, **$p \leq 0.01$, respectively). $n_{control} = 91$ and $n_{treated} = 51$. (I-K) in presence of 0.3 M mannitol. Representative images of root meristems of 9-day-old seedlings expressing SUN1-GFP in absence (I) or presence (J-K) of 0.3 M mannitol (16h-treatment). Merge are presented combining DIC and fluorescent channels (GFP, green, for NE, and PI, magenta, for cell wall). White arrows indicate plasma membrane detachment in a few cells. Scale bars are 5 µm.

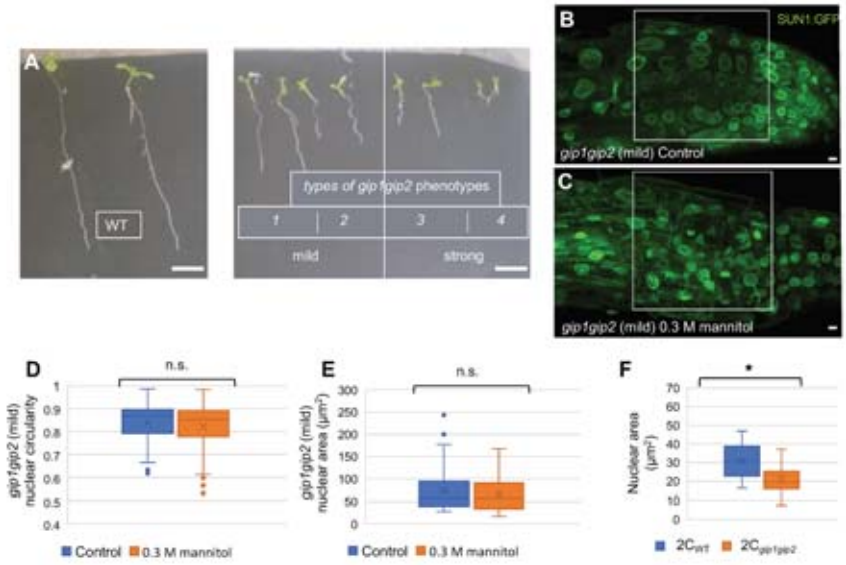

Figure S2. Characterization of the *gip1gip2* mutant, related to Figure 2: (A) Nine days-old-seedlings : mild (type 1-2) and severe (type 3-4) phenotypes of the *gip1gip2* mutant can be distinguished from WT based on the length of their main root. Scale bar is 0.5 cm (B-E) Nuclear shape analysis in root meristems of mild *gip1gip2* phenotype in the presence of 0.3 M mannitol (B-C). Representative images of root meristems of 9-day-old seedlings expressing SUN1-GFP in absence (B) or presence (C) of 0.3 M mannitol (16h-treatment). Scale bars are 5 µm. (D-E) Quantification of nuclear circularity (D) and area (E). The *p*-values after Student's t-test are 0.34 and 0.24, indicating no significant nuclear changes after 0.3M mannitol treatment (n.s.). $n_{control} = 55$ and $n_{treated} = 62$ (F) Nuclear area was evaluated in flow sorted nuclei isolated from root of WT and mild *gip1gip2* phenotype as described in [S1]. Using a Student's t-test significant difference was obtained between $2C_{WT}$ nuclei (n = 18) and $2C_{gip1gip2}$ nuclei (n =19), *p*-value 0.0014 (*).

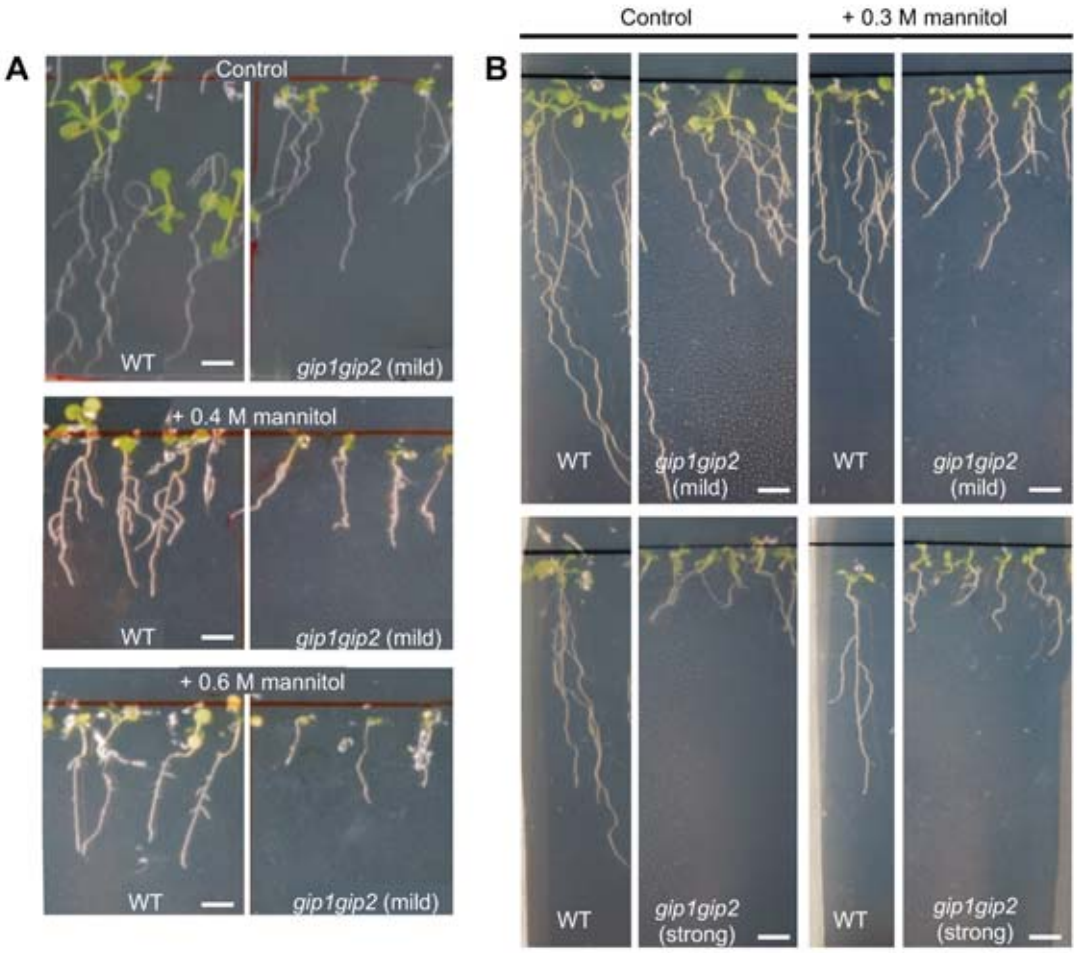

Figure S3. Phenotype of the *gip1gip2* mutant and WT seedlings in presence of various mannitol concentrations, related to Figure 3. (A) mild *gip1gip2* phenotype and WT 9-day-old seedlings grown in normal conditions were transferred on control, or 0.4 and 0.6M mannitol media and observed after 2 days. (B) mild and strong *gip1gip2* and WT 9-day-old seedlings were transferred on 0.3 M mannitol and control media and observed after 5 days. Scale bars are 0.5 cm.

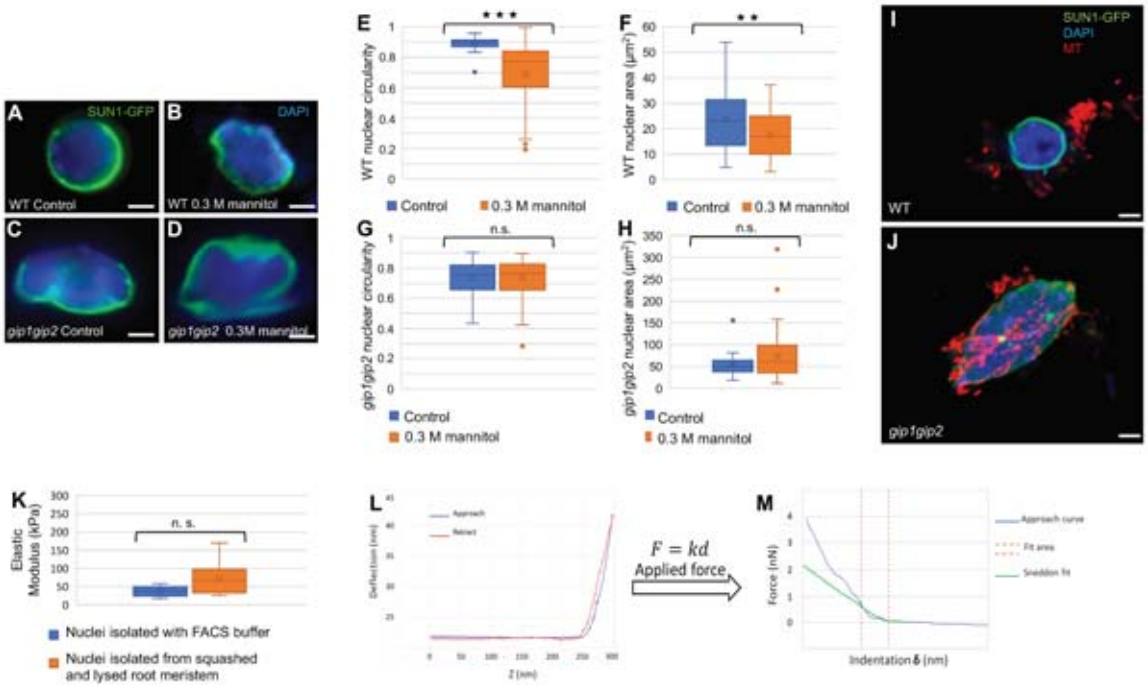

Figure S4. Characterization of nuclei used for nuclear rigidity measurements, related to Figure 4. (A-D) Nuclei were isolated from root tips using FACS buffer in presence of DAPI. Experiments were performed on 9-day-old seedlings expressing SUN1-GFP in WT control (n = 33) (A) and WT treated with 0.3 M mannitol (n = 57) (B) as well as in *gip1gip2* control (n =34) (C) and *gip1gip2* treated with 0.3 M mannitol (n = 53) (*D*). Scale bars are 2 µm. (E-H) Nuclear circularity (E-G) and nuclear area (F-H) were quantified. Using Student's t-test, significant differences were observed between WT control and WT 0.3M mannitol for nuclear circularity and area, respectively, with *p* values of 2.7e-9 (***) and 0.0079 (**); but not for *gip1gip2* with *p* values of 0.94 and 0.083, respectively (n.s.). (I-J) Immunostaining with anti-tubulin antibody performed on isolated nuclei from 9-day-old seedlings expressing SUN1-GFP in WT (I) and *gip1gip2* (*J*), as used in micro-rheometry experiments. Fixation and immunostaining were performed as described in [S1]. Scale bars, 2 µm. (K) AFM measurements comparing the elastic moduli of isolated nuclei as used in micro-rheometry (n = 5) to those of nuclei from squashed root meristems AFM (n = 6). Using Mann Whitney test no significant difference was observed (n.s.) with a *p* value of 0.193. (L-M) AFM measurements details. Calibration of the AFM probe with approach (blue) and retraction (red) (L). (M) Example of a force-indentation curve for one nucleus.

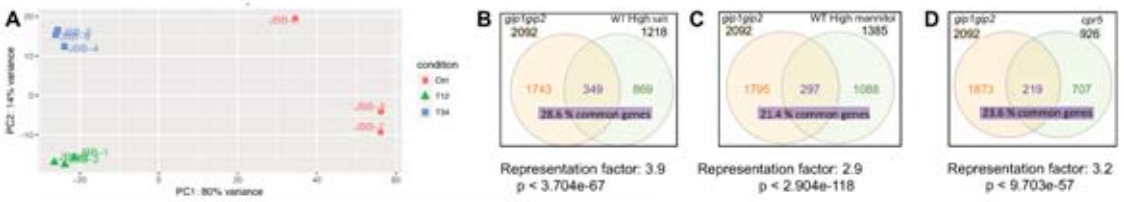

E

Accession number	Genes	Description	log 2 fold change in mild phenotype *gip1gip2*	log 2 fold change in strong phenotype *gip1gip2*	fold change in the touch response
AT5G37770	*TOUCH2 (TCH2)*	Encodes CaM-like proteins (CML24)	2.41	2.52	6.55
AT2G41100	*TOUCH3 (TCH3)*	Encodes CaM-like proteins (CML12)	3.86	3.80	2.37
AT5G57560	***TOUCH4 (TCH4)***	Encodes a xyloglucan endotransglucosylase/hydrolase	1.24	1.73	21.17
AT4G31800	***WRKY family transcription factor (WRKY18)***	Pathogen-induced transcription factor	4.06	4.61	19.56
AT2G38470	*WRKY family transcription factor (WRKY33)*	Pathogen-induced transcription factor	1.86	2.74	12.39
AT1G80840	***WRKY family transcription factor (WRKY40)***	Pathogen-induced transcription factor	5.14	5.81	43.1
AT1G27730	***Salt tolerance zinc finger (Salt tolerance)***	Transcriptional repressor, involved in response to several abiotic stresses	3.29	4.49	29.4
AT5G66210	*Calcium-dependent protein kinase (CPK28)*	Abscisic acid-activated signalling pathway	2.11	2.61	13.07
AT3G57530	*Calcium-dependent protein kinase (CPK32)*	Abscisic acid-activated signalling pathway	1.50	1.92	11.50
AT4G27280	*Calcium-binding EF-hand family protein (CA)*	Response to karrikin	2.43	3.09	12.68
AT3G50930	***AAA-type ATPase family (AAA)***	Involved in cell death	3.50	4.26	10.69
AT3G55980	*SZF1*	Transcription factor, involved in Chitin response	3.19	3.96	18.7
AT1G76600	*A2 unknown function*	Unknown function	1.67	2.08	10.51
AT1G21910	*DREB2E*	Transcription factor, encodes an AP2 type	1.60	1.13	4.07
AT5G67300	*Myb44*	Transcription factor, involved in mediating plant responses to several abiotic stresses	2.32	2.56	5.35
AT4G37370	***CYP81D8***	Encodes cytochrome P450 family proteins	1.44	1.88	2.26
AT5G06320	*NHL3*	Positive regulator of plant defense	1.86	2.63	3.34
AT2G40000	***HSPRO2***	Encodes salicylic acid-responsive positive regulator of basal resistance	1.36	1.82	18.5

Figure S5. Transcriptomic analyses of the *gip1gip2* mutant, related to Figure 5. (A) PCA analysis of the samples used for the transcriptome study to confirm that the 9 samples cluster correctly according to their genotype (DESeq2 package), *i.e.* in 3 groups WT and two populations (T12, mild phenotype and T34, strong phenotype) of *gip1gip2* mutants. (B-D) A list of genes found up-regulated in both mild and severe *gip1gip2* phenotypes was established. Venn diagrams show the overlap between up-regulated genes in *gip1gip2*, WT high salt (B), WT high mannitol (C) and *cpr5* (D) respectively [S2, S3]. The pourcentage of common genes are indicated as well as the representative factor. Statistical significance of the overlap is determined by the exact hypergeometric test (P is indicated) (E) Comparison of the fold change difference in expression for genes analyzed in the hyperosmotic stress response and in *gip1gip2* (mild and strong phenotypes). Bold genes are upregulated in high hyperosmotic conditions (salt, mannitol), and none of the 18 genes are found up regulated in *cpr5*.

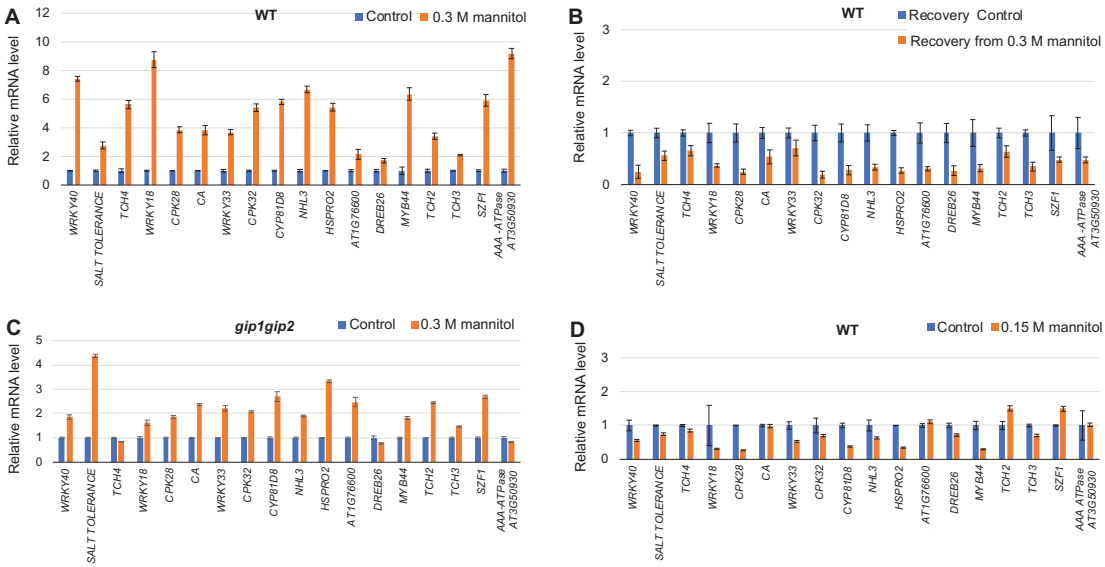

Figure S6. Relative mRNA level of touch induced genes in response to various osmotic stresses, related to Figure 6. (A) RNA was extracted from the roots of WT seedlings treated with 0.3 M mannitol for 16 hours and in control conditions. (B) RNA was extracted from WT root seedlings treated with 0.3 M mannitol for 16 hours followed by 7 hours of recovery in normal growth conditions. (C) RNA was extracted from 9-day-old *gip1gip2* seedlings treated with 0.3 M mannitol for 16 hours and control conditions. (D) RNA was extracted from 9-day-old WT seedlings treated with 0.15 M mannitol for 16 hours and control conditions. All the experiments were performed with 3 technical replicates and 2 biological replicates. SDs are indicated.

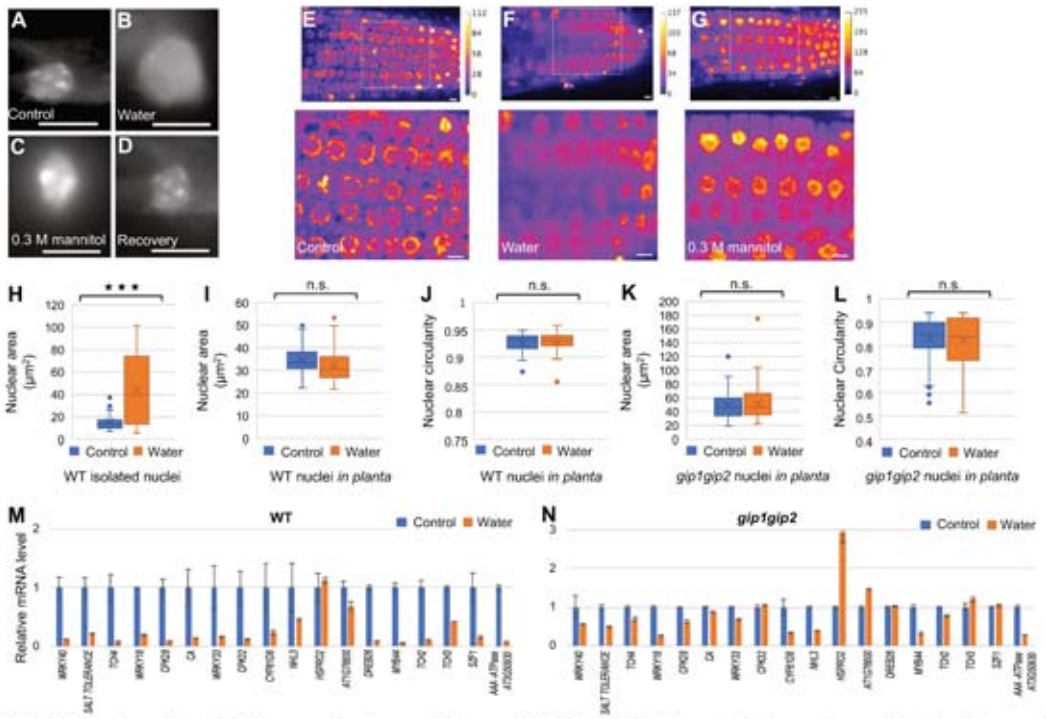

Figure S7. Analysis of nucleus and transcriptional responses to various osmotic stresses, related to Figure 7. (A-D) Representative fluorescence images of isolated nuclei compressed between parallel plates during micro-rheometry mechanical measurements. Nuclei were isolated from root tips of seedlings in control conditions using FACS buffer in presence of DAPI (A, n = 7), or after a 16h-water treatment (B, n = 5) compared to a 16h-0.3M mannitol treatment (C, n = 11) and recovery from 0.3 M mannitol (D, n = 8). Scale bars are 5 µm. (E-G) Nuclei in root tips of seedlings in control conditions (E), or after a 16h-water treatment (F) compared to a 16h - 0.3M mannitol treatment (G) using a 10 min incubation of the roots in FACS buffer in presence of DAPI. Images were adjusted to the same background level and signal intensity was color-coded using the ImageJ Fire lookup table. Calibration bar is indicated on the right side of each picture. Magnification of dotted square are presented below each picture. Scale bars are 5 µm. (H-L) Nuclear area was evaluated in isolated nuclei from root tips (H) of WT seedlings treated in control conditions (n = 45), or a 16h -water treatment (n = 32) and a significant difference was observed using Student's-t test with a p value of 9.06e-8 (***). Similar analyses were performed on nuclei *in planta* (I) in WT control (n =164) and water-treated WT seedlings (n = 174) as well as in mild phenotype *gip1gip2* (K) ($n_{control}$ = 80 and $n_{treated}$ = 57) but no significant differences were observed for nuclear area between control and treated seedlings, with p-values of 0.4 and 0.361, respectively. Nuclear circularity was also not significantly modified by water treatment with a p-value of 0.12 for WT and 0.553 for *gip1gip2* (M-N) Analysis of the transcriptional response of touch induced genes in seedlings after a 16h-water treatment compared to control conditions in WT (M) and in *gip1gip2* (N). All the experiments were performed with 3 technical replicates and 2 biological replicates. SDs are indicated.

GO	Count	%	PValue	List Total	Pop Hits	Pop Total	Fold Enrichment	Bonferroni	Benjamini	FDR
single-organism cellular process	831	40,22	3,86E-15	1644	7640	18449	1,220614944	4,59E-13	4,59E-14	4,45E-1
response to stress	670	32,43	2,33E-91	1644	3697	18449	2,033744399	2,75E-89	2,75E-89	2,67E-8
single-organism metabolic process	610	29,53	1,75E-39	1644	4317	18449	1,585691886	2,07E-37	5,17E-38	2,01E-3
response to chemical	512	24,78	5,95E-62	1644	2884	18449	1,992258657	7,02E-60	3,51E-60	6,81E-5
response to abiotic stimulus	380	18,39	5,43E-51	1644	2004	18449	2,127927843	6,41E-49	2,14E-49	6,21E-4
cellular response to stimulus	342	16,55	6,16E-07	1644	3022	18449	1,269996908	7,27E-05	6,61E-06	7,05E-0
response to endogenous stimulus	303	14,67	8,66E-32	1644	1757	18449	1,935271427	1,02E-29	1,28E-30	9,91E-2
response to external stimulus	300	14,52	1,01E-36	1644	1631	18449	2,064136014	1,19E-34	1,70E-35	1,15E-3
response to biotic stimulus	258	12,49	5,19E-38	1644	1282	18449	2,258409533	6,12E-36	1,22E-36	5,94E-3
response to other organism	250	12,10	6,83E-38	1644	1224	18449	2,292079139	8,06E-36	1,34E-36	7,82E-3
immune response	89	4,31	9,50E-20	1644	351	18449	2,845469323	1,12E-17	1,24E-18	1,09E-1
regulation of response to stimulus	84	4,07	1,29E-05	1644	584	18449	1,614126087	0,00152201	1,17E-04	0,0147715
regulation of immune system process	28	1,36	8,92E-07	1644	110	18449	2,856514046	1,05E-04	8,77E-06	0,0010203
immune effector process	18	0,87	7,10E-05	1644	68	18449	2,970534564	0,00834467	5,98E-04	0,0812383
interspecies interaction between organisms	30	1,45	7,57E-05	1644	153	18449	2,200395973	0,00889146	5,95E-04	0,0865831
single organism signaling	230	11,13	1,80E-04	1644	2064	18449	1,250515735	0,02096223	0,00132319	0,205255C
single-organism localization	196	9,49	2,90E-04	1644	1735	18449	1,267732458	0,03366872	0,00201259	0,331613C
positive regulation of response to stimulus	32	1,55	0,00100479	1644	194	18449	1,851054757	0,11185862	0,00656857	1,1439006
hormone metabolic process	28	1,36	0,00131436	1644	164	18449	1,915954543	0,14375262	0,00813494	1,4939167
multi-organism cellular process	25	1,21	0,00574709	1644	156	18449	1,798400555	0,49344035	0,03343397	6,3833243
positive regulation of immune system process	13	0,63	0,00683841	1644	61	18449	2,391577919	0,55501016	0,03782345	7,5525837
regulation of multi-organism process	18	0,87	0,01023072	1644	104	18449	1,9422726	0,70282758	0,05366295	11,102602
seed oilbody biogenesis	4	0,19	0,01876494	1644	7	18449	6,412582551	0,89304021	0,09261374	19,490394
negative regulation of circadian rhythm	3	0,15	0,02236962	1644	3	18449	11,22201946	0,93071916	0,10526956	22,811009
maintenance of location	12	0,58	0,03701776	1644	68	18449	1,980356376	0,98833306	0,16309094	35,058652
cell wall organization or biogenesis	81	3,92	0,04106787	1644	742	18449	1,225045252	0,99290473	0,17330568	38,116705
detection of stimulus	16	0,77	0,04524346	1644	105	18449	1,710022014	0,99576033	0,18318558	41,131403
activation of immune response	8	0,39	0,05418344	1644	39	18449	2,301952711	0,99860294	0,2092423	47,140253
circadian rhythm	17	0,82	0,05904587	1644	118	18449	1,616731618	0,99923954	0,21935975	50,168125
negative regulation of response to stimulus	22	1,06	0,06083046	1644	165	18449	1,496269262	0,99939216	0,21874455	51,23908
protein folding	37	1,79	0,08717799	1644	320	18449	1,297546001	0,99997884	0,29333818	64,791832

Table S1. GO annotations of biological functions linked to the most upregulated genes, related to Figure 5, in the *gip1gip2* transcriptome when compared to WT. In red are GO with FDR (False discovery rate < 0.05)

Genes	AGI	Forward primer	Reverse Primer
TCH2	AT5G37770	GTCGACGGTGATGATTCGTA	CATCAATCACCACATACTTCTAGGG
TCH3	AT2G41100	GGAATCTTTCAGGTTATTCGACA	AGGGAAAACATCACGGTACG
TCH4	AT5G57560	CCATGT TGTTCCAGGTGATTTCAAG	CCTCTGGTTCTGGATTCAAC
WRKY family transcription factor (*WRKY18*)	AT4G31800	CATCGGACACAAGCTTGACAGTT	TGCGCTGCGTTGTACCTTC
WRKY family transcription factor (*WRKY33*)	AT2G38470	GGGGACAATGAAACAAATGGTG	CGATTCTCGGCTCTCTCACTG
WRKY family transcription factor (*WRKY40*)	AT1G80840	CCAAGAGCTTACTTCAAATGTGC	CCTCCACACTTCTCTGAACCTT
Salt tolerance zinc finger (*SALT TOLERANCE*)	AT1G27730	ATCACACGTTTGCACCATCTG	CTTCGTAGTGGCACCGCT
Calcium-dependent protein kinase (*CPK28*)	AT5G66210	ATAACGCCTGAGGAACTTCG	TCCCATCTCTGTCTATGTCTGC
Calcium-dependent protein kinase (CPK32)	AT3G57530	GGGAAGCCTTGTCTGACGAAC	TGTTCCTGTTTTCATCATCGTTACAA
Calcium-binding EF-hand family protein (*CA*)	AT4G27280	TGTGTTGATGTTTAGGCTTAGCCC	TCCTCAATGACCTCCGTGACGA
AAA-type ATPase family (*AAA*)	AT3G50930	AGGTATTGAGGCGACAGAGG	ACAGAGTCATTTCTCATAAGCTGTTC
SZF1	AT3G55980	TCCAACTTTCTTCTCAATTTCATTC	TGTTAAGGTTCTTGAAGAGCAGAG
Unknown function (*A2*)	AT1G76600	GTCGCGATTGAGAAAGCAG	CGTCACAACCGGAGAGATTC
DREB26	AT1G21910	ACGATGCTCGATGAATACTTCTACG	TTAATTGAAACTCCAAAGCGGAATGTCAG
Myb44	AT5G67300	GCAACGTCATTGTCTCTCTCC	CAACTAGTACTGAGCTTAGCTTTAGGC
CYP81D8	AT4G37370	TCGTATCATTAAAGGAAACATGCTCGC	GGATGGTTCAACACGTTCGACAA
NHL3	AT5G06320	ACGGTGGTTGGAACTAAACTCG	TCCTCTCTCCGCCGTCAAG
HSPRO2	AT2G40000	TCATTTGCTTCAGGGGATG	CGCCACTAACTGCCTATACCC

Table S2. List of primers used in qRT-PCR experiments, related to Figures 5 and 6

Supplemental references:

S1: Batzenschlager, M., Lermontova, I., Schubert, V., Fuchs, J., Berr, A., Koini, M.A., Houlne, G., Herzog, E., Rutten, T., Alioua, A., et al. (2015). Arabidopsis MZT1 homologs GIP1 and GIP2 are essential for centromere architecture. Proc Natl Acad Sci U S A 112, 8656-8660.

S2: Sewelam, N., Oshima, Y., Mitsuda, N., and Ohme-Takagi, M. (2014). A step towards understanding plant responses to multiple environmental stresses: a genome-wide study. Plant Cell Environ 37, 2024-2035.

S3: Gu, Y., Zebell, S.G., Liang, Z., Wang, S., Kang, B.H., and Dong, X. (2016). Nuclear Pore Permeabilization Is a Convergent Signaling Event in Effector-Triggered Immunity. Cell 166, 1526-1538 e1511.

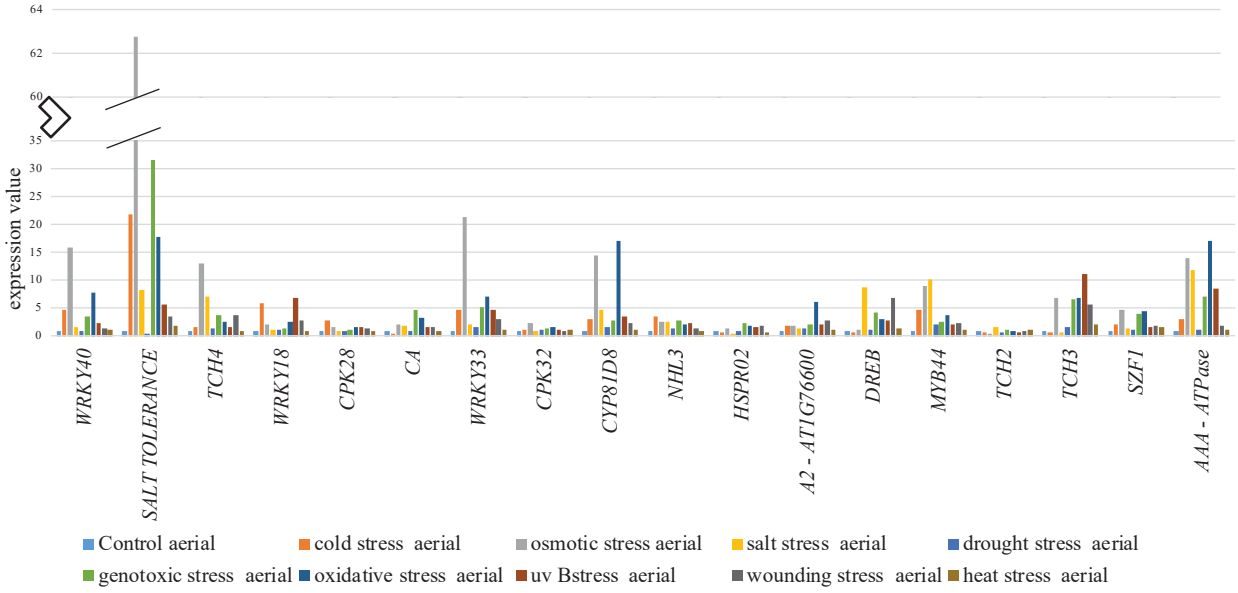

Figure 2. Expression of 18 genes under different abiotic stresses in the aerial parts after 24 hours

Additional Data –

1. Expression analysis and data clustering

We have highlighted that the *gip1gip2* mimics a constitutive stress response at the transcriptional level, with GO annotations of induced genes linked to various stress responses (osmotic stress, oxidative stress, salt stress, cation induced stress). Based on transcriptional response in *gip1gip2*, mechanical stress induced in hyper-osmotic, touch and sound vibration responses (Lee *et al.*, 2004; Ghosh *et al.*, 2016), we have identified 18 genes i.e. *TCH2, TCH3, TCH4, WRKY* family transcription factor (*WRKY18*), *WRKY33, WRKY40*, Salt tolerance zinc finger (SALT TOLERANCE), Calcium-dependent protein kinase (*CPK28*), *CPK32*, Calcium-binding EF-hand family protein (CA), AAA-type ATPase family (AAA), *SZF1*, Unknown function (A2), *DREB26*, *Myb44, CYP81D8, NHL3, HSPRO2.* In order to know whether these genes can also be induced in response to other stresses, we have investigated their expression patterns in various abiotic stresses.

Expression data of these genes have been collected by using AtGenExpress Visualization Tool (http://jsp.weigelworld.org/expviz/expviz.jsp) which has now been discontinued but the data is still visible in Arabidopsis eFP browser, hosted at the University of Toronto (http://bar.utoronto.ca/efp/cgi-bin/efpWeb.cgi?dataSource=Abiotic_Stress). Expression data comprises analysis on 18 day-old Arabidopsis seedlings after cold stress (continuous 4°C), osmotic stress (300 mM Mannitol), salt stress (150 mM NaCl), wind-induced drought stress (exposure to airstream for 15 minutes in loop), genotoxic stress (bleomycin 1.5 µg/ml and mitomycin 22 µg/ml), oxidative stress (10 µM methyl viologen), UV-B stress (15 min UV-B lights), wounding stress (a custom made 16 needdles containing tool punctuated the leaves for 3 times), heat stress (3 hours at 38 degrees) (Figures 2 and 3).

The genes tested show variable responses to these abiotic stresses. All of the above-mentioned genes exhibit up-regulation in response to hyperosmotic stress by salt (2 - 263 fold) and mannitol (1.38 - 6.56 fold) after 24 hours in the root tissue as we observed after 16h of treatment by salt or mannitol (Figures 2 and 3). Interestingly, for the aerial part, mannitol is able to induce all these genes except *TCH2* (Figure 7) but salt stress is unable to induce *WRKY18, CPK28, CPK32, HSPR0, TCH3* (Figures 4, 5, 6, 7).

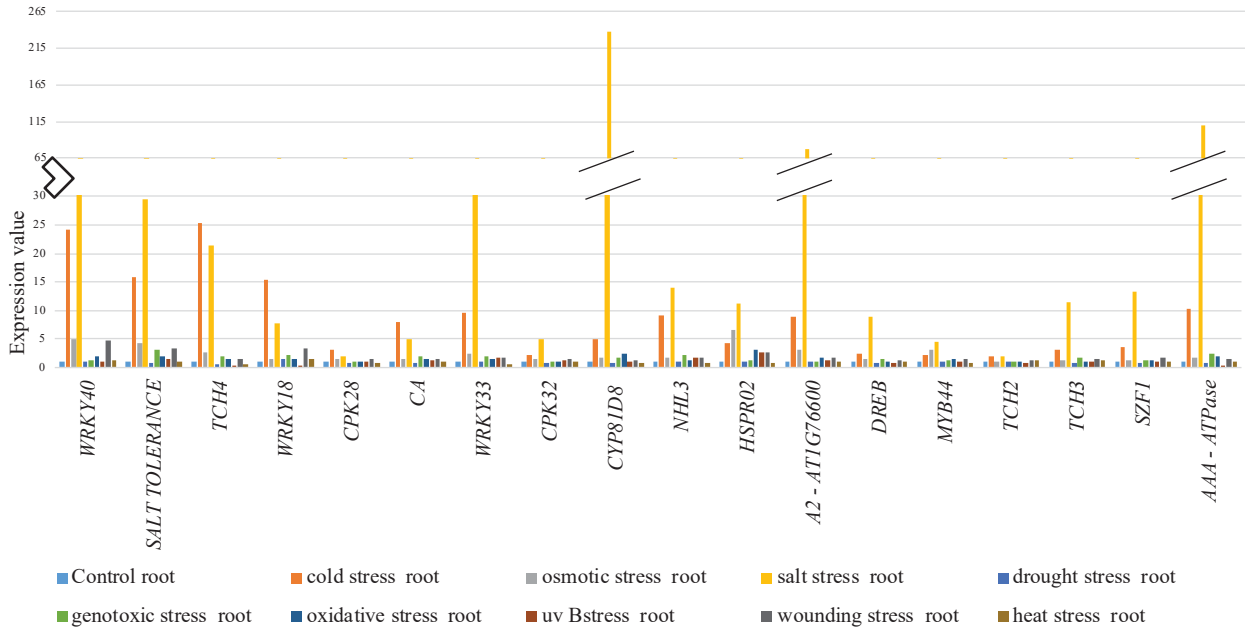

Figure 3. Expression of 18 genes under different abiotic stresses in root tissue after 24 hours

The level of expression of all these genes in root tissues is the highest in conditions of salt and cold stresses. In the aerial parts of the seedlings, a higher-level induction was observed in response to osmotic stress compared to other abiotic stress of the following genes: *WRKY40, SALT TOLERANCE, TCH4, WRKY 33, CYP81D8, NHL3, CA, WRKY33, CPK32, MYB44*, *TCH3, AAA-ATPase, SZF1,* (Figures 4, 5, 6, 7, 8). ROS accumulation is common response to salt (Leshem *et al.*, 2007) and sorbitol induced (Martinière *et al.*, 2019) osmotic stress. Some of the other abiotic stress could mimic osmotic stress via accumulation of ROS for example genotoxic, UV-B and oxidative stress responses. Indeed, these stresses were able to induce the expression of the genes (*WRKY40, SALT TOLERANCE, TCH4, WRKY 33, CYP81D8, NHL3, CA, WRKY33, MYB44*, *TCH3, AAA-ATPase, SZF1*) upregulated by osmotic stress in the areal part as well.

Tissues might be more or less permeable to salt and mannitol. Salt induced signaling response primarily originates in root tissue (Julkowska & Testerink, 2015). Differential tissue specific stress response is shown during Jasmonic asid (defense response induction comparable to wounding response) induction. Root and shoot act differently in context of the signal induction and the signaling cascade in *Brassica oleracea* (Tytgat *et al.*, 2013). Molecular players responsible for organ specific differential stress response is yet to be fully understood. Tissue context, cell type specific response, and stress gradient are likely to be involved (Pierik & Testerink, 2014).

2. Promoter Analysis for putative binding of Transcription factors-

Certain transcription factors (TFs) have been found to be master regulators of the hyperosmotic stress response. Ghorbani *et al.*, 2019 observed 109 (about 6.6%) and 223 (about 7.7%) genes encoding transcription factors in leaves and 234 (about 7.4%) and 396 (about 10.5%) genes in roots which are differentially regulated in response to drought and salt stress, respectively. Although they categorized these TFs in 28 and 34 groups in leaves, and 37 and 40 groups in roots, in response to drought and slat stress, the majority belonged to the *AP2/ERF, MYB* and NAC families but *bZIP, HSF, C2H2* and *WRKY* are also worth to mention (Ghorbani *et al.*, 2019). Here we have analysed the putative transcription factor binding sites on the 18 genes to understand the regulation of these mechanoresponsive genes which were upregulated under osmotic stress or in conditions of reduced levels of GIPs in our study. We studied the promoter regions of our genes to understand the regulation of these genes by using http://bioinformatics.sdstate.edu/go/. Interestingly, various putative transcription binding sites

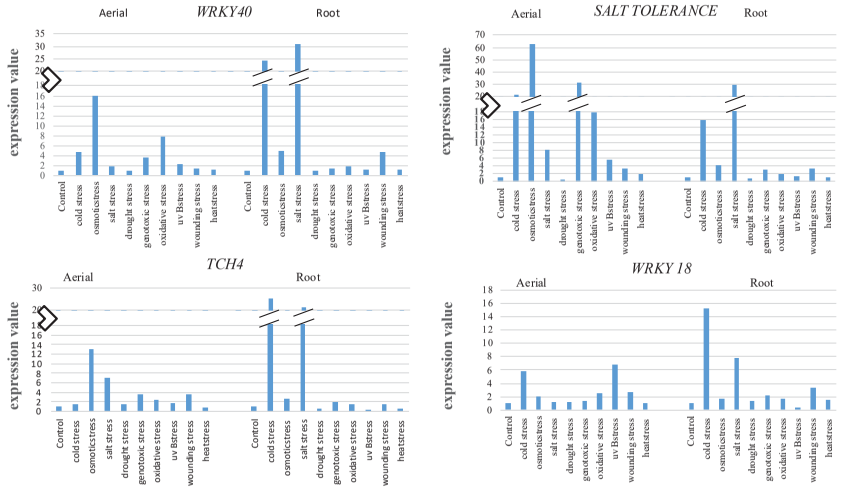

Figure 4. *WRKY40, SALT TOLERANE, TCH 4 and WRKY 18* expression in aerial and root tissue after 24 hours

were identified in the promoter regions (up to 600 pb upstream the coding regions), such as the binding myb box 3 in 10 genes (*AT1G21910 _ DREB26, AT1G27730_salt tolerance, AT1G76600_ A2 unknown function, AT1G80840_WRKY 40, AT2G38470_ WRKY 33, AT3G50930_ AAA-type, AT4G27280_ calcium-binding EF-hand family protein, AT4G37370_CYP81D8, AT5G57560 _TCH4, AT5G67300_ Myb44*), the myb box 1 in 11 genes (*AT1G21910 _ DREB26, AT1G27730_salt tolerance, AT1G76600_ A2 unknown function, AT1G80840_WRKY 40, AT2G38470_ WRKY 33, AT3G50930_ AAA-type, AT4G27280_ calcium-binding EF-hand family protein, AT4G37370_CYP81D8, AT5G57560 _TCH4, AT5G67300_ Myb44, AT2G41100_TOUCH 3*) and finally the myb box 2 in 8 genes (*AT1G21910 _ DREB26, AT1G27730_salt tolerance, AT1G76600_ A2 unknown function, AT2G38470_ WRKY 33, AT5G57560 _TCH4, AT2G41100_TOUCH 3, AT2G40000_HSPR02, AT5G06320_NHL3*) (Table 1). So, 13 out of 18 genes (72%) have at least one putative MYB binding site. This analysis is preliminary, but it depicts a scenario where the mechano-responsive genes could be under control of specific transcription factors involved in the abiotic stress response including mechanoresponsive genes (*TCH*s and *CML*s).

Interestingly, *MYB44* and *DREB26* TF promoters have TF binding site MYB box 3 and MYB box 1, but no DREB binding site. DREB26 can regulate 5 of these mechanoresponsive genes, notably salt tolerance (STZ), which could critical in mediating stress tolerance to salt and drought (Ghorbani *et al.*, 2019). This could suggest an existence of a signaling cascade where MYB factors may regulate *DREB26* and target genes towards a more specific response to hyperosmotic stress. Similarly, *WRKY33* also has MYB binding sites whereas MYB 44 does not have a direct WRKY binding site (Table 1). *WKRY 33* (not WRKY 40) has DREB transcription factor binding site and *DREB26* as well have WRKY binding site in their promoter region meaning a possible co-regulated expression of these genes. But WRKY could regulate a wider range of the tested mechanoresponsive genes. Touch induces strongly the expression of *WRKY 40* when compared to *MYB44* through transcriptome analysis as well as by RT-qPCR under hyperosmotic stress and in control conditions in *gip1gip2* (Goswami *et al.*, 2020).

TCH 4 has TF binding site for MYB, HSF, WRKY, bZIP, bHLH ARF; TCH 3 for MYB, HSF, WRKY, NAC; TCH 2 for NAC, bHLH (Table 1). A common regulation of genes encoding

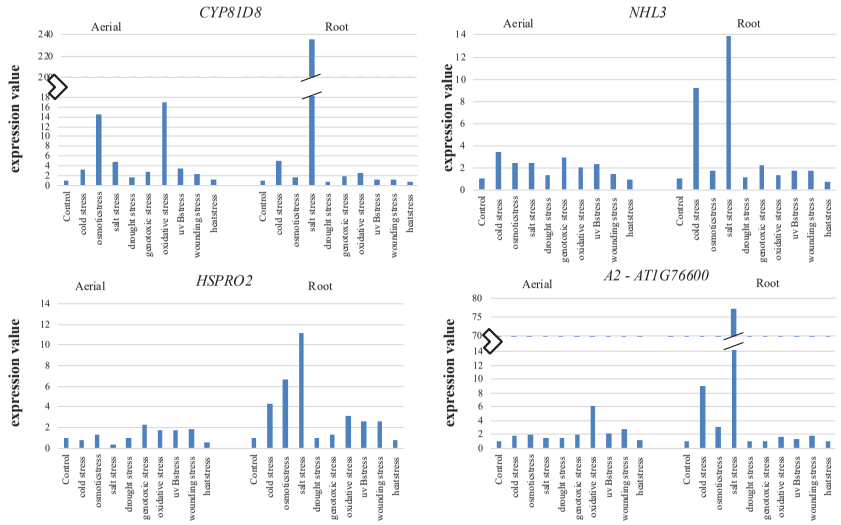

Figure 5. *CYP81D8, NHL3, HSPRO2* and *A2* expression in aerial and root tissue after 24 hours

cell wall modifying and calcium signaling proteins could mean they belong to a common signaling cascade or as target genes of a particular type of stress.

Discussion

Under hyperosmotic stress, *Arabidopsis* nucleus becomes abnormally shaped and mechanically stiffer, although transiently. But in absence of the nuclear envelope protein GIP the nuclear response is constitutive at the level of nuclear shape and mechanics. Changes in nuclear characteristics hugely affects stress gene expression (Goswami *et al.*, 2020). These genes upregulated by mechanical changes are also induced by other abiotic stress albeit to a lower extent, when compared to hyperosmotic stress in root tissue. Interestingly in root tissue, most of these genes were also upregulated in cold stress which modifies membrane fluidic properties (Xiong *et al.*, 2002), leads to higher ROS production, induction of dehydration (extracellular ice formation due in subzero level), change in secondary DNA structure (Pareek *et al.*, 2017) etc. which can change the mechanical property of the cell and subcellular structures. The transcriptional response to mechanical stress may also be compared to the wounding response sharing a large overlap in genes induced with both abiotic and biotic stresses and thus may represent the initial general stress response of *Arabidopsis.* Interestingly many stress related genes are regulated by the repressive marks H3K27me3, for which the nuclear envelope environment is critical to maintain a repressive transcriptional state (see review Barneche & Baroux, 2017). That suggests that derepression of genes loaded by H3K27me3 might be linked to changes in 3D chromatin organization as recently suggested (Nützmann *et al.*, 2020). It appears also that MYB transcription factors, which target 70% of the mechanically induced genes (13 among 18 studied genes) and their respective sites on promoters, may be important to drive drought stress response in plants but also are involved in crosstalk among different abiotic stress responses, where they be upstream in the signaling cascades (Baldoni *et al.*, 2015). `

The nuclear envelope seems to be important to regulate stress responses, especially nucleoporins and nucleoskeleton proteins (Groves *et al.*, 2018). In Rice (*Oryza sativa*) the gene encoding the nuclear lamin like protein *OsNMCP1* is induced by drought through hyperosmotic stress and confers resistance. OsNMCP1 modulates the chromatin accessibility by interacting physically with OsSWI3C which is a SWITCH/SUCROSE NONFERMENTING (SWI/SNF) ATP-dependent chromatin remodeling complex (CRC) protein. It helps to remove the negative

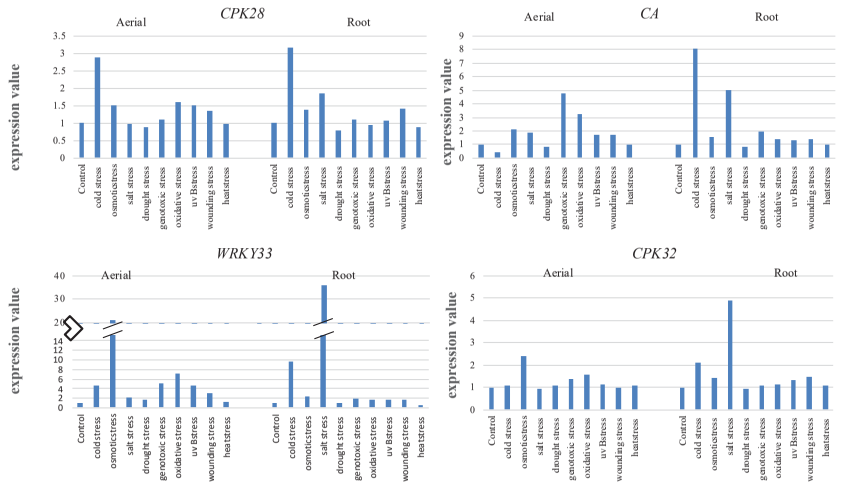

Figure 6. *CPK28, CA, WRKY33* and *CPK32* expression in aerial and root tissue after 24 hours

effect of OsSWI3C on gene expression and ensure array of drought responsive gene expression including *OsNAC10, OsERF48, OsSGL, SNAC1, and OsbZIP23* (Yang *et al.*, 2020). In a way this regulation could be different for NMCP homologous CRWN proteins in Arabidopsis, since CRWN1 was found to negatively regulate gene expression through maintaining repressive state by interacting with the polycomb associated factor PWO1 (Mikulski *et al.*, 2019). GIPs also are negative regulators of touch responsive genes in the hyperosmotic stress response.

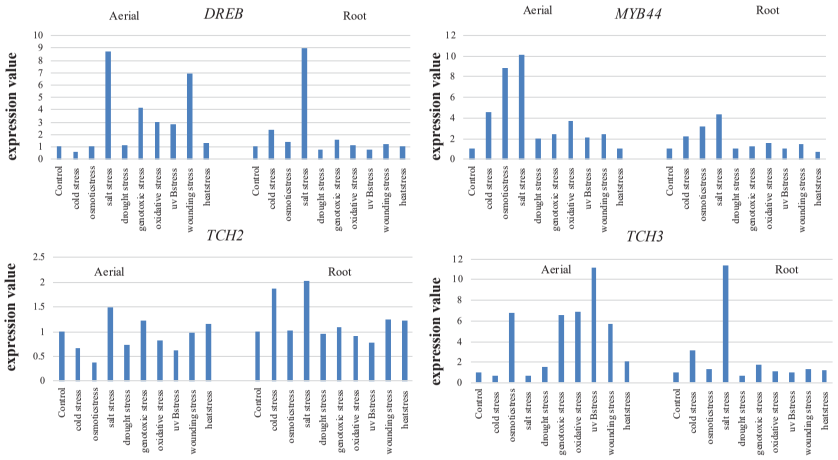

Figure 7. *DREB, MYB44, TCH2* and *TCH3* expression in aerial and root tissue after 24 hours

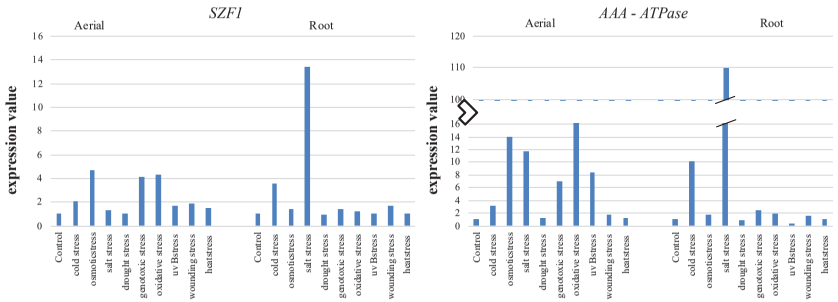

Figure 8. *SZF1* and *AAA-ATPase* expression in aerial and root tissue after 24 hours

Table 1. Transcription factor binding sites in 18 mechanoresponsive genes (n means not applicable)

Enrichment	FDR	Genes in list	Functional	Category	AT1G21910_DREB26	AT1G27730_salt tolerance	AT1G76600_A2 unknown function	AT1G80840_WRKY 40	AT2G38470_WRKY 33	AT3G50930_AAA-type	AT4G27280_calcium-binding EF-hand family protein	AT4G37370_CYP81D8	AT5G57560_TCH4	AT5G67300_Myb44	AT2G41100_TOUCH 3	AT2G40000_HSPR02	AT5G06320_NHL3	AT3G55980_SZF1	AT5G37770_TOUCH 2
1.60E-08	10	1276	**Myb box3 MYB target**	AT1G21910	AT1G27730	AT1G76600	AT1G80840	AT2G38470	AT3G50930	AT4G27280	AT4G37370	AT5G57560	AT5G67300	n	n	n	n	n
1.71E-07	11	2340	**Myb box1 MYB target**	AT1G21910	AT1G27730	AT1G76600	AT1G80840	AT2G38470	AT3G50930	AT4G27280	AT4G37370	AT5G57560	AT5G67300	AT2G41100	n	n	n	n
2.21E-07	11	2493	**HSE1 HSF target**	AT1G21910	n	AT1G76600	AT1G80840	AT2G38470	n	AT4G27280	AT4G37370	AT5G57560	AT5G67300	AT2G41100	AT2G40000	AT5G06320	n	n
2.37E-07	8	982	**Myb box2 MYB target**	AT1G21910	AT1G27730	AT1G76600	n	AT2G38470	n	n	n	AT5G57560	n	AT2G41100	AT2G40000	AT5G06320	n	n
3.75E-07	10	2100	**W box WRKY target**	AT1G21910	AT1G27730	AT1G76600	AT1G80840	n	AT3G50930	n	AT4G37370	n	n	AT2G41100	AT2G40000	AT5G06320	AT3G55980	
6.64E-05	6	1029	**Nac box NAC target**	n	AT1G27730	n	n	AT2G38470	n	n	n	n	AT5G67300	AT2G41100	AT2G40000	n	n	AT5G37770
0.00045327	5	938	**G box bHLH target**	n	AT1G27730	AT1G76600	n	n	n	n	AT4G37370	n	n	n	n	n	AT3G55980	AT5G37770
0.00081034	3	250	**C ABRE bZIP target**	n	n	n	n	n	n	n	n	AT5G57560	AT5G67300	n	n	n	AT3G55980	
0.00120961	4	693	**N box bHLH target**	n	n	n	n	n	n	n	AT4G37370	AT5G57560	n	n	n	AT5G06320	AT3G55980	n
0.00206089	5	1416	**AuxRE ARF target**	n	n	AT1G76600	n	n	AT3G50930	n	n	AT5G57560	AT5G67300	AT2G41100	n	n	n	n
0.00331203	4	963	**DREB AP2 EREBP target**	n	AT1G27730	n	n	AT2G38470	AT3G50930	AT4G27280	n	n	n	n	n	AT5G06320	n	n
0.00389406	4	1032	**G box2 bZIP target**	n	n	AT1G76600	n	n	AT3G50930	n	n	n	n	AT2G41100	AT2G40000	n	n	n

Chapter II

Role of nucleoskeletal proteins of *Arabidopsis* under osmotic stress

Preface-

As discussed in the introduction, Nucleoskeletal proteins constitute one of the important mechanical elements of the nucleus which helps to modulate the mechanical properties of the nucleus. In animals, nuclear lamina is constituted of highly conserved lamin proteins (Stuurman *et al.*1998; Dittmer & Misteli, 2011). This nuclear lamina is a mesh like fibrous structure which not only helps in mechanically stabilising the nucleus but also acts as a module for chromatin tethering, signal transduction, transcription factor anchoring (de Leeuw *et al.*, 2018). In addition of lamin proteins, nuclear lamina harbours several integral membrane proteins called lamin binding proteins (such as emerin, lamina- associated polypeptide 2, MAN1 e.t.c.) to tether the meshwork to both the nuclear envelope and chromatin. Although true lamins are exclusive to animals, a similar structural meshwork has been identified in plants (Fiserova *et al.*, 2009) and functional homolog of lamins, called plant lamin-like, have been identified in several model plants: carrot (*Daucus carota*) (Masuda *et al.*, 1993), onion (*Allium cepa*)(Ciska *et al.*, 2013) and *Arabidopsis* (Wang *et al.*, 2013). In Arabidopsis, 4 coil-coiled domain proteins have been identified, the CROWDED NUCLEI (CRWN) proteins which are expressed in all plant tissues. CRWN1 and 4 are located at the nuclear periphery while CRWN2 and 3 are distributed throughout the nucleoplasm(Dittmer *et al.*, 2007; Dittmer & Richards, 2008; Sakamoto & Takagi, 2013). The loss of all CRWN proteins leads to plant lethality, showing their importance in plant development. Interestingly plants lacking both CRWN1 and 2 or CRWN1 and 4, exhibit enhanced defense responses including some resistance to bacterial pathogens (Choi *et al.*, 2019). All of them contribute to maintain the nuclear structure and morphology especially in differentiated tissues: nuclei remain small and rounded in the *crwn* mutants, when compared to elongated nuclei in the WT (Dittmer *et al.*, 2007; Wang *et al.*, 2013; Sakamoto & Takagi, 2013) (Figure 1A). Linked to their localization pattern, CRWN1 and CRWN4 contribute to the chromatin status (Wang *et al.*, 2013; Hu *et al.*, 2019). Another putative lamin-like protein, KAKU4, interacts with CRWN1 and is located at the nuclear envelope, however until now no clear link with chromatin has been established for KAKU4 (Goto *et al.*, 2014). Similar phenotype of nuclear shape in *kaku4* was observed as for *crwn* mutants (Goto *et al.*, 2014) (Figure 1B).

In the previous chapter we established the role of nuclear morphology and mechanics under hyperosmotic stress. So next we wanted to know if nucleoskeleton proteins may be important for the mechanical properties of nucleus and the plant response to osmotic stress.

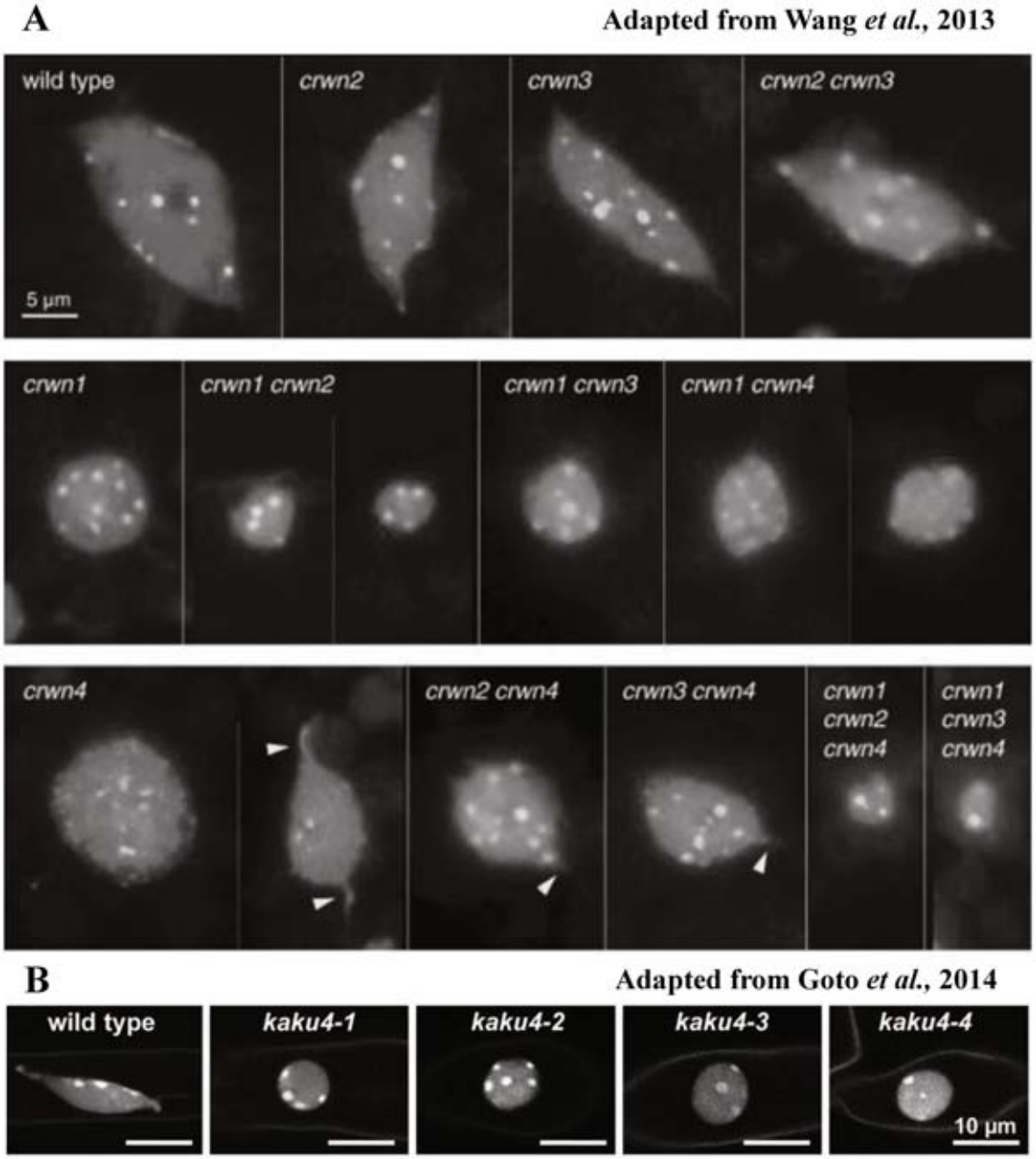

Figure 1. Shape of *Arabidopsis* nucleus in absence of nucleoskeletal proteins.

(A) Shape of the nuclei in single, double and viable triple mutants of *crwn1, crwn2, crwn3* and *crwn4.* In differentiated cells, nucleus loses the typical elongated phenotype and becomes spherical. Adapted from Wang *et al.* (2013).

(B) Shape of the nuclei in absence of CRWN1 and CRWN4 interacting protein KAKU4. Nuclei from differentiated tissue in *kaku4* also becomes spherical. Adapted from Goto *et al.* (2014).

Hyperosmotic stress impacts nucleus lacking the nucleoskeletal proteins at the nuclear periphery

Rituparna Goswami[a,b], Olivier Hamant[b*] and Marie-Edith Chabouté[a*]

[a] Institut de biologie moléculaire des plantes, CNRS, Université de Strasbourg, 67084 Strasbourg, France

[b] Laboratoire de Reproduction et Développement des Plantes, Université de Lyon, UCB Lyon 1, ENS de Lyon, INRA, CNRS, 69364 Lyon, France

Abstract

Animal nuclei posses a filamentous lamina tethered at the envelope which ensures mechanical stability and can also act as a signalling hub. In plants NMCP/CRWN proteins are considered to be functional homologues of lamins and are proposed to provide structural support to the plant nuclei. Arabidopsis CRWN1 and CRWN4 are located at the nuclear cortext and maintain nuclear integrity and chromosomal architecture in differentiated tissue. The role of these proteins in cycling cells is unknown, and whether CRWN1 and CRWN4 exhibit different functions is not documented. Here we show that nuclear area is increased in *crwn1* whereas it is slightly decreased in *crwn4* in root tips. We also show that osmotic stress can induce a decrease of the size and nuclear circularity of the nuclei in both mutants, as observed for WT reported in our previous data. Interestingly, the relative decrease of the size from control to treated plants is twice more important in *crwn1* compared to WT. This finding suggests a primary role of CRWN1 in maintaining the nuclear size in cycling cells.

Introduction

Nucleus is a bi-layered organelle separating the genetic material from the rest of the eukaryotic cell. It has two structural components : the nuclear envelope with the outer and inner nuclear membranes, and associated proteins on the one had, and the chromatin and associated proteins on the other hand. In animals, beneath the inner nuclear membrane lies a mesh like network called lamina which is made of lamin proteins and lamin associated proteins providing mechanical stability to the nucleus (Dahl *et al.*, 2008). Lamin A/C and lamin B are two lamin proteins creating this mesh and the lamin associated proteins (like emerin, lamina-associated polypeptide 2, MAN1 e.t.c) help to tether the network to the nuclear membrane. In regards to the mechanics of the nucleus, lamin A mostly contributes to nucleus viscosity and lamin B to nucleus elasticity (Swift *et al.*, 2013). Both lamins interact with heterochromatin at the level of the lamin associated domains (LADS) (Gruenbaum & Foisner, 2015), whereas only the Lamin

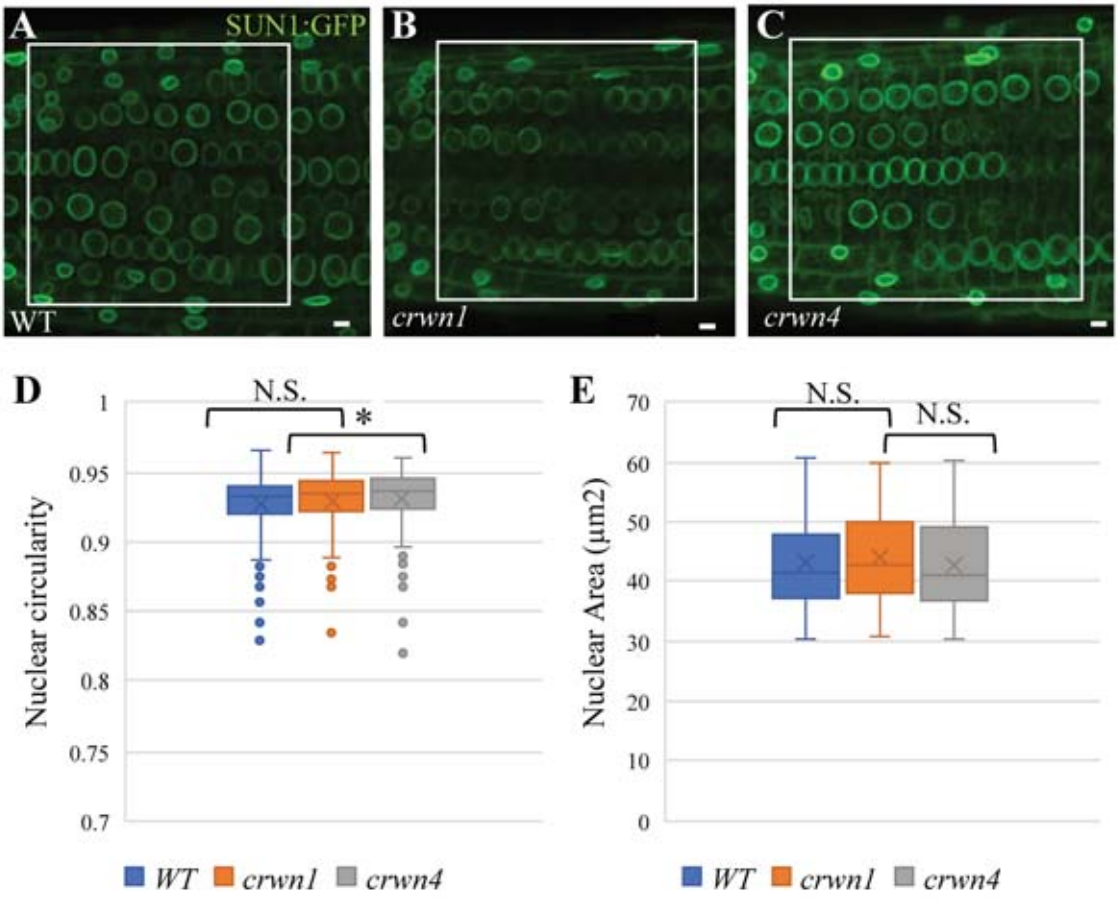

Figure 2. Nuclear morphology does not change in the *crwn1 and crwn4 Arabidopsis* root tip.

(A-B) Analysis of the nuclear shape in root tips by confocal microscopy (Z max, optical sections of 0.7 µm) in 9-day-old WT *pSUN1::SUN1-GFP, crwn1 pSUN1::SUN1-GFP and crwn4 pSUN1::SUN1-GFP* seedlings. Representative images are selected. Scale bars are 5 µm. (C-D) Quantitative measurements of nuclear morphology, circularity (C) in WT (plant, n = 13; nucleus n = 292), *crwn1*(n = 7; nucleus n = 156) and *crwn4* (plant, n =8; nucleus n = 204) shows no significant change ($p > 0.05$, n.s.) and significant minor increase respectively ($p < .05$, *), respectively. *P* value for circularity change by student t test is 0.400 and 0.0192 respectively. Nuclear area (D) in *crwn1*(n = 7; nucleus n = 132) and *crwn4* (plant, n =8; nucleus n = 174) compared to WT (plant, n = 13; nucleus n = 260) was not changing significantly ($p > 0.05$, n.s.). *P* value for area 0.299 and 0.584, respectively. Measurements were done by using NugSec in image J. Region of interest denoted by a white box (A-B).

A/C is found to interact with euchromatin suggesting a more direct expression regulation via lamin modulation (Gesson *et al.*, 2016). In lamin A/C–deficient (lmna−/−) mice, aberrant nuclear shape is observed in cardiac myocytes, fibroblast cells which is linked to the decreased nuclear stiffness, increased nuclear damage and mechanosensitivity.

Presence of lamin genes are unique to animals as there are no sequential or structural homologous are found in higher plants, but rather functional homologs (Dittmer & Misteli, 2011). Although functional homologous of lamin proteins namely Nuclear Matrix Constituent Proteins (NMCPs) have been observed in plants, we do not know their contribution to the structural features of the plant nuclei. The first lamin-like proteins were observed in *Daucus carota* and, by analogy with the animal context, it was postulated to contribute to the structural stability of the nucleus (Masuda *et al.*, 1993). These are coiled-coil proteins forming a nuclear peripheral framework later found in different plant cells like tobacco (*Nicotiana tabacum*) (Fiserova *et al.*, 2009) and onions (*Allium cepa*) (Ciska *et al.*, 2013). *Arabidopsis* has four NMCP orthologous genes which are known as CROWDED NUCLEI (CRWN) (formerly LITTLE NUCLEI (LINC)) (Dittmer *et al.*, 2007; Wang *et al.*, 2013). CRWN1 directly interacts with the heterochromatin via a physical interaction with the PROLINE-TRYPTOPHANE-TRYPTOPHANE- PROLINE (PWWP) INTERACTOR OF POLYCOMBS1 (PWO1) protein (Mikulski *et al.*, 2019). CRWN1 and CRWN4 help to maintain the heterochromatin positioning at the nuclear periphery, particularly CRWN1 has a direct access to repressed chromosomal domains located close to the nuclear envelope (Hu *et al.*, 2019). CRWN1 and CRWN4 deficiency in leaf tissue has been associated with reduced nuclear size whereas absence of CRWN2 and CRWN3 do not have that effect. In absence of CRWN 1 or CRWN4, nuclear shape is affected although CRWN4 acts independently from CRWN1 in maintaining the nuclear shape (Wang *et al.*, 2013). Thus, in the mutants, the nuclei in differentiated cells lose their elongated nuclear morphology linked with development, and showed a more rounded shaped structure. CRWNs have a surprising role in plant immunity, particularly CRWN1 which negatively regulates the pathogen induced response by repressing the gene expression of the defense related protein PR1 (Guo *et al.*, 2017) through the salicylic-acid dependent way (Choi *et al.*, 2019).

Like all physical objects, nucleus shape is also a read out of a pattern of forces and mechanical properties. In our previous study, by studying the shape of nucleus under hyperosmotic stress we could infer the effects of hydrostatic force on nucleus and gene expression (Goswami *et al.*,

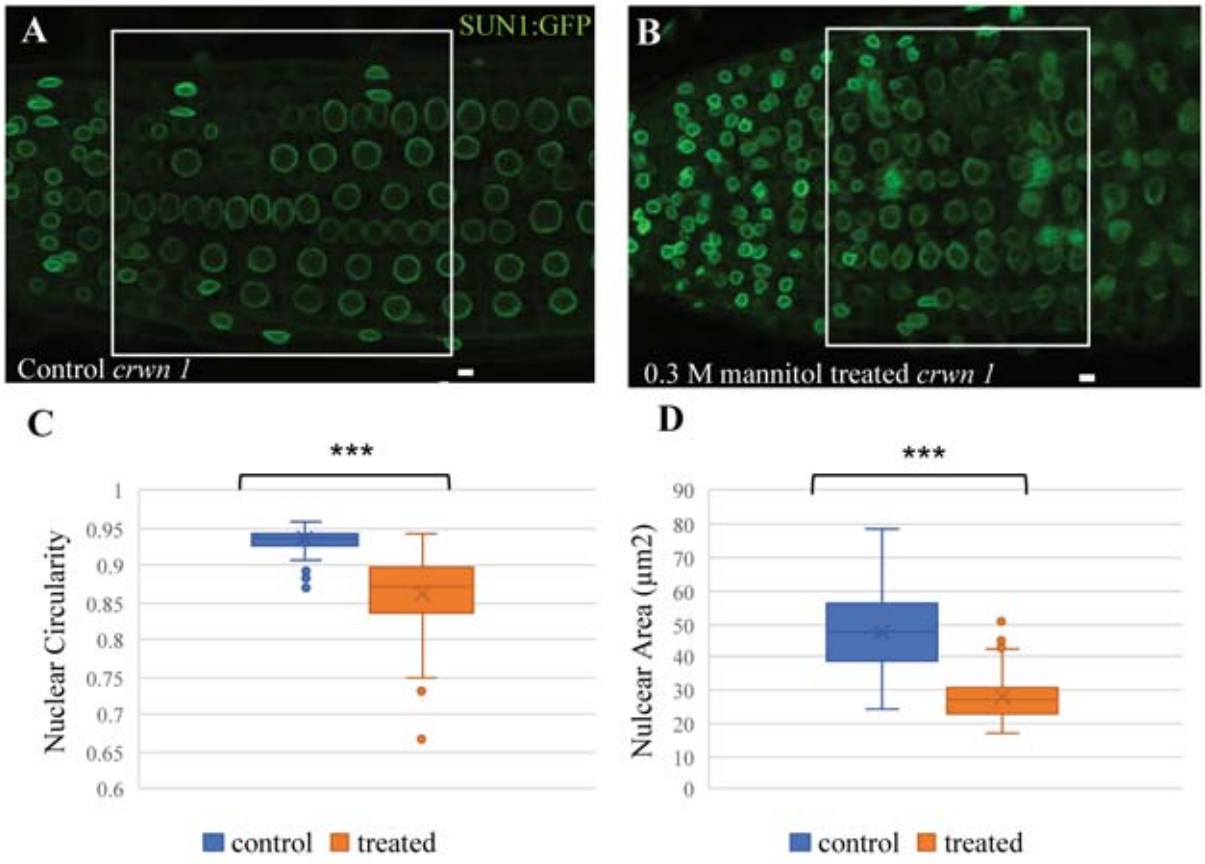

Figure 3. Hyperosmotic stress alters nuclear morphology in *crwn1* similarly as in WT.
(A-B) Confocal images representing nuclear morphology in root tips of 9-day-old *crwn1 pSUN1::SUN1-GFP* seedlings in (A) absence or (B) presence of a 16h-long treatment with 0.3 M mannitol (Z max, optical sections of 0.7 µm). Scale bars are 5 µm.
(C-D) Quantitative analysis of nuclear morphology. (C) Circularity and (D) area changes statistically significantly ($p < 0.001$, ***) before (plant, n =7 ; nucleus n = 146) and after (plant, n =6 ; nucleus n = 148) treatment. *P* value by student t test 1.06027e-40 and 4.65412e-48 respectively. Region of interest denoted by a white box(A-B).

2020). We also observed how the reduced level of GIPs, notably at the nuclear envelope, maintain the nucleus and the cell in a hyper-stressed state, comparable to a constitutive response to hyperosmotic stress. Here, we described the relative roles of the plant lamin-like protein CRWN 1 and CRWN 4 in nuclear shape in the root meristem. We reveal that CRWN1 and CRWN4 are not required for the nucleus shrinking in response to hyperosmotic stress, consistent with a dominant role of chromatin in nucleus shape changes in response to hyper-osmotic stress. We also reveal different contributions of CRWN1 and CRWN4 in nucleus shape control.

Results

CRWN1 and CRWN4 does not affect nuclear morphology in dividing tissue

The typical elongated spindle like shape of differentiated nucleus in *Arabidopsis* is replaced with a rounded nucleus generally found in dividing tissues (Sakamoto & Takagi, 2013). Furthermore, the *crwn4* nuclei sometimes exhibit thin protrusions originated from nuclear periphery (Wang *et al.*, 2013). To understand the contribution of CRWN1 and CRWN4 to nuclear morphology in cycling cells we analysed the nucleus shape in meristematic region of the root in the most external layers (epidermis and cortex, marked by white frame, Figure 2).

Nine-day old *crwn*1 and *crwn*4 seedlings expressing the inner nuclear membrane marker SUN1-GFP were used to analyse the shape of the nucleus by confocal microscopy. Qualitatively, *crwn1* and *crwn4* mutant nuclei exhibited round nuclear shape similar to WT root meristem nuclei (Figures 2A 2B 2C). Beyond qualitative observation, we quantitatively evaluate the nuclear phenotype using the imageJ NucSeg plugin (https://imagej.net/Welcome, https://github.com/mutterer/NucSeg). Nuclear circularity in *crwn1* (0.928± 0.002; plant, n = 7; nucleus n = 156), and *crwn4* (0.931 ± 0.001; plant, n =8; nucleus n = 204) was comparable to WT (0.926 ± 0.002; plant, n = 13; nucleus n = 292) (Figure 2D). Change in circularity for *crwn1* was not statistically significant with a *p* Value of 0.400 by Student's t test and change is only 0.19%. Although the change for *crwn4* is only 0.483 %, it is statistically significant with a pValue 0.019. Nuclear area of *crwn1* was 43.81 ± 0.66 μm^2, (plant, n = 7: nucleus, n = 132) for *crwn4* was 42.57 ± 0.59 μm^2 (plant, n = 8: nucleus n = 174), and for WT 42.97 ± 0.46 μm^2 (plant, n = 13: nucleus n = 260) (Figure 2E). Change in area was 1.95% and 0.95% respectively for *crwn1* and *crwn4* compared to WT and wasn't changing statistically significantly with a *p* Value of 0.299 and 0.584 respectively.

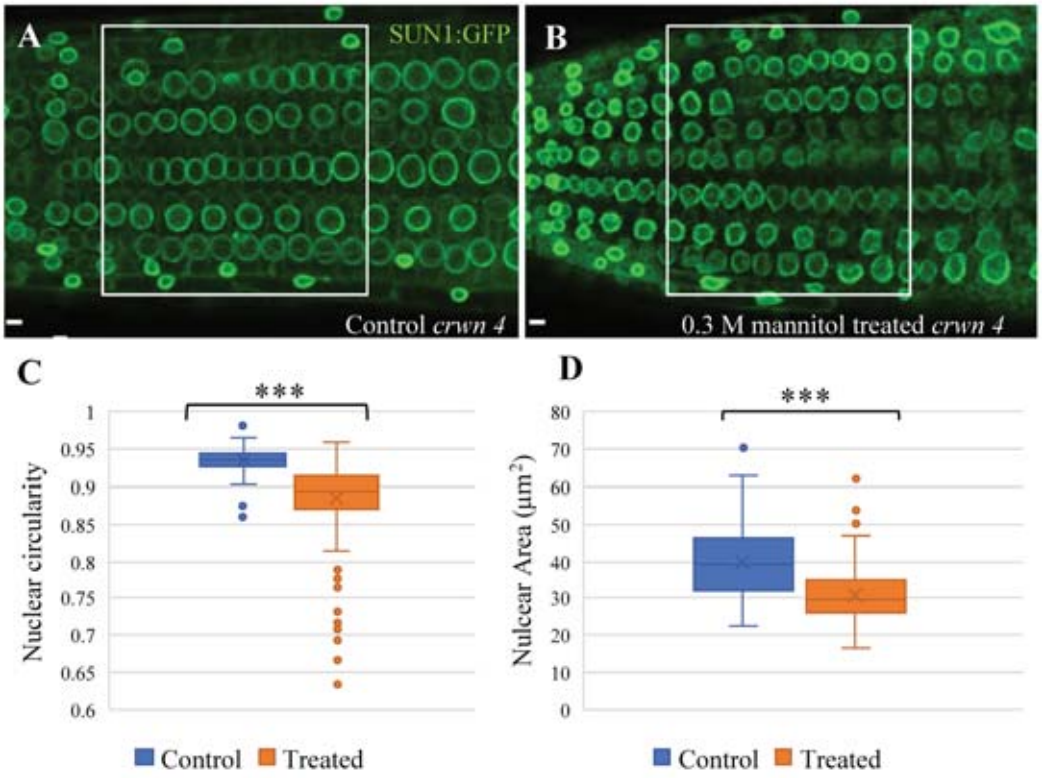

Figure 4. Hyperosmotic stress alters nuclear morphology in *crwn4* similarly as in WT.

(A-B) Nuclear phenotype is analysed by confocal microscopy in root tips of 9-day-old *crwn4 pSUN1::SUN1-GFP* seedlings in (A) absence or (B) presence of a 16h-long treatment with 0.3 M mannitol (Z max, optical sections of 0.7 µm). Scale bars are 5 µm.

(C-D) The change in nuclear shape was quantified. (C) Circularity and (D) area changes statistically significantly ($p < 0.001$, ***) before (plant, n =9 ; nucleus n = 204) and after (plant, n =9 ; nucleus n = 219) treatment. *P* value by student t test 5.37963e-33 and 2.28623e-23 respectively. Region of interest denoted by a white box(A-B).

Altogether these data demonstrate that the nuclear morphology isn't affected by the absence of CRWN1 or CRWN4 in the nucleus from diving cells in the root tip.

Hyperosmotic stress affects nuclear morphology in *crwn1* and *crwn4*

Now, we investigated how hyperosmotic stress affects the nuclei from diving region in the *crwn* mutants. In our previous study we showed that in WT nuclei, nuclear area and circularity were decreasing by 20% and 9% under hyper osmotic stress, respectively (Goswami *et al.*, 2020). We reasoned that hyperosmotic stress may affect three factors: the cytoskeleton (e.g. pulling on the nucleus), the plamina (acting as nucleoskeleton) and chromatin (acting as a gel). Because meristematic cells are rather isodiametric, the cytoplasmic cytoskeleton is rather isotropic, consistent with the round shape of nuclei. Thus, we mainly analyse the relative contribution of nuceloskeleton and chromatin in nuclear shaping. Here we used the *crwn1* and *crwn4* mutant to decipher the contribution of the nucleoskeleton. We subjected 9-days old *crwn1* and *crwn4* seedlings to a 16 -hour-0.3M mannitol treatment. We observed the nuclei in the same region as for WT to obtain comparable and reproducible measurements. Under such mannitol treatment, deformation of the nuclei were observed with decreased circularity and area in both CRWN1 or CRWN4-devoided seedlings after hyperosmotic stress (Figures 3B 4B), when compared to control conditions (Figures 3A 4A).

In case of *crwn1,* nuclear circularity was significantly decreasing from 0.935 ± 0.001 (plant, n =7 ; nucleus n = 146) to 0.862 ± 0.003, (plant, n = 6; nucleus n = 148), with a *p* value by Student's t test 1.06027e-40, similarly as we previously observed in WT (*i.e.* from 0.936 ± 0.001 to 0.854 ± 0.008, (Goswami *et al.*, 2020) (Figure 3C). Interestingly the nuclear area was reducing about twice more [from 47.27 ± 0.85 μm^2 (n = 146), to 27.76 ± 0.54 μm^2 (n = 148), *p* value is 4.65412e-48] in *crwn1* (Figure 3D) compared to WT (a decreased of 22% of the size, from 41.1 ± 0.8 μm^2 in untreated seedlings to 32.1 ± 1.0 μm^2 in treated (Goswami *et al.*, 2020)). *crwn4* nuclei showed similar changes as WT in response to hyperosmotic stress. *Crwn4* nuclei circularity decreased from 0.934 ± 0.001 (plant, n =9 ; nucleus n = 204) to 0.884 ± 0.003 (plant, n =9 ; nucleus n = 219) with a *p* value of 5.37963e-33 by Student's t test (Figure 4C) and the nuclear area reduced as well from 39.75 ± 0.65 μm^2 (n = 204) to 31.06 ± 0.49 μm^2 (n = 219) with *p* value of 2.28623e-23 by Student's t test (Figure 4D).

Although this remains to be consolidated with mechanical measurements of *crwn1/4* nuclei

and the analysis of the double *crwn1crwn4* mutant, this suggests that 1/ CRWN1 and CRWN4 are not required for the nucleus shrinking and mis-shaping in response to hyperosmotic stress, thus suggesting a primary role of chromatin in that response; 2/ Instead, CRWN1, but not CRWN4, would rather act as a negative regulator of nucleus shrinking in response to hyperosmotic stress; 3/ the contributions of CRWN1 and CRWN4 in nuclear shaping could be uncoupled from one another.

Discussion

Plant lamin like NMCP/CRWNs have been identified decades earlier (Masuda *et al.,* 1997) and were found to maintain nuclear shape, size and chromatin organisation (Dittmer *et al.*, 2007; Wang *et al.*, 2013; Sakamoto & Takagi, 2013). While most of the studies were addressed in differentiated tissues in plants, where *crwn* nuclei cannot elongate as WT, we present here a quantification the nuclear changes of *crwn1* and *crwn4* in root meristems. Here we showed that the absence of CRWN1 or CRWN4 does not modify nuclear morphology compared to WT. Interestingly, compared to WT, CRWN1- depleted nuclei reached smaller size in response to hyper-osmotic stress.

It is already established that nuclear envelope components actively regulate the nuclear shape in plants, notably the LINC complexes and nucleoskeleton in differentiated cells (Dittmer *et al.*, 2007; Goto *et al.*, 2014; Zhou *et al.*, 2015), while GIP proteins regulate nuclear shape in both meristematic and differentiated cells (Janski *et al.*, 2012). Interestingly while GIPs proteins help to maintain rounded shape, the *gip1gip2* mutants showed lobulated and bigger nuclei in the root meristematic nuclei (Janski *et al.*, 2012; Goswami *et al.*, 2020) whereas the CRWN1 and CRWN4 proteins doesn't have control over nuclear shape in the meristematic region.

In case of animal nuclear shape change is dependent on cytoskeleton, LINC complexes (Agrawal & Lele, 2019), nucleoskeletal lamins (Swift *et al.*, 2013), and chromatin itself (Stephens *et al.*, 2018). Hyper osmotic stress induces structural change in chromatin as well (Olins *et al.*, 2020). In plants, hyper osmotic stress has been found to decrease nuclear circularity, area and increase nuclear stiffness in relation with mechanically active gene induction in WT *Arabidopsis* plant (Goswami *et al.*, 2020). In *Arabidopsis* hyperosmotic stress induced changes in chromocenters organization which appear more clustered and probably accompanied by changes in 3D chromatin organization allowing the induction of touch

responses for which some of them are transcriptionally regulated by the polycomb complexes, such as WRKY transcriptional factors (Roudier *et al.*, 2011). CRWN1 interacts with chromatin and the chromatin regulator PRC2- associated protein PWO1 mainly in the nuclear periphery and regulate the nuclear shape in a PWO1-dependent manner. PWO1 is suggested to help in maintaining a nuclear envelope bound repressed chromatin structure (Mikulski *et al.*, 2019).

Our findings put forward a scenario where CRWN1 and CRWN4 – nuclear envelope proteins doesn't directly affect nuclear morphology in diving cells but CRWN1 (not CRWN4) acts as a negative regulator under hyper osmotic stress putatively interacting with the important contributor of the nuclear mechanics – the chromatin. This supports the hypothesis of our recent finding (Goswami *et al.*, 2020), that the gel like chromatin contribute significantly towards the morphomechanics of the nuclei under hyperosmotic stress and maintain the nuclear shape by interacting with the nuclear envelope proteins.

This work has still many open questions, that needs to be further investigated. How these nuclear skeleton proteins being regulated under hyperosmotic stress and what is the signalling pathway? As small dynamic GIP proteins have been shown to regulate the nuclear response to hyperosmotic stress, the next question is if and how GIPs and the CRWNs act together in maintaining the nuclear shape and size in WT nucleus in the root meristems. Absence of GIP induces expression of several stress response genes and the nuclear morphology is hugely affected. CRWNs also have an effect on stress responsive gene expression in correlation with the shape change (Choi *et al.*, 2019). This work not only predicts a role of CRWN1 during hyperosmotic stress response but opens a way for new study to understand the control of nuclear structure and gene expression *via* plant lamina.

Materials and Methods

Plants material, seed sterilization and growth medium

Arabidopsis WT pSUN1::SUN1-GFP, are already described in literature (Graumann *et al., 2010*). *crwn1 PSUN1::SUN1-GFP* and *crwn4 pSUN1::SUN1-GFP* plants were established by crossing between the single mutants *crwn1-2* (SALK_025347) (Wang *et al.*, 2013) and crwn4-1 (SALK_079296) (Wang *et al.*, 2013) .

Seed surface was sterilized by using 70% ethanol and 0.1% Triton X100 for 10 minutes, then

96% ethanol for 5 mins and let dried before *in vitro* culture.

For "*in vitro*" growth conditions, 1/2 Murashige and Skoog (MS) medium (SERVA Electrophoresis) complemented with 1% sucrose and 1.2% agar were used. Seedlings were grown under long day (16-h light 70µmol/m2 per second of fluorescent lighting / 8-h dark) at 20 °C.

Hyper osmotic stress induction

Hyperosmotic stress was applied on 9-day-old seedlings following normal germination in control growth conditions. After transfer to liquid culture, the seedlings were maintained for 16h in ½ MS medium supplemented with 0.3 M mannitol (hyperosmotic stress) in parallel of control seedlings in ½ MS medium.

Image recording by Confocal laser scanning microscopy

Whole plant roots where observed under LSM700 confocal microscope (Zeiss, Germany) to obtain z stack and 20×/0.8 NA lens was used. The optical sections were 7 µm apart. GFP is excited by 488 nm wavelength and it emitted wavelength is 510 nm. In all the images for Col-0 *pSUN1::SUN1-GFP, crwn1 pSUN1::SUN1-GFP* and *crwn4::SUN1-GFP*, signal to noise ratio was increased by reducing background noise as much as possible. The laser excitation was maintained same throughout the experiment but the digital gain was modulated to achieve an optimum signal.

Nuclear parameters measurements

All the quantitative analysis of the images acquired in the confocal was done in ImageJ by using NucSeg plugin. The detailed description of the method given in our previous work (Goswami *et al.*, 2020). The values lie within 0-1 and more in leans towards 1 the more circular the measured nucleus is. To maintain the reproducibility and robustness of the measurement we choose a particular segment of the root (the epidermal and cortex layers).

Statistical tests

Statistical analysis of the quantified traits was done using Student t test to study where the difference in the two data sets is significant. The variation of the data was analyzed by F test.

Depending on the variance a two tailed student t test was performed assuming equal or unequal variance.

Acknowledgments and funding

This work was supported by the Centre National de la Recherche Scientifique (CNRS) (defi Mecanobio, NEstress 2016-2018), by Fondation Schlumberger pour l'Education et la Recherche (FSER) (2016-2018), by the European Research Council grants ERC-2013-CoG-615739 ‘‘MechanoDevo,’’ by the IdEX international PhD program (unista, Strasbourg), and by HFSP grant 2018, RGP, 009. We acknowledge discussions with members of the COST Action CA1612 INDEPTH network. We are grateful to K. Graumann for providing fluorescent-tagged SUN1 lines, as well as to Elise Hoffmann for technical help.

Chapter III

Preliminary study of the correlation between cell wall and nuclear mechanics in plants

Preface-

Plant mechanics mainly depend on cell walls (Cosgrove, 2005). We focus our study on the root apical meristem cells where primary cell walls are thinner and less rigid in dividing cells compared to differentiated cells that stop growing (Whaley *et al.*, 1952). Chemically, primary cell wall is a composite material made of cellulose microfibrils embedded in a matrix made of hemicellulose, pectin and structural proteins (Cosgrove, 2005). Cellulose microfibrils are correspond to higher order structures of cellulose, which is a polymer of beta1,4-glucose. As I discussed in the introduction, cellulose microfibrils are thought to be the main load bearing component of the wall: the texture and crystallinity of this polymer is determinant for the mechanical properties of the wall (Rongpipi *et al.*, 2019). The mechanical properties of the wall can be modulated by changing the orientation or the spacing of cellulose microfibrils, and this often involves a contribution of the matrix. In certain cells and tissues, like the pollen tube, the matrix play a dominant role in wall properties (Cosgrove, 2014). Beyond its mechanical role, the cell wall has been postulated as a reservoir of signalling molecules which might contribute to signalling, including mechanical signalling (e.g. through stretch-induced desquestration of these molecules)(Ackermann & Stanislas, 2020). A good candidate for this is Rapid Alkalinisation Factor (RALF) peptides residing in cell wall and plasma membrane has receptor for these peptides (Mecchia *et al.*, 2017).

Although animals do not have cell walls, animal cells and tissue behavior highly depend the mechanical properties of the rigid extracellular matrix and its constituents. Interestingly, any change in the mechanical property of substrate for a single cell in culture (mimicking the ECM environment) could be relayed to nucleus as well (LOVETT *et al.*, 2013). Here we explore whether, in a similar fashion, any change in cell wall properties may also have an effect on nuclear property in plants. One of the main added value of the plant system for this question is the possibility to study the role of wall mechanics on the nucleus in a multicellular context, notably because plant mechanics is simpler to interpret (no cell movement, no cell death). We chose to focus on Cellulose Synthase (CESA) proteins. They are membrane bound proteins responsible for the cellulose synthesis in plants. We chose a mutant line *eli1.1* where the cellulose synthesis is hindered due to a mutation in *CESA3* (Caño-Delgado *et al.*, 2003). These leads to lower cellulose level but ectopic lignin deposition. In this study, we investigate the effect of these change in nuclear morphology and mechanics in the dividing root cells. We use

Atomic Force Microscopy (AFM) to evaluate cell wall and nuclear rigidity as well as live cell imaging to evaluate changes in nuclear shape.

Introduction

Rigid cell wall encases plant cell and predominantly influences the morphology and mechanics of the cell. Plant has two types of cell wall: the primary and secondary cell walls. The primary cell wall is ubiquitous in all plant cell types, thin and deformable in dividing and expanding cells. Thick secondary cell walls appear after cell expansion, e.g. in specialized cell types forming the sclerenchyma (ie tracheids, fibers and vessels) that will confer strong rigidity to the cells (Cosgrove, 2018). The main load-bearing components of cell walls are cellulose microfibrils, which are parallel chains of polymers of glucose linked by 1-4 β glycoside bond. They are embedded in a matrix of hemicellulose, pectin and structural proteins. Recent evidence show that hemicellulose is intertwingled with cellulose microfibrils to form an inaccessible amalgam termed as "mechanical hotspots" and could act as the main modulator of cell wall mechanics (Cosgrove, 2015). But the molecular regulation of these mechanical load bearing junction or how they are formed is still enigmatic. Pectin is also speculated to take part in these hotspots (White *et al.*, 2014). Chemically rhamnogalacturonan I, rhamnogalacturonan II, homogalacturonan, xylogalacturonan, apiogalacturonan, arabinan, and arabinogalactan are the major pectin elements. Pectin contribute to the mechanical characteristics of cell as they can form these gel like networks with variable mechanical properties (mainly stiffness) by having variable proportion of methyl esterification (Wolf *et al.*, 2009).Pectin qualities vary among cell type, environment, tissue, growth and developmental status (Palin & Geitmann, 2012).

Cell wall may be compared with the extracellular matrix (ECM) of animal cells, at least to some extent. ECM is a classically represented as a rigid network where the cells are embedded. Yet, ECMs are more dynamic, in terms of geometry, chemistry and mechanics. Cells receive mechanical signals from the ECM and the surrounding cells (Smith *et al.*, 2017). Change in the mechanical properties of ECM, for example myocardial ECM, is directly related to mechanical malfunctioning of Cardiomyocyte compromising the whole myocardium structure and function (Engler *et al.*, 2008). These changes in cellular function by changing mechanical properties of ECM is spanned to the nucleus. LOVETT et al., found a correlation between the stiffness of the substrate where the cells grow and the nuclear shape. The nucleus in NIH 3T3 fibroblasts is spherical in a soft substrate with a rigidity of 0.4kPa but loses the sphericity as the substrate stiffness increases and becomes flattened in a highly rigid substrate with rigidity of 308kPa (LOVETT *et al.*, 2013). In an earlier study Engler et al., showed just by increasing

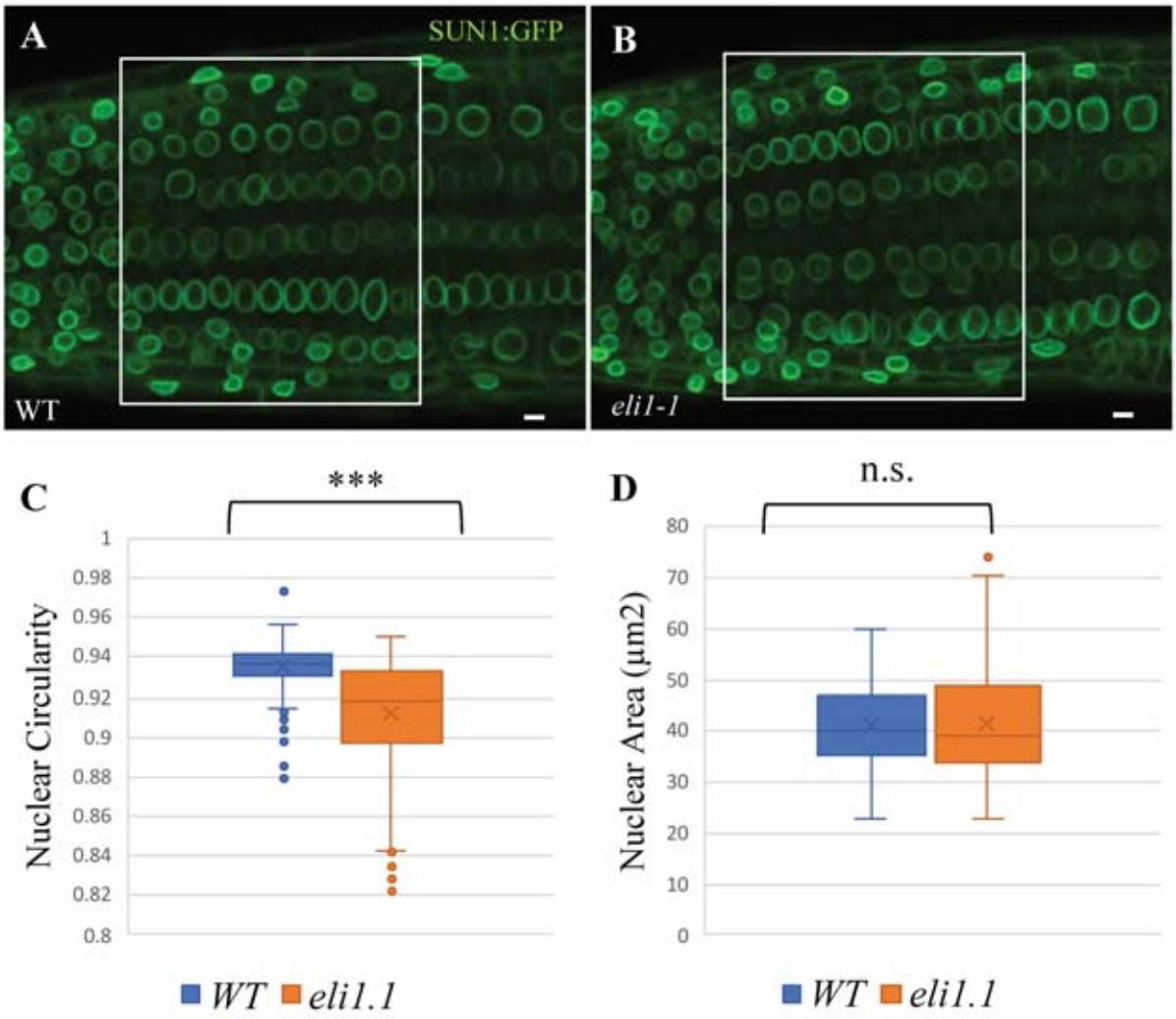

Figure 1: Nuclear circularity but not the area is affected in the *eli1-1 Arabidopsis* root tip. (A-B) Analysis of the nuclear shape in root tips by confocal microscopy (Z max, optical sections of 0.7 µm) in 9-day-old WT *pSUN1::SUN1-GFP and eli pSUN::SUN1-GFP* seedlings. Representative images are selected. Scale bars are 5 µm. (C-D) Quantitative measurements of nuclear morphology, circularity (C) and nucleus area (D) was done using NugSec in image J in WT (nuclei n = 131; plant n = 7) and *eli1.1* (nuclei, n = 142 ; plants, n = 7). The *p*-values after Student's t-test are 1.48981e-15 and 0.69239677, respectively indicating significant decrease in circularity ($p < 0.001$, ***) and no significant differences between the area (n.s.). Region of interest is denoted by a white box (A-B).

the substrate rigidity one can play with the differentiation of a mesenchymal stem cell (Engler *et al.*, 2006). Later, the same team showed that cytoskeleton and nucleoskeleton mechanical properties scale with ECM properties (Swift *et al.*, 2013). This quite nicely illustrates the importance of ECM-dependent change in nuclear morphology and the putative role it could have in development.

The putative link between cell wall properties and nuclear shape has not been yet investigated in plants. As cell wall structure depends on the deposition of cellulose microfibrils, it is tightly controlled by Cellulose Synthase enzymes (CESA). CESAs belong to the CELLULOSE SYNTHASE COMPLEXES (CSC), which is a large complex composed of 6x6 CESA proteins together with associated proteins. CESA1, CESA3 and CESA6 are responsible for primary cell wall formation whereas CESA4, CESA7 and CESA8 for secondary cell wall (Cosgrove, 2005). To correlate a changed in the cell wall with nuclear deformation, we chose *eli1-1,* a mutant affected in *CESA3*, resulting in reduced cellulose content but ectopic lignification of the walls, hence the name *ectopic lignin* 1. Thus the mutant show reduced cell expansion, causing reduced root and shoot growth resulting in a short and stunted phenotype (Caño-Delgado *et al.*, 2000).

Here we study the effects of changes in cell wall composition on the nuclear properties in this mutant: the morphology and mechanical properties. We investigate also, whether that also affects the nuclear response to hyperosmotic stress.

Results

Nuclear morphology is slightly altered in *eli1.1*

In case of animals, change in extracellular stiffness results into change in nuclear morphology. To build on that result, we studied the nuclear morphology of 9-day-old *Arabidopsis* Col-0 and *eli1-1* seedlings expressing the nuclear envelope SUN1-GFP in root meristems (epidermis and cortex marked by white frame). Nuclei exhibited minor deformation (Figure 1B) compared to Wild type (Figure 1A). After quantification of the nuclear shape, by using NucSeg plugin in Image analysis software ImageJ, the nuclear circularity was slightly reduced in the *eli1-1* mutant, when compared to WT from 0.934 ± 0.001 to 0.912 ± 0.002 (nuclei WT = 131; plants WT = 7; *eli1-1*nuclei = 142; plants, n = 7). The decrease in circularity was limited (2.45%,) but statistically significant with a *p*-value of 1.48981e-15 by Student's t test (Figure 1C). However, we could not detect significant difference in the mutant compared to WT [area WT

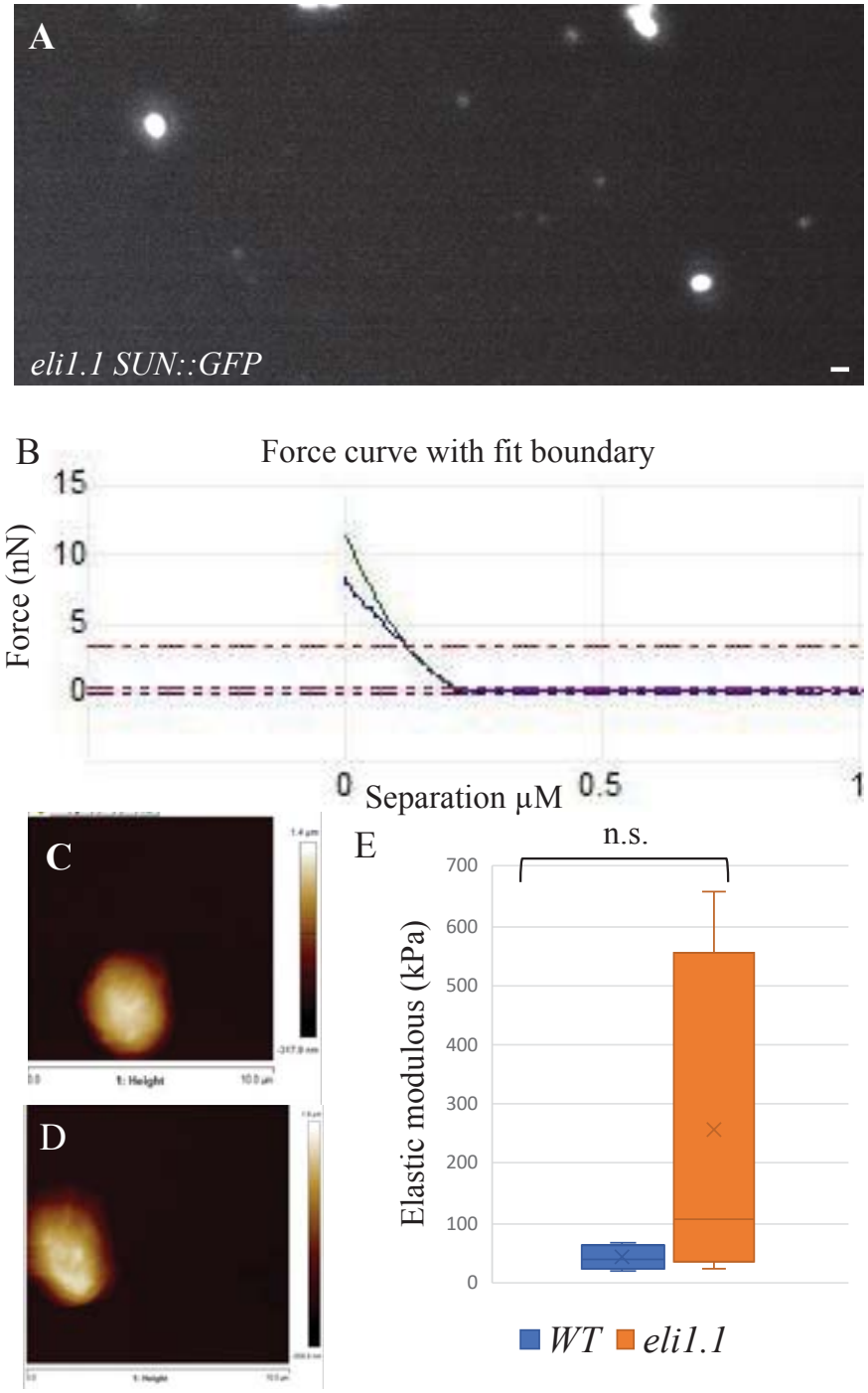

Figure 2. Physical measurements of nuclear property by AFM

(A) Nucleus was selected depending on the fluorescence observes. (scale bar 5µm)

(B) Representative force curve obtained from AFM

(C-D) Nuclear topography of (C) control and (D) *eli1-1* nuclei

(E) Elastic modulus is measured in WT (n = 6 nuclei in 3 independent roots) and *eli1-1* nuclei (n = 5 nuclei in 3 independent roots); *p* values from Mann-Whitney test are 0.1211 (not significant).

(41.13 ± 0.71 µm^2; Nucleus, n = 131; plants, n = 7) and *eli1-1* (41.58 ± 0.88 µm^2 ; Nucleus, n = 142 ; plants, n = 7) with a *p*-value of 0.69239677 by Student's t test (Figure 1D).

Altogether this data shows that the nuclear shape changes but the size is unaffected in the root tip nucleus of *eli1.1*.

***eli1.1* has stiffer nuclei in normal growth conditions**

The shape of an object can reflect its physical properties. As the shape of the nucleus was changing in *eli1.1* in normal growth conditions, we were interested in studying the nuclear mechanics. In our previous study, we show that decreased in nuclear circularity of WT nuclei under hyper osmotic stress is linked to increased nuclear stiffness (Goswami *et al.*, 2020). As nuclear circularity is slightly reduced in *eli1-1,* one would predict slightly stiffer nuclei in *eli1-1*, at least in the simplest scenario.

To assess nuclear stiffness in *eli1-1*, we used atomic force microscopy (AFM) in the root tip of 9-day-old WT *pSUN1::SUN1-GFP* and *eli1-1 pSUN1::SUN1-GFP*. Note that we had to digest cell wall prior to these measurements, thus we make the assumption that nuclear properties reflect the long-term state of the cell (or that rapid changes in cell properties do not immediately translate into changes in nuclear mechanics). This strong and debatable assumption is based on the observation that mutants with altered nuclear shapes, like *gip1gip2*, keep their shape even after nuclei are extracted from the cell (Goswami 2020). Nuclear shape and integrity were visualised by the presence of SUN1-GFP under the fluorescence microscope (Figure 2A).

A pyramidal tip attached with a flexible cantilever, was used for acquisition of the topography and indentation. The root tip was enzymatically digested and then squashed on a poly -L-Lysine coated plastic Petri dishes. After recording the topography of the nucleus (Figures 2C 2D) in 2D by using the peakforce QNM (quantitative Nanomechanical mapping) mode, a Point and Shoot was then used to define to perform standard force-distance curves and then the Young's modulus was quantified by using processing software Nanoscope Analysis 2.0 (Bruker). Average stiffness (apparent elastic modulus) of the WT root tip nucleus was 42 ± 9 kPa (nuclei = 6; roots= 3). The stiffness of the nucleus from the root tip of *eli1-1* was 257 ± 126 kPa (nuclei= 5, roots= 3) (Figure 2E). Even though the nucleus of the mutant appeared stiffer compared to WT the difference was not statistically significant with a *p* value of 0.1211,

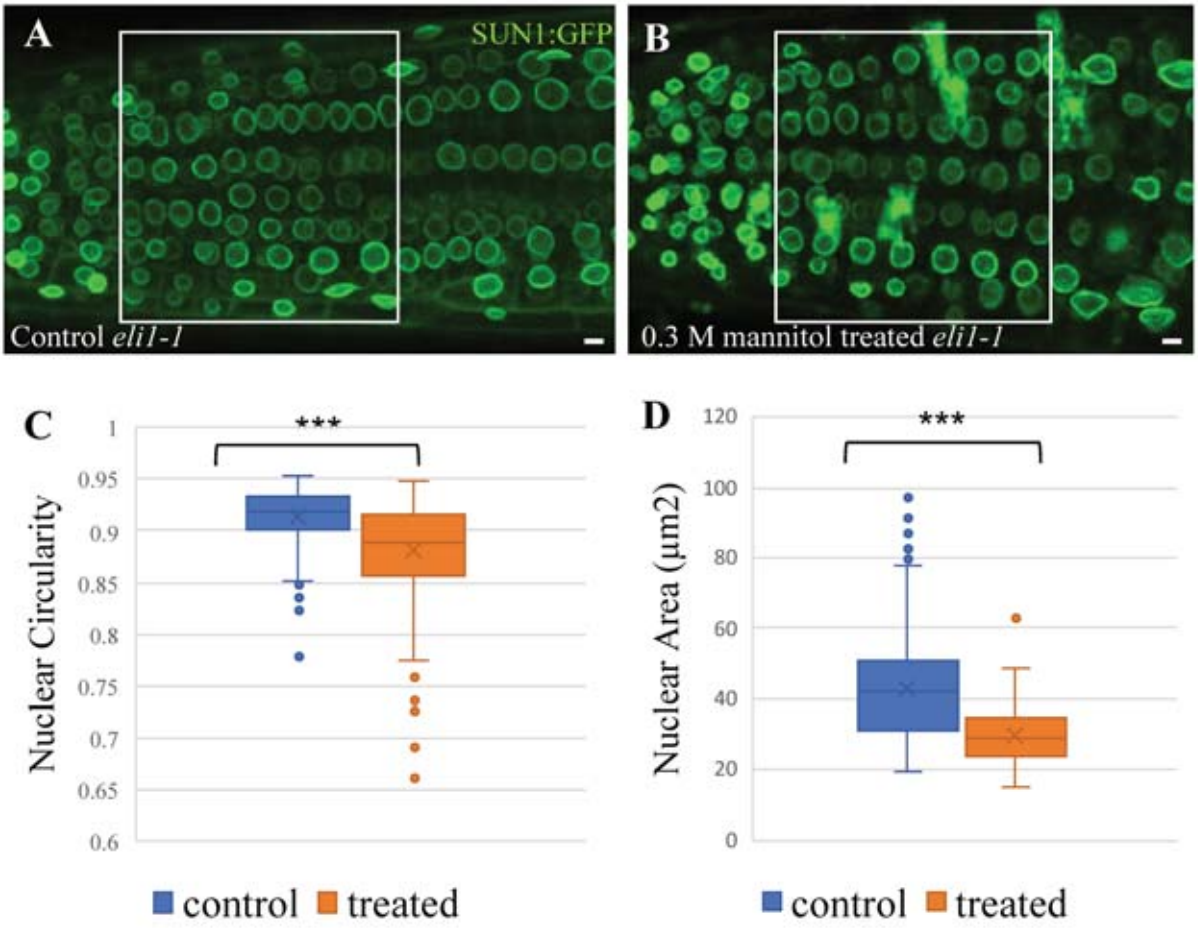

Figure 3. Hyperosmotic stress alters nuclear morphology in *eli1-1*.
(A-B) Nuclear phenotype is analysed by confocal microscopy in root tips of 9-day-old *eli1-1 pSUN1::SUN1-GFP* seedlings in (A) absence or (B) presence of a 16h-long treatment with 0.3 M mannitol (Z max, optical sections of 0.7 µm). Scale bars are 5 µm. (C-D) The change in nuclear shape was quantified. (C) Circularity and (D) area change statistically significantly ($p < 0.001$, ***) from control (nucleus, n = 284; plant, n= 17) to treated (nucleus, n = 270; plant, n=16). *P* value by student t test 3.39114e-05 and 1.08258e-06 respectively. Region of interest denoted by a white box (A-B).

by Mann Whitney. This is in fact easily explained by the high standard deviation observed in the mutant. We thus need to confirm these data sets with more data points to get more robust results.

Hyper osmotic stress changes nuclear morphology

Hyperosmotic stress alters the nuclear shape, size and mechanics in WT nuclei (Goswami *et al.*, 2020). To know whether hyperosmotic stress would also affect nuclei in cell wall mutants, nine-day-old *eli1-1* seedlings were treated for 16 hours with 0.3M mannitol. As we did previously (Goswami *et al.*, 2020), we analysed the nuclear shape changes in the root meristem nuclei. We observed that the nuclear morphology changed and the size of the nucleus decreases in *eli1-1* after hyperosmotic stress (Figures 3A 3B).

Upon hyperosmotic stress in *eli1-1*, nuclear circularity changed from 0.912 ± 0.001 in the control (nucleus, n = 284; plant, n= 17) to 0.881 ± 0.002 in the treated seedlings, (nucleus, n = 270; plant, n=16) with a *p*-value by Student's t-test 4.13842e-19 (Figure 3C). Interestingly in the response, nuclear circularity was decreasing of 3.4% in *eli1-1* from its initial circularity in the control in *eli1-1,* while it was decreasing of 9% in WT in our previous work (i.e. from 0.936 ± 0.001 to 0.854 ± 0.008) (Goswami *et al.*, 2020). This trend suggests that in response to hyperosmotic stress, the change in nuclear circularity observed in *eli1-1 i*s milder compared to WT. In *eli1-1*, nuclear area was 43.11± 0.89 µm2 (nucleus, n = 284; plant, n= 17) in control conditions, and was decreasing significantly to 29.61 ± 0.47 µm2 (nucleus, n = 270; plant, n=16) in response to hyperosmotic stress with a p value of 1.08802e-25 (Figure 3D). The change was 31% which is although slightly higher from the 22% change observed in WT in our previous work (from 41.1 ± 0.8 µm2 in untreated seedlings to 32.1± 1.0 µm2 in treated seedlings) (Goswami *et al.*, 2020). Thus, the difference between *eli1-1* and WT was mild.

These data suggest that nuclear morphology (but not size) is less malleable in case of *eli1-1* compared to WT under hyperosmotic stress. It correlates with the already slightly deformed nuclei of *eli1-1,* which could confer this reduced sensitivity of nuclear morphology towards change under hyperosmotic stress.

Discussion

This work represents a first attempt to link wall and nuclear properties. In principle, the *eli1-1* mutant offers a good genetic context for this study. Yet, the compensation mechanism, involving lignification in response to cellulose deficiency, may make the interpretation of our results more complex.

We observed that the nuclear shape slightly changed in *eli1-1* and we also observed stiffer nuclei in the mutant. At this stage, this basis of this correlation remains unclear. Many factors could contribute to the observed nuclear rigidity such as changes in chromatin organisation that is known also critical to modify the mechanical properties of the nucleus (Heo *et al.*, 2016). Lignin deposition is also known involved in the mechanical response towards pathogen infection and *eli1-1* shows upregulation of defence-related genes (Caño-Delgado *et al.*, 2003) that could be linked to changes in chromatin organization. This could be also correlated to the increased nuclear stiffness in the *gip1gip2* which presents a constitutive up-regulation of stress responsive genes and notably those linked to the mechanical touch response (Goswami *et al.*, 2020).

Although our preliminary observations suggest that the *eli1-1* nucleus is slightly deformed (but not smaller) compared to WT, the *eli1-1* nuclear shape and size changes with hyper osmotic stress. That means that *in vivo*, the slight nuclear deformation observed in the mutant has not reached a maximal threshold and can be further deformed in response to hyperosmotic stress. This is not comparable to *gip1gip2* which is likely reached already a maximal nuclear deformation in normal growth conditions and is no more deformable in response to hyperosmotic stress (Goswami *et al.*, 2020).

This study would require a more thorough analysis of cell wall properties in the root. Cell wall is a complex structure with cellulose microfibrils embedded in a matrix. Cellulose is deposited on the cell wall by CESA proteins, any change in these proteins are often lethal. A non-lethal *eli1-1* with mutated CESA3 gene important for cellulose synthesis in primary cell wall shows lower cellulose but higher lignin composition. This compensatory effect could be essential for the survival of these plants. We tried to measure the mechanics of the root tip. Due to curve nature of the root it always intervened with the measurement and we were unable to fix it. Also, the cylindrical nature of the root gave a very small attachment area which was not enough to hold them exactly on position while a force exerted to measure the elastic property. In the

literature, no measurement for the root elastic modulus has been observed. Although viscoelastic properties of the live whole root cell wall at the nano scale was studied, the measure was done using a model to measure the "Index of Plasticity" which converted the elastic properties to viscoelastic (Fernandes *et al.*, 2012). AFM measurement was impossible on whole root as file of outer epidermal cells remained attached to the surface. Although by using a glue we were able to fix the roots to some extent, yet very heterogenous data were obtained suggesting other components were not completely eliminated from the measurements. In future we need to investigate other plant tissues to investigate the change of cell wall mechanics and nuclear mechanics.

As a prospect, we may consider using other mutants in the future. For example, we could treat the sample with cellulase, to check whether short-term modifications can lead to nucleus shape defects, and conversely, use other cell wall mutants, with various degree of compensation to better assess the correlation between nuclear and wall stiffness. Last, it might be easier to do this work in the shoot apical meristem where wall mutants have been shown to exhibit strong morphological defects, without lignification, and where wall properties can be probed and nucleus shape monitored.

Materials and methods

Plants material

Arabidopsis Col-0 *pSUN::SUN1-GFP* (Graumann et al., 2010) were crossed with. *eli1-1* (Caño-Delgado *et al.*, 2000) to give rise to the *eli1-1 pSUN::SUN1-GFP* line.

Before *in vitro* experiments, seeds were sterilized by a chemical treatment. After a treatment at 70% ethanol in presence of 0.1% Triton X100 for 10 minutes, seeds were treated with 96% ethanol for 5 min before letting dried. Seedlings were grown on 1/2 Murashige and Skoog (MS) medium (SERVA Electrophoresis) complemented with 1% sucrose and 1.2% agar, under long day (16-h light 70µmol/m2 per second of fluorescent lighting / 8-h dark) at 20 °C.

Confocal microscopy

Confocal microscopy was performed using LSM700 confocal microscope (Zeiss, Germany) and 20×/0.8 NA lens. Whole seedling was deposited on a glass slide and then cover with a coverslip using tape to separate the coverslip from the slide in order to prevent mechanical

Figure 4. Instrumental set up of AFM

(A) AFM head in mounted on top of the Inverted fluorescence microscope.
(B) Laser calibration equipment.
(C) Leica DMI 6000B fluorescence microscope.
(D) Used AFM tips.

pressure. Observation was done in presence of Propidium Iodide (PI) (Sigma Aldrich, 2µg/ml) in order to detect cell wall in living cells. Root meristem was observed making z stack with optical sections of 0.7µm. GFP is excited by 488 nm wavelength and it emitted wavelength is 510 nm. In case of PI, excitation was done at 555 nm and emission wavelength is 617 nm. In all the images for *Col-0 pSUN1::SUN1-GFP, eli1-1 pSUN1::SUN1-GFP*, the background noise was reduced and higher signal to noise ratio was applied. Digital gain was modulated depending on the image in order to achieve an optimum signal while the laser excitation was maintained constant for each experiment.

Nuclear parameters measurements

Acquired confocal images were analyzed quantitatively by ImageJ by using NucSeg plugin. These methods are discussed in details in our previous work (Goswami *et al.*, 2020). The values lie within 0-1 and more in leans towards 1 the more circular the measured nucleus is. A particular segment of the root (the epidermal and cortex layers) was selected to maintain reproducibility.

Statistical tests

Quantified data was statistically validated by using Student t test and Mann-Whitney test (or low data number) to study the significance. The variation of the data was analyzed by F test. Two types of student t test were used based on the variance of the data sets one assuming the variance equal and the other assuming its unequal.

Root digestion before AFM analysis

Poly L lysin coated plastic Petri dishes were prepared after plasma cleaning and/or ethanol washing by adding a drop of poly L-lysin (1% solution in MTBS) in the centre of the plate and let dried. Before coating, the Petri dishes were treated with ethanol overnight. Nine-day- old WT pSUN1 :: SUN1-GFP and *eli1.1* p SUN1 :: SUN1-GFP plants were placed in the Poly L lysin coated plastic Petri dishes and the root tip was incubated in presence of a mixture of cell wall digestion enzymes fro 10 min (2.5 % pectinase, 2.5 % cellulase, 2.5 pectolyase) in MTBS buffer (followed Batzenschlager *et al.*, 2015). Then the root tip was rinsed by MTBS (50 mM Pipes, 5 mM EGTA, and 5 mM MgSO4, pH 6.9) and squashed.

Microscope mounting to AFM

In our experiment all the nucleus squeezed out of the cell had their nuclear envelope, easily detectable with the fluorescence of the inner nuclear membrane SUN1 protein tagged with GFP. The attachment of the nucleus on poly-lysine coated plate was extremely fragile. To separate the debris from nucleus we needed a fluorescence microscope. A Bioscope Catalyst atomic force microscope (Bruker, Figure 4B), was adapted onto an inverted microscope stage (LEICA DMI 6000B Figure 4C) in order to detect the fluorescent nuclei. Micro Manager an open source control software based on ImageJ, has been used for image acquisition.

AFM

AFM was performed with a Bioscope Catalyst from Bruker (Figure 4A). The topographic acquisitions were done in PeakForce QNM® mode, using an amplitude of 1 µm and a frequency of 0.5 kHz. Typical scanned areas were of 10 x 10 µm² with 128 x 128 pixels. Point and Shoot was then used to define, based on the acquired topography, to set a grid of points where to perform standard force-distance curves (typically 10 to 100 points). The ramp size was 3 µm with 512 data points per segment, the ramp rate was of 1 Hz and the trigger threshold force was set to 8 nN. The cantilever type used in all the experiments was a ScanAsyst Air (Bruker), having a nominal spring constant of 0.4 N/m and a pyramidal tip (nominal tip height 2.5-8 µm, nominal tip apex radius 2 nm). Cantilever calibration was performed following the standard thermal noise method. We measured the deflection sensitivity using a linear fitting of the contact part of a force curve acquired on sapphire in MTBS. Then, we determined the spring constant by acquiring the thermal noise spectrum of the cantilever and fitting the first normal mode peak using a single harmonic oscillator model. A same tip was used for several experiments in different days as long as possible (Figure 4D). In order to reduce the offsets in force that may be introduced by each new calibration, especially by the measurements of the deflection sensitivity, we followed the SNAP protocol (Schillers *et al.*, 2017). Since our cantilevers have not been independently calibrated by the producer, we consider the spring constant value found at the first calibration as the reference value. In the following calibrations, we correct the deflection sensitivity following SNAP, in order to obtain the same spring constant each time by thermal tune analysis. Then, the new deflection sensitivity and the reference spring constant will be set in the instrument software. All the experiments where performed in MTBS medium at room temperature (around 23°C).

AFM data analysis

Quantification of the Young's modulus was done by using processing software Nanoscope Analysis 2.0 (Bruker). Force vs. Height Sensor curves were first flattened by removing the result of a linear fit to the non-contact part of the force curve (Baseline correction), in order to set this part to 0 force. The force vs. tip-sample distance (Figure 2B) was then obtained calculating a new axis of distances by the formula of

$$\text{tip-sample distances} = \text{Height Sensor [m]} - \text{tip deflection } \Delta d \text{ [m]}.$$

Young's modulus was obtained by fitting the extend segment of force vs. tip-sample distance curves with a Linearized Sneddon model (approximating the pyramidal tip by a cone) setting a tip half-angle of 18° and a Poisson ratio ν of 0.5 (incompressible material). Since adhesion was always very small of absent, we chose to use a model neglecting it.

Considering the finite thickness of the nuclei, we decided to adopt a 10% indentation rule: according to this rule, we have to indent at maximum 10% of the total height of the nucleus, otherwise the measured elastic moduli will be affected by the finite thickness of the sample and by the presence of the stiff substrate (see (Dimitriadis *et al.*, 2002)for a more detailed explanation). On each curve a 5%-40% fit boundary on the force was found appropriate, in average, to respect this rule (Figure 2B). The same fitting parameters are then used to analyse in batch all the curves of each Point and Shoot acquisition.

Discussion-Conclusion

In my PhD, I have observed the morphological and mechanical changes of plant nucleus under internal and external stresses using *Arabidopsis* root tip as a model system and hyperosmotic stress as a physiological mechanical stress. I studied the correlation of changes in nuclear envelope shape and mechanics with changes in chromatin condensation and gene expression. This study provides the first steps to address the role of nuclear mechanics and mechanotransduction in plants.

Nuclear envelope proteins and/or chromatin – regulators of plant nuclear mechanics under osmotic stress

As a physical object, the nucleus can vary in its morphology and this can be correlated with nuclear mechanics. We found that a 0.3M mannitol hyperosmotic stress on plant root tip nuclei was inducing a decrease of the nuclear volume and sphericity but an increase in nuclear stiffness with changes in stress-related gene expression. Such responses were transient and induced above a threshold of osmotic stress, suggesting that plant nucleus may act as a mechanical rheostat. The hypoosmotic stress induced by water induced no significantly change in the nuclear size or morphology in the root meristematic tissue context, but had an effect on isolated nuclei leading to an increased nuclear size, and a very likely reduction in nucleus stiffness.

The nuclear envelope appears as an important nexus for stress induced modification of the nuclear shape. In animals, nuclear envelope proteins like LINC complexes (SUN and KASH proteins) are direct link between cytoskeleton (providing mechanical stature to the cell) and nucleoskeleton (providing mechanical stature to the nucleus). Nesprin-2 giant – a KASH domain protein can sense cellular tension and affect the nuclear shape (Arsenovic *et al.*, 2016). Nucleus is positioned in migrating cells in the point of maximal tension and acts as a force propagator depending on the LINC complex functionality (Alam *et al.*, 2015). In plants disruption in LINC complex proteins results into a spherical nucleus compared to the typical elongated shape- nucleus in differentiated tissues (Tamura *et al.*, 2015). In plants too, GIP1 and GIP2 are small proteins present on both sides of the nuclear envelope, interacting with the ER TSA1 protein, the microtubule nucleation complexes at the outer nuclear membrane and the centromeric histone close to the inner nuclear membrane (Janski *et al.*, 2012; Batzenschlager *et al.*, 2013, 2015). The knocked down mutant *gip1gip2* nuclei mimics a response to hyperomostic stress, in terms of nuclear deformation, stiffness and gene expression. Increased nuclear stiffness observed in the presence of hyperosmotic stress on isolated nuclei

in the WT, is unlikely to be caused by a difference in osmotic pressure since the nucleus has large nuclear pores allowing the entry of mannitol. Similarly, this is unlikely due to the cytoskeleton, as isolated nuclei exhibit the same response. This response thus has to do with the nuclear architecture (nucleoskeleton and/or the chromatin), for which GIP proteins play a key role (Batzenschlager *et al.*, 2013, 2015).

Based on studies in animal single cells, the nucleoskeleton is as an important contributor to mechanical properties of the nucleus, where the lamins components, such as lamins A are described to interact with chromatin and the nuclear envelope SUN proteins (Haque *et al.*, 2010). For example, it has been observed that the nuclear deformation is a rate limiting factor in the cell migration, and reduced level of lamins A/C enhances the transit efficiency (Davidson *et al.*, 2014). Many cancer cells and immune cells express lower levels of lamin A/C leading to higher nuclear deformability helping them to migrate through stringent conditions. In lamin A/C–deficient (Lmna−/−) mice aberrant nuclear shape is also observed in cardiac myocytes, fibroblast cells which is linked to a decreased nuclear stiffness, increased nuclear damage and mechanosensitivity (Hah & Kim, 2019). In *Arabidopsis,* the nuclear lamin-like proteins CRWN1 helps to maintain nuclear shape in differentiated cells. Our finding suggests that these proteins do not affect the nuclear morphology in meristematic cells, ie dividing cells. CRWN1 helps to tether heterochromatin at the nuclear periphery in order to maintain a repressed chromatin state (Hu *et al.*, 2019) and is also connected with the facultative heterochromatin by interacting with the polycomb associated factor PWO1 (Mikulski *et al.*, 2019). In case of rice (*Oryza sativa*) hyperosmotic stress induces expression of the gene encoding the nuclear lamin like protein OsNMCP1. OsNMCP1 interacts with chromatin with the help of a protein called OsSWI3C, a part of the chromatin remodelling enzyme SWITCH/SUCROSE NONFERMENTING (SWI/SNF) ATP-dependent chromatin remodelling complex (CRC) (Yang *et al.*, 2020). Interestingly, in Arabidopsis CRWN1 is found phosphorylated in leaves in response to mild mannitol stress (Nikonorova *et al.*, 2018), that could be in favour in changes of protein/protein interactions at the nuclear envelope, but in this study this was not correlated to changes in nuclear shape. We show in diving cells of root tip in *Arabidopsis crwn1* that nuclei squeeze twice more compared to WT in response to hyperosmotic stress, depicting here a negative role of CRWN1 in maintaining the nuclear shape via interaction with chromatin.

As the nuclear envelope is too porous to maintain a constant resistance from the cytoskeletal force, the role of chromosome architecture behind the nuclear mechanics needs to be analysed.

Beyond nuclear lamins, chromatin is an important mechanoresponsive element in animals. Lamins interact with chromatin but the function of these two components (lamina and chromatin) can be distinct, where lamina provides mechanical stability under larger force, chromatin reacts to smaller deformation (Stephens *et al.*, 2018). Force is propagated with the help of integrins and cytoskeleton to nucleus directly (Maniotis *et al.*, 1997) and is able to modulate organization of chromosome territory directly (Tajik *et al.*, 2016). In chondrocytes hyperosmotic stress induces nuclear deformation related to chromatin condensation in particular regions (Irianto *et al.*, 2013). For plants, hyperosmotic stress results into chromatin clustering. For example, in *Arabidopsis* root meristem cells, hyperosmotic stress changes the chromocenter structure and heterochromatin fraction which is increasing compared to euchromatin (Wang *et al.*, 2015). Our data show that in *Arabidopsis* root tip diving cells, the heterochromatin was condensing with hyperosmotic stress and decondensing with loss of chromocenters with hypo-osmotic stress. We propose that this response may dominate to explain the presence of stiffer nuclei in hyperosmotic conditions: the chromatin would act like a structural gel for the nucleus.

The mechanical control of gene expression

Any stress generates a signalling leading to particular gene expression. Force can modify gene expression via modulation of the organisation of chromosome territories (Tajik *et al.*, 2016). A clear example of the effect of mechanical force on chromosome territories organization has not been yet described in plants.

Because they are sessile organisms, plants likely have developed strategies to integrate internal and external mechanical cues for the control of gene expression. The subtle change in Arabidopsis plant morphology under constant touch could also generate higher transcription level of a specific set of genes called *TOUCH* genes (Braam & Davis, 1990; Lee *et al.*, 2004). Lee *et al.*, showed that within 30 mins of the touch stimuli, 2.5% of the Arabidopsis genome (589 genes) was upregulated whereas 171 genes were down-regulated as well. Among these upregulated genes *TCH1, TCH2* and *TCH3* are involved in calcium signalling related protein synthesis such as calmodulin, and calmodulin like proteins. Whereas other induced genes *TCH4* is responsible for the expression of the xyloglucan endotransglucosylase/hydrolase (*XTH22*) which is a cell wall modifying enzymes which makes sense in coordinating mechanical stress response induced by growth alterations. Supporting this idea, more than 2-fold increase was observed by Lee *et al.,* in 19 *CML*s and 12 *XTH*s (tested 48 *CML* and 33

XTH) in response to touch. Other abiotic stresses like dark, cold or warm led to similar upregulation of genes upregulated by touch. For instance, 30 mins dark induction increased the transcription of the genes, when analysed 50 % of the genes were shared by the touch induced response (Lee *et al.*, 2004).

Recently it has been shown that the quick touch response of Arabidopsis plant is dependent on RNA Polymerase II-associated factor 1 (Paf1) complex. Vernalisation independence 3 (VIP3) protein of this complex is required for H3K36 methylation and for upregulation of *TCH3* and *TCH4* loci during touch stimulation (Jensen *et al.*, 2017). In an interesting proteomic study by Ghosh *et al.,* showed that sound vibration is able to induce array of genes involved in several pathways also including mechanically upregulated genes (39% of the total induced genes was common with upregulated genes with the (Lee *et al.*, 2004) study) including *TCH4* (Ghosh *et al.*, 2016).

Gene induction by direct mechanical stress *via* plant stem bending has been observed. In case of poplar, single bending led to increase in radial growth and induction of the transcription factor *ZINC-FINGER-PROTEIN 2 (PtaZFP2*). Total bending of stem is proportional to *ZFP* transcription (Coutand *et al.*, 2009). This induction is only achieved by bending of the stem and not by other abiotic stresses (Leblanc-Fournier *et al.*, 2008), showing some specificity in the response.

Hyperosmotic stress induces various stress responsive genes (Seki *et al.*, 2002; Sewelam *et al.*, 2014; Jensen *et al.*, 2017; Ghorbani *et al.*, 2019). In case of dehydration induced by hyperosmotic stress, mechanically important genes are upregulated (25% dehydration induced genes overlapped with touch induced genes) including 33 xyloglucan endotransglucosylase/hydrolase (*XTH*), 10 calmodulin-like (*CML*) protein genes (Urano *et al.,* 2016). A strong coupling between osmotic and mechanical stress is evident including the role of nucleus. We observed that 18 genes selected from touch and sound induced genes (Lee *et al.*, 2004; Ghosh *et al.*, 2016), are upregulated with 0.3M hyperosmotic stress : i.e. *TCH2, TCH3, TCH4, WRKY* family transcription factor (*WRKY18*), *WRKY33, WRKY40*, Salt tolerance zinc finger (SALT TOLERANCE), Calcium-dependent protein kinase (*CPK28*), *CPK32*, Calcium-binding EF-hand family protein (CA), AAA-type ATPase family (AAA), *SZF1*, Unknown function (A2), *DREB26*, *Myb44, CYP81D8, NHL3, HSPRO2* (Goswami *et al.*, 2020). Gene expression analysis further enforced the expression of this gene in hyperosmotic stresses, but also showed the stresses which have common secondary signaling molecule like

ROS linked to the expression of *WRKY40, SALT TOLERANCE, TCH4, WRKY 33, CYP81D8, NHL3, CA, WRKY33, MYB44*, *TCH3, AAA-ATPase, SZF1*. All the tested 18 mechanically induced genes were upregulated in root tissue but in areal part 17 (except *TCH2*) genes were upregulated by mannitol stress and 13 genes (except *WRKY18, CPK28, CPK32, HSPR0, TCH3*) by salt stress was induced. Although molecular players of organ specific expression are not clear, indeed the root is more vulnerable to osmotic stress, making the plant to be more sensitive towards this stress. Hyper osmotic stress in able to upregulate several transcription factors (TFs) including *AP2/ERF, MYB* , *bZIP, HSF, C2H2*, *WRKY* are also worth to mention (Ghorbani *et al.*, 2019). 70% of our tested genes (upregulated in *gip1gip2* and in response to hyperosmotic stress, touch and sound response) have MYB binding site Myb box1 Myb box 2 or Myb box, in their promoter region but a more specific TF like AP2 EREBP target region DREB is present in the promoter of only 28% of the genes. Thus, MYB could be a master regulator for hyperosmotic stress, which share a crosstalk with other abiotic stress and confers specificity via the induction of a specific set of TFs.

In our study we observed that the *gip1gip2* and touch induced transcriptomes share 57% of homology. All the previously mentioned 18 genes upregulated in hyperosmotic stress were also upregulated in *gip1gip2*. The plant lamin-like protein OsNMCP1 in rice (*Oryza sativa*) ensures an array of drought responsive gene expression including *OsNAC10, OsERF48, OsSGL, SNAC1* and *OsbZIP23* by physically interacting with the negative regulator OsSWI3C (Yang *et al.*, 2020). In *Arabidopsis* NMCP homologue CRWN1 negatively regulate gene expression (Mikulski *et al.*, 2019). Nine genes among the above mentioned 18 genes upregulated by touch, sound and hyperosmotic stress are common in *gip1gip2* and *crwn1* induced upregulated transcriptome i.e. *HSPRO2, NHL3, WRKY33, CPK28, TCH2, SZF1, AAA-type ATPase family (AAA), WRK18, WRK40*. Although many other stress induced genes are upregulated in *crwn1*, we cannot extend or analysis due to the limited available resource (Choi *et al.*, 2019).

Monitoring nuclear shape to diagnose the physiological state of the cell

Nuclear shape is modified by mechanical stress which is correlated with changes in nuclear mechanics and the mechanical environment of the cell. Mechanical stress also induces gene expression via direct modulation of the chromatin or by shuttling transcription factors. In animals YAP/TAZ transcriptional co activator of Hippo signalling pathway has been shown to

be regulated by substrate stiffness and cellular architecture (Dupont *et al.*, 2011). Physiological stress originates in disease and development at multicellular organisms. In addition, organisms specially plants use environmental and mechanical cues to fine tune developmental processes. Taking all these points into account, the nuclear shape change could be studied as an indicator of response towards mechanical stress generated physiologically, in addition in the context of environmental stress particularly in plants.

Disease and development

Nuclear shape alterations have been linked to several disease conditions like cancer and several nuclear envelopathies, aging related diseases. Breast cancer cells could be identified more robustly by nuclear morphology than cellular morphology. An increase in nuclear shape and size variation is often correlated with cancer progression. Nuclear morphology and size are often used as markers to identify several cancers. Specific nuclear features mark specific cancers, for example a recent finding on urothelial carcinomas suggests that cancerous cells can be distinguished by their particularly large nuclei from the normal cells (Poropatich *et al.*, 2016). In most of the cancer cells, the nuclear dysfunction is caused by the depletion of lamin A/C leading to a softer mechanically flexible nuclei aiding towards cancer cell movement but also contributing to misfunction of signalling pathways (Bell & Lammerding, 2016). In general, nuclear envelopathies result from mutated nuclear envelope proteins such as lamins, lamin associated proteins like lamin B receptors etc. Laminopathies are linked to diseases related to changes in lamin for example muscular laminopathies or Hutchinson-Gilford progeria etc. Muscle fiber cells from Emery-Dreifuss muscular dystrophy patients have abnormally shaped and damaged nuclei in 25% of the cases (Fidziańska & Hausmanowa-Petrusewicz, 2003).

When murine embryonic stem (ES) cells differentiate to primitive endoderm cells, nuclear shape changes are observed: the flattened and oval nuclei become more spherical and with a slight decrease in their volume (Smith *et al.*, 2017). In case of bovine and human Mesenchymal stem cells nuclear deformability decreases with fibrochondrogenic differentiation in nanofibrous scaffolds (Heo *et al.*, 2016). MSCs with altered nuclear morphology are not able to reach projected differentiation (McColloch *et al.*, 2019). Although this list is not exhaustive, it appears that nucleus shape and stiffness reflect the physiological status of the cell.

Plant - opening new perspectives

Plant development hugely depend on external cues, including aggressive ones. This leads to the expression of stress response genes. Particularly, mechanical stress in an important regulator of development (Hamant, 2017). Mechanical stress can affect cell wall integrity which is highly important for plant immunity (Bacete & Hamann, 2020). For example, *Arabidopsis irregular xylem (irx)* plants with mutated secondary cell wall synthesis show enhanced resistance to pathogens like *Plectosphaerella cucumerina, Botrytis cinerea, Fusarium oxysporum* e.t.c. (Bacete *et al.*, 2018). Change in cell wall composition could be sensed directly by RLKs or indirectly by MSLs with changes in mechanical properties of plasma membrane. It has been shown that during early MAMP (molecular pattern-triggered immunity), the microbial molecule perceived by plant cell surface receptors induced signalling to the nucleus for massive transcriptional reprogramming for the host defence response. In this process, WRKY18, 40 and 33 are important transcriptional factors targeting specific loci (Birkenbihl *et al.*, 2017). MT is an important constituent of cell mechanics, helping the cell to change stress anisotropy to isotropy during development (Hamant *et al.*, 2019) and MT is physically linked to cell wall via cellulose synthase interacting protein 1 (CSI1). Yet how this signals exactly transduce and modulate the nucleus and ensures specific gene response is unclear. Absence of nuclear envelope proteins like SUN and KASH domain proteins, which have been shown in animals to have mechanically important role, doesn't really affect the development and growth of Arabidopsis (Tamura *et al.*, 2015; Meier *et al.*, 2017). Such LINC complexes have been shown to be linked to the actin skeleton (Tamura *et al.*, 2015). The same is true for single mutants of genes encoding nucleo skeletal proteins – CRWN1-4, although double mutant *crwn1crwn2* as well as triple mutant *crwn1crwn2crwn*4 have impaired growth.

CRWN proteins also negatively regulate-defence response, loss of CRWN1 and/or CRWN 4 results into spontaneous defence response with the upregulation of defence-related genes (Choi *et al.*, 2019). Cell wall is one of the most important mechanical contributor of plant cell. When the main load bearing component cellulose is reduced and compensated by lignin in a CESA3 mutant *eli1-1*, upregulation of defence-related genes is also observed via chromatin modulation (Caño-Delgado *et al.*, 2003). GIP interacts with the mechanically important microtubules outside the nucleus and could be postulated to contribute in a direct link between cell wall and nucleus via microtubule. *gip1* or *gip2* single mutants also doesn't show any change in

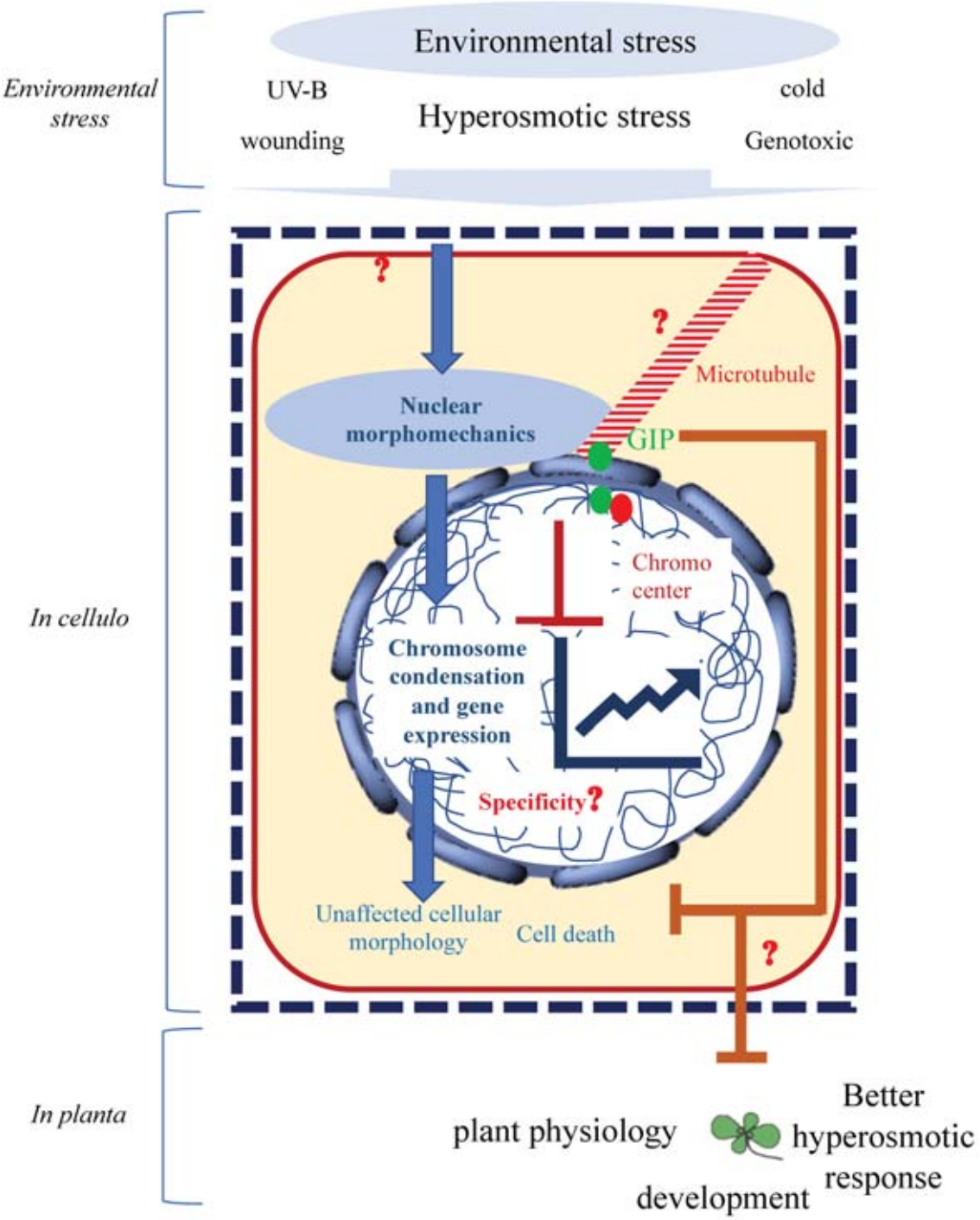

Figure 1: Nuclear morphomechanics under hyper osmotic stress: importance of nuclear envelope and chromatin

phenotype, yet double mutant *gip1gip2* has hugely altered plant phenotype, with short root, dwarfism, sterility in presence of a highly lobulated and wavy nuclear phenotypes. In *gip1gip2* the cell structure is highly disturbed as well as the cell plate formation after division resulting into polyploidy (Janski *et al.*, 2012) and several stress responsive genes are induced, including defence-related genes (4% of the upregulated transcriptome). We observed in our preliminary studies that the nucleus becomes slightly misshaped and stiffer in *eli 1-1* in normal growth conditions and also in response to hyper osmotic stress however the change in nuclear misshaping is three time less (decrease of 3%) compared to WT (decrease of 9%). Although we need to confirm this data in a more architecturally stable tissue like shoot apical meristem. This could open better understanding of the role of cell wall components on the nuclear morphology maintenance. Altogether this could provide a link from the cell wall modification to modification of nuclear architecture.

We observed in our study that *gip1gip2* nucleus and plant are insensitive to further hydrostatic force induced by hyperosmotic treatment. These plants show mildly to no change in root growth when compared to WT and cell death was reduced even in harsher osmotic conditions. So, GIPs act as negative regulators of the hyperosmotic response, and when nuclei are already deformed, they are primed to resist hyperosmotic stress linked to changes in the nuclear mechanical properties, and nucleus may act as a shield. Although osmotic stress and mechanical stress are strongly coupled, the role of the plant nucleus in development induced by mechanical cues is yet to be elucidated. Our work opens an avenue to understand the role of environmental cues during development, through the lens of nuclear mechanics and mechanotransduction.

Conclusion

We propose that a gel-like chromatin based nuclear mechanical response exists in presence of hyperosmotic stress which leads to specific gene expression and GIPs act as negative regulator (Figure 1). Our current model suggests that hyperosmotic stress results into transient highly disturbed nuclear morphology with reduced circularity, area, that echoes changes in nuclear mechanical property which becomes stiffer. The porous nature of the nucleus likely makes it ill-equipped to withstand changes in osmotic stress, thus suggesting a role of chromatin in modulating the mechanical properties of the nucleus when osmotic conditions change. Heterochromatin condensation seems to occur with hyper osmotic stress and decondensation with hypoosmotic stress, modulating thus the expression of mechanically relevant gene

expression. This is consistent with the reported aberrant centromeric chromatin organisation in *gip1gip2*, the misshaped nuclei and the interaction of CRWN1 with repressed heterochromatin *via* PWO1.

GIPs and CRWN1 might regulate the response of gel-like chromatin to osmotic stress through changes in the 3D chromatin organization as already shown for CRWN1 (Hu *et al.*, 2019). While contrary data were obtained on the role of CRWN1 in the transcriptional response (Choi *et al.*, 2019; Hu *et al.*, 2019), further studies are needed at the chromatin level to correlate changes in nuclear shape and gene expression, including HI-C data and epigenetic landscape, as well as nuclear translocation of specific transcription factors. Next challenges will be to understand how the specificity of molecular pathways are achieved under such global changes or how the nuclear envelope mechanics is integrated in plant development. The mechanical signalling interactions between cell wall property, wall sensing, cytoskeleton (mainly microtubules) and nucleus remains largely unknown in plants. Our findings clearly open new avenue to understand the role of nuclear morphomechanics in response to environmental stresses in plants. This could also help to understand plant susceptibility to pests in response to mechanical stress to increase plant immunity (Coutand, 2020).

References

Ackermann F, Stanislas T. **2020**. The Plasma Membrane–An Integrating Compartment for Mechano-Signaling. *Plants* **9**: 505.

Agrawal A, Lele TP. **2019**. Mechanics of nuclear membranes. *Journal of Cell Science*: 8.

Alam SG, Lovett D, Kim DI, Roux KJ, Dickinson RB, Lele TP. **2015**. The nucleus is an intracellular propagator of tensile forces in NIH 3T3 fibroblasts. *Journal of Cell Science* **128**: 1901–1911.

Alcaraz J, Buscemi L, Grabulosa M, Trepat X, Fabry B, Farré R, Navajas D. **2003**. Microrheology of Human Lung Epithelial Cells Measured by Atomic Force Microscopy. *Biophysical Journal* **84**: 2071–2079.

Alonso-Serra J, Shi X, Peaucelle A, Rastas P, Bourdon M, Immanen J, Takahashi J, Koivula H, Eswaran G, Muranen S, *et al.* 2020. ELIMÄKI Locus Is Required for Vertical Proprioceptive Response in Birch Trees. *Current Biology* **30**: 589-599.e5.

Al-Zube LA, Robertson DJ, Edwards JN, Sun W, Cook DD. **2017**. Measuring the compressive modulus of elasticity of pith-filled plant stems. *Plant Methods* **13**.

Ambrose C, Wasteneys GO. **2014**. Microtubule Initiation from the Nuclear Surface Controls Cortical Microtubule Growth Polarity and Orientation in Arabidopsis thaliana. *Plant and Cell Physiology* **55**: 1636–1645.

Arsenovic PT, Ramachandran I, Bathula K, Zhu R, Narang JD, Noll NA, Lemmon CA, Gundersen GG, Conway DE. **2016**. Nesprin-2G, a Component of the Nuclear LINC Complex, Is Subject to Myosin-Dependent Tension. *Biophysical Journal* **110**: 34–43.

Bacete L, Hamann T. **2020**. The Role of Mechanoperception in Plant Cell Wall Integrity Maintenance. *Plants* **9**: 574.

Bacete L, Mélida H, Miedes E, Molina A. **2018**. Plant cell wall-mediated immunity: cell wall changes trigger disease resistance responses. *The Plant Journal* **93**: 614–636.

Baldoni E, Genga A, Cominelli E. **2015**. Plant MYB Transcription Factors: Their Role in Drought Response Mechanisms. *International Journal of Molecular Sciences* **16**: 15811–15851.

Balland M, Richert A, Gallet F. **2005**. The dissipative contribution of myosin II in the cytoskeleton dynamics of myoblasts. *European Biophysics Journal* **34**: 255–261.

Barneche F, Baroux C. **2017**. Unreeling the chromatin thread: a genomic perspective on organization around the periphery of the Arabidopsis nucleus. *Genome Biology* **18**.

Barton DA, Vantard M, Overall RL. **2008**. Analysis of Cortical Arrays from Tradescantia virginiana at High Resolution Reveals Discrete Microtubule Subpopulations and Demonstrates That Confocal Images of Arrays Can Be Misleading. *The Plant Cell* **20**: 982–994.

Batzenschlager M, Lermontova I, Schubert V, Fuchs J, Berr A, Koini MA, Houlné G, Herzog E, Rutten T, Alioua A, *et al.* 2015. *Arabidopsis* MZT1 homologs GIP1 and GIP2 are essential for centromere architecture. *Proceedings of the National Academy of Sciences* **112**: 8656–8660.

Batzenschlager M, Masoud K, Janski N, Houlné G, Herzog E, Evrard J-L, Baumberger N, Erhardt M, Nominé Y, Kieffer B, *et al.* 2013. The GIP gamma-tubulin complex-associated proteins are involved in nuclear architecture in Arabidopsis thaliana. *Frontiers in Plant Science* **4**.

Beauzamy L, Derr J, Boudaoud A. **2015a**. Quantifying Hydrostatic Pressure in Plant Cells by Using Indentation with an Atomic Force Microscope. *Biophysical Journal* **108**: 2448–2456.

Beauzamy L, Louveaux M, Hamant O, Boudaoud A. **2015b**. Mechanically, the Shoot Apical Meristem of Arabidopsis Behaves like a Shell Inflated by a Pressure of About 1 MPa. *Frontiers in Plant Science* **6**.

Bell ES, Lammerding J. **2016**. Causes and consequences of nuclear envelope alterations in tumour progression. *European journal of cell biology* **95**: 449–464.

Beloussov LV, Grabovsky VI. **2006**. Morphomechanics: goals, basic experiments and models. *The International Journal of Developmental Biology* **50**: 81–92.

Besson S, Dumais J. **2011**. Universal rule for the symmetric division of plant cells. *Proceedings of the National Academy of Sciences of the United States of America* **108**: 6294–6299.

Bidhendi AJ, Geitmann A. **2019**. Methods to quantify primary plant cell wall mechanics. *Journal of Experimental Botany* **70**: 3615–3648.

Birkenbihl RP, Kracher B, Roccaro M, Somssich IE. **2017**. Induced Genome-Wide Binding of Three Arabidopsis WRKY Transcription Factors during Early MAMP-Triggered Immunity. *The Plant Cell* **29**: 20–38.

Blancaflor EB, Hasenstein KH. **1995**. Growth and Microtubule Orientation of Zea mays Roots Subjected to Osmotic Stress. *International Journal of Plant Sciences* **156**: 774–783.

Borassi C, Sede AR, Mecchia MA, Salgado Salter JD, Marzol E, Muschietti JP, Estevez JM. **2016**. An update on cell surface proteins containing extensin-motifs. *Journal of Experimental Botany* **67**: 477–487.

Bovio S, Long Y, Monéger F. **2019**. Use of Atomic Force Microscopy to Measure Mechanical Properties and Turgor Pressure of Plant Cells and Plant Tissues. *Journal of Visualized Experiments*: 9.

Boyer JS, Cavalieri AJ, Schulze E-D. **1985**. Control of the rate of cell enlargement: Excision, wall relaxation, and growth-induced water potentials. *Planta* **163**: 527–543.

Braam J. **2004**. In touch: plant responses to mechanical stimuli: Tansley review. *New Phytologist* **165**: 373–389.

Braam J, Davis RW. **1990**. Rain-, wind-, and touch-induced expression of calmodulin and calmodulin-related genes in Arabidopsis. *Cell* **60**: 357–364.

Budday S, Raybaud C, Kuhl E. **2014**. A mechanical model predicts morphological abnormalities in the developing human brain. *Scientific Reports* **4**.

Bufi N, Durand-Smet P, Asnacios A. **2015**. Single-cell mechanics: The parallel plates technique. In: Methods in Cell Biology. Elsevier, 187–209.

Caño-Delgado AI, Metzlaff K, Bevan MW. **2000**. ELI1 regulates cell expansion and secondary wall formation. : 11.

Caño-Delgado A, Penfield S, Smith C, Catley M, Bevan M. **2003**. Reduced cellulose synthesis invokes lignification and defense responses in Arabidopsis thaliana. *The Plant Journal* **34**: 351–362.

Cazalé A-C, Droillard M-J, Wilson C, Heberle-Bors E, Barbier-Brygoo H, Laurière C. **1999**. MAP kinase activation by hypoosmotic stress of tobacco cell suspensions: towards the oxidative burst response? *The Plant Journal* **19**: 297–307.

Chebli Y, Geitmann A. **2017**. Cellular growth in plants requires regulation of cell wall biochemistry. *Current Opinion in Cell Biology* **44**: 28–35.

Chen W, Lou J, Evans EA, Zhu C. **2012**. Observing force-regulated conformational changes and ligand dissociation from a single integrin on cells. *The Journal of Cell Biology* **199**: 497–512.

Choi J, Strickler SR, Richards EJ. **2019**. Loss of CRWN Nuclear Proteins Induces Cell Death and Salicylic Acid Defense Signaling1[OPEN]. *Plant Physiology* **179**: 1315–1329.

Christmann A, Grill E, Huang J. **2013**. Hydraulic signals in long-distance signaling. *Current Opinion in Plant Biology* **16**: 293–300.

Ciska M, Masuda K, Moreno Díaz de la Espina S. **2013**. Lamin-like analogues in plants: the characterization of NMCP1 in Allium cepa. *Journal of Experimental Botany* **64**: 1553–1564.

Conde A, Chaves MM, Geros H. **2011**. Membrane Transport, Sensing and Signaling in Plant Adaptation to Environmental Stress. *Plant and Cell Physiology* **52**: 1583–1602.

Cosgrove D. 1986. Biophysical Control of Plant Cell Growth. ***Annual Review of Plant Physiology*****: 29.**

Cosgrove DJ. **1993**. Wall extensibility: its nature, measurement and relationship to plant cell growth. *New Phytologist* **124**: 1–23.

Cosgrove DJ. **2005**. Growth of the plant cell wall. *Nature Reviews Molecular Cell Biology* **6**: 850–861.

Cosgrove DJ. **2014**. Re-constructing our models of cellulose and primary cell wall assembly. *Current opinion in plant biology* **22**: 122–131.

Cosgrove DJ. **2015**. Plant expansins: diversity and interactions with plant cell walls. *Current opinion in plant biology* **25**: 162–172.

Cosgrove DJ. **2018**. Nanoscale structure, mechanics and growth of epidermal cell walls. *Current Opinion in Plant Biology* **46**: 77–86.

Cosgrove DJ, Jarvis MC. **2012**. Comparative structure and biomechanics of plant primary and secondary cell walls. *Frontiers in Plant Science* **3**.

Costa KD, Sim AJ, Yin FC-P. **2006**. Non-Hertzian Approach to Analyzing Mechanical Properties of Endothelial Cells Probed by Atomic Force Microscopy. *Journal of Biomechanical Engineering* **128**: 176–184.

Coutand C. **2020**. The Effect of Mechanical Stress on Plant Susceptibility to Pests: A Mini Opinion Review. *Plants* **9**: 632.

Coutand C, Martin L, Leblanc-Fournier N, Decourteix M, Julien J-L, Moulia B. **2009**. Strain Mechanosensing Quantitatively Controls Diameter Growth and PtaZFP2 Gene Expression in Poplar. *Plant Physiology* **151**: 223–232.

Cox CD, Bavi N, Martinac B. **2019**. Biophysical Principles of Ion-Channel-Mediated Mechanosensory Transduction. *Cell Reports* **29**: 1–12.

Cramer LP, Siebert M, Mitchison TJ. **1997**. Identification of Novel Graded Polarity Actin Filament Bundles in Locomoting Heart Fibroblasts: Implications for the Generation of Motile Force. *Journal of Cell Biology* **136**: 1287–1305.

Dahl KN, Engler AJ, Pajerowski JD, Discher DE. **2005.** Power-Law Rheology of Isolated Nuclei with Deformation Mapping of Nuclear Substructures. *Biophysical Journal*: 10.

Dahl KN, Ribeiro AJS, Lammerding J. **2008**. Nuclear shape, mechanics, and mechanotransduction. *Circulation research* **102**: 1307–1318.

Darling EM, Topel M, Zauscher S, Vail TP, Guilak F. **2008**. Viscoelastic properties of human mesenchymally-derived stem cells and primary osteoblasts, chondrocytes, and adipocytes. *Journal of biomechanics* **41**: 454–464.

Davidson PM, Denais C, Bakshi MC, Lammerding J. **2014**. Nuclear deformability constitutes a rate-limiting step during cell migration in 3-D environments. *Cellular and molecular bioengineering* **7**: 293–306.

Decreux A, Messiaen J. **2005**. Wall-associated Kinase WAK1 Interacts with Cell Wall Pectins in a Calcium-induced Conformation. *Plant and Cell Physiology* **46**: 268–278.

Desprat N, Richert A, Simeon J, Asnacios A. **2005**. Creep Function of a Single Living Cell. *Biophysical Journal* **88**: 2224–2233.

Desprat N, Supatto W, Pouille P-A, Beaurepaire E, Farge E. **2008**. Tissue Deformation Modulates Twist Expression to Determine Anterior Midgut Differentiation in Drosophila Embryos. *Developmental Cell* **15**: 470–477.

Dimitriadis EK, Horkay F, Maresca J, Kachar B, Chadwick RS. **2002**. Determination of elastic moduli of thin layers of soft material using the atomic force microscope. *Biophysical Journal* **82**: 2798–2810.

Dittmer TA, Misteli T. **2011**. The lamin protein family. *Genome Biology* **12**: 222.

Dittmer TA, Richards EJ. **2008**. Role of LINC proteins in plant nuclear morphology. *Plant Signaling & Behavior* **3**: 485–487.

Dittmer TA, Stacey NJ, Sugimoto-Shirasu K, Richards EJ. **2007**. *LITTLE NUCLEI* Genes Affecting Nuclear Morphology in *Arabidopsis thaliana*. *The Plant Cell* **19**: 2793–2803.

Dupont S, Morsut L, Aragona M, Enzo E, Giulitti S, Cordenonsi M, Zanconato F, Le Digabel J, Forcato M, Bicciato S, *et al.* 2011. Role of YAP/TAZ in mechanotransduction. *Nature* **474**: 179–183.

Durand-Smet P, Chastrette N, Guiroy A, Richert A, Berne-Dedieu A, Szecsi J, Boudaoud A, Frachisse J-M, Bendhamane M, Hamant O, *et al.* 2014. A Comparative Mechanical

Analysis of Plant and Animal Cells Reveals Convergence across Kingdoms. *Biophysical Journal* **107**: 2237–2244.

Emons AMC, Höfte H, Mulder BM. **2007**. Microtubules and cellulose microfibrils: how intimate is their relationship? *Trends in Plant Science* **12**: 279–281.

Engler AJ, Carag-Krieger C, Johnson CP, Raab M, Tang H-Y, Speicher DW, Sanger JW, Sanger JM, Discher DE. **2008**. Embryonic cardiomyocytes beat best on a matrix with heart-like elasticity: scar-like rigidity inhibits beating. *Journal of cell science* **121**: 3794–3802.

Engler AJ, Sen S, Sweeney HL, Discher DE. **2006**. Matrix Elasticity Directs Stem Cell Lineage Specification. *Cell* **126**: 677–689.

Errera L. **1886**. Sur une condition fondamentale d'équilibre des cellules vivantes. *Annales de la Société belge de microscopie* **13**: 12–16.

Esehaghbeygi A, Hoseinzadeh B, Khazaei M, Masoumi A. **2009**. Bending and Shearing Properties of Wheat Stem of Alvand Variety. : 6.

Fabry B, Maksym GN, Butler JP, Glogauer M, Navajas D, Fredberg JJ. **2001**. Scaling the Microrheology of Living Cells. *Physical Review Letters* **87**.

Felekis D, Vogler H, Mecja G, Muntwyler S, Nestorova A, Huang T, Sakar MS, Grossniklaus U, Nelson BJ. **2015**. Real-time automated characterization of 3D morphology and mechanics of developing plant cells. *The International Journal of Robotics Research* **34**: 1136–1146.

Feng W, Kita D, Peaucelle A, Cartwright HN, Doan V, Duan Q, Liu M-C, Maman J, Steinhorst L, Schmitz-Thom I, *et al.* 2018. The FERONIA Receptor Kinase Maintains Cell-Wall Integrity during Salt Stress through Ca2+ Signaling. *Current Biology* **28**: 666-675.e5.

Fernandes AN, Chen X, Scotchford CA, Walker J, Wells DM, Roberts CJ, Everitt NM. **2012**. Mechanical properties of epidermal cells of whole living roots of *Arabidopsis thaliana* : An atomic force microscopy study. *Physical Review E* **85**: 021916.

Fidziańska A, Hausmanowa-Petrusewicz I. **2003**. Architectural abnormalities in muscle nuclei. Ultrastructural differences between X-linked and autosomal dominant forms of EDMD. *Journal of the Neurological Sciences* **210**: 47–51.

Fink J, Carpi N, Betz T, Bétard A, Chebah M, Azioune A, Bornens M, Sykes C, Fetler L, Cuvelier D, *et al.* 2011. External forces control mitotic spindle positioning. *Nature Cell Biology* **13**: 771–778.

Fiserova J, Kiseleva E, Goldberg MW. **2009**. Nuclear envelope and nuclear pore complex structure and organization in tobacco BY-2 cells. *The Plant Journal* **59**: 243–255.

Fujita S, Pytela J, Hotta T, Kato T, Hamada T, Akamatsu R, Ishida Y, Kutsuna N, Hasezawa S, Nomura Y, *et al.* 2013. An Atypical Tubulin Kinase Mediates Stress-Induced Microtubule Depolymerization in Arabidopsis. *Current Biology* **23**: 1969–1978.

Fung YC. **1991**. What are the residual stresses doing in our blood vessels? *Annals of Biomedical Engineering* **19**: 237–249.

Fung YC, Liu SQ. **1989**. Change of residual strains in arteries due to hypertrophy caused by aortic constriction. *Circulation Research* **65**: 1340–1349.

Galletti R, Verger S, Hamant O, Ingram GC. **2016**. Developing a 'thick skin': a paradoxical role for mechanical tension in maintaining epidermal integrity? *Development* **143**: 3249–3258.

Geitmann A, Ortega JKE. **2009**. Mechanics and modeling of plant cell growth. *Trends in Plant Science* **14**: 467–478.

Georges PC, Miller WJ, Meaney DF, Sawyer ES, Janmey PA. **2006**. Matrices with Compliance Comparable to that of Brain Tissue Select Neuronal over Glial Growth in Mixed Cortical Cultures. *Biophysical Journal* **90**: 3012–3018.

Gesson K, Rescheneder P, Skoruppa MP, Haeseler A von, Dechat T, Foisner R. **2016**. A-type lamins bind both hetero- and euchromatin, the latter being regulated by lamina-associated polypeptide 2 alpha. *Genome Research* **26**: 462–473.

Ghorbani R, Alemzadeh A, Razi H. **2019**. Microarray analysis of transcriptional responses to salt and drought stress in Arabidopsis thaliana. *Heliyon* **5**.

Ghosh R, Mishra RC, Choi B, Kwon YS, Bae DW, Park S-C, Jeong M-J, Bae H. **2016**. Exposure to Sound Vibrations Lead to Transcriptomic, Proteomic and Hormonal Changes in Arabidopsis. *Scientific Reports* **6**.

Gibson WT, Veldhuis JH, Rubinstein B, Cartwright HN, Perrimon N, Brodland GW, Nagpal R, Gibson MC. **2011**. Control of the Mitotic Cleavage Plane by Local Epithelial Topology. *Cell* **144**: 427–438.

Goffin JM, Pittet P, Csucs G, Lussi JW, Meister J-J, Hinz B. **2006**. Focal adhesion size controls tension-dependent recruitment of α-smooth muscle actin to stress fibers. *Journal of Cell Biology* **172**: 259–268.

Goswami R, Asnacios A, Milani P, Graindorge S, Houlné G, Mutterer J, Hamant O, Chabouté M-E. **2020**. Mechanical Shielding in Plant Nuclei. *Current Biology* **30**: 2013-2025.e3.

Goto C, Tamura K, Fukao Y, Shimada T, Hara-Nishimura I. **2014**. The Novel Nuclear Envelope Protein KAKU4 Modulates Nuclear Morphology in Arabidopsis[W]. *The Plant Cell* **26**: 2143–2155.

Graumann K, Runions J, Evans DE. **2010**. Characterization of SUN-domain proteins at the higher plant nuclear envelope. *The Plant Journal* **61**: 134–144.

Green PB. **1968**. Growth Physics in Nitella: a Method for Continuous in Vivo Analysis of Extensibility Based on a Micro-manometer Technique for Turgor Pressure 1. *Plant Physiology* **43**: 1169–1184.

Groves NR, Biel AM, Newman-Griffis AH, Meier I. **2018**. Dynamic Changes in Plant Nuclear Organization in Response to Environmental and Developmental Signals. *Plant Physiology* **176**: 230–241.

Gruenbaum Y, Foisner R. **2015**. Lamins: Nuclear Intermediate Filament Proteins with Fundamental Functions in Nuclear Mechanics and Genome Regulation. *Annual Review of Biochemistry* **84**: 131–164.

Guck J, Schinkinger S, Lincoln B, Wottawah F, Ebert S, Romeyke M, Lenz D, Erickson HM, Ananthakrishnan R, Mitchell D, *et al.* 2005. Optical Deformability as an Inherent Cell Marker for Testing Malignant Transformation and Metastatic Competence. *Biophysical Journal* **88**: 3689–3698.

Guilak F, Tedrow JR, Burgkart R. 2000. Viscoelastic Properties of the Cell Nucleus. *BIOCHEMICAL AND BIOPHYSICAL RESEARCH COMMUNICATIONS* **269**: 6.

Guo T, Mao X, Zhang H, Zhang Y, Fu M, Sun Z, Kuai P, Lou Y, Fang Y. 2017. Lamin-like Proteins Negatively Regulate Plant Immunity through NAC WITH TRANSMEMBRANE MOTIF1-LIKE9 and NONEXPRESSOR OF PR GENES1 in Arabidopsis thaliana. *Molecular Plant* **10**: 1334–1348.

Haas KT, Wightman R, Meyerowitz EM, Peaucelle A. 2020. Pectin homogalacturonan nanofilament expansion drives morphogenesis in plant epidermal cells. *Science* **367**: 1003–1007.

Hah J, Kim D-H. 2019. Deciphering Nuclear Mechanobiology in Laminopathy. *Cells* **8**.

Hamant O. 2017. Mechano-devo. *Mechanisms of Development* **145**: 2–9.

Hamant O, Haswell ES. 2017. Life behind the wall: sensing mechanical cues in plants. *BMC Biology* **15**.

Hamant O, Heisler MG, Jonsson H, Krupinski P, Uyttewaal M, Bokov P, Corson F, Sahlin P, Boudaoud A, Meyerowitz EM, *et al.* 2008. Developmental Patterning by Mechanical Signals in Arabidopsis. *Science* **322**: 1650–1655.

Hamant O, Inoue D, Bouchez D, Dumais J, Mjolsness E. 2019. Are microtubules tension sensors? *Nature Communications* **10**: 2360.

Hamant O, Traas J. 2010. The mechanics behind plant development. *New Phytologist* **185**: 369–385.

Hamilton ES, Jensen GS, Maksaev G, Katims A, Sherp AM, Haswell ES. 2015. Mechanosensitive channel MSL8 regulates osmotic forces during pollen hydration and germination. *Science* **350**: 438–441.

Hammerick KE, Huang Z, Sun N, Lam MT, Prinz FB, Wu JC, Commons GW, Longaker MT. **2011**. Elastic Properties of Induced Pluripotent Stem Cells. *Tissue Engineering. Part A* **17**: 495–502.

Haque F, Mazzeo D, Patel JT, Smallwood DT, Ellis JA, Shanahan CM, Shackleton S. **2010**. Mammalian SUN Protein Interaction Networks at the Inner Nuclear Membrane and Their Role in Laminopathy Disease Processes. *The Journal of Biological Chemistry* **285**: 3487–3498.

Harris DM, Corbin K, Wang T, Gutierrez R, Bertolo AL, Petti C, Smilgies D-M, Estevez JM, Bonetta D, Urbanowicz BR, *et al.* 2012. Cellulose microfibril crystallinity is reduced by mutating C-terminal transmembrane region residues CESA1A903V and CESA3T942I of cellulose synthase. *Proceedings of the National Academy of Sciences* **109**: 4098–4103.

Hashimoto T. **2015**. Microtubules in Plants. *The Arabidopsis Book / American Society of Plant Biologists* **13**.

Haswell ES, Peyronnet R, Barbier-Brygoo H, Meyerowitz EM, Frachisse J-M. **2008**. Two MscS Homologs Provide Mechanosensitive Channel Activities in the Arabidopsis Root. *Current Biology* **18**: 730–734.

Haswell ES, Verslues PE. **2015**. The ongoing search for the molecular basis of plant osmosensing. *The Journal of General Physiology* **145**: 389–394.

Heisler MG, Hamant O, Krupinski P, Uyttewaal M, Ohno C, Jönsson H, Traas J, Meyerowitz EM. **2010**. Alignment between PIN1 Polarity and Microtubule Orientation in the Shoot Apical Meristem Reveals a Tight Coupling between Morphogenesis and Auxin Transport. *PLoS Biology* **8**.

Heller I, Hoekstra TP, King GA, Peterman EJG, Wuite GJL. **2014**. Optical Tweezers Analysis of DNA–Protein Complexes. *Chemical Reviews* **114**: 3087–3119.

Heo S-J, Driscoll TP, Thorpe SD, Nerurkar NL, Baker BM, Yang MT, Chen CS, Lee DA, Mauck RL. **2016**. Differentiation alters stem cell nuclear architecture, mechanics, and mechano-sensitivity. *eLife* **5**.

Higuchi A, Ling Q-D, Chang Y, Hsu S-T, Umezawa A. **2013**. Physical Cues of Biomaterials Guide Stem Cell Differentiation Fate. *Chemical Reviews* **113**: 3297–3328.

Hochmuth RM. **2000**. Micropipette aspiration of living cells. *Journal of Biomechanics* **33**: 15–22.

Hofmeister W. **1863**. Zusatze und Berichtigungen zu den 1851 vero¨ ffentli- chen Untersuchungengen der Entwicklung ho¨ herer Kryptogamen. *Jahrbucher für Wissenschaft und Botanik* **3**: 259–293.

Hooke R, Allestry J, Martyn J. **1665**. *Micrographia, or, Some physiological descriptions of minute bodies made by magnifying glasses :with observations and inquiries thereupon /*. London : Printed by Jo. Martyn and Ja. Allestry, printers to the Royal Society ... ,.

Hu S, Chen J, Butler JP, Wang N. **2005**. Prestress mediates force propagation into the nucleus. *Biochemical and Biophysical Research Communications*: 6.

Hu B, Wang N, Bi X, Karaaslan ES, Weber A-L, Zhu W, Berendzen KW, Liu C. **2019**. Plant lamin-like proteins mediate chromatin tethering at the nuclear periphery. *Genome Biology* **20**: 87.

Huang T-L, Wang H-J, Chang Y-C, Wang S-W, Hsia K-C. **2020**. Promiscuous Binding of Microprotein Mozart1 to γ-Tubulin Complex Mediates Specific Subcellular Targeting to Control Microtubule Array Formation. *Cell Reports* **31**: 107836.

Humble GD, Raschke K. **1971**. Stomatal Opening Quantitatively Related to Potassium Transport. *Plant Physiology* **48**: 447–453.

Hutchins JRA, Toyoda Y, Hegemann B, Poser I, Heriche JK, Sykora MM, Augsburg M, Hudecz O, Buschhorn BA, Bulkescher J, *et al.* 2010. Systematic Analysis of Human Protein Complexes Identifies Chromosome Segregation Proteins. *Science* **328**: 593–599.

Hyskova V, Ryslava H. **2018**. Hyperosmotic versus Hypoosmotic Stress in Plants. *Biochemistry & Analytical Biochemistry* **07**.

İnce A, Uğurluay S, Güzel E, Özcan MT. **2005**. Bending and Shearing Characteristics of Sunflower Stalk Residue. *Biosystems Engineering* **92**: 175–181.

Ingber DE. **2008**. Tensegrity-Based Mechanosensing from Macro to Micro. *Progress in biophysics and molecular biology* **97**: 163–179.

Irianto J, Swift J, Martins RP, McPhail GD, Knight MM, Discher DE, Lee DA. **2013**. Osmotic Challenge Drives Rapid and Reversible Chromatin Condensation in Chondrocytes. *Biophysical Journal* **104**: 759–769.

Janski N, Masoud K, Batzenschlager M, Herzog E, Evrard J-L, Houlne G, Bourge M, Chaboute M-E, Schmit A-C. **2012**. The GCP3-Interacting Proteins GIP1 and GIP2 Are Required for -Tubulin Complex Protein Localization, Spindle Integrity, and Chromosomal Stability. *The Plant Cell* **24**: 1171–1187.

Jensen GS, Fal K, Hamant O, Haswell ES. **2017**. The RNA Polymerase-Associated Factor 1 Complex Is Required for Plant Touch Responses. *Journal of Experimental Botany* **68**: 499–511.

Julkowska MM, Testerink C. **2015**. Tuning plant signaling and growth to survive salt. *Trends in Plant Science* **20**: 586–594.

Keller TS, Mao Z, Spengler DM. **1990**. Young's modulus, bending strength, and tissue physical properties of human compact bone. *Journal of Orthopaedic Research* **8**: 592–603.

Kim D-H, Khatau SB, Feng Y, Walcott S, Sun SX, Longmore GD, Wirtz D. **2012**. Actin cap associated focal adhesions and their distinct role in cellular mechanosensing. *Scientific Reports* **2**: 555.

Kim D, Langmead B, Salzberg SL. **2015**. HISAT: a fast spliced aligner with low memory requirements. *Nature methods* **12**: 357–360.

Komis G, Apostolakos P, Galatis B. **2002**. Hyperosmotic Stress Induces Formation of Tubulin Macrotubules in Root-Tip Cells of Triticum turgidum: Their Probable Involvement in Protoplast Volume Control. *Plant and Cell Physiology* **43**: 911–922.

Kretschmann DE. **2008**. The influence of juvenile wood content on shear parallel, compression, and tension perpendicular to grain strength and mode I fracture toughness of loblolly pine at various ring orientation. **58**: 8.

Kumar MN, Jane W-N, Verslues PE. **2013**. Role of the Putative Osmosensor Arabidopsis *Histidine Kinase1* in Dehydration Avoidance and Low-Water-Potential Response. *Plant Physiology* **161**: 942–953.

Kutschera U, Niklas KJ. **2007**. The epidermal-growth-control theory of stem elongation: An old and a new perspective. *Journal of Plant Physiology* **164**: 1395–1409.

Lamport DTA, Kieliszewski MJ, Chen Y, Cannon MC. **2011**. Role of the Extensin Superfamily in Primary Cell Wall Architecture1. *Plant Physiology* **156**: 11–19.

Lanza RP, Atala A (Eds.). **2014**. *Essentials of stem cell biology*. Amsterdam: Elsevier/Academic Press.

Leblanc-Fournier N, Coutand C, Crouzet J, Brunel N, Lenne C, Moulia B, Julien J-L. **2008**. Jr-ZFP2, encoding a Cys2/His2-type transcription factor, is involved in the early stages of the mechano-perception pathway and specifically expressed in mechanically stimulated tissues in woody plants. *Plant, Cell & Environment* **31**: 715–726.

Lee D, Polisensky DH, Braam J. **2004**. Genome-wide identification of touch- and darkness-regulated Arabidopsis genes: a focus on calmodulin-like and XTH genes. *New Phytologist* **165**: 429–444.

de Leeuw R, Gruenbaum Y, Medalia O. **2018**. Nuclear Lamins: Thin Filaments with Major Functions. *Trends in Cell Biology* **28**: 34–45.

Leshem Y, Seri L, Levine A. **2007**. Induction of phosphatidylinositol 3-kinase-mediated endocytosis by salt stress leads to intracellular production of reactive oxygen species and salt tolerance. *The Plant Journal* **51**: 185–197.

Lévy R, Maaloum M. **2002**. Measuring the spring constant of atomic force microscope cantilevers: thermal fluctuations and other methods. *Nanotechnology* **13**: 33–37.

Li QS, Lee GYH, Ong CN, Lim CT. **2008**. AFM indentation study of breast cancer cells. *Biochemical and Biophysical Research Communications* **374**: 609–613.

Lin T, Neuner A, Flemming D, Liu P, Chinen T, Jäkle U, Arkowitz R, Schiebel E. **2016**. MOZART1 and γ-tubulin complex receptors are both required to turn γ-TuSC into an active microtubule nucleation template. *Journal of Cell Biology* **215**: 823–840.

Lindström H, Harris P, Nakada R. **2002**. Methods for measuring stiffness of young trees. *Holz als Roh- und Werkstoff* **60**: 165–174.

Lintilhac PM, Vesecky TB. **1984**. Stress-induced alignment of division plane in plant tissues grown in vitro. *Nature* **307**: 363–364.

Lionetto F, Del Sole R, Cannoletta D, Vasapollo G, Maffezzoli A. **2012**. Monitoring Wood Degradation during Weathering by Cellulose Crystallinity. *Materials* **5**: 1910–1922.

Liu H, Wen J, Xiao Y, Liu J, Hopyan S, Radisic M, Simmons CA, Sun Y. **2014**. *In Situ* Mechanical Characterization of the Cell Nucleus by Atomic Force Microscopy. *ACS Nano* **8**: 3821–3828.

Long Y, Cheddadi I, Mosca G, Mirabet V, Dumond M, Kiss A, Traas J, Godin C, Boudaoud A. **2020**. Cellular Heterogeneity in Pressure and Growth Emerges from Tissue Topology and Geometry. *Current Biology* **30**: 1504-1516.e8.

Lopez R, Badel E, Peraudeau S, Leblanc-Fournier N, Beaujard F, Julien J-L, Cochard H, Moulia B. **2014**. Tree shoot bending generates hydraulic pressure pulses: a new long-distance signal? *Journal of Experimental Botany* **65**: 1997–2008.

Louveaux M, Julien J-D, Mirabet V, Boudaoud A, Hamant O. **2016**. Cell division plane orientation based on tensile stress in Arabidopsis thaliana. *Proceedings of the National Academy of Sciences of the United States of America* **113**: E4294–E4303.

LOVETT DB, SHEKHAR N, NICKERSON JA, ROUX KJ, LELE TP. **2013**. Modulation of Nuclear Shape by Substrate Rigidity. *Cellular and molecular bioengineering* **6**: 230–238.

Mahaffy RE, Park S, Gerde E, Käs J, Shih CK. **2004**. Quantitative Analysis of the Viscoelastic Properties of Thin Regions of Fibroblasts Using Atomic Force Microscopy. *Biophysical Journal* **86**: 1777–1793.

Maksaev G, Haswell ES. **2012**. MscS-Like10 is a stretch-activated ion channel from Arabidopsis thaliana with a preference for anions. *Proceedings of the National Academy of Sciences of the United States of America* **109**: 19015–19020.

Malivert A, Hamant O, Ingram G. **2018**. The contribution of mechanosensing to epidermal cell fate specification. *Current Opinion in Genetics & Development* **51**: 52–58.

Maniotis AJ, Chen CS, Ingber DE. **1997**. Demonstration of mechanical connections between integrins, cytoskeletal filaments, and nucleoplasm that stabilize nuclear structure. *Proceedings of the National Academy of Sciences* **94**: 849–854.

Mao Y, Baum B. **2015**. Tug of war—The influence of opposing physical forces on epithelial cell morphology. *Developmental Biology* **401**: 92–102.

Marga F, Grandbois M, Cosgrove DJ, Baskin TI. **2005**. Cell wall extension results in the coordinate separation of parallel microfibrils: evidence from scanning electron microscopy and atomic force microscopy. *The Plant Journal* **43**: 181–190.

Martí M, Mulero L, Pardo C, Morera C, Carrió M, Laricchia-Robbio L, Esteban CR, Belmonte JCI. **2013**. Characterization of pluripotent stem cells. *Nature Protocols* **8**: 223–253.

Martinière A, Fiche JB, Smokvarska M, Mari S, Alcon C, Dumont X, Hematy K, Jaillais Y, Nollmann M, Maurel C. **2019**. Osmotic Stress Activates Two Reactive Oxygen Species Pathways with Distinct Effects on Protein Nanodomains and Diffusion. *Plant Physiology* **179**: 1581–1593.

Martino F, Perestrelo AR, Vinarský V, Pagliari S, Forte G. **2018**. Cellular Mechanotransduction: From Tension to Function. *Frontiers in Physiology* **9**.

Masuda K. **1997**. Peripheral Framework of Carrot Cell Nucleus Contains a Novel Protein Predicted to Exhibit a Long a-Helical Domain. *Experimental Cell Research* **232**: 173–181.

Masuda K, Takahashi S, Nomura K, Arimoto M, Inoue M. **1993**. Residual structure and constituent proteins of the peripheral framework of the cell nucleus in somatic embryos from Daucus carota L. *Planta* **191**.

McColloch A, Rabiei M, Rabbani P, Bowling A, Cho M. **2019**. Correlation between Nuclear Morphology and Adipogenic Differentiation: Application of a Combined Experimental and Computational Modeling Approach. *Scientific Reports* **9**.

McQueen-Mason S, Durachko DM, Cosgrove DJ. **1992**. Two endogenous proteins that induce cell wall extension in plants. *The Plant Cell* **4**: 1425–1433.

Mecchia MA, Santos-Fernandez G, Duss NN, Somoza SC, Boisson-Dernier A, Gagliardini V, Martínez-Bernardini A, Fabrice TN, Ringli C, Muschietti JP, *et al.* 2017. RALF4/19 peptides interact with LRX proteins to control pollen tube growth in *Arabidopsis*. *Science* **358**: 1600–1603.

Meier I, Richards EJ, Evans DE. **2017**. Cell Biology of the Plant Nucleus. *Annual Review of Plant Biology* **68**: 139–172.

Miedes E, Suslov D, Vandenbussche F, Kenobi K, Ivakov A, Van Der Straeten D, Lorences EP, Mellerowicz EJ, Verbelen J-P, Vissenberg K. **2013**. Xyloglucan endotransglucosylase/hydrolase (XTH) overexpression affects growth and cell wall mechanics in etiolated Arabidopsis hypocotyls. *Journal of Experimental Botany* **64**: 2481–2497.

Mikulski P, Hohenstatt ML, Farrona S, Smaczniak C, Stahl Y, Kalyanikrishna K, Kaufmann K, Angenent GC, Schubert D. **2019a**. The chromatin-associated protein PWO1 interacts with plant nuclear lamin-like components to regulate nuclear size. *The Plant Cell*: tpc.00663.2018.

Milani P, Gholamirad M, Traas J, Arnéodo A, Boudaoud A, Argoul F, Hamant O. **2011**. In vivo analysis of local wall stiffness at the shoot apical meristem in Arabidopsis using atomic force microscopy. *The Plant Journal* **67**: 1116–1123.

Milloud R, Destaing O, de Mets R, Bourrin-Reynard I, Oddou C, Delon A, Wang I, Albigès-Rizo C, Balland M. **2017**. αvβ3 integrins negatively regulate cellular forces by phosphorylation of its distal NPXY site: αvβ3 integrins and cell forces regulation. *Biology of the Cell* **109**: 127–137.

Mitrossilis D, Fouchard J, Guiroy A, Desprat N, Rodriguez N, Fabry B, Asnacios A. **2009**. Single-cell response to stiffness exhibits muscle-like behavior. *Proceedings of the National Academy of Sciences* **106**: 18243–18248.

Moeendarbary E, Harris AR. **2014**. Cell mechanics: principles, practices, and prospects. *Wiley Interdisciplinary Reviews. Systems Biology and Medicine* **6**: 371–388.

Mouille G, Ralet M-C, Cavelier C, Eland C, Effroy D, Hématy K, McCartney L, Truong HN, Gaudon V, Thibault J-F, *et al.* 2007. Homogalacturonan synthesis in Arabidopsis thaliana requires a Golgi-localized protein with a putative methyltransferase domain. *The Plant Journal* **50**: 605–614.

Moulia B. **2013**. Plant biomechanics and mechanobiology are convergent paths to flourishing interdisciplinary research. *Journal of Experimental Botany* **64**: 4617–4633.

Munevar S, Wang Y, Dembo M. **2001**. Traction force microscopy of migrating normal and H-ras transformed 3T3 fibroblasts. *Biophysical Journal* **80**: 1744–1757.

Nakagawa Y, Katagiri T, Shinozaki K, Qi Z, Tatsumi H, Furuichi T, Kishigami A, Sokabe M, Kojima I, Sato S, *et al.* 2007. Arabidopsis plasma membrane protein crucial for Ca2+ influx and touch sensing in roots. *Proceedings of the National Academy of Sciences of the United States of America* **104**: 3639–3644.

Nakayama N, Smith RS, Mandel T, Robinson S, Kimura S, Boudaoud A, Kuhlemeier C. **2012**. Mechanical Regulation of Auxin-Mediated Growth. *Current Biology* **22**: 1468–1476.

Naumanen P, Lappalainen P, Hotulainen P. **2008**. Mechanisms of actin stress fibre assembly. *Journal of Microscopy* **231**: 446–454.

Nezhad AS, Naghavi M, Packirisamy M, Bhat R, Geitmann A. **2013**. Quantification of the Young's modulus of the primary plant cell wall using Bending-Lab-On-Chip (BLOC). *Lab on a Chip* **13**: 2599.

Nikonorova N, Van den Broeck L, Zhu S, van de Cotte B, Dubois M, Gevaert K, Inzé D, De Smet I. **2018**. Early mannitol-triggered changes in the Arabidopsis leaf (phospho)proteome reveal growth regulators. *Journal of Experimental Botany* **69**: 4591–4607.

Nussenzveig HM. **2018**. Cell membrane biophysics with optical tweezers. *European Biophysics Journal* **47**: 499–514.

Nützmann H-W, Doerr D, Ramírez-Colmenero A, Sotelo-Fonseca JE, Wegel E, Di Stefano M, Wingett SW, Fraser P, Hurst L, Fernandez-Valverde SL, *et al.* 2020. Active and repressed biosynthetic gene clusters have spatially distinct chromosome states. *Proceedings of the National Academy of Sciences* **117**: 13800–13809.

Olins AL, Gould TJ, Boyd L, Sarg B, Olins DE. **2020**. Hyperosmotic stress: in situ chromatin phase separation. *Nucleus* **11**: 1–18.

Oria R, Wiegand T, Escribano J, Elosegui-Artola A, Uriarte JJ, Moreno-Pulido C, Platzman I, Delcanale P, Albertazzi L, Navajas D, *et al.* 2017. Force loading explains spatial sensing of ligands by cells. *Nature* **552**: 219–224.

Orssengo G. **1999**. Determination of the True Intraocular Pressure and Modulus of Elasticity of the Human Cornea in vivo. *Bulletin of Mathematical Biology* **61**: 551–572.

Ounkomol C, Xie H, Dayton PA, Heinrich V. **2009**. Versatile Horizontal Force Probe for Mechanical Tests on Pipette-Held Cells, Particles, and Membrane Capsules. *Biophysical Journal* **96**: 1218–1231.

Palin R, Geitmann A. **2012**. The role of pectin in plant morphogenesis. *Biosystems* **109**: 397–402.

Paluch E, Heisenberg C-P. **2009**. Biology and Physics of Cell Shape Changes in Development. *Current Biology* **19**: R790–R799.

Paredez AR. **2006**. Visualization of Cellulose Synthase Demonstrates Functional Association with Microtubules. *Science* **312**: 1491–1495.

Pareek A, Khurana A, Sharma AK, Kumar R. **2017**. An Overview of Signaling Regulons During Cold Stress Tolerance in Plants. *Current Genomics* **18**: 498–511.

Park YB, Cosgrove DJ. **2012**. Changes in Cell Wall Biomechanical Properties in the Xyloglucan-Deficient *xxt1/xxt2* Mutant of Arabidopsis. *Plant Physiology* **158**: 465–475.

Parre E, Geitmann A. **2005**. Pectin and the role of the physical properties of the cell wall in pollen tube growth of Solanum chacoense. *Planta* **220**: 582–592.

Pear JR, Kawagoe Y, Schreckengost WE, Delmer DP, Stalker DM. **1996**. Higher plants contain homologs of the bacterial celA genes encoding the catalytic subunit of cellulose synthase. *Proceedings of the National Academy of Sciences of the United States of America* **93**: 12637–12642.

Peaucelle A, Wightman R, Höfte H. **2015**. The Control of Growth Symmetry Breaking in the Arabidopsis Hypocotyl. *Current Biology* **25**: 1746–1752.

Pellegrin S, Mellor H. **2007**. Actin stress fibres. *Journal of Cell Science* **120**: 3491–3499.

Pelloux J, Rusterucci C, Mellerowicz E. **2007**. New insights into pectin methylesterase structure and function. *Trends in Plant Science* **12**: 267–277.

Peyronnet R, Tran D, Girault T, Frachisse J-M. **2014**. Mechanosensitive channels: feeling tension in a world under pressure. *Frontiers in Plant Science* **5**.

Pierik R, Testerink C. **2014**. The Art of Being Flexible: How to Escape from Shade, Salt, and Drought. *Plant Physiology* **166**: 5–22.

Poropatich K, Yang JC, Goyal R, Parini V, Yang XJ. **2016**. Nuclear size measurement for distinguishing urothelial carcinomas from reactive urothelium on tissue sections. *Diagnostic Pathology* **11**: 57.

Proseus TE, Boyer JS. **2007**. Tension required for pectate chemistry to control growth in Chara corallina. *Journal of Experimental Botany* **58**: 4283–4292.

Reiser V, Raitt DC, Saito H. **2003**. Yeast osmosensor Sln1 and plant cytokinin receptor Cre1 respond to changes in turgor pressure. *Journal of Cell Biology* **161**: 1035–1040.

Ricci D, Tedesco M, Grattarola M. **1997**. Mechanical and morphological properties of living 3T6 cells probed via scanning force microscopy. *Microscopy Research and Technique* **36**: 165–171.

Robertson DJ, Julias M, Gardunia BW, Barten T, Cook DD. **2015**. Corn Stalk Lodging: A Forensic Engineering Approach Provides Insights into Failure Patterns and Mechanisms. *Crop Science* **55**: 2833–2841.

Robertson D, Smith S, Gardunia B, Cook D. **2014**. An Improved Method for Accurate Phenotyping of Corn Stalk Strength. *Crop Science* **54**: 2038–2044.

Robinson S, Burian A, Couturier E, Landrein B, Louveaux M, Neumann ED, Peaucelle A, Weber A, Nakayama N. **2013**. Mechanical control of morphogenesis at the shoot apex. *Journal of Experimental Botany* **64**: 4729–4744.

Robinson S, Kuhlemeier C. **2018**. Global Compression Reorients Cortical Microtubules in Arabidopsis Hypocotyl Epidermis and Promotes Growth. *Current Biology* **28**: 1794-1802.e2.

Rongpipi S, Ye D, Gomez ED, Gomez EW. **2019**. Progress and Opportunities in the Characterization of Cellulose – An Important Regulator of Cell Wall Growth and Mechanics. *Frontiers in Plant Science* **9**.

Roppolo D, Geldner N. **2012**. Membrane and walls: who is master, who is servant? *Current Opinion in Plant Biology* **15**: 608–617.

Roudier F, Ahmed I, Bérard C, Sarazin A, Mary-Huard T, Cortijo S, Bouyer D, Caillieux E, Duvernois-Berthet E, Al-Shikhley L, *et al.* 2011. Integrative epigenomic mapping defines four main chromatin states in Arabidopsis. *The EMBO Journal* **30**: 1928–1938.

Routier-Kierzkowska A-L, Weber A, Kochova P, Felekis D, Nelson BJ, Kuhlemeier C, Smith RS. **2012**. Cellular Force Microscopy for in Vivo Measurements of Plant Tissue Mechanics1[W][OA]. *Plant Physiology* **158**: 1514–1522.

Roychoudhury A. **2019**. Osmolytes and their Role in Abiotic Stress Tolerance in Plants. : 15.

Sakamoto Y, Takagi S. **2013**. LITTLE NUCLEI 1 and 4 Regulate Nuclear Morphology in Arabidopsis thaliana. *Plant and Cell Physiology* **54**: 622–633.

Sampathkumar A, Krupinski P, Wightman R, Milani P, Berquand A, Boudaoud A, Hamant O, Jönsson H, Meyerowitz EM. **2014**. Subcellular and supracellular mechanical stress prescribes cytoskeleton behavior in Arabidopsis cotyledon pavement cells. *eLife* **3**.

Sampathkumar A, Peaucelle A, Fujita M, Schuster C, Persson S, Wasteneys GO, Meyerowitz EM. **2019**. Primary wall cellulose synthase regulates shoot apical meristem mechanics and growth. *Development* **146**: dev179036.

Savin T, Kurpios NA, Shyer AE, Florescu P, Liang H, Mahadevan L, Tabin CJ. **2011**. On the growth and form of the gut. *Nature* **476**: 57–62.

Saxe F, Weichold S, Reinecke A, Lisec J, Döring A, Neumetzler L, Burgert I, Eder M. **2016**. Age Effects on Hypocotyl Mechanics (S Amancio, Ed.). *PLOS ONE* **11**: e0167808.

Scheller HV, Ulvskov P. **2010**. Hemicelluloses. *Annual Review of Plant Biology* **61**: 263–289.

Schillers H, Rianna C, Schäpe J, Luque T, Doschke H, Wälte M, Uriarte JJ, Campillo N, Michanetzis GPA, Bobrowska J, *et al.* 2017. Standardized Nanomechanical Atomic Force Microscopy Procedure (SNAP) for Measuring Soft and Biological Samples. *Scientific Reports* **7**: 5117.

Schopfer P. **2006**. Biomechanics of plant growth. *American Journal of Botany* **93**: 1415–1425.

Seki M, Narusaka M, Ishida J, Nanjo T, Fujita M, Oono Y, Kamiya A, Nakajima M, Enju A, Sakurai T, *et al.* 2002. Monitoring the expression profiles of 7000 Arabidopsis genes under drought, cold and high-salinity stresses using a full-length cDNA microarray. *The Plant Journal* **31**: 279–292.

Sewelam N, Oshima Y, Mitsuda N, Ohme-Takagi M. **2014**. A step towards understanding plant responses to multiple environmental stresses: a genome-wide study. *Plant, Cell & Environment* **37**: 2024–2035.

Sharir A, Barak MM, Shahar R. **2008**. Whole bone mechanics and mechanical testing. *The Veterinary Journal* **177**: 8–17.

Sharma A, Shahzad B, Kumar V, Kohli SK, Sidhu GPS, Bali AS, Handa N, Kapoor D, Bhardwaj R, Zheng B. **2019**. Phytohormones Regulate Accumulation of Osmolytes Under Abiotic Stress. *Biomolecules* **9**.

Sherman VR, Yang W, Meyers MA. **2015**. The materials science of collagen. *Journal of the Mechanical Behavior of Biomedical Materials* **52**: 22–50.

Shih H-W, Miller ND, Dai C, Spalding EP, Monshausen GB. **2014**. The Receptor-like Kinase FERONIA Is Required for Mechanical Signal Transduction in Arabidopsis Seedlings. *Current Biology* **24**: 1887–1892

Shiu J-Y, Aires L, Lin Z, Vogel V. **2018**. Nanopillar force measurements reveal actin-cap-mediated YAP mechanotransduction. *Nature Cell Biology* **20**: 262–271.

Shoji T, Suzuki K, Abe T, Kaneko Y, Shi H, Zhu J-K, Rus A, Hasegawa PM, Hashimoto T. **2006**. Salt Stress Affects Cortical Microtubule Organization and Helical Growth in Arabidopsis. *Plant and Cell Physiology* **47**: 1158–1168.

Simon A, Cohen-Bouhacina T, Porté MC, Aimé JP, Amédée J, Bareille R, Baquey C. **2003**. Characterization of dynamic cellular adhesion of osteoblasts using atomic force microscopy. *Cytometry Part A* **54A**: 36–47.

Smith L, Cho S, Discher DE. **2017**. Mechanosensing of matrix by stem cells: From matrix heterogeneity, contractility, and the nucleus in pore-migration to cardiogenesis and muscle stem cells in vivo. *Seminars in Cell & Developmental Biology* **71**: 84–98.

Somerville C. **2006**. Cellulose Synthesis in Higher Plants. *Annual Review of Cell and Developmental Biology* **22**: 53–78.

Stephens AD, Liu PZ, Banigan EJ, Almassalha LM, Backman V, Adam SA, Goldman RD, Marko JF. **2018**. Chromatin histone modifications and rigidity affect nuclear morphology independent of lamins. *Molecular Biology of the Cell* **29**: 220–233.

Strohmeyer N, Bharadwaj M, Costell M, Fässler R, Müller DJ. **2017**. Fibronectin-bound α5β1 integrins sense load and signal to reinforce adhesion in less than a second. *Nature Materials* **16**: 1262–1270.

Stuurman N, Heins S, Aebi U. **1998**.Nuclear Lamins: Their Structure, Assembly, and Interactions. : 25.

Swift J, Ivanovska IL, Buxboim A, Harada T, Dingal PCDP, Pinter J, Pajerowski JD, Spinler KR, Shin J-W, Tewari M, *et al.* 2013. Nuclear Lamin-A Scales with Tissue Stiffness and Enhances Matrix-Directed Differentiation. *Science (New York, N.Y.)* **341**: 1240104.

Tajik A, Zhang Y, Wei F, Sun J, Jia Q, Zhou W, Singh R, Khanna N, Belmont AS, Wang N. **2016**. Transcription upregulation via force-induced direct stretching of chromatin. *Nature Materials* **15**: 1287–1296.

Takai E, Costa KD, Shaheen A, Hung CT, Guo XE. **2005**. Osteoblast elastic modulus measured by atomic force microscopy is substrate dependent. *Annals of Biomedical Engineering* **33**: 963–971.

Takeda S, Tadele Z, Hofmann I, Probst AV, Angelis KJ, Kaya H, Araki T, Mengiste T, Scheid OM, Shibahara K, *et al.* 2004. BRU1, a novel link between responses to DNA damage and epigenetic gene silencing in Arabidopsis. *Genes & Development* **18**: 782–793.

Tamura K, Goto C, Hara-Nishimura I. **2015**. Recent advances in understanding plant nuclear envelope proteins involved in nuclear morphology. *Journal of Experimental Botany* **66**: 1641–1647.

Taylor NG. **2008**. Cellulose biosynthesis and deposition in higher plants. *New Phytologist* **178**: 239–252.

Teo S-S, Ho C-L, Teoh S, Rahim RA, Phang S-M. **2009**. Transcriptomic Analysis of Gracilaria Changii (rhodophyta) in Response to Hyper- and Hypoosmotic Stresses1. *Journal of Phycology* **45**: 1093–1099.

Thompson DW. **1917**. On Growth and Form. *Cambridge, UK: Cambridge University Press*.

Titushkin I, Cho M. **2007**. Modulation of Cellular Mechanics during Osteogenic Differentiation of Human Mesenchymal Stem Cells. *Biophysical Journal* **93**: 3693–3702.

Tran D, Galletti R, Neumann ED, Dubois A, Sharif-Naeini R, Geitmann A, Frachisse J-M, Hamant O, Ingram GC. **2017**. A mechanosensitive Ca2+ channel activity is dependent on the developmental regulator DEK1. *Nature Communications* **8**.

Tytgat TOG, Verhoeven KJF, Jansen JJ, Raaijmakers CE, Bakx-Schotman T, McIntyre LM, van der Putten WH, Biere A, van Dam NM. **2013**. Plants Know Where It Hurts: Root and Shoot Jasmonic Acid Induction Elicit Differential Responses in Brassica oleracea (G Bonaventure, Ed.). *PLoS ONE* **8**: e65502.

Urano K, Maruyama K, Jikumaru Y, Kamiya Y, Yamaguchi-Shinozaki K, Shinozaki K. **2016**. Analysis of plant hormone profiles in response to moderate dehydration stress. *The Plant Journal*: 20.

Uyttewaal M, Burian A, Alim K, Landrein B, Borowska-Wykręt D, Dedieu A, Peaucelle A, Ludynia M, Traas J, Boudaoud A, *et al.* 2012. Mechanical Stress Acts via Katanin to Amplify Differences in Growth Rate between Adjacent Cells in Arabidopsis. *Cell* **149**: 439–451.

Varanasi P, Katsnelson J, Larson DM, Sharma R, Sharma MK, Vega-Sánchez ME, Zemla M, Loque D, Ronald PC, Simmons BA, *et al.* 2012. Mechanical Stress Analysis as a Method to Understand the Impact of Genetically Engineered Rice and Arabidopsis Plants. *Industrial Biotechnology* **8**: 238–244.

Verger S, Long Y, Boudaoud A, Hamant O. **2018**.A tension-adhesion feedback loop in plant epidermis. *eLife* **7**.

Verslues PE, Juenger TE. **2011**. Drought, metabolites, and Arabidopsis natural variation: a promising combination for understanding adaptation to water-limited environments. *Current Opinion in Plant Biology* **14**: 240–245.

Wang Z, Casas-Mollano JA, Xu J, Riethoven J-JM, Zhang C, Cerutti H. **2015**. Osmotic stress induces phosphorylation of histone H3 at threonine 3 in pericentromeric regions of *Arabidopsis thaliana*. *Proceedings of the National Academy of Sciences* **112**: 8487–8492.

Wang H, Dittmer TA, Richards EJ. **2013**. Arabidopsis CROWDED NUCLEI (CRWN) proteins are required for nuclear size control and heterochromatin organization. *BMC Plant Biology* **13**: 200.

Wang C, Li J, Yuan M. **2007**. Salt Tolerance Requires Cortical Microtubule Reorganization in Arabidopsis. *Plant and Cell Physiology* **48**: 1534–1547.

Wang N, Tolić-Nørrelykke IM, Chen J, Mijailovich SM, Butler JP, Fredberg JJ, Stamenović D. **2002**. Cell prestress. I. Stiffness and prestress are closely associated in adherent contractile cells. *American Journal of Physiology-Cell Physiology* **282**: C606–C616.

Wang T, Zabotina O, Hong M. **2012**. Pectin–Cellulose Interactions in the *Arabidopsis* Primary Cell Wall from Two-Dimensional Magic-Angle-Spinning Solid-State Nuclear Magnetic Resonance. *Biochemistry* **51**: 9846–9856.

Webster KD, Crow A, Fletcher DA. **2011**. An AFM-Based Stiffness Clamp for Dynamic Control of Rigidity (I Sokolov, Ed.). *PLoS ONE* **6**: e17807.

Wenger MPE, Bozec L, Horton MA, Mesquida P. **2007**. Mechanical Properties of Collagen Fibrils. *Biophysical Journal* **93**: 1255–1263.

Whaley WG, Mericle LW, Heimsch C. **1952**. THE WALL OF THE MERISTEMATIC CELL. *American Journal of Botany* **39**: 20–26.

White PB, Wang T, Park YB, Cosgrove DJ, Hong M. **2014**. Water–Polysaccharide Interactions in the Primary Cell Wall of *Arabidopsis thaliana* from Polarization Transfer Solid-State NMR. *Journal of the American Chemical Society* **136**: 10399–10409.

Wisniewska J. **2006**. Polar PIN Localization Directs Auxin Flow in Plants. *Science* **312**: 883–883.

Wohlbach DJ, Quirino BF, Sussman MR. **2008**. Analysis of the *Arabidopsis* Histidine Kinase ATHK1 Reveals a Connection between Vegetative Osmotic Stress Sensing and Seed Maturation. *The Plant Cell* **20**: 1101–1117.

Wolf S, Mouille G, Pelloux J. **2009**. Homogalacturonan Methyl-Esterification and Plant Development. *Molecular Plant* **2**: 851–860.

Wolf S, Mravec J, Greiner S, Mouille G, Höfte H. **2012**. Plant Cell Wall Homeostasis Is Mediated by Brassinosteroid Feedback Signaling. *Current Biology* **22**: 1732–1737.

Wu P-H, Aroush DR-B, Asnacios A, Chen W-C, Dokukin ME, Doss BL, Durand-Smet P, Ekpenyong A, Guck J, Guz NV, *et al.* 2018. A comparison of methods to assess cell mechanical properties. *Nature Methods* **15**: 491–498.

Wymer CL, Wymer SA, Cosgrove DJ, Cyr RJ. **1996**. Plant cell growth responds to external forces and the response requires intact microtubules. *Plant Physiology* **110**: 425–430.

Xiong L, Schumaker KS, Zhu J-K. **2002**. Cell Signaling during Cold, Drought, and Salt Stress. *The Plant Cell* **14**: S165–S183.

Yamaguchi-Shinozaki K, Shinozaki K. **2006**. TRANSCRIPTIONAL REGULATORY NETWORKS IN CELLULAR RESPONSES AND TOLERANCE TO DEHYDRATION AND COLD STRESSES. *Annual Review of Plant Biology* **57**: 781–803.

Yang J, An B, Luo H, He C, Wang Q. **2019**. AtKATANIN1 Modulates Microtubule Depolymerization and Reorganization in Response to Salt Stress in Arabidopsis. *International Journal of Molecular Sciences* **21**.

Yang J, Chang Y, Qin Y, Chen D, Zhu T, Peng K, Wang H, Tang N, Li X, Wang Y, *et al.* 2020. A lamin-like protein OsNMCP1 regulates drought resistance and root growth through chromatin accessibility modulation by interacting with a chromatin remodeller OsSWI3C in rice. *New Phytologist* **227**: 65–83.

Yang W, Sherman VR, Gludovatz B, Schaible E, Stewart P, Ritchie RO, Meyers MA. **2015**. On the tear resistance of skin. *Nature Communications* **6**: 6649.

Yoneda A, Ohtani M, Katagiri D, Hosokawa Y, Demura T. **2020**. Hechtian Strands Transmit Cell Wall Integrity Signals in Plant Cells. *Plants* **9**: 604.

Yuan F, Yang H, Xue Y, Kong D, Ye R, Li C, Zhang J, Theprungsirikul L, Shrift T, Krichilsky B, *et al.* 2014. OSCA1 mediates osmotic-stress-evoked Ca2+ increases vital for osmosensing in Arabidopsis. *Nature* **514**: 367–371.

Zhang H, Liu K-K. **2008**. Optical tweezers for single cells. *Journal of the Royal Society Interface* **5**: 671–690.

Zhang T, Zheng Y, Cosgrove DJ. **2016**. Spatial organization of cellulose microfibrils and matrix polysaccharides in primary plant cell walls as imaged by multichannel atomic force microscopy. *The Plant Journal* **85**: 179–192.

Zhou X, Groves NR, Meier I. **2015**. Plant nuclear shape is independently determined by the SUN-WIP-WIT2-myosin XI-i complex and CRWN1. *Nucleus* **6**: 144–153.

Résumé étendu

La caractérisation biochimique et moléculaire des processus biologiques a été un axe majeur d'étude en biologie dans la seconde moitié du XXe siècle. Les scientifiques ont identifié et caractérisé d'innombrables acteurs moléculaires et des hypothèses fortes concernant les mécanismes associés ont été avancées. Pourtant, les organismes biologiques sont aussi des objets physiques. Ainsi, les voies identifiées doivent être intégrées dans un cadre plus physique aussi, et à toutes les échelles. En effet, les propriétés mécaniques du matériel vivant peuvent contribuer à un contrôle global de ces voies moléculaires et nous aider à comprendre comment ces voies se coordonnent pour générer des réponses physiologiques de la division cellulaire à la différenciation au cours du développement. Bien que l'explication physique des systèmes biologiques était déjà dynamique au 19ème siècle (voir par exemple Sachs, Hofmeister, D'Arcy Thompson), le domaine a pris de l'ampleur au cours des dernières décennies avec les améliorations technologiques de l'imagerie en direct, de la micromécanique et de la modélisation informatique permettant l'étude des propriétés physiques des systèmes biologiques.

Lorsqu'une structure supporte une contrainte de traction préexistante avant qu'une charge externe ne soit appliquée, l'état initial de la structure est appelé « préconstraint ». Lors de l'étude des propriétés mécaniques de l'organisme, une présence de condition précontrainte est observée comme dans les artères (Fung & Liu, 1989), le cerveau humain (Budday et al., 2014), les vaisseaux sanguins (Fung, 1991), l'embryon en développement (Beloussov & Grabovsky, 2006). Cette mécanique « stressée » contribue à la forme et aux propriétés mécaniques de l'organisme. Ces organes sont formés par une organisation complexe des tissus. Les tissus ont une large gamme de propriétés élastiques avec le cerveau comme exemple de tissu mou avec un module de Young inférieur à 1 kPa (Georges et al., 2006) tandis que les os sont les plus rigides chez les vertébrés avec une rigidité de l'ordre du GPa (Keller et al., 2006) al., 1990). Notez que la rigidité mesurée du tissu n'est pas la somme des éléments individuels, mais qu'elle dépend plutôt de la structure et de la topologie du tissu. Dans tout tissu, l'unité fonctionnelle est la cellule. Cela implique une coordination locale et globale. En fin de compte, la mécanique des cellules devient une pièce importante du puzzle pour comprendre la mécanique derrière un organisme.

L'état de précontrainte est partagé dans tous les règnes. Les plantes sont des organismes à parois, et ce qui peut être unique dans leur mécanique est la grande rigidité de leurs parois, qui leur permet également d'accumuler une pression de turgescence élevée, de l'ordre du MPa. Parce que toutes les cellules sont collées les unes aux autres, ce qui est vrai à l'échelle des cellules

individuelles, peut être vrai aussi à l'échelle de l'organe, présentant une auto- similitude, au moins dans une certaine mesure. En dehors des contraintes internes, les plantes sont régulièrement soumises à des contraintes mécaniques externes notamment la gravité et le vent. C'est peut-être l'un des avantages évolutifs des structures précontraintes : elles sont robustes aux fluctuations environnementales. L'unité de l'architecture végétale est la cellule végétale rigide enfermée dans une paroi cellulaire qui est comparable à la matrice extracellulaire dictant l'adhésion et l'interaction des cellules avec d'autres cellules ainsi qu'avec des facteurs biotiques/abiotiques. Cette mécanique cellulaire est la clé pour comprendre la modulation de la taille et de la forme des cellules, la production de la paroi cellulaire, l'interaction cellule-cellule pour fournir un support mécanique à une architecture stable et favoriser la croissance.

Ainsi, les acteurs clés de la mécanique chez les plantes sont la pression de turgescence et la paroi cellulaire rigide. Les plantes sont également capables de détecter les forces mécaniques. Par exemple, chez les plantes d'Arabidopsis, si elles sont touchées et brossées régulièrement (10 passages par jour), elles deviennent plus courtes, dans un processus appelé thigmomorphogenèse (Jensen et al., 2017). Fondamentalement, les cellules végétales traduisent une déformation élastique (par le toucher ou le vent) en une réponse plastique (parois plus rigides et croissance réduite ; (Braam, 2004). Un large éventail d'activités cellulaires sont sensibles aux signaux mécaniques et influencent la morphologie et croissance cellulaire (polarité, division) et la différenciation cellulaires ou la décision du destin cellulaire. Lorsque ces signaux pénètrent dans la cellule, ils doivent atteindre le noyau pour produire les réponses. Or, au-delà de sa nature biochimique, le noyau est aussi un objet physique. Il existe de plus en plus de preuves que sa mécanique joue un rôle clé dans l'expression des gènes, l'organisation du cytosquelette, et plus généralement dans la biologie cellulaire et du développement. Le noyau a des caractéristiques mécaniques spécifiques. Lorsqu'il est sondé par la diffusion de nanoparticules internalisées, la structure nucléaire révèle des micro-domaines transitoires de 300 nm de faibles modules d'élasticité (~20 Pa) et viscosités (~50 Pa.s) (Tseng et al., 2004). Le noyau se déforme sous contrainte constante imposée (expérience de fluage), il présente un comportement en loi de faible puissance libre à l'échelle du temps, avec un module viscoélastique allant de 1 à 10 kPa, et un exposant α ~ 0,2-0,3 (Dahl et al., 2005). Ceci correspond à un comportement mécanique dominé par l'élasticité, avec, à une échelle de temps typique de la seconde, un module élastique apparent d'environ 5 kPa, et une viscosité apparente de ~300 Pa.s. Les propriétés mécaniques des principaux éléments mécaniquement pertinents du noyau (enveloppe nucléaire, lamines et chromatine) modulent la mécano-détection

nucléaire, conduisant au concept de rhéostat nucléaire. L'hétérochromatine est enrichie à la périphérie nucléaire, qui est un environnement transcriptionnel plutôt silencieux (Fransz et al., 2002 ; Fransz & de Jong, 2011 ; Bi et al., 2017), tandis que l'euchromatine est organisée en domaines actifs topologiquement associés, qui définissent des unités régulatrices à l'intérieur des territoires chromosomiques. Alors que des domaines actifs sont trouvés dans le riz et le coton, des « régions de type frontière » ont été principalement trouvées chez Arabidopsis permettant la séparation des régions transcriptionnellement actives des régions inactives (Wang et al., 2015b; Liu et al., 2017; Szabo et al., 2019). La lamina est un maillage rigide du nucléosquelette comprenant les lamines A/C et B. Alors que les lamines A/C et B interagissent avec l'hétérochromatine à la périphérie nucléaire (Gruenbaum & Foisner, 2015), seule la lamine A/C interagit avec l'euchromatine via le polypeptide associé à la lamine. 2α permettant une régulation plus directe de l'expression des gènes (Gesson et al., 2016). Chez les plantes, alors que l'architecture de l'enveloppe nucléaire est principalement conservée (Fal et al., 2017), il n'existe pas de véritables lamines. Pourtant, des homologues fonctionnels spécifiques sont présents (Ciska & Moreno Diaz de la Espina, 2014). Cela inclut les protéines de domaine enroulé CRWN/NMPC trouvées initialement dans la carotte en tant que NMPC (Masuda et al., 1997) et identifiées en outre chez Arabidopsis en tant que CRWN1-4 (Dittmer et al., 2007; Wang et al., 2013). À l'aide d'expériences FRET, il a été démontré que CRWN1 interagit avec le domaine N-terminal du nucléoplasme de SUN1 (Graumann, 2014). Il a été démontré que d'autres protéines interagissent physiquement avec SUN1 en utilisant ue approche double hybride en levure, comme KAKU4 de type lamine spécifique à la plante (Goto et al., 2014) ou la protéine associée à l'hétérochromatine facultative PWO1 (Mikulski et al., 2019). Chez Arabidopsis, alors que CRWN1 et KAKU4 peuvent maintenir la morphologie nucléaire grâce à leur interaction avec le NE, ils peuvent déformer le NE indépendamment (Goto et al., 2014). Fait intéressant, les interactions génétiques entre les mutants simples et doubles révèlent que PWO1 et CRWN1 contrôlent la taille et la forme nucléaires dans la même voie génétique (Mikulski et al., 2019). Cependant, la relation de la déformation nucléaire en réponse au stress mécanique n'a pas encore été étudiée chez les plantes. L'envelope nucléaire a ses propres propriétés mécaniques, l'élasticité, la viscosité et la plasticité de la NE qui sont assurées et modulées par plusieurs protéines clés (2005). Elle se compose de deux membranes bicouches lipidiques, à savoir les membranes nucléaires externe (ONM) et interne (INM), qui sont séparées par un espace périnucléaire ~35-50 nm. Ces membranes fusionnent sur les sites du complexe de pores nucléaires (NPC) donnant lieu à une topologie ultra-donut (Torbati et al., 2016). L'écart géométrique entre les membranes nucléaires est principalement maintenu via les

protéines SUN1 et SUN2 (Crisp et al., 2006). Les protéines SUN1 et SUN2 sont situées au niveau de l'INM et interagissent, via leur domaine SUN C-terminal (domaine d'homologie Sad1/UNC-84), avec le domaine KASH (homologie Klarsicht/ANC-1/SYNE) des protéines de la famille KASH situées à l'ONM. Ces complexes SUN-KASH, également connus sous le nom de complexes LINC (LINker of Nucleoskeleton and Cytoskeleton) se retrouvent chez tous les eucaryotes (Crisp et al., 2006 ; Graumann et al., 2010; Murphy et al., 2010; Zhou et al., 2012, 2014). Dans le cas des vertébrés, SUN1 est également connecté aux lamines A/C (Haque et al., 2006). Des signaux mécaniques peuvent atteindre l'enveloppe nucléaire pour modifier l'architecture du génome et induire des gènes spécifiques. La taille, la forme et la mécanique du noyau peuvent varier en fonction de la forme et de la fonction de la cellule. Typiquement, le noyau est le plus gros organite (avec un diamètre de ∼5 à 20 μm) et aussi le plus rigide à l'intérieur d'une cellule (Dahl et al., 2008). Considérant un tel élément structurel à l'intérieur de la cellule, il n'est donc pas surprenant de trouver des relations entre les propriétés mécaniques du noyau et ses fonctions.

Nous montrons l'importance de la mécanique nucléaire dans les racines exposées aux contraintes osmotiques. Les cellules végétales sont capables de réguler activement la pression osmotique en synthétisant des osmolytes ou cette pression osmotique est régulée par des changements de concentration de soluté extracellulaire. Ce changement de pression osmotique est observé en réponse au sel, à la sécheresse, au gel ou au stress thermique (Conde et al., 2011). Il crée une force sur la membrane est a donc une composante mécanique impliquant des éléments mécanosensibles. Ainsi nous avons pu mesurer la rigidité du noyau par microscopie à force atomique et micro-rhéométrie, dans des plantes contrôles et stressées par un stress osmotique (mannitol 0, 3M). Nous avons constaté qu'un stress hyperosmotique de mannitol 0,3 M sur les noyaux de la pointe des racines des plantes induisait une diminution du volume et de la sphéricité des noyaux mais une augmentation de la rigidité nucléaire. Le stress hypo-osmotique induit par l'eau n'a pas entraîné de changement significatif dans la taille ou la morphologie du noyau dans le contexte du tissu méristématique de la racine, mais a eu un effet sur les noyaux isolés conduisant à une augmentation de la taille du noyau et à une réduction très probable de la rigidité du noyau. De telles réponses étaient transitoires et induites au-dessus d'un seuil de stress osmotique, suggérant que le noyau de la plante peut agir comme un rhéostat mécanique. L'hétérochromatine se condensait avec un stress hyper-osmotique et se décondensait avec une perte de chromocentres avec un stress hypo-osmotique, dans les cellules

du méristème racinaire d'Arabidopsis. Ainsi, la chromatine agirait comme un gel dont la structure peut changer au sein du noyau.

Les tissus végétaux sont généralement beaucoup plus rigides que ceux des animaux, car les cellules végétales sont fortement pressurisées avec une pression de turgescence de l'ordre du MPa et entourées d'une paroi cellulaire rigide. Pourtant, les cellules végétales subissent encore des conflits mécaniques contribuant à déterminer leur forme et la croissance des tissus. Les réseaux de microtubules corticaux jouent un rôle majeur dans l'orientation du complexe de cellulose synthase (CSC) pour réguler la paroi cellulaire et ses propriétés physiques. Les microtubules corticaux s'alignent avec la direction de la contrainte de traction maximale dans la paroi cellulaire, renforçant ainsi la paroi cellulaire pour résister à la contrainte de traction (Hamant et al., 2008). Les complexes de nucléation des MTs sont présents à l'enveloppe nuclaire, et les protéines GIP homologues de MZT1sont des régulateurs de ces complexes (Janski et al., 2012). Il est intéressant de noter que les γ tubulines, se trouvent dans différents complexes : les complexes de nucléation des MTs mais aussi en complexe avec les protéines SUN1 à l'INM. De manière intéressante les GIPs forment un complexe avec la chromatine centromérique via CENH3 en périphérie de l'INM (Batzenschlager et al., 2015 ; Chumová et al., 2019). L'enveloppe nucléaire est une barrière à l'interface nucléo-cytoplasmique d'une cellule eucaryote. Elle possède également ses propres propriétés mécaniques, notamment grâce à son nucléosquelette au niveau du cortex du noyau et grâce à la chromatine à l'intérieur du noyau. Par conséquent, le hub de γ tubuline/GIP pourrait avoir un rôle spécifique dans la mécano-transduction nucléaire chez les plantes. Fait intéressant, dans le méristème racinaire, les noyaux des mutants *gip1gip2* ont un phénotype de déformation nucléaire proche de celui observé en réponse au stress hyperosmotique. Cela suggère en outre que non seulement les protéines de l'enveloppe nucléaire jouent un rôle important dans les signaux mécaniques dérivés de la croissance, mais qu'elles peuvent également être impliquées dans la réponse de la plante à son environnement mécanique. De manière intéressante, nous avons également constaté que les mutants *gip1gip2* sont plus résistants aux conditions osmotiques extrêmes. Cela suggère que l'absence de GIP peut en fait sensibiliser la plante vers des conditions hyper-osmotiques. Sous le stress hyperosmotique, le noyau d'Arabidopsis se déforme et se rigidifie de manière transitoire. En présence de quantités réduites des protéines GIP, les noyaux sont déformés constitutivement et sont plus rigides.

L'enveloppe nucléaire semble être importante pour réguler les réponses au stress, en particulier les nucléoporines et les protéines du nucléosquelette (Groves et al., 2018). Chez le

riz (Oryza sativa), le gène codant pour la protéine de type lamine nucléaire OsNMCP1 est induit par la sécheresse par le biais d'un stress hyperosmotique et confère une résistance. OsNMCP1 module l'accessibilité de la chromatine en interagissant physiquement avec OsSWI3C qui est une protéine du complexe de remodelage de la chromatine (CRC) dépendant de l'ATP (SWITCH/SUCROSE NON FERMENTING). Il aide à éliminer l'effet négatif d'OsSWI3C sur l'expression des gènes et à garantir une gamme d'expression de gènes sensibles à la sécheresse, notamment OsNAC10, OsERF48, OsSGL, SNAC1 et OsbZIP23 (Yang et al., 2020). D'une certaine manière, cette régulation pourrait être différente pour les protéines CRWN homologues du NMCP chez Arabidopsis, car CRWN1 s'est avérée réguler négativement l'expression des gènes de stress, en maintenant l'état répressif en interagissant avec le facteur PWO1 associé au polycomb (Mikulski et al., 2019). Les GIP sont également des régulateurs négatifs des gènes sensibles au toucher dans la réponse au stress hyperosmotique.

Les noyaux animaux possèdent une lamina filamenteuse attachée à l'enveloppe qui assure la stabilité mécanique et qui peut également constituer un hub de signalisation. Dans les plantes, les protéines NMCP/CRWN sont considérées comme des homologues fonctionnels des lamines et sont proposées pour fournir un support structurel aux noyaux. Les protéines CRWN1 et CRWN4 sont situées au niveau du cortex nucléaire et maintiennent l'intégrité nucléaire et l'architecture chromosomique dans les tissus différenciés. Le rôle de ces protéines dans le cycle cellulaire est inconnu, et si CRWN1 et CRWN4 présentent des fonctions différentes n'est pas documenté. Ici, nous montrons que la surface nucléaire est augmentée dans le mutant *crwn1* alors qu'elle est légèrement diminuée dans *crwn4* dans les cellules de la pointe racinaire. Nous montrons également que le stress osmotique peut induire une diminution de la taille et de la circularité nucléaire des noyaux chez les deux mutants, comme observé pour le WT rapporté dans nos données précédentes. Fait intéressant, la diminution relative de la taille des noyaux des plantes témoins par rapport aux plantes traitées est deux fois plus importante dans *crwn1* que le WT. Cette découverte suggère un rôle principal de CRWN1 dans le maintien de la taille nucléaire dans les cellules cyclantes mais aussi comme un stabilisateur en réponse au stress hyperosmotique puisque son absence conduit à un noyau plus déformé. De par son association à la chromatine, on ne peut pas exclure un effet conjugué de la chromatine à la morphodynamique des noyaux (Goswami et al., 2020).

Tout stress génère une signalisation conduisant à une expression génique particulière. La force peut modifier l'expression des gènes via la modulation de l'organisation des territoires

chromosomiques (Tajik et al., 2016). Les changements dans les caractéristiques nucléaires affectent énormément l'expression des gènes de stress (Goswami et al., 2020). Le stress hyperosmotique induit divers gènes sensibles au stress (Seki et al., 2002 ; Sewelam et al., 2014 ; Jensen et al., 2017 ; Ghorbani et al., 2019). En cas de déshydratation induite par le stress hyperosmotique, des gènes mécaniquement importants sont régulés à la hausse (25 % de gènes induits par la déshydratation le sont aussi en réponse au toucher) dont ceux codant pour la 33 xyloglucane endotransglucosylase/hydrolase (XTH), 10 protéines de type calmoduline (CML) (Urano et al. , 2016). Un fort couplage entre le stress osmotique et mécanique est évident. Nous avons observé que 18 gènes sélectionnés parmi les gènes induits par le toucher et le son (Lee et al., 2004 ; Ghosh et al., 2016), sont régulés positivement par un stress hyperosmotique de 0,3M : c'est-à-dire *TCH2, TCH3, TCH4*, facteur de transcription de la famille *WRKY (WRKY18) , WRKY33, WRKY40*, doigt de zinc de tolérance au sel (SALT TOLERANCE), protéine kinase dépendante du calcium (CPK28), *CPK32*, protéine de la famille EF fixant le calcium (CA), famille des ATPases de type AAA (AAA), SZF1, fonction inconnue (A2), *DREB26, Myb44, CYP81D8, NHL3, HSPRO2* (Goswami et al., 2020). Ces gènes sont induits en réponse au stress hyperosmotique (mannitol), et certains sont aussi associés à une signalisation ROS (gènes *WRKY40, SALT TOLERANCE, TCH4, WRKY 33, CYP81D8, NHL3, CA, WRKY33, MYB44, TCH3, AAA-ATPase, SZF1*). Tous les 18 gènes induits mécaniquement testés ont été régulés positivement dans le tissu racinaire en réponse au stress mannitol. Dans la partie aérienne, seul TCH2 n'est pas régulé positivement par le stress mannitol et treize gènes sont induits par le stress salin sauf *WRKY18, CPK28, CPK32, HSPR0, TCH3*). Bien que les acteurs moléculaires de l'expression spécifique de ces gènes ne soient pas clairement définis, il convient de mentionner que le stress hyperosmotique peut positivement plusieurs facteurs de transcription (TF), notamment AP2/ERF, MYB, bZIP, HSF, C2H2, WRKY (Ghorbani et al., 2019). Plus de 70% des 18 gènes testés (induits constitutivement dans *gip1gip2* et en réponse au stress hyperosmotique, au toucher et à la réponse sonore dans une plante WT) ont un site de liaison MYB dans leur région promotrice. Bien que MYB soit impliqué dans d'autres stress abiotiques il pourrait conférer une spécificité dans la réponse au stress hyperosmotique via une copérativité avec d'autres facteurs comme le facteur DREB. Dans notre étude, nous avons observé que les transcriptomes induits dans *gip1gip2* et en réponse au toucher chez le WT partagent 57% d'homologie. Tous les 18 gènes mentionnés précédemment induits en stress hyperosmotique le sont aussi de manière constitutive dans *gip1gip2*. La protéine de type lamine végétale OsNMCP1 dans le riz (Oryza sativa) régule l'expression d'un panel de gènes sensibles à la sécheresse, notamment OsNAC10, OsERF48, OsSGL, SNAC1 et OsbZIP23 en interagissant

physiquement avec le régulateur négatif OsSWI3C (Yang et al., 2020). Chez Arabidopsis, l'homologue du NMCP CRWN1 régule négativement l'expression des gènes de stress (Mikulski et al., 2019). Neuf gènes parmi les 18 gènes mentionnés ci-dessus régulés à la hausse par le toucher, le son et le stress hyperosmotique sont communs aux transcriptomes induits dans *gip1gip*2 et *crwn1*, à savoir *HSPRO2, NHL3, WRKY33, CPK28, TCH2, SZF1, AAA-type ATPase family (AAA), WRK18, WRK40*.

Ces gènes régulés à la hausse par des changements mécaniques sont également induits par d'autres stress abiotiques, bien que dans une moindre mesure, par rapport au stress hyperosmotique dans le tissu racinaire. Fait intéressant dans le tissu racinaire, la plupart de ces gènes ont également été régulés à la hausse dans le stress froid qui modifie les propriétés fluidiques de la membrane (Xiong et al., 2002), conduisant à une production plus élevée de ROS, à l'induction de la déshydratation (formation de glace extracellulaire due au niveau inférieur à zéro), au changement de structure secondaire de l'ADN (Pareek et al., 2017) etc. qui peuvent modifier la propriété mécanique des structures cellulaires et subcellulaires. La réponse transcriptionnelle au stress mécanique peut également être comparée à la réponse de blessure partageant un grand chevauchement dans les gènes induits à la fois par des stress abiotiques et biotiques et peut donc représenter la réponse initiale de stress général chez Arabidopsis. Il est intéressant de noter que de nombreux gènes liés au stress sont régulés par les marques répressives H3K27me3, pour lesquelles l'environnement de l'enveloppe nucléaire est essentiel pour maintenir un état transcriptionnel répressif (voir la revue Barneche & Baroux, 2017). Cela suggère que la dérépression des gènes chargés par H3K27me3 pourrait être liée à des changements dans l'organisation de la chromatine 3D comme récemment suggéré (Nützmann et al., 2020).

Notre travail représente une première approche pour lier les propriétés de la paroi cellulaire à celles du noyau. En principe, le mutant *eli1-1* offre un bon contexte génétique pour cette étude. Nous avons observé que la forme des noyaux changeait légèrement dans *eli1-1* et nous avons également observé des noyaux plus rigides chez le mutant. Pourtant, nous devons prendre en compte le mécanisme de compensation existant dans *eli1-1*, impliquant une lignification en réponse à une carence en cellulose. Le dépôt de lignine est également connu pour être impliqué dans la réponse mécanique à l'infection pathogène et *eli1-1* montre une régulation à la hausse des gènes liés à la défense (Caño-Delgado et al., 2003) qui pourrait être liée à des changements dans l'organisation de la chromatine. Cela pourrait également être corrélé à l'augmentation de

la rigidité nucléaire et une augmentation de la paroi cellulaire observée dans le *gip1gip2* qui présente une régulation positive constitutive des gènes de réponse au stress et notamment ceux liés à la réponse mécanique au toucher (Goswami et al., 2020). Bien que nos observations préliminaires suggèrent que le noyau *eli1-1* est légèrement déformé (mais pas plus petit) par rapport au WT, la forme et la taille du noyau *eli1-1* changent avec le stress hyperosmotique. Cela signifie qu'*in vivo*, la légère déformation nucléaire observée chez le mutant n'a pas atteint un seuil maximal et peut se déformer davantage en réponse au stress hyperosmotique. Ce n'est pas comparable à *gip1gip2* qui a probablement déjà atteint une déformation nucléaire maximale et n'est plus déformable en réponse au stress hyperosmotique (Goswami et al., 2020). Cette étude nécessiterait une analyse plus approfondie des propriétés de la paroi cellulaire dans la racine. La paroi cellulaire est une structure complexe avec des microfibrilles de cellulose intégrées dans une matrice. La cellulose se dépose sur la paroi cellulaire par les protéines CESA, toute modification de ces protéines est souvent mortelle. Le mutant *eli1-1* non létal avec un gène CESA3 muté important pour la synthèse de la cellulose dans la paroi cellulaire primaire montre une composition plus faible en cellulose mais plus élevée en lignine. Cet effet compensatoire pourrait être essentiel pour la survie de ces plantes. Alternativement, nous pourrions traiter l'échantillon avec de la cellulase, pour vérifier si des modifications à court terme peuvent conduire à des défauts de forme du noyau, et inversement, utiliser d'autres mutants de la paroi cellulaire, avec divers degrés de compensation pour mieux évaluer la corrélation entre la rigidité nucléaire et la paroi. Enfin, il pourrait être plus facile de faire ce travail dans le méristème apical de la pousse où il a été démontré que les mutants de la paroi présentent de forts défauts morphologiques, sans lignification, et où les propriétés de la paroi peuvent être sondées et la forme du noyau surveillée.

En conclusion, j'ai observé des changements morphologiques et mécaniques du noyau végétal sous stress interne et externe en utilisant la pointe racinaire d'Arabidopsis comme système modèle et le stress hyperosmotique comme stress mécanique physiologique. J'ai étudié la corrélation des changements dans la forme et la mécanique de l'enveloppe nucléaire avec les changements dans la condensation de la chromatine et l'expression des gènes. Cette étude fournit les premières étapes pour aborder le rôle de la mécanique nucléaire et de la mécanotransduction dans les plantes. Nous proposons qu'une réponse mécanique nucléaire basée sur la chromatine de type gel existe en présence d'un stress hyperosmotique qui conduit à l'expression de gènes spécifiques et que les GIP agissent comme régulateur négatif. Notre modèle actuel suggère que le stress hyperosmotique entraîne un changement transitoire de la

morphologie du noyau qui font écho aux changements des propriétés mécaniques du noyau. La condensation de l'hétérochromatine semble se produire avec un stress hyper-osmotique et une décondensation avec un stress hypo-osmotique, modulant ainsi l'expression de gènes de stress mécanosensibles. L'induction constitutive de ces gènes dans le mutant *gi1gip2* pourrait être aussi corrélée à des défauts d'organisation de l'hétérochromatine centromérique (Batzenschlager et al. 2015), de même le mutant *crwn1* montre des défauts d'organisation de l'hétérochromatine à la périphérie nucléaire (Hu et al., 2019). Des études supplémentaires sont nécessaires au niveau de la chromatine pour corréler les changements de forme du noyau et d'expression des gènes, y compris données Hi-C données et modifications épigénétiques, ainsi que la translocation nucléaire de facteurs de transcription spécifiques. Les prochains défis seront de comprendre la spécificité des voies moléculaires dans de tels changements globaux ou comment la mécanique de l'enveloppe nucléaire est intégrée dans le développement des plantes. Les interactions de signalisation mécanique entre la propriété de la paroi cellulaire, la détection de la paroi, le cytosquelette (principalement les microtubules) et le noyau restent largement inconnues chez les plantes. Par ailleurs, l'analyse des réponses multi-stress est également facilitée chez les plantes du fait de leur développement plastique et de leur nature sessile, ce qui permet d'envisager l'étude éco-devo de la mécanotransduction nucléaire chez les plantes. Nos résultats ouvrent clairement une nouvelle voie pour comprendre le rôle de la morphomécanique nucléaire en réponse aux stress environnementaux dans les plantes. Cela pourrait également aider à comprendre la sensibilité des plantes aux ravageurs en réponse à un stress mécanique pour augmenter l'immunité des plantes (Coutand, 2020). Au total, cela introduit la mécanotransduction nucléaire comme un nouveau domaine de recherche dans la communauté végétale, avec des implications allant bien au-delà d'une comparaison avec les noyaux animaux.

Rituparna GOSWAMI

Characterization of the nuclear envelope mechano-transduction in Arabidopsis: from supracellular stress to chromatin remodeling

Résumé

Les cellules végétales détectent et répondent à divers stimuli mécaniques externes comme le toucher ou le vent, et internes comme la pression osmotique et la tension des parois cellulaires. Dans cette étude, j'ai démontré que la forme et la rigidité du noyau sont affectées de manière réversible en condition de stress hyperosmotique et sont corrélées à l'expression de gènes. Afin d'identifier les bases moléculaires de cette réponse, nous avons étudié différents mutants. En particulier, les protéines GIP lient cytosquelette, enveloppe nucléaire et chromatine ; nous avons observé que le mutant *gip1gip2* présente une réponse nucléaire de type hyperosmotique constitutive et acquiert même une résistance physiologique au stress hyperosmotique. De façon plus exploratoire, j'ai commencé à analyser l'impact du nucléosquelette (mutant *crwn1*) et de la paroi (mutant *eli1*) sur la forme des noyaux et leurs réponses au stress hyperosmotique. Notre étude ouvre le champ de la mécanotransduction nucléaire chez les plantes, et offre de nombreuses perspectives.

Mots clés: mécanique nucléaire; micro-rhéométrie; AFM; forme du noyau; enveloppe nucléaire; stress hyperosmotique; Arabidopsis; mérsitème racinaire; géne en réponse au toucher, *gip1gip2*, *crwn1*, *eli-1*, analyse de l'expression de gènes.

Anglaise

Plant cells sense and respond to external mechanical stimuli such as touch or wind, and to internal mechanical stimuli, such as turgor pressure and cell wall tension. In this study I have demonstrated that the nuclear shape and mechanics are impacted upon hyperosmotic stress in a reversible manner and are correlated with gene expression. To identify the molecular bases of this response, we have investigated different mutants. First the GIP proteins are at the nexus between cytoskeleton, nuclear envelope, and chromatin. We found that the *gip1gip2* mutant defects exhibits a constitutive hyperosmotic nuclear response and is already primed to resist hyperosmotic stress. As a more exploratory work, I also analysed the contribution of the nucleoskeleton (*crwn1* mutant) and cell wall (*eli1* mutant) on nucleus behaviour in response to hyperosmotic stress. Our study opens the path to nuclear mechanotransduction in plants, while also offering several prospects for future research in this area.

Key words : Nuclear mechanics; micro-rheometry; AFM; nuclear shape; nuclear envelope; hyperosmotic stress; touch gene; *Arabidopsis*; root meristem; *gip1gip2*, *crwn1*, *eli1-1*, gene expression analysis